DEPARTMENT OF THE INTERIOR
GEOLOGICAL SURVEY

MINUTES OF THE NATIONAL EARTHQUAKE PREDICTION EVALUATION COUNCIL

March 29-30, 1985
Pasadena, California

by
Clement F. Shearer[1]

Open File Report 85-507

This report is preliminary and has not been edited or reviewed for conformity with U.S. Geological Survey publication standards and stratigraphic nomenclature.

---

[1] U.S. Geological Survey, 106 National Center
Reston, Virginia 22092

TABLE OF CONTENTS

Page

Preface iii

List of members, National Earthquake Prediction Evaluation Council iv

Minutes of the March 1985 meeting 1

Appendices:

A. Summaries of presentations given at March 1985 meeting

1. Southern California Earthquake Probabilities - 13
2. The Pattern of Deformation from Small Earthquakes Along the Transform Boundary in California: Evidence for Block Rotation - L. Seeber 17
3. Depth of Seismicity and its Relationship to Heat Flow and Large Earthquake Potential - Hiroo Kanamori 29
4. Southern San Andreas Fault Geometry and Fault-Zone Deformation and Implications for Earthquake Prediction in the Coachella Valley, California - Roger Bilham 44
5. Slip Rates of Active Faults - Malcolm Clark 66
6. Tectonic Framework of the South-Central Transverse Ranges - Jonathan C. Matti 70
7. Evidence on Large Southern California Earthquakes from Historical Records - Duncan Agnew 76
8. Earthquake Potentials along the San Andreas Fault - Kerry Sieh 91
9. Forecast Model for Large and Great Earthquakes in Southern California - W. D. Stuart 98

Page

10. Foreshocks and Time-Dependent Earthquake Hazard Assessment in Southern California - Lucille M. Jones 123

11. CIT (California Institute of Technology) - USGS Catalog Events 1979-1984 - C. Johnson 142

12. A Review of Earthquake Stress Drop Determination Along the San Andreas and San Jacinto Fault Zones, Southern California - Arthur Frankel 144

B. Parkfield Correspondence

1. Council letter to Director, U.S. Geological Survey 166

2. U.S. Geological Survey Statement to California Office of Emergency Services 172

3. U.S. Geological Survey Press Release 175

C. U.S. Geological Survey Statements on Southern California Earthquake Hazard

1. 1976 letter to Alex Cunningham, Director, Office of Emergency Services, California 178

2. 1980 letter to Alex Cunningham, Director, Office of Emergency Services, California 181

3. 1981 letter to Alex Cunningham, Director, Office of Emergency Services, California 184

D. Proceedings of Southern California Special Study Areas Workshop San Diego, California, February 28-March 2, 1985 186

PREFACE

The National Earthquake Prediction Evaluation Council (NEPEC) was established in 1979 pursuant to the Earthquake Hazards Reduction Act of 1977 to advise the Director of the U.S. Geological Survey (USGS) in issuing any formal predictions or other information pertinent to the potential for the occurrence of a significant earthquake. It is the Director of the USGS who is responsible for the decision whether and when to issue such a prediction or information.

NEPEC, also referred to in this document as the Council, according to its charter is comprised of a Chairman, Vice Chairman, and from 8 to 12 other members appointed by the Director of the USGS. The Chairman shall not be a USGS employee, and at least one-half of the membership shall be other than USGS employees.

The USGS recently has begun to publish the minutes of NEPEC meetings. This open-file report is the second in an anticipated series of routinely published proceedings of the Council.

NATIONAL EARTHQUAKE PREDICTION EVALUATION COUNCIL

Dr. Lynn R. Sykes CHAIRMAN	Higgins Professor of Geological Sciences Lamont-Doherty Geological Observatory of Columbia University Palisades, New York 10964 Office: 914/359-2900 Home: 914/359-7428
Dr. John R. Filson VICE CHAIRMAN	Chief, Office of Earthquakes, Volcanoes, and Engineering U.S. Geological Survey National Center, MS 905 Reston, Virginia 22092 Office: 703/860-6471 Home: 703/860-2807
Dr. Clement F. Shearer EXECUTIVE SECRETARY	Hazards Information Coordinator Office of the Director U.S. Geological Survey National Center, MS 106 Reston, Virginia 22092 Office: 703/860-6208 Home: 703/620-9422
Dr. Keiiti Aki	Department of Geological Sciences University of Southern California Los Angeles, California 90007 Office: 213/743/3510 Home: 213/559-1350
Dr. John N. Davis	State Seismologist, Alaska Department of Natural Resources, Division of Geological and Geophysical Surveys, and, Adjunct Associate Professor, Geophysical Institute, University of Alaska 794 University Avenue, Basement Fairbanks, Alaska 99701 Office: 907/474-7190 Home: 907/455/6311
Dr. James F. Davis	State Geologist, California Department of Conservation California Division of Mines and Geology 1416 Ninth Street, Room 1341 Sacramento, California 95814 Office: 916/445-1923 Home: 916/487-6125

Dr. James H. Dieterich	Research Geophysicist Branch of Tectonophysics U.S. Geological Survey 345 Middlefield Road, MS 977 Menlo Park, California 94025 Office: 415/323-8111, ext. 2573 Home: 415/856-2025
Dr. William L. Ellsworth	Chief, Branch of Seismology U.S. Geological Survey 345 Middlefield Road, MS 977 Menlo Park, California 94025 Office: 415/323-8111, ext. 2782 Home: 415/322-9452
Dr. Hiroo Kanamori	Division of Geological & Planetary Science California Institute of Technology Pasadena, California 91125 Office: 818/356-6914 Home: 818/796-8452
Dr. Thomas V. McEvilly	Department of Geology and Geophysics University of California, Berkeley Berkeley, California 94720 Office: 415/642-4494 Home: 415/549-0967
Dr. I. Selwyn Sacks	Department of Terrestrial Magnetism Carnegie Institution of Washington 5241 Broad Branch Road, N.W. Washington, D.C. 20015 Office: 202/966-0863 Home: 301/657-3271
Dr. Wayne Thatcher	Chief, Branch of Tectonophysics U.S. Geological Survey 345 Middlefield Road, MS 977 Menlo Park, California 94025 Office: 415/323-8111, ext. 2120 Home: 415/326-4680
Dr. Robert E. Wallace	Chief Scientist, Office of Earthquakes, Volcanoes, and Engineering U.S. Geological Survey 345 Middlefield Road, MS 977 Menlo Park, California 94025 Office: 415/323-8111, ext. 2751 Home: 415/851-0249

Dr. Robert L. Wesson
Research Geophysicist
Branch of Seismology
U.S. Geological Survey
National Center, MS 922
Reston, Virginia 22092
Office: 703/860-7481
Home: 703/476-8815

Dr. Mark D. Zoback
Professor of Geophysics
Department of Geophysics
Stanford University
Stanford, California 94305
Office: 415/497-9438
Home: 415/322-9570

National Earthquake Prediction Evaluation Council
Minutes of the Meeting
March 29 & 30, 1985
Pasadena, California

Council members present

Dr. Lynn Sykes, Chairman-Lamont-Doherty Geological Observatory
Dr. John R. Filson, Vice-Chairman-U.S. Geological Survey (USGS)
Dr. Clement F. Shearer, Executive Secretary-USGS
Dr. Keiiti Aki-University of Southern California
Dr. John N. Davies-Alaska Dept. of Natural Resources
Dr. James F. Davis-California Dept. of Conservation
Dr. James H. Dieterich-USGS
Dr. William L. Ellsworth-USGS
Dr. Hiroo Kanamori-California Institute of Technology
Dr. Thomas V. McEvilly-Univ. of California, Berkeley
Dr. I. Selwyn Sacks-Carnegie Institution of Washington
Dr. Wayne Thatcher-USGS
Dr. Robert E. Wallace-USGS
Dr. Robert L. Wesson-USGS
Dr. Mark D. Zoback-Stanford University

Invited Speakers

A. G. Lindh
L. Seeber
H. Kanamori
Roger Bilham
Malcolm Clark
J. Matti
Carl Johnson
Duncan Agnew
K. Sieh
Clarence Allen
William Stuart
T. Hanks
Lucille Jones
Arthur Frankel

MARCH 29

REVIEW OF SAN ANDREAS AND SAN JACINTO FAULTS, SOUTHERN CALIFORNIA

Chairman **Sykes** opened the meeting with a brief summary of the last meeting and outlined the agenda for the present meeting. He noted that at the November 1984 meeting the Council agreed to periodically review several particularly important earthquake-prone areas in the United States, and that this meeting was to be devoted to the San Andreas and San Jacinto faults in southern California. Dr. Sykes emphasized that in selecting these two faults the Council fully recognizes that there are significant earthquake risks in other areas in southern California. Some of these areas may be discussed in future Council meetings. Also, at the previous meeting the Council endorsed the results of research indicating a high probability of a magnitude 6 earthquake near Parkfield, California, between 1985-1993. An update of that discussion was presented later in the meeting. Additionally, this meeting will include discussion of probabilistic statements made for various segments of the San Andreas and San Jacinto faults and consider revision of hazard statements for southern California made by the USGS.

Thatcher summarized the Southern California Special Study Areas Workshop held by the USGS in San Diego, California, from February 28 to March 2, 1985. The workshop's goal was to identify and reach consensus on specific 30-km long segments of the southern San Andreas and San Jacinto fault zones appropriate for detailed earthquake prediction studies using clustered monitoring equipment. The workshop was an adjunct to a Department of the Interior request to the USGS for a proposal to develop a prototype earthquake prediction network in southern California. The proposal was discussed in more detail at the last NEPEC meeting. At the San Diego workshop there was overall unanimity on the need to focus efforts in selected regions of southern California; with or without additional funds. It was generally accepted that the Parkfield prediction experiment is the prototype or model for future experiments in southern California, however, it was noted strongly that one can't treat all areas in exactly the manner of the Parkfield experiment. Instead it was clearly articulated at the workshop that there is the need for expanded regional coverage outside the special study zone. Further, for some areas in southern California there is the need for preliminary site investigations that may span several years just to decide what particular 30-km. segments to study in detail. In addition, in order to fulfill the goals of the prediction network it may be necessary to sustain and improve the regional seismic and geodetic coverage. Although opinion differed on which areas are the best for inclusion in the network, the following areas were repeatedly mentioned: the Anza slip gap on the San Jacinto fault, the southernmost end of the San Andreas fault near the Salton Sea, and the complex junction zone of the San Andreas and San Jacinto faults near Cajon Pass.

Comparison of Various Probability Estimates

Al Lindh presented a figure showing probability estimates for southern California that he produced some time ago and a figure of more detailed southern California conditional probability estimates more recently produced by Sykes and Nishenko. Lindh is now less confident than when he started that there is adequate information for some of the shorter segments and that using a time dependent probabilistic formulation is appropriate. He divided probabilistic estimates for southern California into two groups - first, a Mojave segment and a Carrizo segment, where probability estimates have some significance and second, all other segments, where the probability estimates are of lesser significance because the recurrence interval estimates are conjectural. He suggested that sometimes increased information on a segment leads to an increase in the range of estimated probabilities and thus an apparent increase in the associated uncertainties. And, he opined that varying the length of the probability distribution would be preferable to quoting ranges of probabilities. He cautioned against the extrapolation of the Parkfield methodology for estimating probability to other areas for the purposes of selecting sites for clustered monitoring experiments because of both the limits of the statistics and the lack of adequate geological and geophysical investigations. **Sykes** questioned whether the data are of too poor a quality for numerical estimates. He stated that they generally are sufficient to rank areas in the following three categories - high, medium, and low risk - for the next 10 to 50 years. Such estimates would have social utility. **Aki** suggested that the approach discussed is a quantitative estimate of the intuition and uncertainties of experts, with the implication that this does have some public utility. **Wesson** stated that if we are going to do clustered monitoring we must start focusing on certain areas into which we can cast and test our hypotheses.

Deformation along the Transform Boundary, California

L. Seeber presented evidence for block rotation as the pattern of deformation from small earthquakes along the transform boundary. He then discussed how this work led to new ideas or approaches to understanding the dynamics of generating large earthquakes. The major through-going faults in the right-lateral transform system of California clearly can be identified from their structural expression and as the locus of the major earthquake ruptures. The lack of direct correlation between these faults and current seismicity has long been noticed. In some areas, notably along the Transverse Ranges, current seismicity is obvously occurring on secondary faults. Thus, low-magnitude "background" seismicity during the interseismic periods cannot be a reliable indicator of the major faults. However, this seismicity may reveal the detailed pattern of deformation as it evolves in space and time before a major earthquake. Arrival-time data was inverted for local velocity structure and for accurate hypocenters. Earthquakes were then grouped according to their first-motion data. Composite fault-plane solutions were considered acceptable when one of the planes in the solution coincided with the plane or planes defined by the spatial distribution of hypocenters in that solution. The investigators then interpreted these in light of other structural and deformation data. Much of the seismicity is not on the main strands; a lot of the seismicity, however, is on left-lateral northeast striking subsidiary faults. In some cases these faults are related to a system of rotating blocks which may explain the long-term geologic deformation and play a part in the long-term nucleation of large earthquakes.

Depth of Seismicity and its Relation to Heat Flow and Large Earthquake Potential

Hiroo Kanamori described research of earthquakes in southern California conducted to see whether there is any pattern of stress release and also to make some predictions on the location of possible future earthquakes in the region. He stressed that relocation of earthquakes can be very important, especially in the Imperial Valley where the sediment cover is very thick. Hiroo described the study by Dianne Roser and himself of the Imperial Valley earthquake of 1979. One of the most interesting results is that most of the pre-seismic activity occurred near, but not in, the zone of pre-sesimic activity, and again in the aftershock sequence the seismic activity occurred in the zone of pre-seismic activity. So, in a sense the slip zone slipped only at the time of the main shock. He then described other researchers' work which argues that in the places where co-seismic displacement is very large there were few aftershocks. In describing the San Jacinto fault zone, he noted that there is a linear distribution of earthquakes near the bottom of the seismogenic zone which changes in depth along strike, becoming shallower nearer the Imperial Valley region of high heat flow. Also, seismicity is concentrated in the bottom of the seismogenic zone. And, along strike clusters of activity are separated by relatively quiet segments, the quietest of which, except for the Anza seismic gap, are coincident with the rupture zones of the largest historic earthquakes. These observations indicate that the maximum depth of the seismogenic zone can vary by a factor of two, which may affect the repeat time of large earthquakes along different fault segments and also the observability of strain related phenomena at the surface before large earthquakes. That most seismicity occurs at the base of the seismogenic zone implies that seismological precursors to future large earthquakes might be found near the base of the brittle fault zone. It was also noted that heatflow and temperature seem to be controlling the thickness and crustal properties of the seismogenic zone and perhaps also the size of the earthquakes and the average repeat time. Since seismicity patterns alone do not permit short-time prediction, it is important to begin looking at the bottom of the seismogenic zone. Events near the bottom of the seismogenic zone may be different from events at shallow depth, at least suggesting that properties change as a function of depth and time.

Transpression and Earthquake Prediction, Coachella Valley, Southern California

Roger Bilham described recent work on relationships between a seismic deformation and geometry of the San Andreas fault in the Coachella Valley. Seismicity in the valley is almost absent, and what does exist isn't occurring on the San Andreas fault. His investigations lead to a number of geometric properties that may be very important for locating crustal deformation monitoring instruments and long-term geodetic arrays. The mapped, most recent fractures on the southern San Andreas in the valley form a sequence of straight segments, 9 to 14-km long, with bends of 4 to 11 degrees between the segments. These changes in strike determine the fault's physical behavior. Where the fault is parallel to the inferred slip vector the fault zone is poorly expressed and at a low elevation. Where the fault strikes oblique to the slip vector the fault zone is clearly expressed within elevated and folded rocks and exhibits triggered slip in response to strong ground motion from nearby earthquakes. Knowing the geometry and the slip vector it is possible to more or less predict what kind of strain field will be produced at these asperities. The important point for siting instruments is that since the segments have dimensions on the order of 10-km., and the developing strain fields also have wavelengths of 10-km. they are smaller than the baselines of most existing geodetic lines. Dyke injection at depth in the period 1974-1978 appears to be a plausible mechanism to account for Brawley swarm activity, leveling data near Bombay Beach and Salton Sea-level data. Spreading caused increased loading of the Imperial Fault resulting in rupture in 1979. Increased loading of the southern San Andreas Fault is confirmed by recent fault creep and sea-level data. It is possible that rupture of the southern San Andreas Fault will be triggered by a future spreading episode SE of Bombay Beach.

Slip Rates for California Faults

Malcolm Clark began the discussion by stating some of the problems with assigning slip rates. In short, he felt that the present rates are poor but can be improved with more data. He also noted that there is little data for southern San Andreas and San Jacinto faults. He discussed problems in determining slip rates. Although the formula (rate = displacement/age) is simple, measurements of both slip and time are rarely straight-forward. Such measurements generally include crucial assumptions and significant measurement uncertainties. He advocated that investigators give estimates of minimum and maximum rates and a preferred rate. He also advocated that the investigators give a quality assessment of the rates. He concluded with a description of the California slip-rate map and table, and cited some examples of the quality assessments he and his colleagues gave to a selected number of southern California slip rates.

Tectonic Elements - San Gorgonio Pass

J. Matti described faults and seismicity of the San Gorgonio Pass region, fault rupture scenarios of great earthquakes in the region, and locationsfor prediction experiments. The San Gorgonio Pass fault system is a series of Quaternary wrench faults; the system overprints the older Banning fault zone. The San Andreas fault system in this region is a NW-oriented zone with multiple strands - the Banning fault, San Andreas fault zone which in itself consists of a Wilson Creek strand, Mission Creek strand, Mill Creek strand, and San Bernardino strand, and the Crafton Hills horst and graben complex. The San Gorgonio Pass region has been a problem for the San Andreas fault system throughout its history: the Wilson Creek strand, Mission Creek strand, and Mill Creek strands were deformed in this region, and the San Bernadino strand has a complicated relationship with the Coachella Valley segment of the Banning fault. The Coachella Valley segment is probably a Holocene fault and enters the complex San Gorgonio Pass region where it interacts with the San Gorgonio Pass fault system. Also, it is likely the relationship between this neotectonic strand of the Banning fault and the neotectonic San Bernardino strand and is somehow involved in the neotectonic structural knot in the San Gorgonio Pass region. He tends to associate the zig-zag faulting pattern with the interaction between the Coachella Valley segment of the Banning fault and the San Bernardino strand. This complexity in the modern San Andreas fault zone coincides spatially with left-lateral faults that have also had a neotectonic history. Matti agrees that this region is an attractive site for a monitoring and prediction experiment but also feels that its complexity necessitates a greater understanding of the actual distribution of the fault strands and requires a major geologic effort.

Evidence of Large Southern California Earthquakes from Historical Records

Duncan Agnew gave a discussion of what evidence the non-instrumented seismic record gives for the occurrence of large earthquakes on the central San Jacinto fault (Anza Gap) and the southern San Andreas fault. He considered four possible earthquakes: (A) an Anza earthquake with 1 meter of slip; (B) a Cajon - Salton Sea event with 4 meters of slip; (C) and (D) Whitewater - Salton events with 2 and 4 meters of slip respectively. Specifically, he addressed the question of how recently there could have been a large earthquake in these areas that we didn't know about because nobody wrote it down and it didn't get into the Townley and Allen catalog. For each candidate earthquake there are two separate problems to be considered. First, whether there are events in the historical record which might be the one under investigation. If no candidate is suggested from the record, there is the more difficult problem of deciding whether or not the candidate earthquake could have been missed or obscured in the historical record. This in turn breaks down into three questions: (1) what intensity distribution would have been expected?, (2) what other records exist?, and (3) how likely is a particular intensity event to be recorded in any given class of records? In trying to decide whether the absence of historical accounts genuinely reflects the absence of earthquakes, we must be sure that the shaking could not have been ignored. Places which were not continuously inhabited by literate people may thus be excluded. And other things being equal, the more often a record (e.g. a daily journal versus a weekly) is made the lower the intensity that is likely to be recorded. The period before 1850 is generally unfavorable for earthquake reporting. Duncan ruled out the first candidate event, A, occurring after 1880. Event B probably last occurred before 1790; and events C & D can very probably be ruled out after 1850.

Earthquake Potentials along the San Andreas Fault - next 50 years

Clarence Allen presented the discussion for **Kerry Sieh,** who wasn't able to attend the meeting. Sieh divided the fault into areas of high and low danger, the high areas having a 50 percent or greater probability for an earthquake over the next 50 years. The high risk areas include those around Cholame (segment 2), Pallett Creek (segment 5), Cajon Creek to Salton Sea (segment 6). The other three of his segments; north of Cholame, i.e., the creeping zone (segment 1), Wallace Creek (segment 3), and from Mill Potrero to Three Points (segment 4) are all of low risk.

Segment 5 is the southern portion of that reach of the fault which last broke in 1857. Offsets along segment 5 have commonly been about 3 meters and the average recurrence interval between the latest 12 large slip events is between 100 and 200 years. The probability of a large, M7, earthquake along this segment is about 50 percent. Segment 6 is the only portion of the San Andreas fault that has not sustained large offsets in the period of the historical record. Nevertheless, the record of the geologically recent past leaves no doubt that this segment is as active as other segments. The long-term slip rate of this segment is about 25mm/yr. Work in progress near Indio suggests that this segment of the fault produces large earthquakes about as often as those historically active sections to the northwest. This observation coupled with the historical dormancy of the segment and its local low-level creep, lends credence to suggestions that segment 6 has a high probability of generating a large earthquake within the next several decades.

Overview of San Andreas and San Jacinto Fault Systems

Clarence Allen presented a slide "field trip" of the San Andreas and San Jacinto fault systems from Tejon Pass to the Salton Sea.

Prediction of Large Earthquakes along the San Andreas in Southern California

William Stuart discussed his work at combining physical theory, specifically an instability model, with field data to predict large earthquakes. He supposes that the upper 12-km. of the fault zone is brittle and represents it as a patch whose strength varies along strike. He then models offset data by sectioning the patch. Below the patch it is assumed that the fault has zero strength and slides freely. Repeated measures of earthquake offsets are used to constrain the strength along strike. In his model Stuart represented the San Andreas and San Jacinto faults by many rectangular areas, and he imposed a slip rate for the entire San Jacinto fault (earthquakes not allowed in model) and part of the San Andreas fault. In the variable strength patch the fault will have very small slip for centuries and then suddenly rupture during the instability. The model can be used to predict earthquakes by simulating what happened in the past and then running the simulations into the future. This method gives time and location but isn't any better than using existing probability recurrence intervals. A second way is to compute ground deformation as it would occur in the model before the instabilities, as measured by fault creep or motion of geodetic bench marks.

Overview - San Jacinto Fault

Tom Hanks began by noting both the difference between the Anza seismicity gap and the seismic slip gap, and that of the five biggest earthquakes in southern California, four were north of the Transverse Ranges and the fifth was actually in Mexico. They occurred at the rate of about one every 25 years and exhibited a range of focal mechanisms. The rate of seismic moment release has plainly dropped since 1850; about two orders of magnitude in the past 150 years. Obviously this rate of decrease is impossible to continue over the long term. In southern California we should be looking for 5 to 6 cm/yr of plate motion, and seismically this has not been noticed. The decline in seismic moment seems to be real but what does it all mean. Is it somehow related to some larger scale, both in space and time, aftershock sequence? Could it be that a lot of the activity in northern Baja was somehow related to the 1892 earthquake? And is the Mammoth Lake activity somehow related to the 1872 earthquake? And, is seismicity on the San Jacinto fault since 1890 somehow related to or driven by the great 1857 earthquake? This last question is important for two reasons. First, if this relationship is true, we may not see significant activity along the San Jacinto fault until we have the next great earthquake along the San Andreas fault at Fort Tejon. Second, if that mechanism is real, the question becomes whether it is possible that the San Jacinto fault is somehow short-circuiting the San Andreas fault in southern California. Based on the slip rate, and history of the last 90 years the northern San Jacinto fault, and Anza Gap in particular, seems to be a likely location for a magnitude 6 to 7 earthquake in the near future. And, existing information and instrumentation, location of the fault in crystalline rock, and relative simplicity of the fault zone all argue in favor of the region for designation as a special study area.

Foreshocks and Short-Term Earthquake Prediction

Lucille Jones discusssed the possibility of using foreshocks to make short-term earthquake predictions. She first determines the percentage of earthquakes by magnitude that were followed by earthquakes of larger magnitude in southern California, and from this the probability that an earthquake will be a foreshock. She noted that in the past 20 years one-half of the strike-slip earthquakes in southern California have had foreshocks within the previous day. And, there is a slight suggestion that the larger the earthquake the more likely it is to have a foreshock. She believes that there is at least a 50 percent chance that there will be a foreshock for whatever large earthquake occurs in southern California. Foreshocks and non-foreshocks were assumed to have a binomial distribution, the percentage of earthquakes that have foreshocks then is the probability that a future earthquake will be a foreshock. The data used in her analysis includes all earthquakes greater then magnitude three in the past 50 years. An earthquake is defined as a foreshock if it occurs within 5 days and 10-km. of a larger earthquake. In southern California there is a

6 percent probability of an earthquake greater than magnitude three being followed by a large event within 5 days and 10-km. Further, there is a magnitude dependence such that a magnitude three or greater earthquake has a 1 percent chance of being followed by a magnitude 5 mainshock but a magnitude 5 or greater earthquake has a 6.5 percent chance of being followed by another magnitude 5 or greater earthquake. **Dieterich, Wallace,** and **Wesson** all agreed that this work is potentially fruitful and should be used, including that in principal it could be used at Parkfield to give an earthquake probability estimate for a short period following a shock of a given size.

Geometric Considerations of Recent Seismicity-Clustered Monitoring Experiments

C. Johnson presented an overview and analysis of the distribution of recent seismicity in southern California. Most significant is a zone of seismicity surrounding the southernmost section of the San Andreas fault and representing the locus of the highest seismicity in southern California. The seismicity along the San Andreas fault is predominantly strike-slip, the most prevalent mechanism being right-lateral. The Imperial Valley area can be characterized as an oblique spreading zone representing the locus of the spreading center between the Imperial and San Andreas faults. The seismicity confirms other evidence indicating that strain is building up on the southern section of the San Andreas fault. In the San Gorgonio-Mission Creek-Banning area there's a deepening of seismicity that shallows going into the seismically quieter area. The lower boundary of seismicity in the locked area is shallow and becomes deeper towards the Imperial Valley. The seismicity in the Brawley seismic zone is responding to something related to the seismic cycle on the adjoining strike-slip faults, in particular the Imperial, and possibly the San Andreas fault. The places where the shallow seismic zones are impinging on the major strike-slip faults tend to be the focus of major earthquakes on the strike-slip faults. The Bombay Beach area should be seriously considered as one of the more likely places for the nucleation of major earthquakes on the San Andreas fault.

Review of Earthquake Stress Drop along the San Andreas-San Jacinto Faults

Art Frankel reviewed several studies of stress drops of earthquakes in southern California concentrating on determinations of static stress drops for events along the San Andreas and San Jacinto faults. While we actually know very little about the temporal and spatial variations of seismic stress drops along these fault zones, there is encouraging but limited evidence that stress drop determinations when carefully corrected for path effects are useful for the prediction of moderate-sized earthquakes in this area. Wyss and Brune concluded that most events along these fault zones had average apparent stresses. Earthquakes near San Gorgonio Mountain in the Big Bend region of the San Andreas fault had higher than average apparent stresses. However, the study had many limitations, such as the lack of depth and path corrections and the inadequacy of the M_L scale for the estimation of energy for small events. Thatcher and Hanks calculated the stress drops for over 100 events in southern California. The central finding of this study was that stress drops generally ranged from about 1 to 100 bars, independent of the seismic moment for events between magnitudes 3.5 and 6.8. Again, confirmation of possible regional differences in stress drop awaits higher quality recordings at smaller epicentral distances. Many seismologists have suggested the use of stress drop determinations of microearthquakes (M_L>3)for earthquake prediction purposes. However, recent observations of the spectra and pulse widths of microearthquakes have indicated that the path effects (i.e., the site response) often contaminate stress drop determinations for these small events. The wave forms of microearthquakes (M_L<2.2) can be used as empirical Green's functions in the determination of stress drops of earthquakes with magnitudes greater than about 3.5, whose source durations are long enough to be separated from pulse broadening caused by path effects. Frankel and Kanamori found that earthquakes in southern California exhibit significant differences in stress drop and that these differences may sometimes be indicative of impending larger shocks. It is premature to evaluate the limited stress drop calculations available for earthquakes in the vicinity of the San Andreas and San Jacinto faults in terms of earthquake prediction. Seismic network instrumentation with reasonable sampling rates and high dynamic range are required to obtain stress drops of events greater than M_L 3.5 corrected for path effects. The upgrade of relatively few, about 20, stations of the southern California network would provide the necessary data to judge the utility of seismic stress drop for the monitoring of tectonic stress levels and the discrimination of foreshock sequences.

MARCH 30

PARKFIELD UPDATE

William Ellsworth, Chief of the Branch of Seismology, USGS, reviewed recent data from the Parkfield experiment. There has been very little seismic activity; the rate of earthquakes greater than magnitude 1.5 has been low, averaging one or two events in a 2-week period. Data from the 2-color laser suggests a mode of strain accumulation more complex than one might have anticipated. Also, some operational problems had created gaps in data from the laser. He reported that looking at a N-S line one sees a period of relative stability in the line lengths covering most of late 1984, since then there's been a significant shortening of the line. One gets an opposite picture.in the E-W lines, a period of E-W extention while the N-S lines were relatively stable and which is now stabilized while the N-S lines are shortening. He discussed the records of several creepmeters. The Slack Canyon meter shows a rate that has returned to that prior to the Coalinga earthquake indicating that creep has more or less recovered from the Coalinga earthquake. The Middle Mountain meter, established in 1979, shows a clear rate disruption by the Coalinga earthquake, but shows a return to eventful right-lateral creep in 1984 at about 1/2 the pre-Coalinga rate, and is slowly returning to the pre-event rate. The Parkfield meter has been flat since Coalinga showing that the rate is not returning to what it was before the Coalinga earthquake.

STATUS OF THE COUNCIL'S STATEMENT TO USGS REGARDING PARKFIELD PREDICTION

John Filson brought the Council up-to-date on the USGS reaction to the Council's recommendation that the agency issue a statement regarding the Council's endorsement of the Parkfield prediction. In summary, the USGS has written a letter to the Director, California Office of Emergency Services in which it summarizes the results of the USGS Parkfield prediction experiment (The letter was issued on April 4, 1985). **Jim Davis** presented a summary of the California Earthquake Prediction Evaluation Council's (CEPEC) role in this matter. The California Council played a pivitol role in reinforcing the NEPEC finding of a high probability for a magnitude 6 earthquake near Parkfield between 1985 and 1993, and in helping to coordinate the issuance of the statement among the California Department of Conservation, Division of Mines and Geology; California Office of Emergency Services; and U.S. Geological Survey. It also helped the State of California in deciding what actions might be taken in response to the forecast. Also CEPEC advised the USGS to make an effort at short-term prediction and to increase its monitoring effort without waiting for the normal budget process. And, as part of its advisory process CEPEC, furnished the State of California with an intensity map indicating the Modified Mercalli intensity VII isoseismal. It was reported that the California Office of Emergency Services is planning a workshop in the Parkfield area to explain the situation to local residents and officials.

The Council next discussed the amount of time the USGS seems to need to fully consider the Council's recommendations and whether any steps could be taken by the Council and the USGS to reduce this amount of time. The Council was particularly anxious about this matter because conditions at Parkfield may mandate a very quick reaction by the Council and the U.S. Geological Survey.

As part of this discussion **Wesson** offered that if we are to move from making intermediate-term predictions to timely and effective short-term statements we will have to develop some pre-arranged scenarios and statements in consultation with the Director, USGS, that could be publicly issued by people like William Ellsworth, Chief of the Branch of Seismology, USGS. Specifically, he suggested that Thatcher's and Ellsworth's group develop a matrix of trigger events and probabilities for Parkfield that would then be presented to the Council at the next meeting. It is intended that these tables or matrices would be approved by the USGS, State of California, and the two evaluation councils. **Davis** urged the early inclusion of the California Council in NEPEC's deliberations, including holding a joint meeting.

The Council next discussed how it could include probablity statements in both a forecast that an event will occur and a statement that reassesses the forecast should the predicted event not occur in a specified interval. **Aki** suggested that this could be accomplished with the implementation of Lucy Jones' probability calculations for Parkfield.

SOUTHERN CALIFORNIA DISCUSSION - UPDATING THE USGS STATEMENT ON SOUTHERN CALIFORNIA: SOUTHERN CALIFORNIA PROBABILITY ESTIMATES

The Council's discussion of probability estimates began with **Davis** reiterating Lindh's two main points - one concerning the validity of probability calculations and his opinion that the estimates are adequate for the Parkfield, Carrizo, and Mojave segments of the San Andreas fault but not for the other segments of the fault, which have poor data sets. The other point is how to express this data to different audiences. **Kanamori** noted that while some long-term probabilities are independent of models, annual probabilities are highly dependent on the model used and its assumptions. Annual probabilities therefore can be very misleading to the public. He suggested that we have to decide an appropriate time window over which the probabilities are to be calculated. **Wesson** suggested that the Council should formulate a new letter on southern California that both reviews the situations which lead to the original 1976 USGS statement and their present status and states our concern regarding the mid-range probability. He further noted that while annual probabilities are too model dependent, 30 yr. probabilities aren't always helpful and suggested using something like 10-yr. probabilities or the length of time where the model begins to lose credibility. **Davis** noted that these statements and long-term predictions have had a positive impact in that they have lead to good building codes, programs such as the Southern California Earthquake Preparedness Project (SCEPP), and in general helped to create a more appropriate understanding of the earthquake threat. He believes it is advisable to establish an annual NEPEC advisory to provide a continuity of communication regarding California's earthquake hazards.

Sykes observed that at least three independent probability maps have good agreement in several areas of California and suggested that this level of agreement should be made known in public statements about California earthquake probabilities. The Council had considerable debate about the mechanisms and utility of issuing summary probability maps. The consensus of the Council is that it will:

- o annually update a probability advisory on California seismicity using qualitative estimates of probabilities. The first annual update will be on southern California, the next on all of California;
- o recommend that the USGS issue the update; and
- o draft summary information on the following points for the USGS to include in an update of its 1976 and 1980 letters to the Director, California Office of Emergency Services, on southern California seismic hazards:
  - * possibility for a 6 1/2 magnitude earthquake anywhere in the State;
  - * qualitative update of southern California probability;
  - * current USGS, California Division of Mines and Geology programs; and
  - * changes in physical parameters since the last statement.

The Council agreed on the following probabilistic statements for fault segments in southern California with the acknowledgement that work is continuing and the assessment can change substantially.

- o Carrizo segment - low probability
- o Tejon to Cajon Pass - moderate to high
- o San Gorgonio Pass - an area that may break in great earthquakes, work is in progress and there is still substantial uncertainty in sizes of characteristic earthquakes, repeat times, or probability estimates
- o San Andreas fault, Salton Sea to Palm Springs - investigations are underway, preliminary indications that the hazard may be more significant than previously thought
- o Northern San Jacinto fault - there may be a high probability on some segments but more work needs to be done before a risk assessment can be made.

In the Council's discussion of clustered monitoring experiments I. **Sachs** warned that the short-term precursors we hope to capture don't always happen on the major faults or the ones we are monitoring. He suggested that the clusters need auxiliary instruments, or outliers, to improve the prospects for capturing these phenomena. **Wesson** agreed that we need some reasonable level of regional coverage with the clusters being focused experiments within that regional coverage. He also suggested that Council and the USGS working groups begin to focus their attention on which areas are to be monitored, determine what instrumentation is needed, define the experiment, and move into the analysis and testing of our hypotheses. **Sykes** endorsed the working group concept as a good way to synthesize data coming from different sources. The Council agreed that it would be worthwhile to suggest that working groups be established for a few places that appear profitable for clustered experimentation. He further offered that these groups be drawn from the community of researchers working in the areas of interest.

LEGAL LIABILITY

As its last agenda item the Council briefly expressed its concern about the ambiguity concerning its limits of legal liability, particularly the liability of its non-governmental members. The Council's conclusion was that it should state its assumptions about this matter in a letter to the Director, USGS, and ask for a written response.

FUTURE MEETINGS

The Council tentatively plans to hold two meetings this summer. The first meeting will probably be convened in the San Francisco Bay area in late July. The topic will be further discussion of Parkfield, principally the presentation of a draft decision matrix. The second meeting is scheduled for early September in Anchorage, Alaska. At that meeting the Council will discuss updating the USGS statement on the Yakataga seismic gap, the seismicity along the Castle Mountain and Border Ranges faults, the Shumagin gap, and other areas of potentially high risk.

Clement F. Shearer
EXECUTIVE SECRETARY
National Earthquake Prediction
Evaluation Council

APPENDIX A. 1.

Southern California Earthquake Probabilities

Allan G. Lindh

29 March 1985

Southern California Earthquake Probabilities

Allan G. Lindh
U.S.G.S

Conditional probabilities from Sykes and Nishenko (1984) and Lindh and Ellsworth (1985?) for fault segments in southern California are summarized in Table 1. For the Parkfield, Carrizo, and Mojave segments where the questions are well posed and the data adequate, they agree well. In most other cases they also agree, but I believe this reflects only the similarity of our assumptions, and the lack of adequate data.

In the case of most relatively short fault segments (earthquakes of magnitude less than 7) I am less convinced than I previously was that a time dependent probabilistic formulation, such as that used to generate the probabilities in Table 1, is always appropriate. It seems to me that some reasonable way must be found to identify those cases in which we do not have enough information to calculate a time dependent probability (Weibel function for instance), and then be content with one parameter (Poisson) estimates. Then as we progress to better understood fault segments and associated earthquakes, some means is needed to smoothly translate our increased information into bolder (ie time dependent) and less uncertain estimates. Some way must be found to avoid the unfortunate situation which sometimes arises now of increased information on a segment leading to an increase in the range of estimated probabilities, and thus an apparent increase in the associated uncertainties.

One simple approach to accomplishing this would be to adjust the breadth of the a priori Gaussian probabiltiy density function on the basis of how much information one had about the earthquake. In the case of Parkfield where multiple lines of evidence point to an earthquake in the near future, the standard deviation could be set as small as 10-20% of the mean recurrence time. This results in a probability function sharply peaked around 1988, with an associated conditional probability that increases very rapidly around that time; this is of course just a quantitative way of describing a "long-term earthquake prediction".

For the Mojave segment a standard deviation of 30% of the mean recurrence interval seems consistent with the available data, and results in a relatively smooth conditional probabiltiy curve. This curve does differ significantly from the flat conditional probability of a Poisson distribution, and thus accurately reflects our confidence that earthquakes on that segment have a quasi-periodic distribution in time.

For the short segment just south of Parkfield which I have called the Red Hills segment in Table 1 (but which has previously been described as the Simmler or Kerry Sieh segment), the picture is less clear. We have only one piece of evidence for a M6-7 earthquake on that segment -- the 3 m of slip in 1857 -- and that interpretation depends on a series of untested assumptions. Similarly the recurrence interval for that segment is somewhat conjectural, since we have no idea how the strain around the end of a major segment is accomodated, certainly anelastic deformation must play some part. In this case a standard deviation of 40-50% of the mean reccurence interval would seem appropriate.

It seems to me that varying the breadth of the probability distribution would be preferable to quoting ranges of probabilties, particularly since all of these probabilites contain a large subjective component. The test of whether they should be taken seriously and quoted to the public should be whether sufficient information exists to make them significantly better than the simple Poisson estimate. I believe that we have accomplished some good in communicating our work to the public through the use of probabilites, but I believe we could run the risk of over stating the case, and eroding our credibility, if we get carried away and forget that they really are just our "best informed guesses" in most cases. As a guide for research they are clearly better than nothing, but they should be used with great caution in talking to the public, or to public officials, in all but the best constrained cases. The bottom line is that statistics cannot add information to what one knows about a problem, but only summerize what one already knows in a convenient way.

Table 1

Segment name	Magnitude	Probabilities (% / yr)	
		Annual	20 yr cumulative
SAN ANDREAS FAULT			
Parkfield	6 / 6	/ 8.3	62-81 / 98
Red Hills	6.6 /		58-71 /
Carrizo	8 / 8	/ 0.2	3-5 / 5
San Emigdio			4-17 /
Mojave	7.5 / 7.5	/ 1.2	19-49 / 26 (7-60+)
Indio	7.6 / 7.5	/ 2.1	21-61 / 37
SAN JACINTO FAULT			
Caj P to Riv	6.6 /		3-81 /
Riverside	6 /		2-59 /
Riv to Anza	6.7 / 6.7	/ 1.1	15-34 / 28
Anza to C M	6.6 / 6.7	/ 2.1	4-86 / 43
Coyote Mtn	6.4 / 6.7	/ 0.1	.4-19 / 3
Super Mtn	6.6 /		1-34 /
IMPERIAL FAULT			
Imperial	6.6 /		12-22

THE PATTERN OF DEFORMATION FROM SMALL EARTHQUAKES ALONG THE TRANSFORM BOUNDARY IN CALIFORNIA: EVIDENCE FOR BLOCK ROTATION

Extended Abstract for the National Earthquake Prediction Evaluation Concil,
29 March 1985 prepared by L. Seeber

This work is the result of a collaborative effort by C. Nicholson, P. Williams L. Seeber and L. Sykes.

The major through-going faults in the right-lateral transform system of California can be clearly identified from their stuctural expression and as the locus of the major earthquake ruptures. The lack of direct correlation between these faults and current seismicity has long been noticed (e.g., Allen et al., 1965). In some areas, notably along the Transverse Ranges, current seismicity is obviously occurring on secondary faults. Thus, low-magnitude "background" seismicity during the interseismic periods cannot be a reliable indicator of the major faults. However, this seismicity may reveal the detailed pattern of deformation as it evolves in space and time before a major earthquake.

We have begun a systematic examination of earthquake data from the Southern California Network and of other pertinent geologic data in an attempt to improve the resolution of current fault kinematics. This interseismic deformation pattern is then compared to the deformation during great earthquakes and to geologic deformation. This approach will hopefully lead to new strategies for earthquake prediction in California by an improved understanding of how deformation on secondary transverse faults interacts with slip on the master faults.

The abundance and high-quality of earthquake data from the Southern California Network (U.S.G.S./Caltech) has allowed fruitful results from a rather simple procedure. Arrival-time data was inverted for local velocity structure and for accurate hypocenters. Earthquakes were then grouped according to their first-motion data. Composite fault-plane solutions were considered acceptible when one of the planes in the solution coincided with the plane or planes defined by the spatial distribution of hypocenters in that solution. We then interpreted these results in light of other structural and deformation data available.

APPENDIX A. 2.

The Pattern of Deformation from Small Earthquakes Along the Transform Boundary in California: Evidence for Block Rotation

L. Seeber

SUMMARY OF RESULTS

San Bernardino- San Gorgonio Pass Area

Using data supplied by the southern California seismic network, we found that although this area is unusually seismogenic, very few earthquakes were occurring in the upper 5 km, or could be directly associated with any of the major through-going faults. Instead, an active system of relatively short left-lateral faults striking north-east to east-west was identified for earthquakes between focal depths of 5 and 10-12 km. This pattern of deformation, in conjunction with an unusual set of both normal and reverse faulting earthquakes, suggested a series of small rigid blocks undergoing clockwise rotation as a result of regional right-lateral shear (Fig. 2). The normal and reverse faulting earthquakes represent the corners of the blocks rotating into or away from the sides of the major bounding faults. If valid, this is the first study to identify blocks undergoing contemporary rotations - rotations that are more commonly identified on the basis of paleomagnetic work and only for much longer time scales.

Other earthquakes that show left-lateral slip on north-east trending structures include several events along sub-parallel features located west of the San Jacinto fault and first identified by Hadley and Combs [1974] (focal mechanism A in Fig. 2). Each of these structures, as well as the northeast trend of earthquakes located under the town of San Bernardino (focal mechanism H in Fig. 2), corresponds to a known vertical aquiclude affecting ground-water migration in the sediments of the San Bernardino valley [Dutcher and Garrett, 1963]. Where these structures intersect the San Jacinto and San Andreas faults, hot springs and thermal wells are evident that are relatively rare for other sections of the San Andreas system [Jennings, 1975]. Thus, motion along these presumed fault structures must have been sufficient to generate a clay fault gouge capable of acting as an effective water barrier. This implies that although these fault segments are relatively short, they may still constitute a significant seismic hazard to the local population. In fact, intensity data suggests that the 1923 magnitude 6¼ earthquake may have actually occurred along the fault segment that parallels the Santa Ana river (focal mechanism G in Fig. 2) rather than along the San Jacinto fault where it is presumed to be located [Laughlin *et al.*, 1923; Toppozada *et al.*, 1982]. If this earthquake did in fact occur along one of these secondary structures, then the northern section of the San Jacinto fault has not experienced a large earthquake since 1899, and so is more highly susceptible to an earthquake rupture in the near future.

Further east, between the Banning and Mission Creek faults, another set of earthquakes occur that also appear to exhibit left-lateral slip on north-east trending features (Fig. 3). These events align along sub-parallel trends that dip steeply to the south and agree quite well with the orientation of the north-east striking nodal plane seen in the composite focal mechanism solution. Slip along the *en echelon* northeast planes would be left-lateral, but with a larger component of reverse faulting. This type of deformation matches the long-term history of the Pinto Mountain and Morrango Valley faults with which these events align, and may indicate that slip along these features may have at one time extended across the Mission Creek fault. Such high-angle reverse faulting has been previously observed in the shallow surface sediments of San Gorgonio Pass [Allen, 1957], although most of the deformation more closely corresponds to slip along right-lateral strike-slip and shallow-angle thrust faults [Matti and Morton, 1983].

An interesting feature of all this seismicity is that those earthquakes exhibiting left-lateral slip on northeast trends all occur at depths less than ≈10 km (see cross section Fig. 3); suggesting that what ever mechanism is controlling this behavior, it is primarily restricted to shallow depths. Furthermore, if these left-lateral faults are the result of small crustal blocks that are currently rotating then this presupposes a detachment surface at depth, decoupling the blocks, and allowing rotational movement. Regional mid-crustal detachments or ductile shear zones have been suggested based on the occurrence of large earthquakes at depth with shallow-angle nodal planes [Webb and Kanamori, 1985], by the regional pattern of teleseismic travel-time residuals [Hadley and Kanamori, 1977], and by the finite elastic thickness of the upper crust [Turcott *et al.*, 1984]. If a detachment is present, then the possibility exists that the geology and/or the deformation observed at the surface is different from the deformation at depth.

In fact the microearthquakes below 10-12 km are distinctly different from those above. At greater depths, regional north-south shortening resulting from the collision of the San Jacinto Mountains with the San Bernardino Mountains, was found to be accommodated by a combination of strike-slip faults interbedded between a series of subparallel shallow-angle thrust faults dipping to the north (Fig. 4). Determinations of velocity structure from the earthquake arrival times also indicate a possible low-velocity layer at about 10 km depth under the San Bernardino Mountains but not under the San Jacinto Mountains [Nicholson and Simpson, 1985]. This is about the same depth as the transition between the block rotations and the deeper deformation, and suggests the overthrust San Bernardino Mountains are allochthonous. Regional gravity data and the distribution of P_g velocities also support this interpretation [Hearn and Clayton, 1984].

Geometric Properties of Rotating Block Systems and the Cycle of Great Earthquakes

The roles played by block rotations in the interseismic period and in the sequences of great earthquakes may be very pertinent to a earthquake prediction effort. The block/fault rotation model applied to interseismic deformation leads to the concept of time-dependent asperities and to repeat times for rupture that depend on the geometry of adjacent block systems.

Figure 17 illustrates a mechanism by which block rotation can play a direct role in determining the timing of failure on an adjacent master fault. The sketch at the top depicts a system of blocks in a fault zone just after the area has been destressed by major slip on the master fault. The regional faults bounding the blocks are characterized by a thick layer of highly fractured rock markedly weaker than the surrounding rocks (e.g., Feng and McEvilly, 1983; Stierman, 1984). In the interseismic period strike-slip displacement is primarily accomplished by block rotation. The secondary deformation caused by block rotation is concentrated in the weak fault zones bounding the blocks (middle sketch). The rotation raises stress across the fault zone increasing its strength (time-dependent asperities). When the main fault strand ruptures (bottom sketch) the blocks rotate back and partially recover the interseismic rotation, the rachet is disengaged and the system is ready to start the next cycle.

Figure 18 shows the possible evolution of stress and strength on the master fault during the cycle depicted in Figure 17. Shear stress and strength are low after the great eartquake. For some time thereafter blocks can easily rotate because the gouge zone they are impinging upon is weak. How rapidly shear stress and strength raise along the master fault probably depends on the mechanical properties of the gouge zone and on the geometry of the system. For the system to operate by stick-slip, strength has to raise faster than stress and remain higher for the interseismic period. Eventually the gouge zone will be compressed at the corners of the rotating blocks to the point where its resistence to further compression will drastically increase (i.e., when all the cracks are closed). Further strike-slip displacement will require the stress to increase rapidly and to rupture the master fault. A model for the interaction between block rotation and rupture on the master fault along the lines suggested in Figures 17 and 18 can be constructed incorporating constraints on the mechanical properties of fault zones and on the kinematics of rotating block systems.

Block rotations in southern California can be detected both from data that integrate deformation over geologic time and from data that detect short term deformation during the interseismic period between great earthquakes. While most of the deformation during a large earthquake on a master right-lateral fault is directly related to the slip on that fault, during the interseismic period much of the deformation seems to be related to slip on left lateral cross faults defining systems of rotating blocks. Some of this deformation may be permanent and contribute to the geologically detected rotations, some of it may be elastic and recovered during the large earthquakes on right lateral master faults. Active systems of rotating blocks typically occur between major strands of a fault zone where current seismicity is often concentrated. Right steps of the active master fault from one strand to another seem~~s~~ to be accommodated by rotating blocks between these strands in a structurally well documented case on the San Jacinto fault at the Coyote ridge and on a seismically well documented case on the Calveras fault for the Coyote Lake earthquake (1979). Block rotation may account for continuity in right lateral displacement across the step and for the required along-strike extension. These rotating block systems are predicted to achieve large rotations in short geologic times and to propagate along a fault zone increasing the length of an active strand at the expenses of another.

Rotating blocks are expected to interact with the adjacent active major strand by increasing normal stress across portions of this fault and locking it. These rotating blocks would generate time-dependent asperities. Elements such as the size of the blocks and the width and mechanical properties of the weak fractured zone along this fault may contribute to determine how long it will take for the shear stress along the fault to overide the ratchet effect of the blocks and to determine the repeat time for failure. Block rotation may play a critical role in the unstable (stick-slip) nature of fault slip.

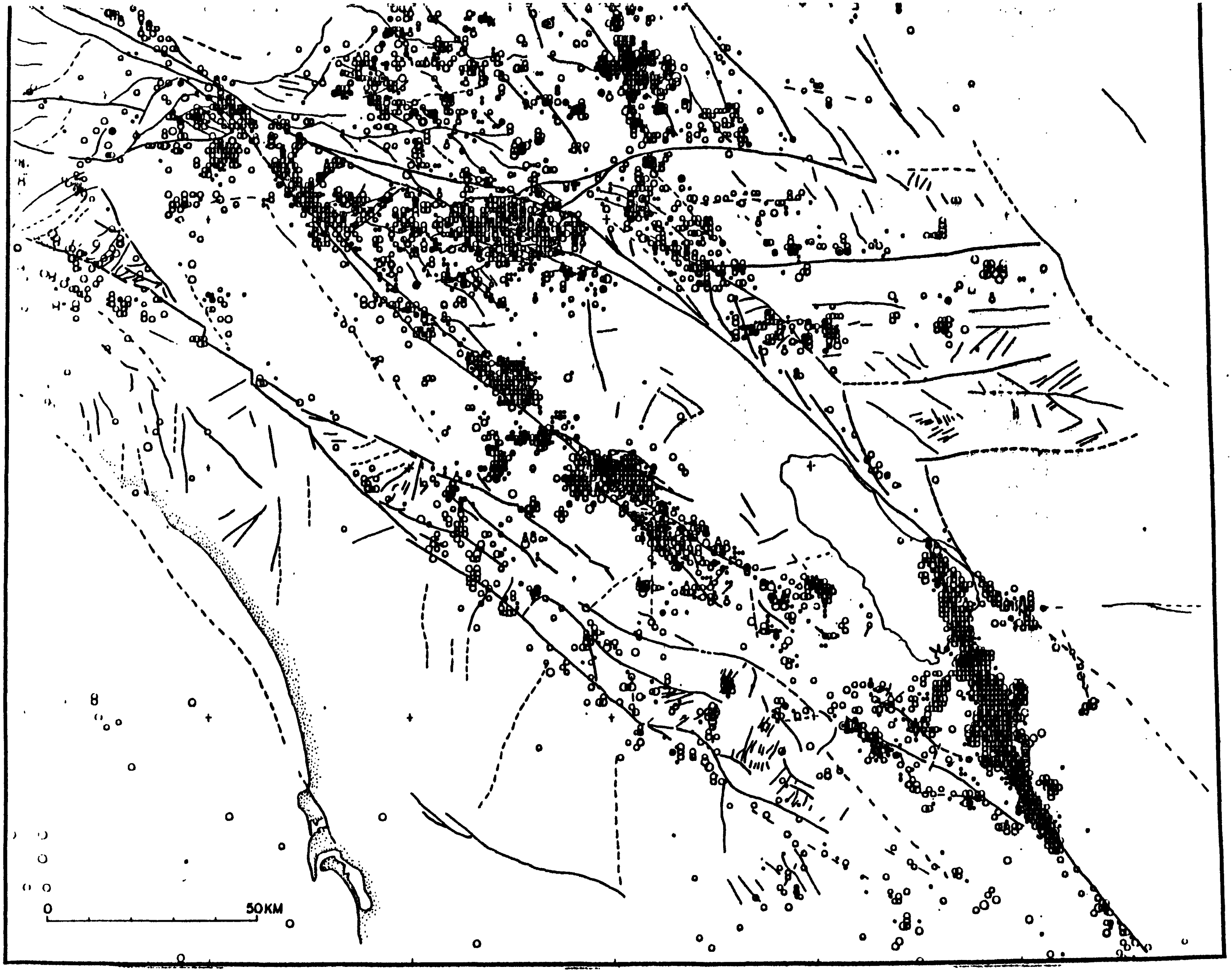

Fig. 1. Well-located 1975-83 hypocenters from the USGS/Caltech network and major faults from the 1:250,000 California Atlas.

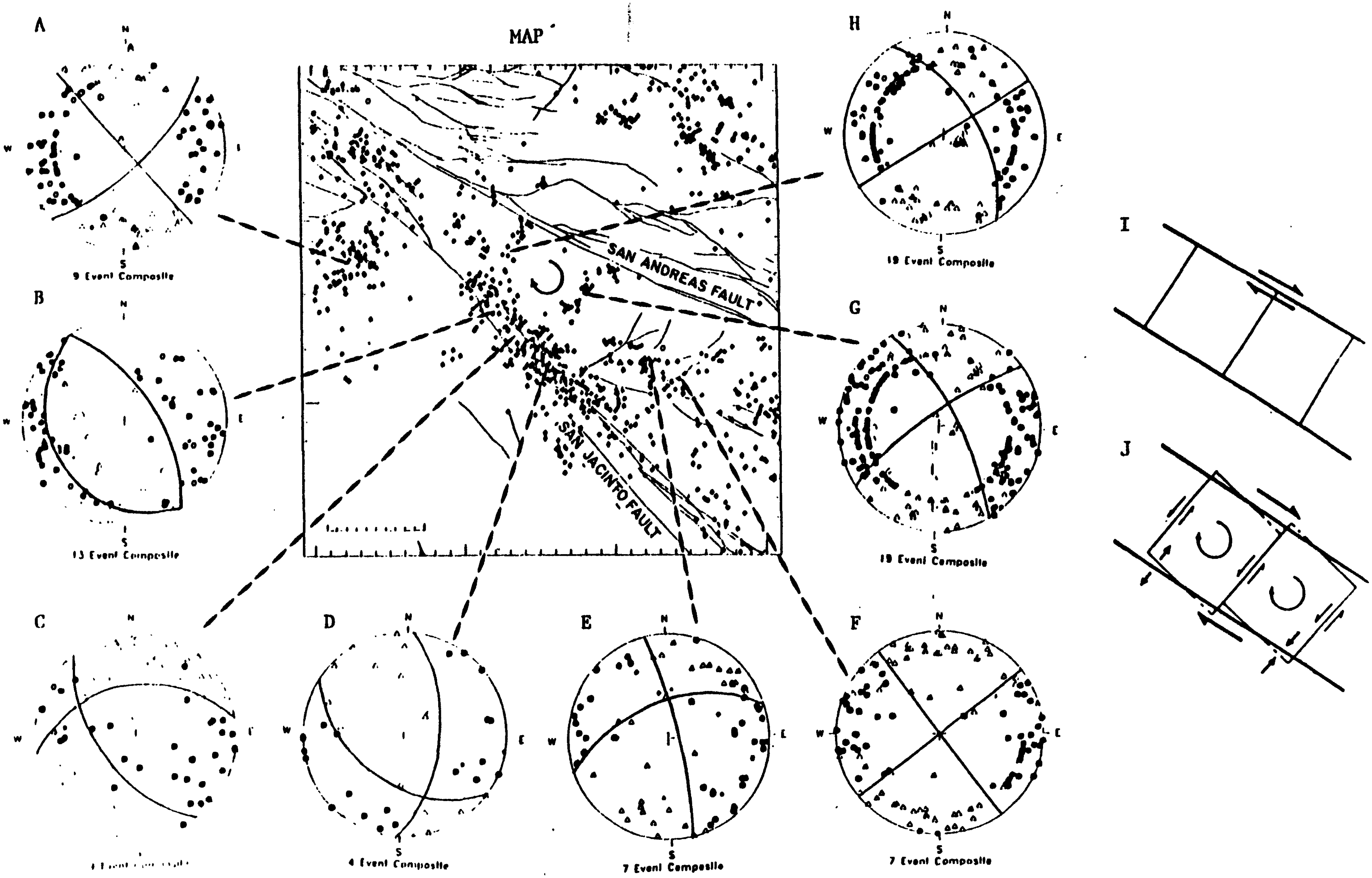
A
B
C
D
E
F
G
H
I
J
MAP
SAN ANDREAS FAULT
SAN JACINTO FAULT
N
S
W
E
9 Event Composite
13 Event Composite
4 Event Composite
7 Event Composite
7 Event Composite
19 Event Composite
19 Event Composite

Figure 2. Shallow seismicity used to define rotating blocks near the intersection of the San Andreas and San Jacinto faults - see map. During a large earthquake right-lateral strike-slip motion (I) occurs on one of the major bounding faults; however, during the inter-seismic period, the major faults become locked causing small blocks in between to rotate (J). This produces a pattern of northeast striking left-lateral faults (E-H), between which alternating groups of normal (B&D), and reverse (C) faulting earthquakes occur that match the particular pattern predicted by the model (compare J with map). Focal mechanism diagrams (A-H) are composite upper hemisphere projections; solid symbols are compressions, open symbols are dilatations. Composite A (upper left) represents a set of sub-parallel left-lateral faults previously identified by Hadley and Combs (1974).

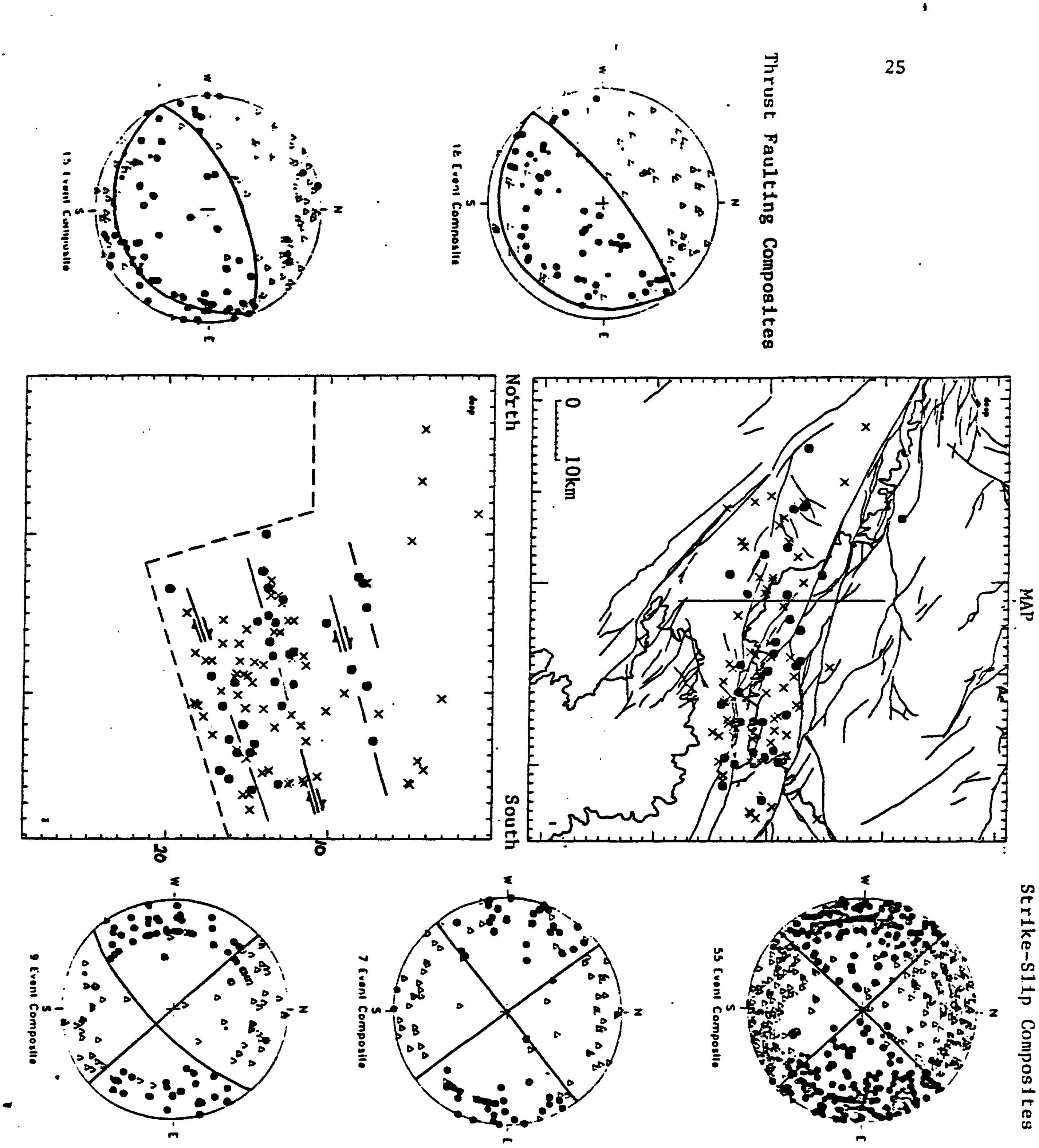
Thrust Faulting Composites
16 Event Composite
13 Event Composite
MAP
0
10km
North
South
10
20
Strike-Slip Composites
55 Event Composite
7 Event Composite
9 Event Composite
N
S
E
W

Figure 4. Map and cross section of the predominately deeper strike-slip (X's) and shallow-angle thrust events (solid circles) near San Gorgonio Pass. The thrust earthquakes define a series of planes that dip to the north and parallel the shallow-dipping interface that defines the base of the seismogenic zone (dashed line) and match the shallow-angle nodal plane seen in the composite focal mechanisms shown at left. The seismicity shows a wedge-shaped volume internally deforming as a result of north-south shortening between the San Bernardino Mts to the north and the San Jacinto Mts to the south. Contours are elevations above 3,000 feet.

fig. 7

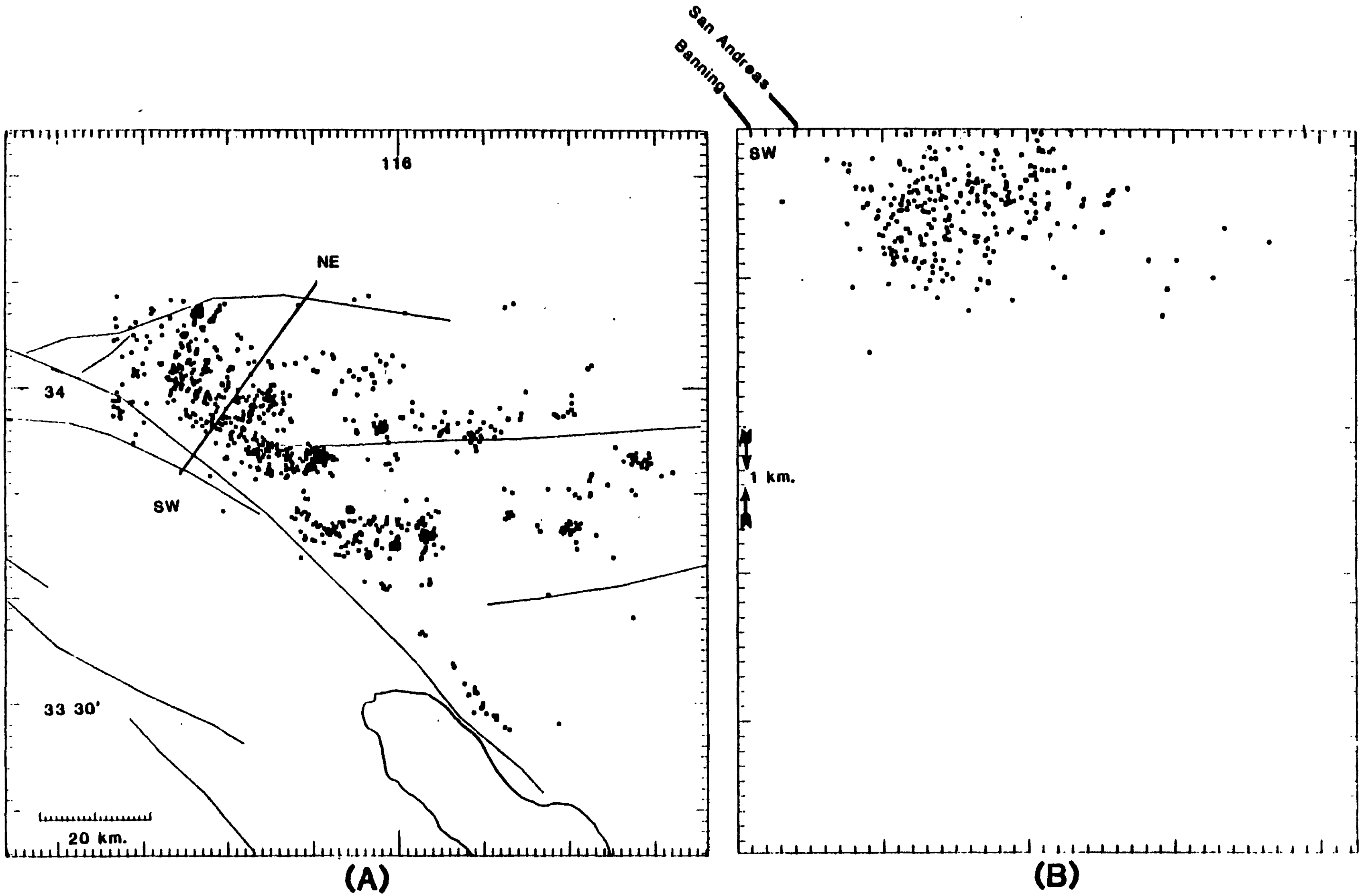
San Andreas
Banning
116
NE
SW
34
33 30'
20 km.
SW
1 km.
(A)
(B)

Figure 5. a) Map of well located earthquakes in the eastern Transverse Ranges for the years 1975-1983. Earthquakes selected are those south of the Pinto Mtn. fault. Note systematic offset of the earthquakes.
b) Vertical cross-section of the earthquakes 10 km to either side of the projected line shown in a). Tick marks are 1 km intervals.

fig. ~~12~~ /

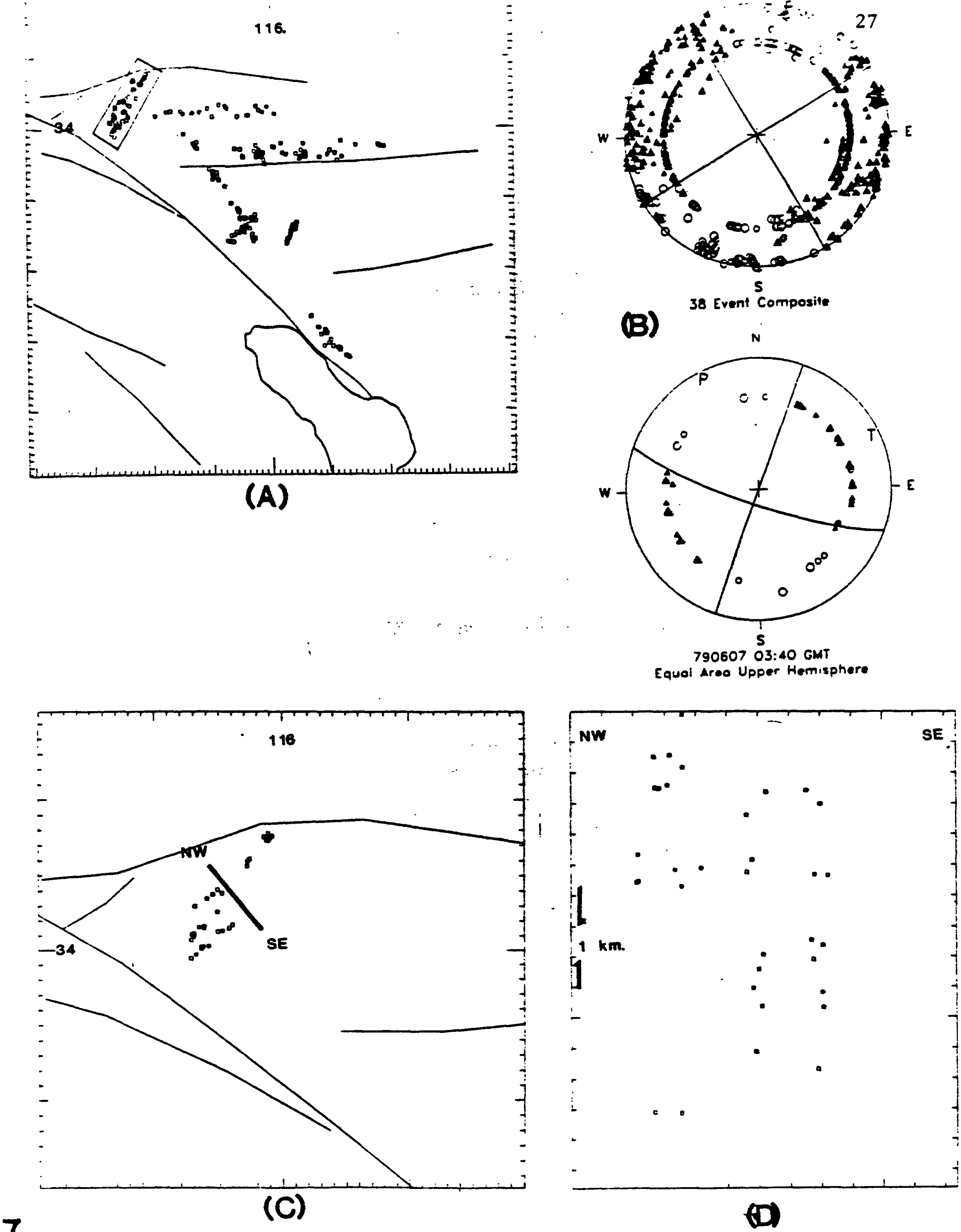
116
34
(A)
W
E
S
38 Event Composite
(B)
N
P
T
W
E
S
790607 03:40 GMT
Equal Area Upper Hemisphere
116
NW
SE
34
(C)
NW
SE
1 km.
(D)

Figure ~~12~~ 7. (a) A well defined NE lineation of seismicity. This group divides the aftershocks of the 1947 Morongo Valley earthquake from the 1948 Desert Hot Springs event.

(b) Dominant focal mechanism exhibiting strike-slip motion on NE and SW nodal planes.

(c) Locations of earthquakes shown in (b). In detail, the earthquakes define an en echelon set of structures.

(d) Cross-section of events shown in (c).

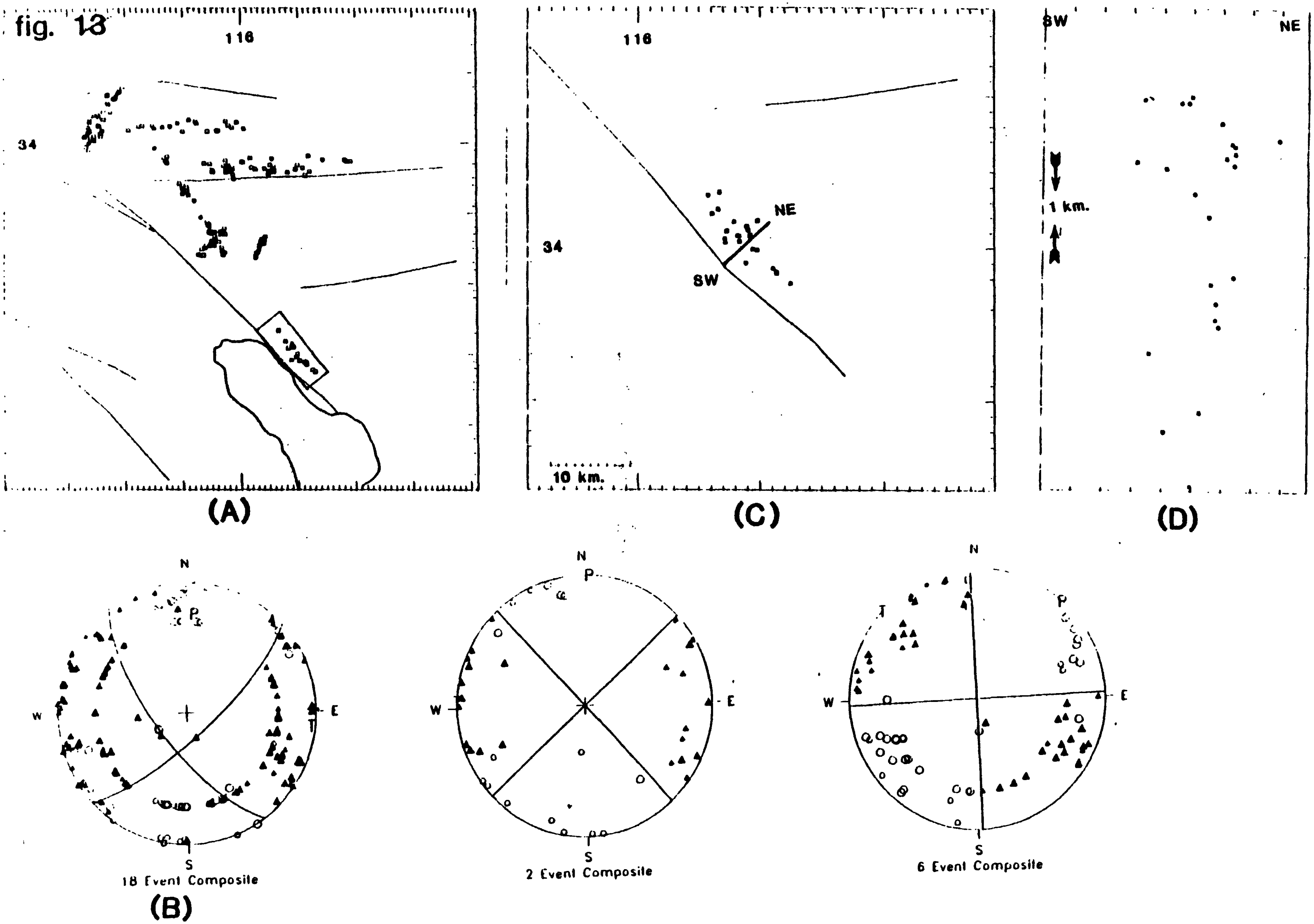
fig. ~~13~~
116
34
(A)
116
34
NE
SW
10 km.
(C)
SW
NE
1 km.
(D)
N
P
T
W
E
S
18 Event Composite
(B)
N
P
W
E
S
2 Event Composite
N
T
P
W
E
S
6 Event Composite

Figure ~~13~~ 8. a) A group of earthquakes close to the San Andreas fault and located northeast of the Salton Sea.
b) Dominant focal mechanism is consistent with right-lateral slip on a NW striking fault plane that dips steeply to the NE. Other focal mechanisms appear to show activity on secondary structures.
c) Locations of the earthquakes used in the dominant focal mechanism shown in b).

APPENDIX A. 3.

Depth of Seismicity and its Relationship to Heat Flow and Large Earthquake Potential

Hiroo Kanamori

Depth of Seismicity in the Imperial Valley Region (1977-1983) and its Relationship to Heatflow, Crustal Structure, and the October 15, 1979 Earthquake

Diane I. Doser and Hiroo Kanamori

Seismological Laboratory, California Institute of Technology, Pasadena, CA 91125

Focal depths from over 1000 earthquakes occuring between 1977 and 1983 in the Imperial Valley-southern Peninsular Ranges are used to study relationships between the depths of seismicity, heat flow, and crustal structure. Earthquakes used in this study are relocated A- and B-quality events from the Caltech catalog that are carefully selected to insure focal depth precision of ± 2 km.

All relocated earthquakes are shown in Figure 1. The size of the symbols in this and following figures reflects distance from the earthquakes to the nearest station. A cross section along the strike of the San Jacinto fault (A-A') is shown in Figure 4. The majority of shallow seismicity lies in the Brawley Seismic Zone. Seismicity in the Imperial Valley outside this zone is diffuse and does not appear to concentrate along mapped surface faults. The concentration of seismicity along distinct segments of the San Jacinto fault and the Anza seismic gap are also visible.

A plot of earthquakes deeper than 10 km (Figure 2) shows that the deeper events in the Imperial Valley are located at the nothern end of the Imperial fault. Little seismicity occurs at depths greater than 10 km along the Coyote Creek-San Jacinto fault system or the northern end of the Brawley Seismic Zone. The majority of deeper seismicity is concentrated along the San Jacinto-Buck Ridge and San Jacinto-Hot Springs fault systems.

Local and regional heat flow in the study area [Lachenbruch et al., 1985] is also compared to earthquakes deeper than 10 km in Figure 2. Most of the Imperial Valley lies within the 100 mW/m^2 heatflow contour. The only area where deeper earthquakes lie within a region with heatflow greater than 200 mW/m^2 is in the Brawley geothermal area (Figure 2). Earthquakes at depths of 8 to 9 km have been observed within 1 to 2 km of the Salton Sea geothermal area (Figure 2) [Gilpin and Lee, 1978], the largest and hottest geothermal area in the Imperial Valley [Renner et al. 1975], suggesting that deeper earthquakes occuring near the edges of a geothermal area may not be uncommon. The deepest seismicity in Imperial Valley correlates with a heatflow low to the south of the Brawley geothermal area. Sass et al.[1984] believe that convective systems in the valley extend to depths of at least 2 km, however it is difficult to determine whether the correlation between the heatflow low and the deep seismicity is coincidental or signifies a deep convective system. The deepest seismicity is also located within the region where Fuis et al. [1982] have evidence for a dome on the subbasement.

Rheologic modeling was used to study the effects of the heatflow low and the subbasement high on the depth to the brittle/ductile transition zone in this region. Although uncertainties in model parameters may change the transition zone depth by several kilometers, the modeling does suggest that the subbasement high alone could depress the depth of the brittle/ductile transition, and that the heatflow low need not be invoked to explain the deeper seismicity.

Earthquakes deeper than 12.5 km are shown in Figure 3. Only 5 earthquakes in the Imperial Valley region occur at this depth and all are located at the northern end of the Imperial fault. The deepest earthquakes in this group occurred at a depth of 13.2 km. A cluster of activity occurs along the San Jacinto-Hot Springs fault system as well as diffuse seismicity along the Elsinore fault. The deepest earthquakes in the Peninsular Ranges occurred at a depth of 16.7 km along the San Jacinto fault northwest of the Anza Gap.

Variations in focal depth across the study area are shown in a cross-section taken along the strike of the San Jacinto fault (Figure 4). Earthquakes located up to 10 km from the cross-section line have been plotted. The deepest earthquakes in the section occur along the northwest end of the cross section with an average depth of 13 km. This correlates with the region with heatflow ≤ 60 mW/m^2 shown in Figure 2. There is a marked shallowing of seismicity south of the northwest end of the Anza Gap to an average depth of 10 km where the heatflow increases to 80 mW/m^2. (Earthquakes shown in the Anza Gap in Figure 4 do not occur along the San Jacinto fault, but are located 2 to 5 km southeast of the surface trace of the fault.) Approaching the Imperial Valley the seismicity shallows to a maximum depth of 10 km as the heatflow reaches 100 mW/m^2. An abrupt increase in depth occurs 10 km northwest of the Brawley fault in an 8 to 10 km wide zone at the northern end of the Imperial fault. This correlates with the heatflow low and subbasement high mentioned previously. This suggests that slip at depth in the Imperial Valley is confined to this narrow band along the Imperial and Brawley faults. The apparent vertical trends of seismicity shown in Figure 4 are an artifact of the scaling used in the cross-section. Cross-sections drawn at larger scales do not exhibit the lineations. Plots of the distribution of earthquakes versus depth show a peak at 7 km for the Imperial Valley region (the region east of the 1968 Borrego Mountain earthquake)and a peak at 11 km for the Southern Peninsular Ranges.

Cross-sections of relocated seismicity along the trace of the Imperial fault for the pre-mainshock, aftershock and post-1979 time periods are shown in Figure 5. Note that point DL on the figures represents the southern limit of earthquakes that could be adequately located with the existing seismic network. The location of the 1979 mainshock hypocenter, the U.S.-Mexican border, and the ends of the surface rupture are shown for reference. Since the southern end of the surface rupture and the mainshock hypocenter are south of point DL, no earthquake relocations are available to study seismic behavior in these regions. The northern end of the surface rupture occurs in the area of deepest seismicity along the Imperial fault, and is also located near the northern end of the subbasement high detected by Fuis et al. [1982]. The southern end of the dome probably is located 3 to 5 km south of the intersection of the Brawley and Imperial faults. It is interesting to note that the region near the southern end of the dome is the region where the Imperial fault undergoes a transition from stick-slip behavior to the southeast to aseismic fault creep to the northwest [Reilinger, 1984].

The frequency-depth distributions for all earthquakes occurring in the Imperial Valley during these three time periods show that aftershocks within the first two months of the mainshock were 2 to 3 km deeper than pre-October 1979 or post-December 1979 earthquakes. This suggests that the immediate afershocks may have served to readjust strain at the base of the seismogenic zone.

Strike-slip offsets of ≥ 1 m from the faulting models of Archuleta [1984] and Hartzell and Heaton [1983] are shown in Figure 5. Both models show large patches of slip along the fault just south of the intersection of the fault with the Brawley fault. Smaller patches of slip are present to the north of this intersection and near the hypocenters in Archuleta's model. The major difference between the models is the depth of the slip zone. Hartzell and Heaton's model shows slip between depths of 6 and 10 km with slip $\geq$ 1.4 m concentrated between 6 and 8 km. Comparison of this model with relocated earthquakes indicates that few earthquakes from 1977 to 1983 occurred in this region of high slip. This would suggest that this portion of the fault slipped only during the mainshock. Archuleta's model, however, shows maximum slip concentrated between 8 and 13 km in depth. Prior to the 1979 earthquake a large number of earthquakes occurred along this part of the fault. Aftershocks occurred in a small cluster within the region of high slip, but not within the region of maximum slip. From 1980-1983 there have been few earthquakes along the Imperial fault south of the Brawley fault. The northern ends of the areas of maximum slip lie near the intersection of the Brawley fault and the edge of the subbasement high, suggesting that both structures may arrest faulting to the northwest.

A relocation of the 1940 (M_S=7.1) Imperial Valley earthquake suggests that the earthquake began north of the main patch of slip during the 1979 mainshock and south of the region of deep seismicity associated with the subbasement high. The location nearly coincides with the small northernmost patch of slip from Archuleta's [1984] model and surface displacements north of the border for both earthquakes were also similar [Sharp, 1982]. These observations suggest that the rupture began just to the north of the portion of the fault where maximum slip occurred in 1979, and that the initial event of the mainshock sequence may have ruptured the same portion of the fault that ruptured in 1979.

References

Archuleta, R. J., Hypocenter for the 1979 Imperial Valley earthquake, *Geophys. Res. Lett.*, *9*, 625-628, 1982.

Archuleta, R. J., A faulting model for the 1979 Imperial Valley earthquake, *J. Geophys. Res.*, *89*, 4559-4585, 1984.

Fuis, G. S., W. D. Mooney, J. H. Healy, G. A. McMechan, and W. J. Lutter, Crustal structure of the Imperial Valley region in The Imperial Valley, California Earthquake of October 15, 1979, *U. S. Geol. Survey Prof. Paper, 1254*, 25-49, 1982.

Gilpin, B. and T-C Lee, A microearthquake study in the Salton Sea geothermal area, California, *Bull. Seism. Soc. Amer.*, *68*, 441-450, 1978.

Hartzell, S. H. and T. H. Heaton, Inversion of strong ground motion and teleseismic waveform data for the fault rupture history of the 1979 Imperial Valley, California, earthquake, *Bull. Seism. Soc. Amer.*, *73*, 1553-1584, 1983.

Reilinger, R., Coseismic and postseismic vertical movements associated with the 1940 M7.1 Imperial Valley, California earthquake, *J. Geophys. Res.*, *89*, 4531-4538, 1984.

Renner, J. L., D. E. White, and D. L. Williams, Hydrothermal convection systems, in Assessment of geothermal resources of the United States-1975, D. E. White and D. L. Williams, eds., *U. S. Geol. Surv. Circular, 720*, 5-57, 1975.

Sass, J. H., S. P. Galanis, Jr., A. H. Lachenbruch, B. V. Marshall, and R. J. Munroe, Temperature, thermal conductivity, heatflow and radiogenic heat production from unconsolidated sediments of the Imperial Valley, California, *U. S. Geol. Surv. Open-File Rept. 84-490*, 1984.

Sharp, R. V., Comparison of 1979 surface faulting with earlier displacements in the Imperial Valley, in the Imperial Valley, California, Earthquake of October 15, 1979, *U. S. Geol. Surv. Prof. Paper, 1254*, 213-221, 1982.

Sharp, R. V., J. J. Lienkaemper, M. G. Bonilla, D. B. Burke, B. F. Fox, D. G. Herd, D. M. Miller, D. M. Morton, D. J. Ponti, M. J. Rymer, J. C. Tinsley, J. C. Yount, J. E. Kahle, E. W. Hart, and K. E. Sieh, Surface faulting in the central Imperial Valley, The Imperial Valley, California, Earthquake, October 15, 1979, *U. S. Geol. Surv. Prof. Paper, 1254*, 119-144, 1982.

Figure Captions

Figure 1. All relocated earthquakes in study area. The type of symbol reflects the quality of location. X's are earthquakes with distance to the nearest station (dmin)$\leq$hypocenter depth, +'s are earthquakes with depth$<$dmin$\leq$1.5 x depth. A-A' is the location of the cross-section shown in Figure 4. The stars denote $M_L>5.5$ earthquakes occurring in the region during the last 20 years and include the Borrego Mountain (1968), Coyote Mountain (1969), and Imperial Valley (1979) earthquakes. The fault abbreviations used in this figure and following figures are: BF=Brawley fault, BRF=Buck Ridge fault, CCF=Coyote Creek fault, EF=Elsinore fault, HSF=Hot Springs fault, IF=Imperial fault, LSF=Laguna Salada fault, SAF=San Andreas fault, SHF=Superstition Hills fault, SJF=San Jacinto fault, SMF=Superstition Mountain fault, and BSZ=Brawley Seismic Zone.

Figure 2. Relocated earthquakes deeper than 10 km and regional heatflow [Lachenbruch et al., 1985] in the study area. The vertical stripes denote regions with heatflow $<$100mW/m^2, the ~~horizontal stripes regions with heatflow $>$200mW/m^2. The letters associated with the dots are~~ abbreviations for geothermal areas. B=Brawley, EB=East Brawley, EM=East Mesa, H=Heber, S=Salton Sea, and W=Westmorland.

Figure 3. Relocated earthquakes deeper than 12.5 km. The box between Brawley and El Centro denotes the possible location of a subbasement dome as discussed by Fuis et al. [1982].

Figure 4. Cross section of earthquakes along A-A'. The cross-section follows the strike of the San Jacinto fault. (See Figure 1 for location) Apparent lineations in the seismicity are a results of the scaling used in plotting and are not seen in larger scale plots of the same region.

Figure 5. Cross-sections of seismicity along the strike of the Imperial fault for the three time periods indicated. The large black dot is the hypocenter for the October 15, 1979 mainshock [Archuleta, 1982]. The vertical dashed line is the U.S.-Mexican border. E denotes the ends of the surface faulting observed during the mainshock [Sharp et al., 1982], B the intersection of the Brawley fault with the Imperial fault, and DL the limit for accurately determining focal depths using the Caltech network. The regions of the fault outlined by solid and dashed lines represent strike-slip offsets of $\geq$ 1 m from the faulting models of Hartzell and Heaton [1983] and Archuleta [1984].

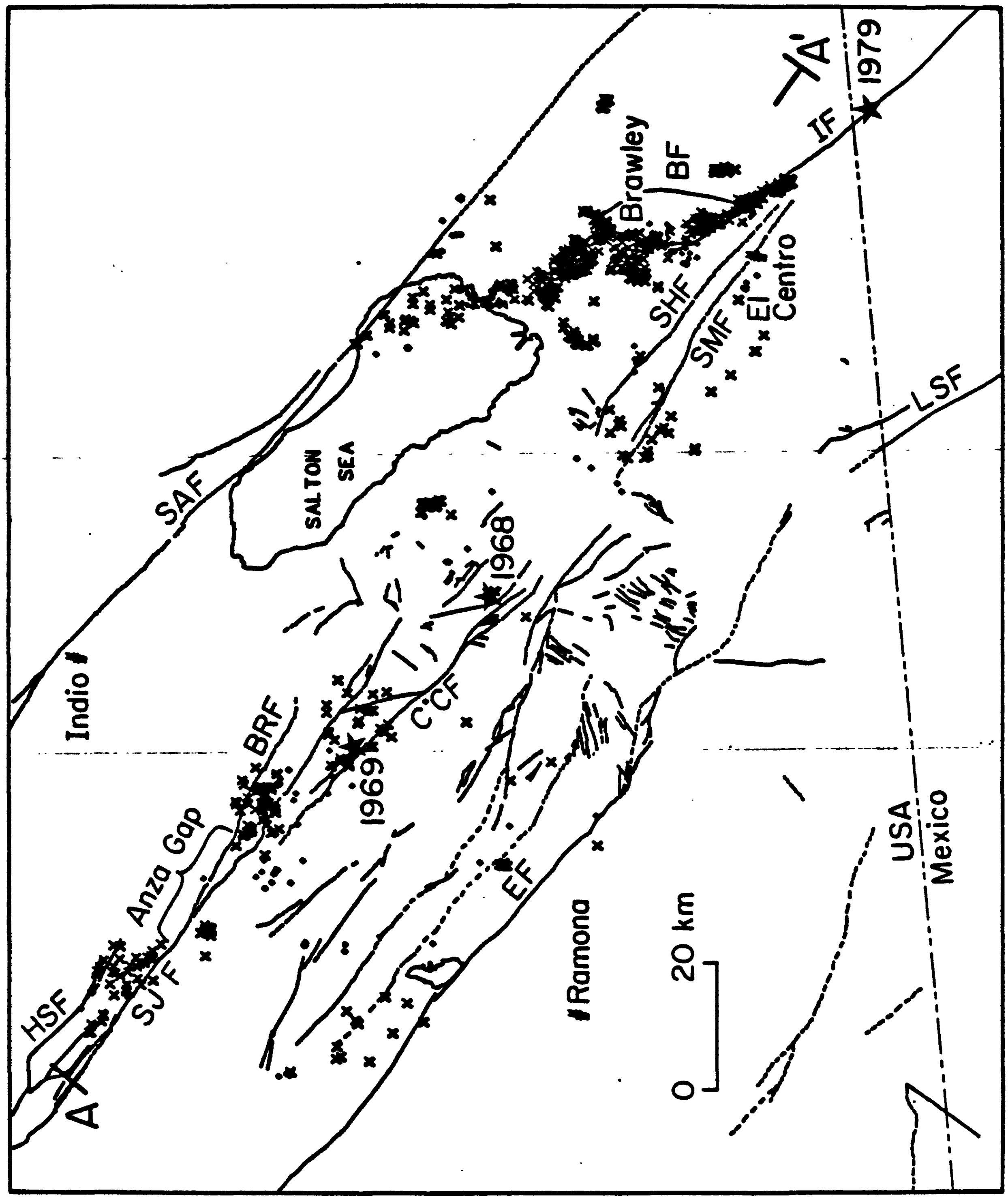
A
HSF
SJF
Anza Gap
BRF
Indio
1969
CCF
EF
Ramona
0
20 km
SAF
SALTON SEA
1968
USA
Mexico
LSF
SMF
SHF
El Centro
Brawley
BF
IF
1979
A'

Figure 1

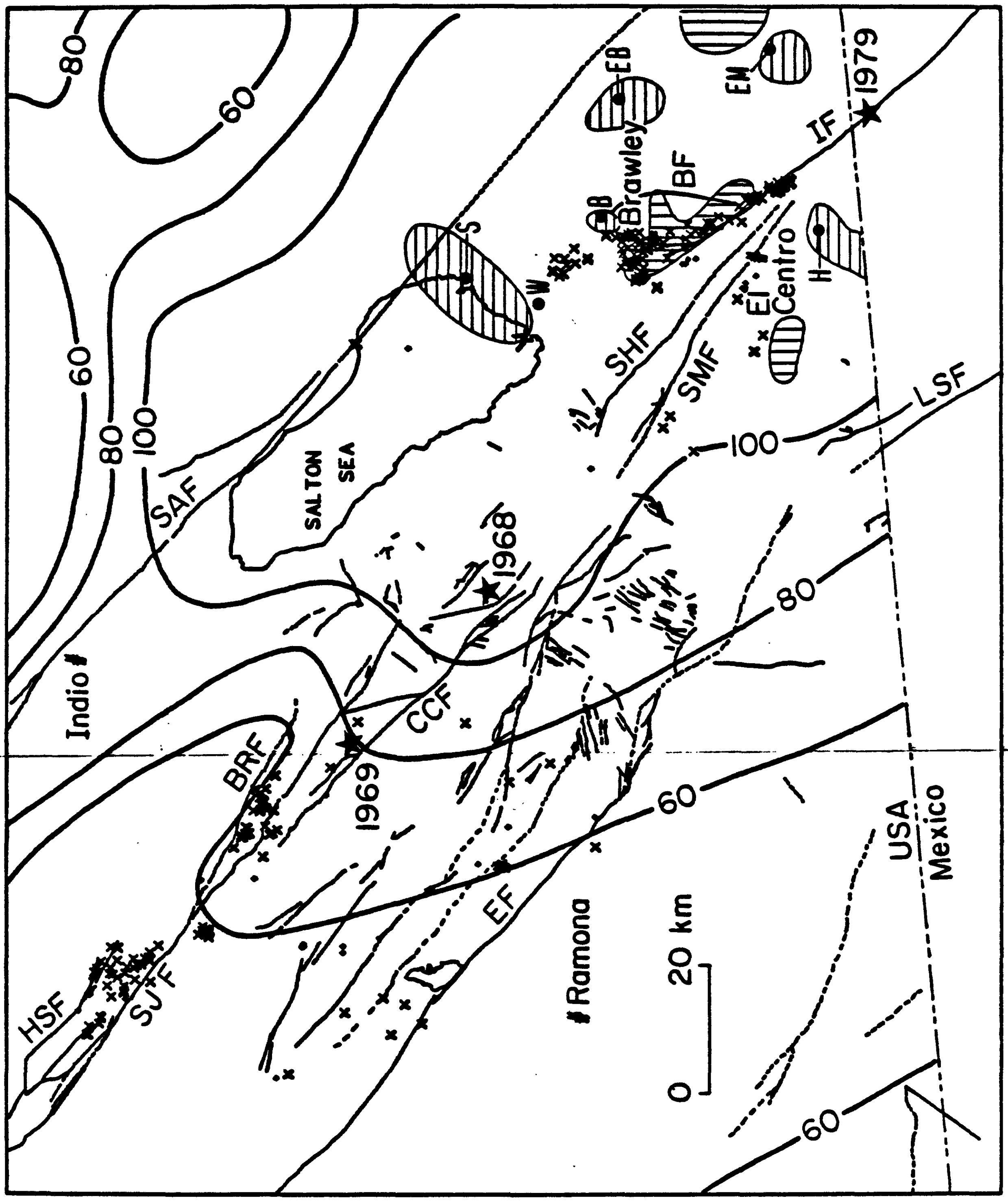
80
60
60
80
100
SAF
Indio
HSF
SJF
BRF
1969
CCF
EF
Ramona
0
20 km
USA
Mexico
60
80
100
60
SALTON
SEA
1968
S
W
B
Brawley
EB
BF
EM
IF
1979
SHF
SMF
El Centro
H
LSF

Figure 2

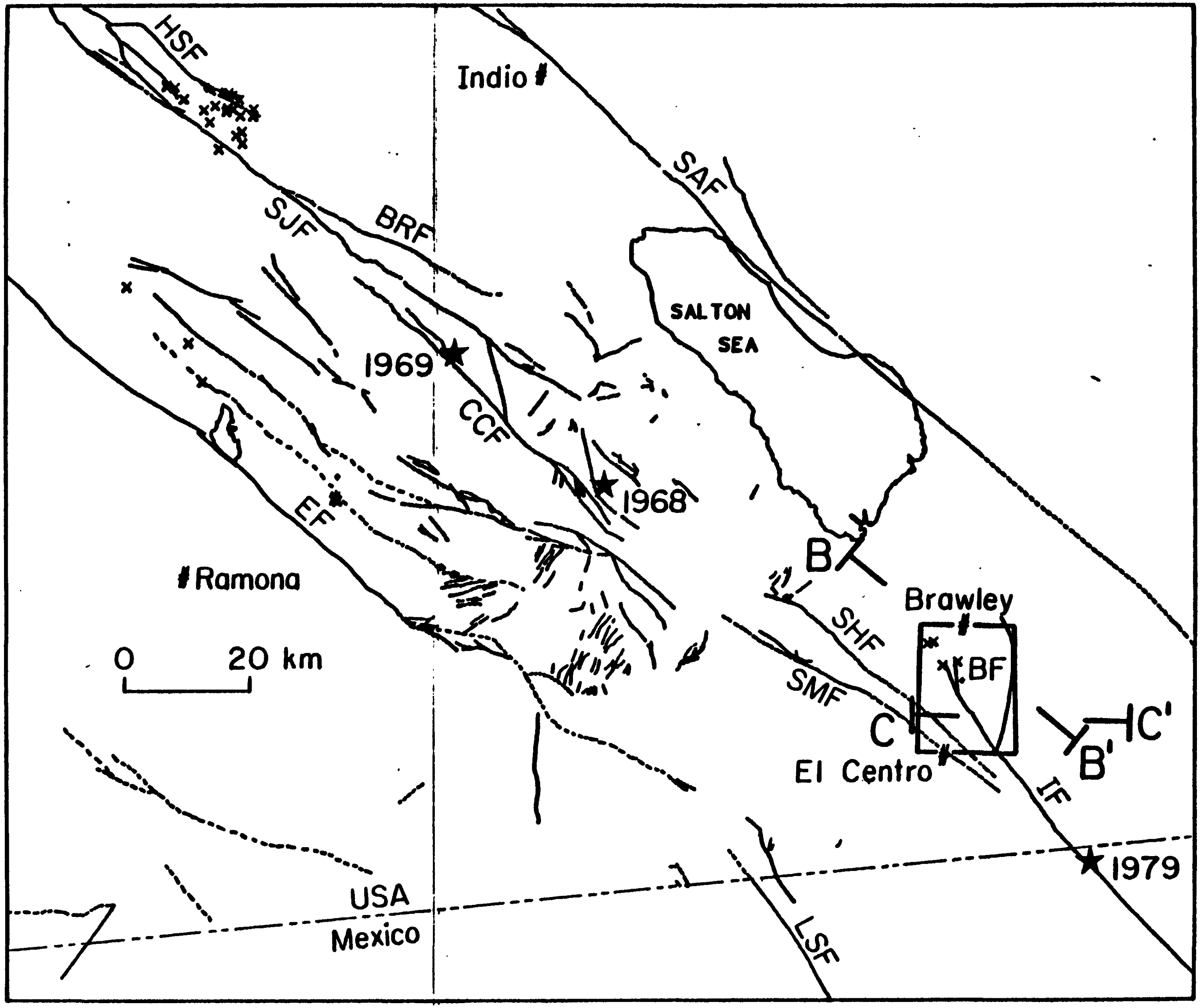
HSF
Indio
SAF
SJF
BRF
SALTON
SEA
1969
CCF
1968
EF
Ramona
B
Brawley
SHF
BF
0
20 km
SMF
C
C'
B'
El Centro
IF
1979
USA
Mexico
LSF

Figure 3

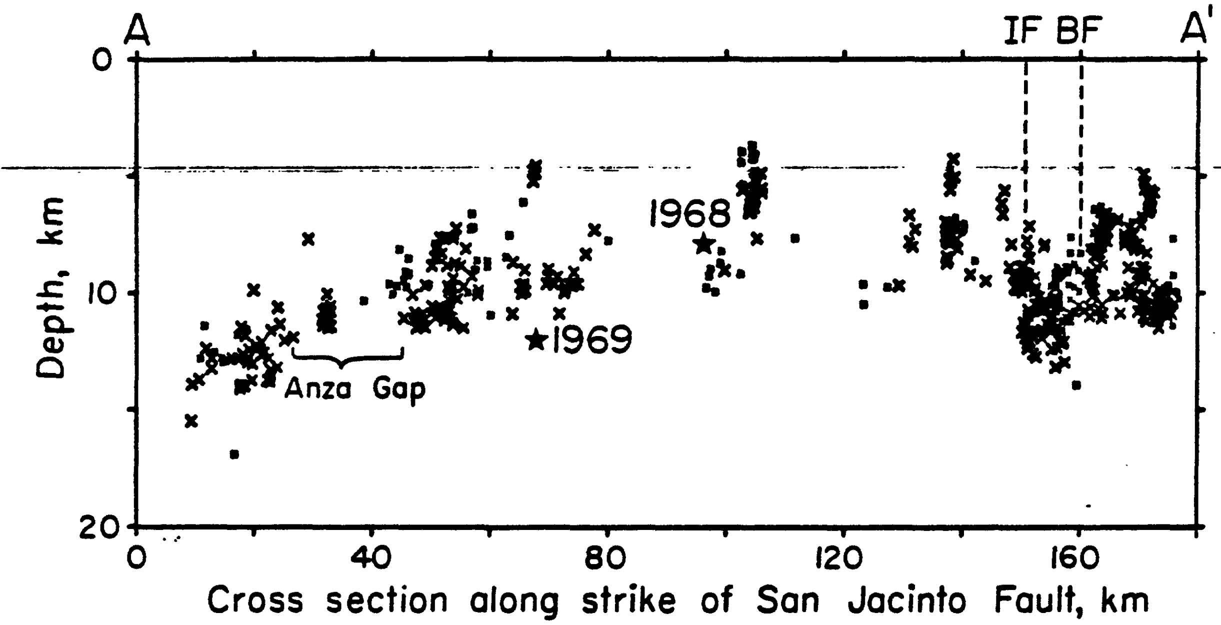
A
IF
BF
A'
0
10
20
Depth, km
1968
1969
Anza Gap
0
40
80
120
160
Cross section along strike of San Jacinto Fault, km

Figure 4

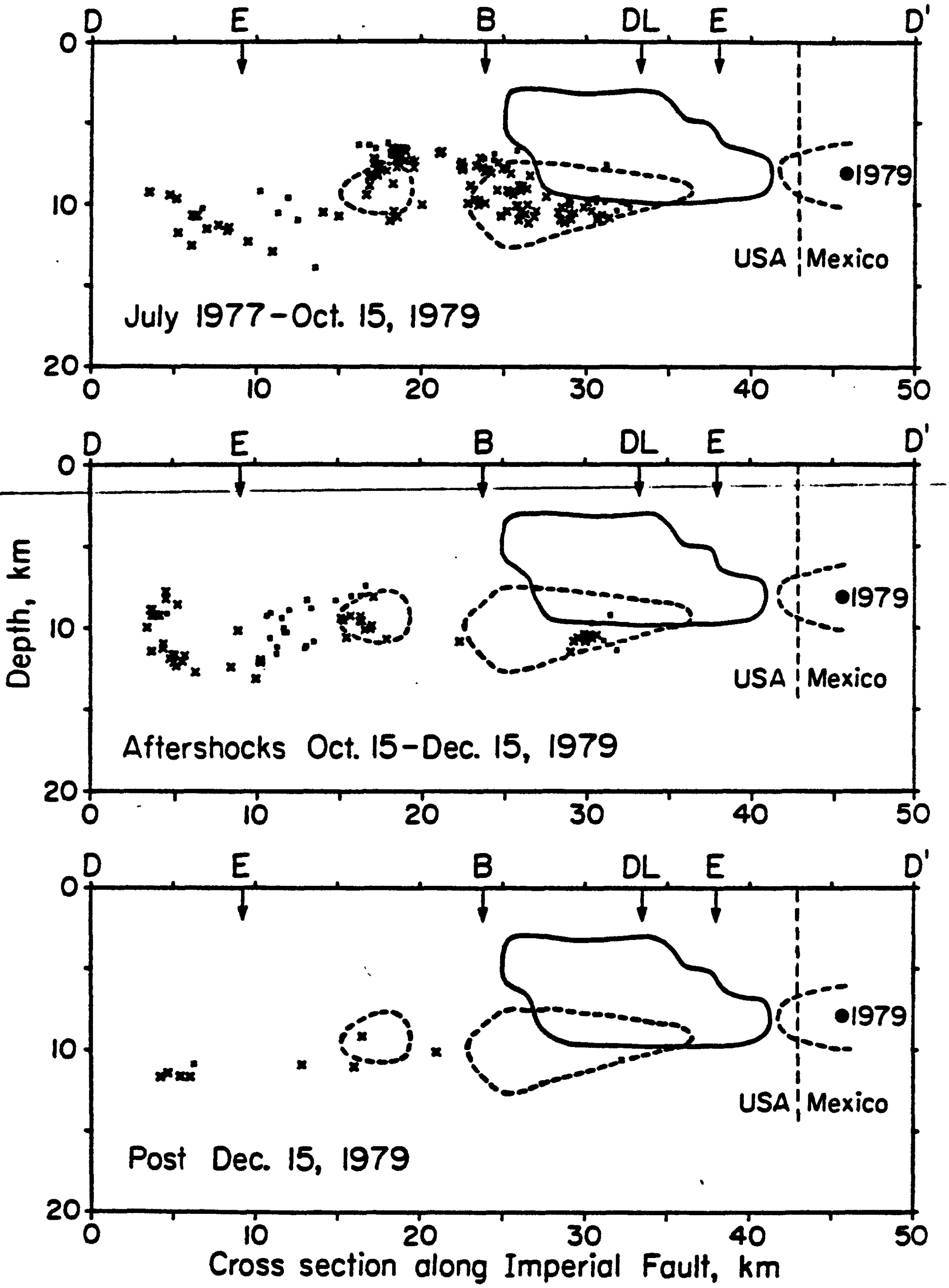
D
E
B
DL
E
D'
0
10
20
30
40
50
●1979
USA
Mexico
July 1977-Oct. 15, 1979
Aftershocks Oct. 15-Dec. 15, 1979
Post Dec. 15, 1979
Depth, km
Cross section along Imperial Fault, km

Figure 5

Depth Distribution of Seismicity Along the San Jacinto Fault Zone and the Relation to Large Earthquake Potential

Chris Sanders and Hiroo Kanamori

Seismological Laboratory, California Institute of Technology, Pasadena, CA 91125

Recent cross-section plots of well determined hypocenters of earthquakes located along the San Jacinto fault zone during the years 1980-1984 reveal new information about the depth distribution of earthquakes along this major strike slip fault zone. Several first order features are apparent:

1. The bottom of the seismogenic zone changes in depth along strike and becomes shallower nearer to the Imperial Valley region of high heat flow.

2. In general, seismicity is concentrated in a band along the bottom of the seismogenic zone, with very little seismicity occurring on the shallower portions of the fault. This is true whether the base of the seismogenic zone lies at 20 or 10 km depth.

3. Along strike, clusters of activity are separated by relatively quiet segments. The clusters are located at the ends of the rupture zones of the largest historic earthquakes (1899-1918, 1954, 1968 had large moments) or coincident with the rupture zones of the smaller large historic earthquakes (1923 and 1937 had small moments). The quietest sections, except for the Anza seismic gap, are coincident with the rupture zones of the largest historic earthquakes.

The first observation indicates that the maximum depth of the seismogenic zone along different sections of the San Jacinto fault zone can vary by as much as a factor of two. This may affect the repeat time of large earthquakes along different fault segments and also the observability of strain related phenomenon at the surface before large earthquakes.

An interpretation of the last two observations is that the quiescent segments of the fault are locked, including the upper 8-12 km of most of the fault zone. That most seismicity occurs at the base of the seismogenic zone and not above suggests that the deeper parts of the fault are under higher shear stresses than the shallower parts. This implies that seismological precursors to future large events might be found near the base of the brittle fault zone. The seismicity in the two years preceding the 1979 Imperial Valley earthquake occurred directly below the asperity which showed the largest displacement during the M_L 6.6 event (Doser and Kanamori, in prep.). The deep seismicity seems to have been indicating the high stresses present along that stretch of the Imperial fault.

In this light we can examine the most apparent seismicity gap along the San Jacinto fault zone, the Anza seismic gap. This 20 km long fault segment has very little seismicity in it at any depth. The lack of seismicity at all depths may be due to high fault-normal compressive stresses caused by the convergence of several active strands of the fault zone to only one strand near Anza. These high normal stresses increase the strength of the fault locally effectively shutting off minor seismicity even in the deeper parts of the fault zone. The greatest concentrations of seismicity in the San Jacinto fault zone occur on either end of the Anza seismic gap. These may be indicating high shear stresses on the faults in the immediate vicinity of the gap. This segment of the fault zone has not ruptured in a large earthquake since at least 1892. Since seismic slip is accumulating at a rate of about 1 cm/yr the potential seismogenic slip on this fault segment must now be about 100 cm or more.

The 60 km section of fault to the northwest of the Anza gap is also relatively aseismic in its upper 12 km and presumably is locked above this depth. This section of fault ruptured during large earthquakes in 1899 (M 7) and 1918 (M_L 6.8). The accumulated potential slip on this fault zone section is now about 60-80 cm.

If an asperity eventually breaks near the Anza gap resulting in a large earthquake the possibility exists for the rupture to propagate northwest many tens of km resulting in a much larger earthquake of around M 7.

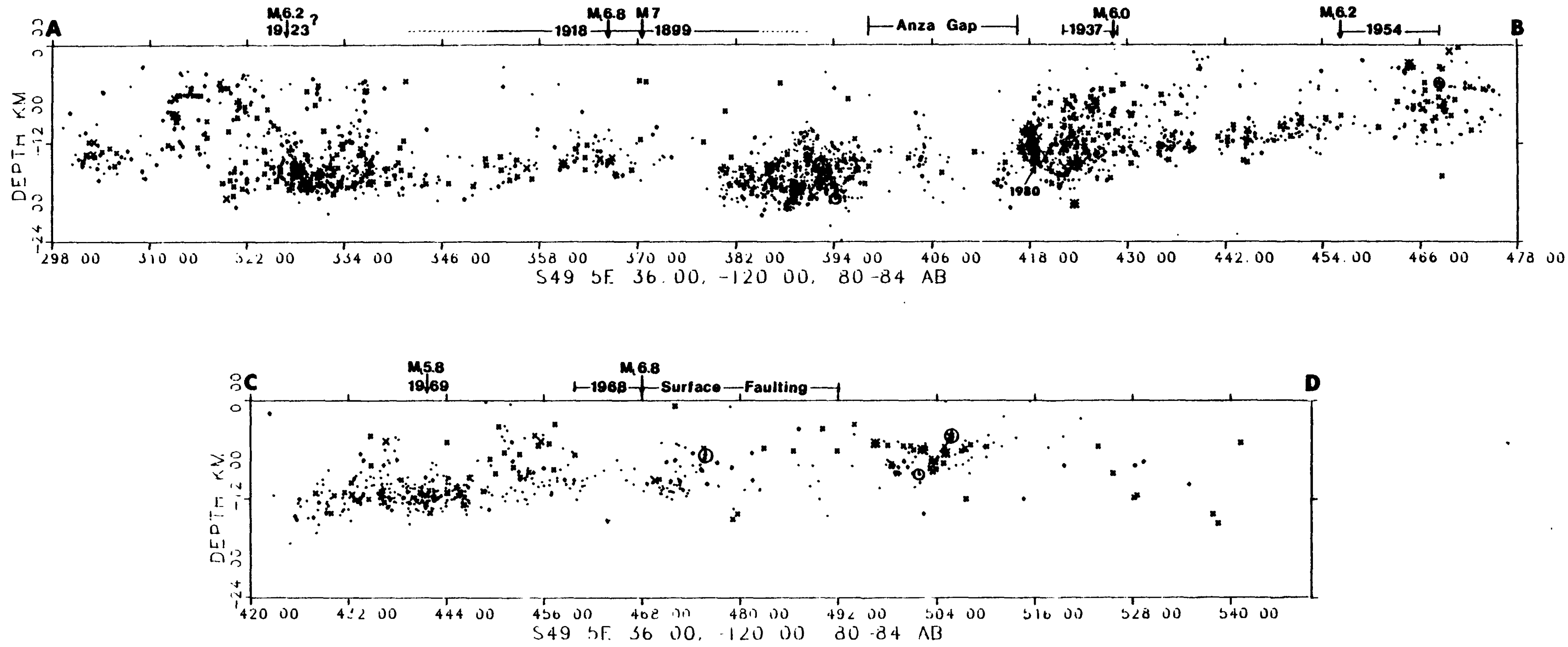

Figure 1. Vertical cross sections A-B along the San Jacinto fault and C-D along the Coyote Creek and Superstition Mountain faults. No vertical exaggeration. These are all of the earthquakes of quality A and B located during the years 1980 to 1984 in the boxes shown on Figure 2. Magnitude key: dot = M≤1, + = M 1.5, x = M 2-2.5, X = M 3, * = M 3.5, o = M 4, O = M 4.5, star = M ≥ 5. This magnitude key holds for Figures 2 and 3 as well.

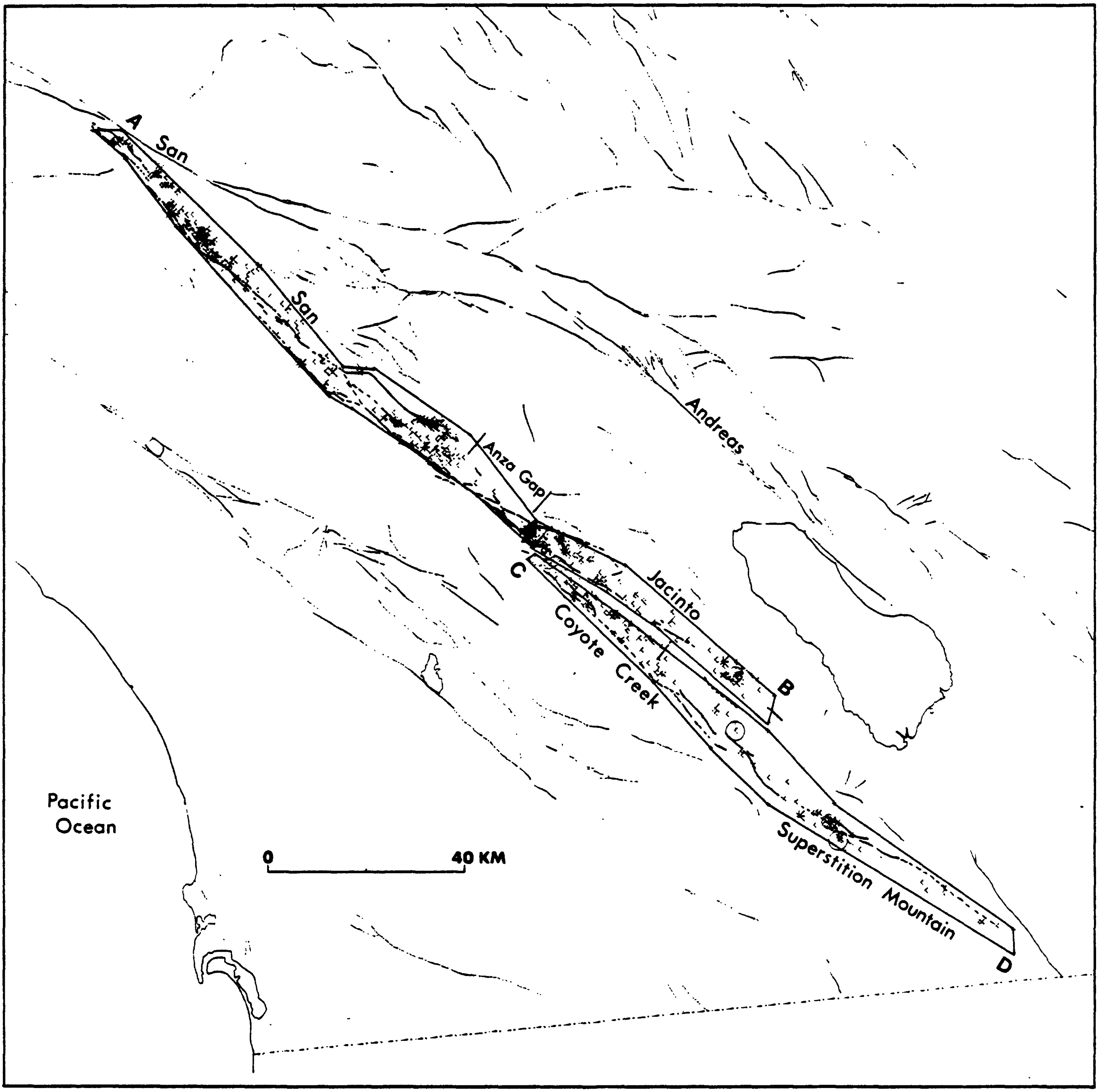
A
B
C
D
San
San
Andreas
Jacinto
Anza Gap
Coyote Creek
Superstition Mountain
Pacific Ocean
0
40 KM

Figure 2. Epicenters of earthquakes used to make cross sections A-B and C-D (Figure 1). The two long boxes along the San Jacinto fault and the Coyote Creek and Superstition Mountain faults contain all quality A and B events of M 1.8 and greater recorded during the years 1980 through 1984. This is a subset of the set of earthquakes used to make the cross sections.

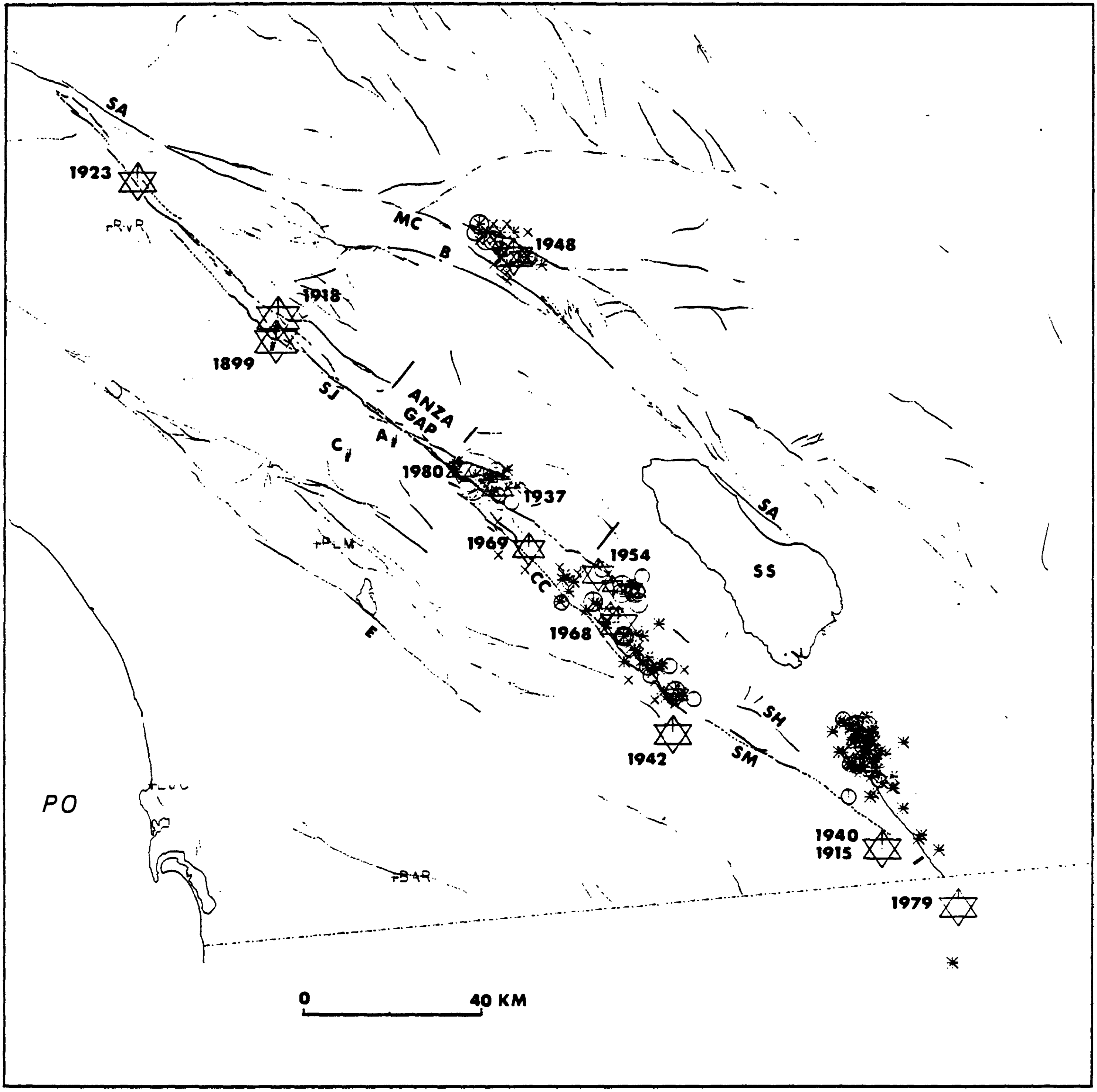
SA
1923
MC
B
1948
1918
1899
SJ
ANZA GAP
A
C
1980
1937
1969
1954
CC
1968
E
SA
SS
SH
SM
1942
1940
1915
1979
PO
0
40 KM

Figure 3. Epicenters of large earthquakes which occurred historically along the San Jacinto, southern San Andreas, and Imperial fault zones. Aftershock zones of the 1937 (M_L 6.0), 1948 (M_L 6), 1954 (M_L 6.2), 1968 (M_L 6.8), 1979 (M_L 6.6), and 1980 (M_L 5.5) events are shown. SA = San Andreas fault, SJ = San Jacinto fault, CC = Coyote Creek fault, SM = Superstition Mountain fault, SH = Superstition Hill fault, I = Imperial fault, E = Elsinore fault, MC = Mission Creek fault, B = Banning fault, SS = Salton Sea, A = Anza, C = Cahuilla, PO = Pacific Ocean.

APPENDIX A. 4.

Southern San Andreas Fault Geometry and Fault-Zone Deformation and Implications for Earthquake Prediction in the Coachella Valley, California

Roger Bilham

SOUTHERN SAN ANDREAS FAULT GEOMETRY AND FAULT-ZONE DEFORMATION : IMPLICATIONS FOR EARTHQUAKE PREDICTION IN THE COACHELLA VALLEY, CALIFORNIA

Roger Bilham*

Lamont Doherty Geological Observatory, Palisades, NY, 10964

Joint Institute for Laboratory Astrophysics,
University of Colorado and National Bureau of Standards, Boulder, CO, 80309

Presented at the
National Earthquake Prediction Evaluation Council meeting,
29 March 1985, Pasadena, California

Summary

The mapped, most-recent fractures of the southern San Andreas fault in the Coachella Valley form a remarkable sequence of straight segments with a dominant length of approximately 12Km. Subtle changes of strike of as small as 3.3 degrees determine the physical behaviour of the fault. Where the fault is parallel to the inferred slip vector the fault-zone is poorly expressed and at a low elevation. Where the fault strikes oblique to the slip vector the fault-zone is clearly-expressed within elevated and folded sedimentary rocks, and exhibits triggered-slip in response to strong-ground motion from nearby earthquakes.

If elastic strain accumulates along the fault zone at oblique-slip segments it is possible to narrow the search for pre-seismic deformation to areas near bends between segments where strainfields will be most intense. Confirmation that these strainfields exist would provide a substantial improvement in our understanding of fault mechanics. Monitoring their development would be an important ingredient in earthquake prediction studies in the area. Existing geodetic coverage of the Coachella Valley is deficient in 1-5Km baseline geodesy capable of examining strainfields arising from fault-zone geometry. Schemes to compliment existing monitoring programs are outlined.

Salton Sea level data suggest that a reversal in tilt coincided with an inferred Brawley spreading event in 1974-78. Deformation on the Durmid segment of the fault is indicated by several other indicators (fault-crossing tilt, creep and leveling data) suggesting that the Brawley event may have loaded the fault zone incrementally in the last several years. Spreading at Cerro Prieto to the south has been invoked to explain the occurence of the 1979 Imperial Valley earthquake and the 1980 Victoria event in Mexico. In view of the similarities between the Cerro Prieto and the Brawley spreading centers, and the Imperial Fault and the southern San Andreas fault, we conclude that slip on the southern San Andreas could be driven by future spreading events near the Salton Sea.

---

* 1985-1986 JILA Visiting Fellow

Introduction

A possible magnitude for a future earthquake on the southern San Andreas has been estimated to be 7.6>Mw<7.8 with a recurrence interval of between 160 and 360 years (Sykes and Nishenko 1984). No reliable data indicate the occurrence of an earthquake in the last century and possibly none has occurred since 1700. The average creep rate in the Coachella Valley (≈2mm/a, Louie et al 1985) is an order of magnitude less than the dextral slip of adjacent sides of the valley observed geodetically (≈20mm/a, Savage 1983). Elastic strain accumulating at 1-µstrain/a in the vicinity of the fault would result in an earthquake approximately every 200 years, approximately that predicted by an instability model of the fault (Stuart, 1985). King & Savage (1983) report a present day shear-strain rate of 0.4-µrad/a and estimate a recurrence interval of 135-570 years.

Fault zone geometry

Detailed mapping of active features of the San Andreas Fault in the Coachella Valley indicates that fault-zone elevation, triggered-slip and active deformation of the San Andreas Fault are related to fault strike. The fault consists of sequence of straight segments that differ in strike by 3-11 degrees (Figure 1A). In this article I discuss the geometric properties of the fault between the Banning Fault and the Salton Sea where five 12Km linear segments alternate in strike between N40W and N47.5W(Table 1). The segments can be defined with an angular accuracy of ±0.45-degrees, and a length accuracy of ±600m (three standard-deviations). Triggered slip, an accelerated manifestation of aseismic fault creep, that occurred shortly after the Borrego Mountain earthquake in 1968 and the Imperial Valley earthquake of 1979, is almost exclusively confined to the N47.5W striking Mecca Hills and Durmid Hill segments (Figure 1b). Recent sedimentary rocks are uplifted and folded within the N47.5W segments by an oblique slip mechanism described as transpression (Sylvester & Smith, 1976, Sanderson & Marchini, 1984). Low ground and unconsolidated sediments are found in the segments parallel, or near-parallel, to the N40W inferred plate slip-vector (Minster & Jordan,1978 and Bird & Rodenstock ,1984). N40W is also the inferred direction of maximum shear in the valley (Savage 1983). Figures 1c and 1d illustrate changes in fault strike graphically.

The observed, subtle changes in fault strike (3.3-7.2 degrees) are barely identifiable in the field and have hitherto been overlooked. However, bends in faults are known to be potential locations for initiating rupture during major earthquakes (Bakun et.al. 1980, Bakun 1980, King and Nabelek 1985). If we assume that this general process is applicable to the Southern San Andreas fault we can narrow the search for deformation precursors to a number of relatively small areas.

If the model is correct we anticipate the development of strainfields with dimensions of the order of a few tens of Km near the fault zone. The existence of strainfields with these dimensions near bends in the fault would confirm that the fault was pinned at these locations. Unfortunately, we are unable to confirm or deny the presence or development of these strainfields because most existing geodetic networks in the valley have baselines of the order of 30Km and span the entire valley. We are not certain that monitoring the predicted strainfields will provide the critical information needed to predict rupture of the southern San Andreas fault, but it is clear that our understanding of fault-zone mechanics would improve considerably with such studies.

The significance of oblique slip in controlling fault movement

In studying the Coachella Valley segment of the San Andreas we confront the kinematic difficulty of modelling dextral movement on a fault with major asperities. A 12.6Km-long fault segment slipping at 7.5 degrees oblique to the slip-vector acts as a 1.6Km-deep, saw-tooth barrier impeding movement of the fault. More than three of these oblique segments exist south of the Indio Hills, effectively locking the fault from movement in the Coachella Valley. How is dextral slip accomodated along the fault zone?

Recent studies show that folding of near-surface rocks occurs at times of active faulting (Yielding et. al. 1983, Stein and King 1984). It is possible to apply these results to the Mecca Hills, Indio Hills and Durmid anticline and conclude that the observed transpressive structures are not the result of interseismic deformation but the direct result of fault *movements.* The distinction has important consequences in interpreting the significance of the N48W segments as slip-controlling asperities. If the transpressive features are a superficial expression of a giant spring we should encourage a strain measurement program to monitor potential failure. If the observed features represent a passive zone of plasticity along the fault we should look elsewhere for precursive signals. A possible indication that the N48W segments are "elastic" barriers is the confinement of triggered slip to the N48W segments. We further argue that fault rupture is energetically more likely to cause the observed transpressive features since it presumably accounts for considerably more relative plate motion than does interseismic creep.

Transpression mechanics on Durmid Hill

Some insight into the process of transpression may be gained from the southernmost of the N48W segments where the Durmid Anticline has been cut through by Salt Creek. If the assumption is made that dextral offset of Salt Creek (850m) and its incised erosion of Durmid Hill (40m) as reported by Babcock (1974) are synchronous, it is possible to conclude that the ratio of dextral slip to uplift is 21:1 (see Figure 2). Curiously, a similar ratio (25:1) was obtained by Keller et. al. (1982) for an affset fan at Biskra Palms on the Indio Hills N48W segment. A 24-36mm/a slip rate results in an age of Durmid Hill of 35-24 Ka, and an uplift rate of 1.1-1.7 mm/a. There is some hope that independent confirmation of this rapid uplift rate (and hence an independent measure of the geological slip rate) may be obtained from a study of ancient Cahuilla shorelines on Durmid Hill. The uplift rate in 1974-78 is approximately twice the estimated geological uplift rate and we attribute this to an inferred spreading event (discussed below).

A suitable mechanism to obtain long term uplift is by thrusting on a plane dipping beneath Durmid hill to the North. If the uplift is formed by simple thrusting, the dip of the fault normal to the strike would need to be approximately 70° to the vertical (1.7mm of uplift for 5mm of convergence). This shallow angle of dip is contrary to the casual observation that the fault is vertical based on the straightness of the trace as it cuts Durmid Hill topography. However, a careful analysis of fault trace elevation and location (Figure 3a) shows that this apparent constraint is weak and a fault zone dipping to the NE or to the SE could exist. A dip to the NE would be consistent with seismic observations and with the sense of vertical throw on faults of the San Andreas system NE of Durmid Hill. If the fault plane were perfectly vertical and subjected to 36mm/a of oblique convergence (at 7.5-degrees), 5mm/a of convergence normal to the fault zone would occur, sufficient to generate the observed transpressive features by Poisson's Ratio (≈0.25) deformation given a 5Km deep deformation zone, 5Km wide. The 120m of sediment shortening required in the last 24Ka by this explanation is much less than the shortening evident in folded pleistocene deposits of the Borrego formation exposed in the Durmid anticlinorium (Babcock, 1972).

Deformation measurements with suitably short baselines to examine near-fault deformation exist in the form of leveling data and trilateration measurements with 1km baselines and approximately 1 p.p.m. accuracy on Durmid Hill. No horizontal deformation has occurred above the noise level of the measurements at Bat Caves Buttes in the last decade (W. Prescott, personal communication 1984) but there appears to have been an episode of 10-15mm of uplift coincident in time with the Brawley seismic swarm in 1974-78. The leveling data are contaminated by a North-South magnetic bias but are lent credence by several other data sets that imply that vertical deformation may have occurred at this time. Salton Sea level data (processed by John Beavan and Ken Hudnut at LDGO) indicate that approximately 2cm of uplift may have occured near North Shore shortly after 1977 (Figure 4). Sharp (1984) monitored 10µrad/a for three years from 1980, and an 8mm creep event was monitored at Mecca

Beach in 1984 (Louie et al 1985).

The absence of horizontal deformation on Durmid Hill in the last decade is difficult to reconcile with the vertical deformation data and merits futher study. If the observed uplift is caused by Poisson's Ratio elastic deformation along a vertical fault. We would anticipate approximately 1 μstrain/a of horizontal strain normal to the fault if the depth and thickness of the deformed zone were each 5Km as indicated by the depth-to-seismicity and width of deformed sediments respectively.

Fault behaviour at bends

We note that the strain fields at bends between faults are more intense than elswhere, that is, strain gradients are high. It is possible, as a consequence that multiple fault breaks may be common near bends, and trench studies across individual strands may result in underestimates of slip. In Figure 5 we show the bend between the Indio Hills segment and the Canal segment parallel to the ancient Cahuilla shoreline. The bend is approximately 1.5-Km south from the Indio trench of Kerry Sieh and almost directly at the Dillon Road alignment array. The Indio Site provides key information concerning historic repeat times and it is obviously of great importance to understand the mechanics of the bend. Several splays are evident in radar profiles and trenches at the Indio site.

Two other observations concerning the Dillon Road bend are recorded here. A 300m-long dry concrete structure known as Wasteway *3 (less than 500m from the alignment array) has been in place across the fault for 34 years and shows no evidence of fracturing, although a subtle flexure is apparent in the structure in the correct sense for dextral slip. A 7-cm dextral shear might have been anticipated if the observed 2mm/a creep rate had been existence for this length of time. A second feature of the canal system nearby is a persistent leakage of the Coachella Canal reported by water engineers approximately 100-m west of the Indio trench site. 15-30cm of overthrust concrete lining was removed when this was repaired in March 1981 (Doyle Cross, personal communication, 1985.) The canal does not cross a mapped fault at this point and although it is close to the mapped fault (150m) it is difficult to envisage dextral fault motion resulting in EW thrusting implied by the sense of fracturing. The significance of these two observations is uncertain since canal structures may undergo significant deformation resulting from hydraulic and thermal pressures. The absence of pronounced fracturing on Wasteway *3 could be explained either by monolithic rotation of the structure, dextral flexure below the threshhold of fracture of the structure, or by invoking the possibility that creep on the fault started in the last two decades.

Speculations on the relationship between the Brawley Seismic Swarm and the southern San Andreas Fault.

Crustal deformation data from the southern San Andreas segment near Bombay Beach are of poor quality and it is perhaps premature to conclude too much from the fragments presently available to us. In Figure 4b we attempt a preliminary interpretation of the Salton-sea-level data, the leveling data and observations of tilt and creep across the fault.

The data appear to be consistent with a model for dyke injection and rifting where the margins of the dyke are downwarped prior to rifting and uplifted during rifting. For the 20 years preceeding the Brawley Seismic Swarm the southern shore of the Salton Sea subsided 20cm. It rose 3-cm during the following 8 years and was accompanied by uplift on the NGS leveling line across Durmid Hill, on either side of the northward extension of the trend of the Brawley swarm. The uplift appears to have been terminated by the 1979 Imperial Valley earthquake that caused triggered slip on the fault. In the most recent few years deformation has occurred along the Durmid segment of the fault. We note that contraction on several geodetic lines in the Coachella Valley was observed after the inferred spreading event, consistent with margin compression on either side of a dyke injection episode.

Silver & Valette-Silver (1985) note that events in the Cerro Prieto area to the south are consistent with a spreading event beneath the Cerro Prieto geothermal field. A model is proposed that suggests that the Imperial and the Victoria earthquakes in the following few years were attributable to increased loading on the transform faults to the north and south respectively. It is possible that loading on the San Andreas fault increases substantially following a spreading episode on the Brawley spreading center. That no earthquake has occured in the last century, whereas several events have occured on the Imperial fault to the south, may be attributable to the Brawley spreading rate being less than the Cerro Prieto spreading rate (Fuis et. al. 1982). A precise estimate of the relative spreading rates of these two zones would be of value in estimating the relative frequency of Imperial Fault events to events on the San Andreas fault.

The Imperial Earthquake (15 October 1979) may have similarities to a future southern San Andreas earthquake. The dimensions of segments on the Imperial Fault defined by the surface break are comparable to those found in the Coachella Valley. That is, the fault can be considered to consist of a 14Km segment trending at approximately N38W from the Mexican border to the intersection with the Brawley Fault. The fault then bifurcates into two segments with irregular breaks extending 12Km to the NE and N respectively. The fault south of the border with no surface break appears to be segmented with a similar wavelength.

During the Imperial event the fault apparently ruptured from one bend to another bend, with the main shock on a third segment to the south. The most significant bends on the southern San Andreas Fault are those at Bombay Beach and at the intersection of the Banning Fault. A possible magnitude-6.7 event (using the three-segment Ms 6.5 Imperial event for scale) could rupture all five segments. Rupture beyond the Banning Fault northward would presumably result in a larger earthquake magnitude. We note that the Imperial event terminated to the south at an apparently insignificant 3-5 degree bend similar to those in the Coachella Valley. The 50-Km Bombay Beach/Banning Fault section of the San Andreas could also fail in shorter segments.

Recommendations for improved monitoring of crustal deformation in the Coachella Valley

Can a geometric model for fault slip be tested before committing USGS resources to a major measurement program involving tiltmeters, extensometers and precise geodesy? Can we devise ways to estimate the ratio of recoverable elastic strain to plastic deformation stored in the N48W segments? How much of the observed surface deformation occurs during motion of the fault? How much during the interseismic period ? What are the horizontal dimensions of elastic strainfields developing near the transpressive zones? Are the observed fault features vertical? Do they continue to the seismogenic zone? Do the segmented features rotate into the average strike of the fault at depth?

If elastic strain continues to increase on the N48W segments of the fault we should anticipate progressive uplift, only partly relieved by creep events on the fault. We might also anticipate a difference in creep behaviour between the N40W segments (fast and uniform) and the N48W segments (slow and erratic).

Tantalisingly, the data tell us little of what we need to know.

1. There was a large (8mm) creep event on the San Andreas fault near North Shore in early 1984. A short leveling line nearby detected 10µrad/a of tilt across the fault in the preceeding three years (Sharp 1983). The line was destroyed before a remeasurement could be made to find out whether the tilt recovered after the creep event. If the tilt was a ≈1 cm vertical manifestation of 8mm of dextral creep on the fault, the ratio of uplift to slip is more than twenty times larger than the observed geological ratio of uplift to dextral slip.

2. Triggered slip in 1979 was preceeded by uplift in 1974-78 on the USGS leveling line with 1µrad/a of tilt on the flanks of the triggered segment (appendix). We do not know whether the uplift subsided after the creep event because the leveling line

was not re-measured.

3. Caltech alignment-arrays and creepmeter measurements embrace this section of the San Andreas fault, but because of the difficulty in precisely locating the fault in the slip-parallel segments, there are few measurements in the N40W, N43W and N22W segments. The creepmeter and alignment arrays at North Shore show no creep in the last decade. If this is true, generally, in the slip-parallel segments it is a curious result and may be of great importance in interpreting the mechanics of fault slip. It is possible, however, that creep is distributed over a wide zone in these segments and may have escaped detection.

The following suggestions and recommendations are intended to remedy the absence of critical data in the Coachella Valley segment of the southern San Andreas fault.

1. The NGS first-order leveling line along the northern shore of the Salton Sea should be remeasured every two years.

We are requesting that the line be repeated by NGS or USGS. Additional leveling lines across the Brawley spreading zone are desireable in order to understand the interaction of inferred spreading and loading of the San Andreas Fault. See 6 below.

2. Short Leveling lines should be installed across the transpressive segments of the fault to monitor ongoing deformation.

Sharp's leveling line should be repaired. Active deformation near Bombay beach (suggested by Babcock (1974) and confirmed by USGS leveling) should be investigated with short leveling lines. A short leveling line exists across the fault at Painted Canyon in the Mecca Hills (A. G. Sylvester, personal communication, 1985) which could be expanded to cross the possibly active Mecca Hills transpressive zone. The emphasis on these short leveling lines should be to understand the relationship between observed fault creep (≈2mm/a) and geodetic slip (≈20mm/a). Leveling ±5Km from the fault may reveal whether or not some of the missing slip is being stored close to the transpressive zones.

3. Better mapping of the San Andreas fault-zone in non-transpressive segments is required.

Ground penetration radar surveys are recommended in the North Shore N40W fault segment, and in the Bombay Beach N22W segments of the fault (Figure 1) to determine the precise location and width of the fault zone.

4. Additional creepmeters and alignment arrays are desireable in the non-transpressive segments of the fault.

It is desireable that these arrays should be wider and but with the same or improved dextral-displacement sensitivity. This implies that measurements will have to be more precise than existing alignment measurements. Deep monuments are suggested. The implementation of these additional measurements would be premature without the improved mapping mentioned in 4. above.

5. Improved horizontal geodesy in the Coachella Valley

Triangulation data to the 1950's (Thatcher, 1979) and trilateration data from the 1970's (Savage, 1983) should be reconciled to form one homogeneous data set.

Trilateration data should be complimented with additional short baseline measurements (1-3Km baselines near the fault., and with 5-10Km baselines extending to the NE side of the fault.

6. Additional sea-level monitors along the Northern and Southern shore of the Salton Sea

The present network of gauges (two LDGO [May,1985] and one USGS gauge) is adequate only for homogeneous tilt. We have ample evidence that the tiltfield is not homogeneous along the San Andreas fault and across the Brawley spreading region. It is possible that subsidence may be occurring at Bombay Beach with uplift on either side. The same process may be occurring at Obsidian Buttes.

7. Bench-mark stability

The surficial materials in the Coachella Valley consist of thick (3-5Km) deposits of sediments. Bench-marks and tigonometrical markers are notoriously unstable in such environments. Preliminary efforts should be directed at gaining experience at installing tiltmeter-end-piers stable to 10µm/a vertically in such materials.

Groundwater withdrawal is a problem near Indio, but more so are the uncertain effects of aquifer recharging that has been an ongoing process since 1948 when the canal was first opened. Recently, deliberate recharging of drinking-well aquifers in the valley has been commenced by engineers from the Coachella Valley Water District. Near much of the San Andreas fault in the North Shore and Durmid segments, aquifer water is unsuited to drinking or irrigation and there are no active wells.

Geodetic bench-marks defining the NGS leveling line parallel to the fault on Durmid Hill are principally on bridge parapets. Disconcertingly, an alarming number of bridges were replaced in early 1985 because of storm damage and it is uncertain how many of the marks are recoverable. Clearly, a more satisfactory array of markers must be installed away from bridge washouts. The markers should consist of deep reference piers isolated from surficial soil motion.

Horizontal deformation markers away from exposed quaternary rocks pose a stability problem. A possible solution is to implement a form of tetrahedral end-mount used for wire strainmeters in Alaska. In this arrangement, three or more rods are driven to refusal in a downward radiating pattern and their free ends are cemented or welded together near the surface. The near-surface ends of the rods would be isolated from surficial motion by plastic collars.

Conclusions

The San Andreas Fault south of the Banning Fault consists of a sequence of straight segments with remarkably similar lengths (≈12-Km) and simple angular relationships. Fault segments elsewhere in the Coachella Valley vary in length from 4-23Km. The segments are remarkable for their straightness and for the fact that fault properties along adjacent segments differ markedly. The strike of the fault changes by as little as 3.3 degrees between fault segments.

Where the strike of a fault segment is oblique to the inferred plate slip vector (N40W) fault motion is accompanied by uplift and folding of sedimentary rocks . Since fault segment strike is known to ±0.45-degrees and the slip vector is inferred to ±1-degree it appears possible to predict the strainfields developing at each of the oblique slip segments impeding fault motion. The precise shape of these strainfields will be determined by the distribution of elastic properties near the fault. The astonishing regularity of fault segmentation suggests that the strainfields may be simple and therefore predictable. Monitoring the development of these predicted strainfields would provide a major contribution to assessing earthquake hazard in the valley, however, at present there are few geodetic networks in the valley with suitably short baselines.

A tentative model to explain deformation data near the Salton Sea is formulated, in which spreading at the Brawley spreading center results in increased loading of the Southern San Andreas fault. A future spreading event may trigger rupture of the fault.

Hitherto, the character of the fault along the southern San Andreas has been considered to be relatively homogeneous. The reported geometric properties of the southern San Andreas fault enable detailed monitoring of the fault zone to be considered within a reasonable budget. It is likely that rupture will propogate from a bend, to a bend. The most significant bends apparent in the Coachella Valley are at Bombay Beach and where the Banning Fault intersects the San Andreas Fault. These bends are each approximately 20 degrees and share the common property of being poorly defined in the near surface. Research is needed to understand the significance of each fault segment in preventing movement of the fault, and to monitor the development of strainfields around fault segments that will tell us where and at what rate elastic strain is accumulating.

ACKNOWLEDGEMENTS

The investigations were stimulated by discussions with Patrick Williams, Nano Seeber and Kerry Sieh, and by numerous subsequent discussions with Art Sylvester, Max Wyss, Lynn Sykes and Chris Scholz. Nano Seeber and John Beavan have kindly reviewed the manuscript. Supported by U.S. Geological Survey contracts 21296 and 21918, National Aeronautic and Space Administration contract NA-5-27237, by the National Geophysical Data Service and by the National Bureau of Standards. Lamont Doherty Contribution Number 3812.

Table 1 Geometric properties of the southern San Andreas Fault in the Coachella Valley, California. (latitudes 33°47' to 33°23'N)

Segment	**Length ±200m**	**Strike ±0.15°**	**Standard Deviation**	**Average Triggered slip**		**Observed Creep rate**
				1968	**1979**	
Indio Hills	12Km	N48.09W	±20m(S 7Km only)	-	-	2mm/a
Canal	12.0Km	N43.78W	±25m	-	-	-
Mecca Hills	12.6Km	N47.42W	±30m	9.5 mm	4mm	3.1mm/a
North Shore	12.6Km	N40.36W	±20m	0.6mm	-	<1mm/a
Durmid Hill	12.6Km	N47.48W	±25m	5 mm	2.5mm	1-2mm/a

The Indio Hills segment is measured from Biskra Palms although it is much fragmented for the first 5Km of the segment and may not represent a continuous fault north of the inferred intersection of the Banning fault. A standard deviation is given only for the southern 7Km of the Indio segment. The Durmid segment is measured to the southern end if the 1979 triggered-slip segment. The deviation from straightness is expressed as a standard deviation from a least-squares fit to all mapped fault strands in each segment. Segment length is determined by the intersection of least-squares fit straight lines from adjacent segments. Triggered slip is calculated from the data of Allen et al (1972) and Sieh (1982). The numerical values are obtained by dividing the sum of the maximum observed slip in each 1-Km section of the fault segment by the length of the segment. Creep data are from Louie et al (1985).

REFERENCES CITED

Allen, C.R., M. Wyss, J. N. Brune, A. Granz and R. Wallace, 1972. Displacements on the Imperial, Superstition Hills and San Andreas fault triggered by the Borrego Mountain earthquake, in The Borrego Mountain Earthquake, U. S. Geological Society Professional Paper 787, p. 87-104

Bakun, W. H., 1980, Seismic Activity on the southern Calaveras Fault in Central California. Seismological Society of America Bulletin v. 70, p. 1181-1197.

Bakun, W. H, R. M. Stewart, C. G. Bufe and S. M. Marks, 1980, Implication of seismicity for failure of a section of the San Andreas fault. Seismological Society of America Bulletin v. 70, p. 185-201.

Babcock, E. A. , 1974, Geology of the NE margin of the Salton Trough, Salton Sea, California, Geological Society of America Bulletin, v. 85, p. 321-332

Bird, P., and R.W. Rosenstock, 1984, Kinematics of present crust and mantle flow in southern California., Geological Society of America Bulletin, v. 95, p. 946-957.

Clark, M. M., 1984, Map showing recently active breaks of the San Andreas Fault and associated faults between Salton Sea and Whitewater River, Mission Creek, California. , Miscellaneous Investigations Series, U. S. Geological Society Map I-1483, Scale 1:24000.

Johnson, C. E. and D. P. Hill, 1982, Seismicity of the Imperial Valley, in The Imperial Valley Earthquake of Oct 15,1979. U. S. Geological Society Professional Paper 1254, p.15-24.

Keller, E. A., M. S. Bonkowski, R. J. Korsch, and R. J. Schlemon, 1982, Tectonic geomorphology of the San Andreas fault zone in the southern Indio Hills, Coachella Valley, California, Geological Society of America Bulletin, 93, 46-56.

King, and Nabelek, 1985, The role of bends in faults in the initiation and termination of earthquake rupture: Implications for earthquake prediction, Science, (in Press)

King, N. E. and J. C. Savage, 1983, Strain Rate Profile across the Elsinore, San Jacinto and San Andreas Faults near Palm Springs, California 1973-1981, Geophysical Research Letters, v. 10, p. 55-57.

Louie, J.N., C. R. Allen, D. C. Johnson, P. C. Haase, and S. N. Cohn, 1985, Fault slip in Southern California. Seismological Society of America Bulletin, (in press)

Mavko, G. M., B. D. Brown, and S. S. Schulz, 1984, Fault Zone Tectonics,. U. S. Geological Survey Open File Report 84-268, p. 232-233

Minster, J. B., and T. H. Jordan, , 1978, Present day tectonic motions, Journal of Geophysical Research, v. 83, p. 5331-5354

Sanderson, J. D. and W. R. D. Marchini, 1984, Transpression, Journal of Structural Geology, v. 6, p. 449-458.

Savage, J. C., 1983, Strain accumulation in western United States, Annual Reviews of Earth and Planetary Sciences, v. 11, p. 11-43

Sharp, R. V., 1972, Tectonic setting of the Salton Trough, . in The Borrego Mountain Earthquake, U. S. Geological Society Professional Paper 787, p. 3-15,

Sharp, R.V., 1983, Salton Trough Tectonics and Quaternary Faulting, U. S. Geological Survey Open-File Report 83-918, p. 133

Sieh, K. E., 1972, Slip along the San Andreas Fault associated with the Earthquake, in The Imperial Valley Earthquake of Oct 15 1979, U. S. Geological Society Professional Paper v.1254, p. 155-160

Silver, P and J. N. Valette-Silver , 1985 , Detection of an on-land spreading event. Potomac Geophysical Society abstract. January 1985

Stein, R. and G. C. P. King, 1984, Seismic potential revealed by surface folding: the Coalinga, California, earthquake. Science v. 224, p. 869-872

Stuart, W. D. 1985, Instability Model for recurring large and great earthquakes in Soiuthern California, Pageoph, in press

Sylvester, A. G. and R. R. Smith, 1976, Tectonic transpression and basement-controlled deformation in the San Andreas fault zone, Salton Trough, California, American Association Petroleum Geologists Bulletin, v. 60, p. 2081-2102,

Sykes, L. R. and S. P Nishenko, 1984, Probabilities of occurrence of large earthquakes for the San Andreas, San Jacinto, and Imperial Faults, California 1823-2003. Journal of Geophysical Research, v. 89, p. 5905-5927.

Thatcher, W., 1979, Horizontal Crustal Deformation from Historic Geodetic Measurements in Southern California, Journal of Geophysical Research, v. 84, p. 2351-2370

Wallace, R.E. Stanford Univ. Geol Sciences Pub. XIII, 1973

Yielding, G, J. A Jackson, G. C. P. King, H. Sinvhal, C. Vita-Finzi and R. M. Wood, 1981, Relations between surface deformation, fault geometry, seismicity and rupture characteristics during the El Asnam (Algeria) earthquake of 10 October 1980. Earth Planet. Sci. Lett. v. 56, p. 287-304.

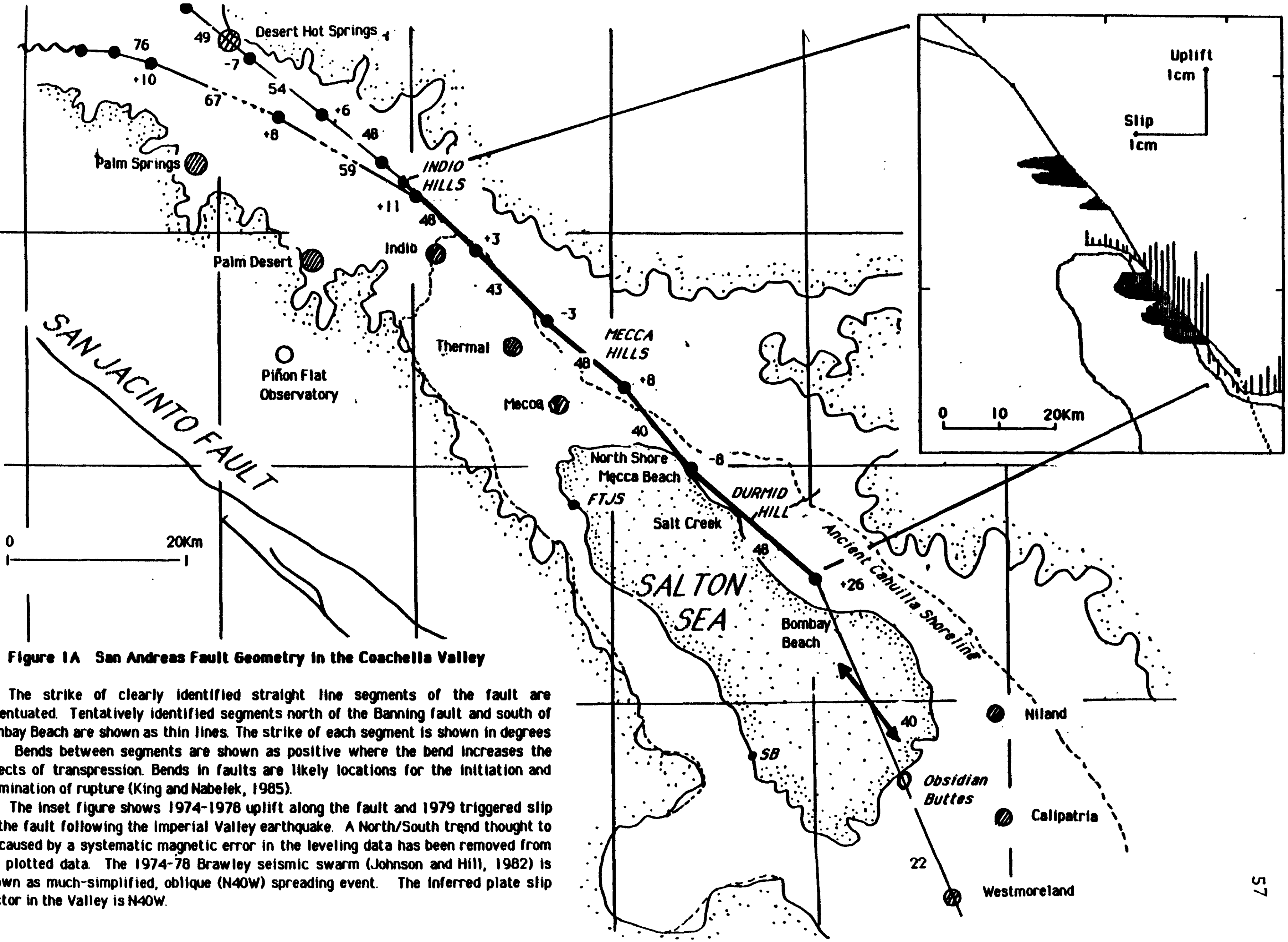
Desert Hot Springs
49
-7
54
+6
48
76
+10
67
+8
59
Palm Springs
INDIO HILLS
+11
48
Indio
+3
43
Palm Desert
-3
MECCA HILLS
Thermal
Piñon Flat Observatory
48
+8
Mecca
40
SAN JACINTO FAULT
0
20Km
North Shore
Mecca Beach
-8
FTJS
DURMID HILL
Salt Creek
48
+26
Ancient Cahuilla Shoreline
SALTON SEA
Bombay Beach
40
SB
Niland
Obsidian Buttes
Calipatria
22
Westmoreland
Uplift 1cm
Slip 1cm
0
10
20Km

Figure 1A San Andreas Fault Geometry in the Coachella Valley

The strike of clearly identified straight line segments of the fault are accentuated. Tentatively identified segments north of the Banning fault and south of Bombay Beach are shown as thin lines. The strike of each segment is shown in degrees NW. Bends between segments are shown as positive where the bend increases the effects of transpression. Bends in faults are likely locations for the initiation and termination of rupture (King and Nabelek, 1985).

The inset figure shows 1974-1978 uplift along the fault and 1979 triggered slip on the fault following the Imperial Valley earthquake. A North/South trend thought to be caused by a systematic magnetic error in the leveling data has been removed from the plotted data. The 1974-78 Brawley seismic swarm (Johnson and Hill, 1982) is shown as much-simplified, oblique (N40W) spreading event. The inferred plate slip vector in the Valley is N40W.

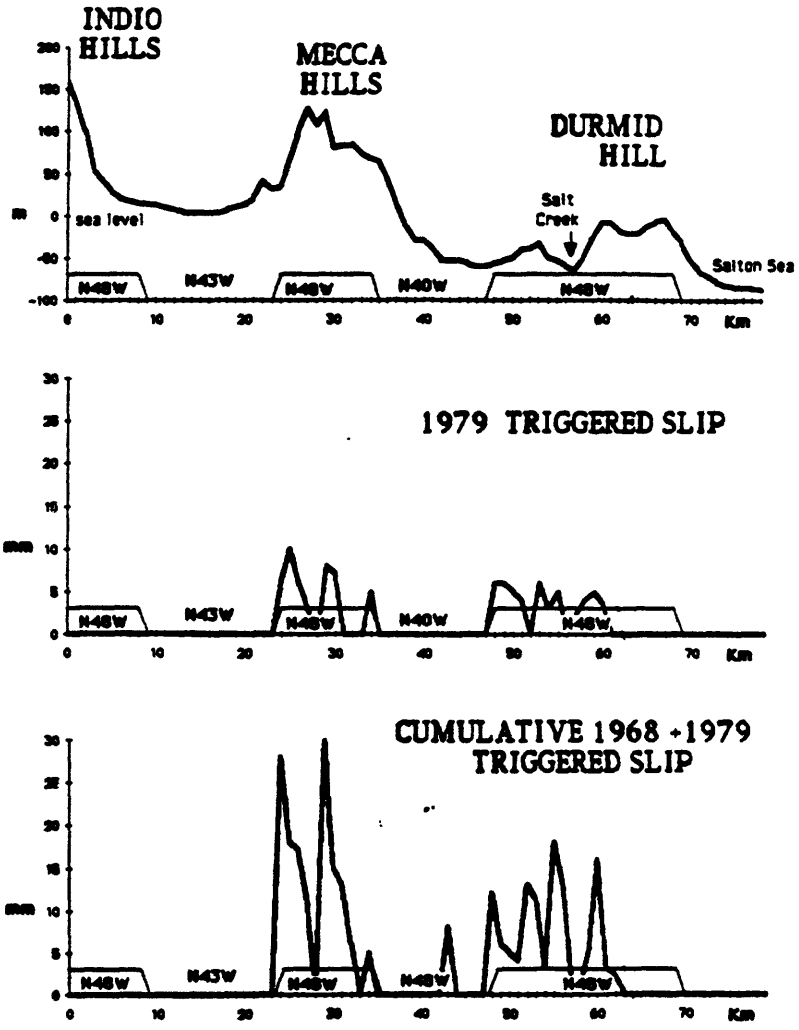

Figure 1B
Relationship between fault strike, fault zone elevation (±100m of the mapped trace) and triggered slip during the 1968 (Borrego Mountain) and 1979 (Imperial) events. The mean, maximum values of triggered slip observed in each 1 Km section of the fault were calculated from the data of Allen et. al. (1972) and Sieh (1982).

The southern end of the Durmid Hill segment meets two 4Km segments (trending at N54Wand N60W) before it meets the projected intersection of the Brawley seismic swarm at Bombay beach. These two segments are poorly defined and in this plot are included with the N48W segment. The southern termination of 1979 triggered slip ends precisely at the bend between the N48W segment and the N54W segment.

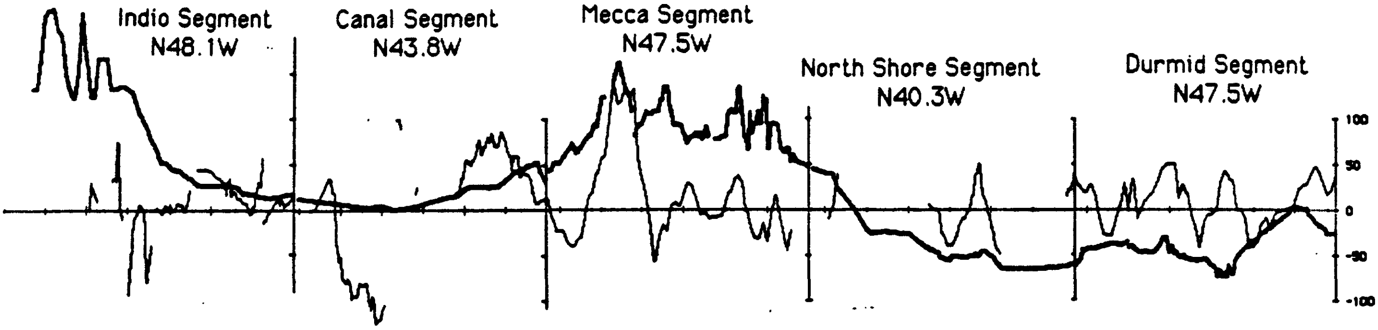

Figure 1c Fault strand elevation and deviation for five segments of the Southern San Andreas Fault

Light curves represent mapped fault traces relative to estimated least-squares straight-line fits for each segment. The mapped location accuracy for each trace is estimated to be not better than 20-30m by Clark (1984). Relative trace location to ±2.5m is beleved possible where multiple fault strands or clear fault-zone topography exists. Bold curves represent elevation of the mapped fault trace (interpolated to ±0.3m). Fault deviation to the NE and elevation above mean sea level are both positive and to the same scale. Vertical/horizontal scale exaggeration ≈40. Tick marks are every 2Km and are measured from the SE (right) end of each segment.

The length of each segment is defined by the intersection of the least-squares fit line derived for that segment with the least-squares fits from adjacent segments. The similarity in length (≈12-Km) of each segment is remarkable.

High ground is associated with segments trending at 7.5-8 degrees to the inferred slip vector. Relatively low ground is found in the North Shore and Canal segments. Departures from straightness are not caused by fault dip, but appear to be related to small scale topographic features.

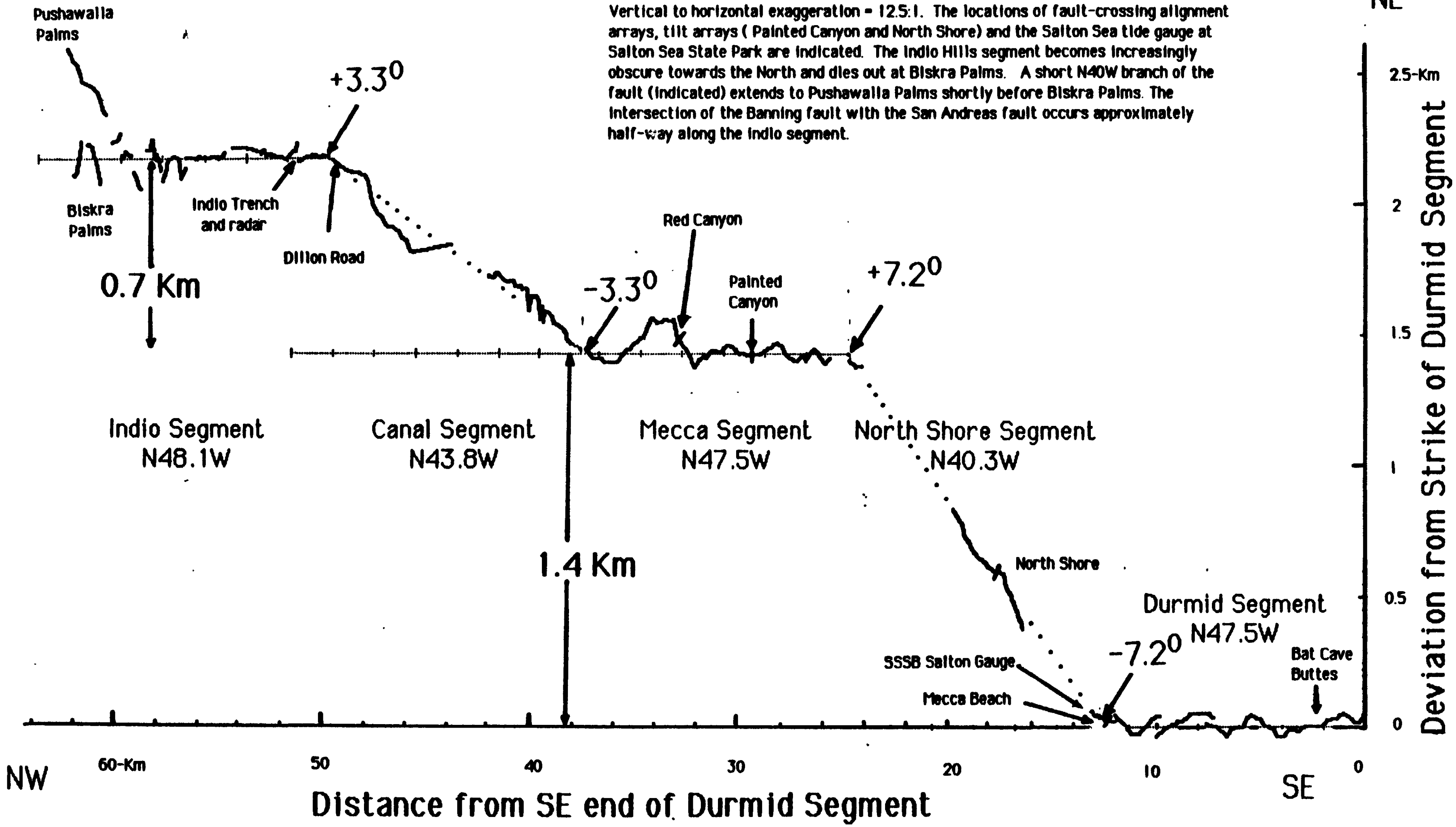

Figure 1d Deviation of the active trace of the San Andreas Fault from the extrapolated strike of the Durmid Hill Segment

Vertical to horizontal exaggeration = 12.5:1. The locations of fault-crossing alignment arrays, tilt arrays (Painted Canyon and North Shore) and the Salton Sea tide gauge at Salton Sea State Park are indicated. The Indio Hills segment becomes increasingly obscure towards the North and dies out at Biskra Palms. A short N40W branch of the fault (indicated) extends to Pushawalla Palms shortly before Biskra Palms. The intersection of the Banning fault with the San Andreas fault occurs approximately half-way along the Indio segment.

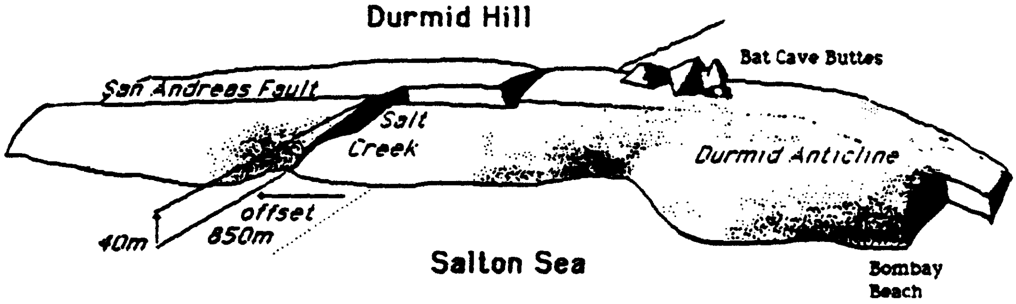
Durmid Hill
San Andreas Fault
Bat Cave Buttes
Salt Creek
Durmid Anticline
offset 850m
40m
Salton Sea
Bombay Beach

Figure 2 Transpression along the Durmid Segment of the San Andreas fault. Salt Creek appears to be an antecedent stream that has been offset approximately 850-m by movement of the San Andreas fault (Babcock 1974). It cuts through a 40-m deep gorge thus providing an approximate estimate of the ratio between uplift and dextral slip. This ratio (.05) is similar to that reported in the Indio Hills segment by Keller et. al.(1982). If we assume that the average dextral slip rate is 24-36mm/a we obtain a minimum age for Durmid Hill of 35-24Ka, and an uplift rate of 1.7-1.1mm/a. A higher uplift rate would be necessary to account for sediments removed by erosion or by gravity sliding.

An uplift rate of 2mm/a would result in 1-m of uplift in 500 year-old lake Cahuilla shorelines surrounding Durmid Hill. Measurements of Cahuilla shorelines may yield an independent estimate of uplift rate , and perhaps slip rate, for this segment of the fault.

Durmid Hill /Elevation/strike/deviation

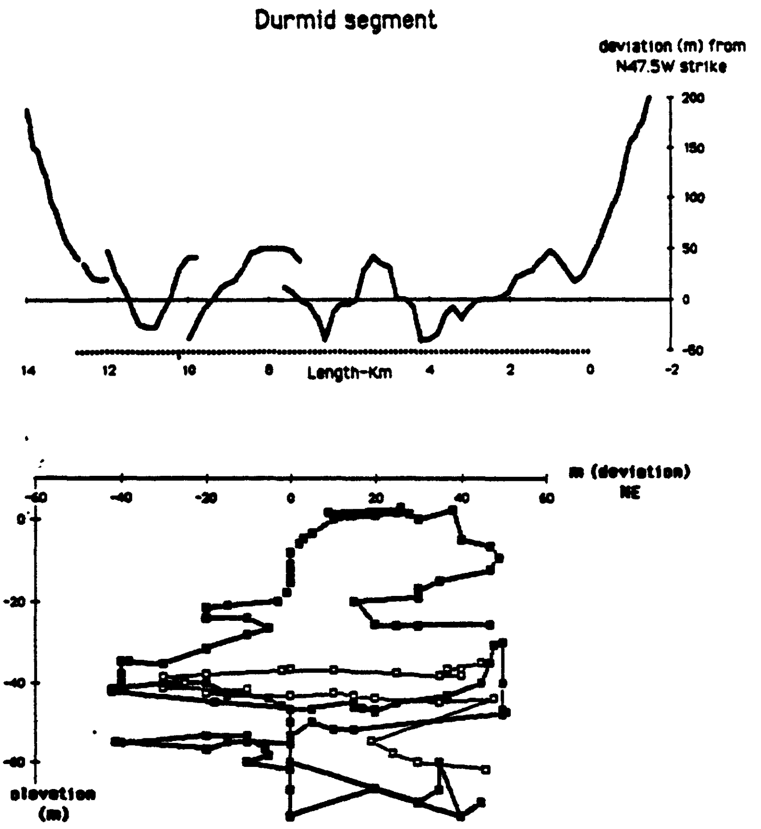

Figure 3

Geometrical analysis of the Durmid Hill segment of the San Andreas Fault. The upper figure illustrates the straightness of the fault by exaggerating (x25) the mapped deviation from an imaginary line striking at N47.48W. The standard-deviation is ±25m and the maximum and minimum deviation are 51m and 41m respectively. The Durmid fault segment (dashed zone) is 12.65±0.2Km long and extends from the southermost 1979 triggered slip fracture (2Km SE of Bat Caves Buttes) to 400m SE of the northmost 1979 fracture (near the Mecca Beach campground). The strike of adjoining segments are plotted for approximately 1Km beyond each bend. The bend itself is defined by the intersection of straight-line, least-squares fits for fault-deviation data-from adjacent fault segments. The fault to the south of this segment (Bombay Beach) is poorly defined but appears to consist of two <4Km long segments before striking to the SE at N22W.

The lower figure illustrates the relationship between fault trace deviation and fault trace elevation within the Durmid Hill segment of the San Andreas Fault. Each strand of the fault follows a curve on the figure. If the fault were vertical we would expect a dominant vertical cluster. A least squares fit to these data give a shallow-dipping fault to the SW, however, it is thought that deviation-details of the fault trace may be strongly influenced by surficial effects making a rigorous analysis misleading. There is some suggestion that the fault is vertical where it is in line with, or parallel to, the mean strike of the segment.

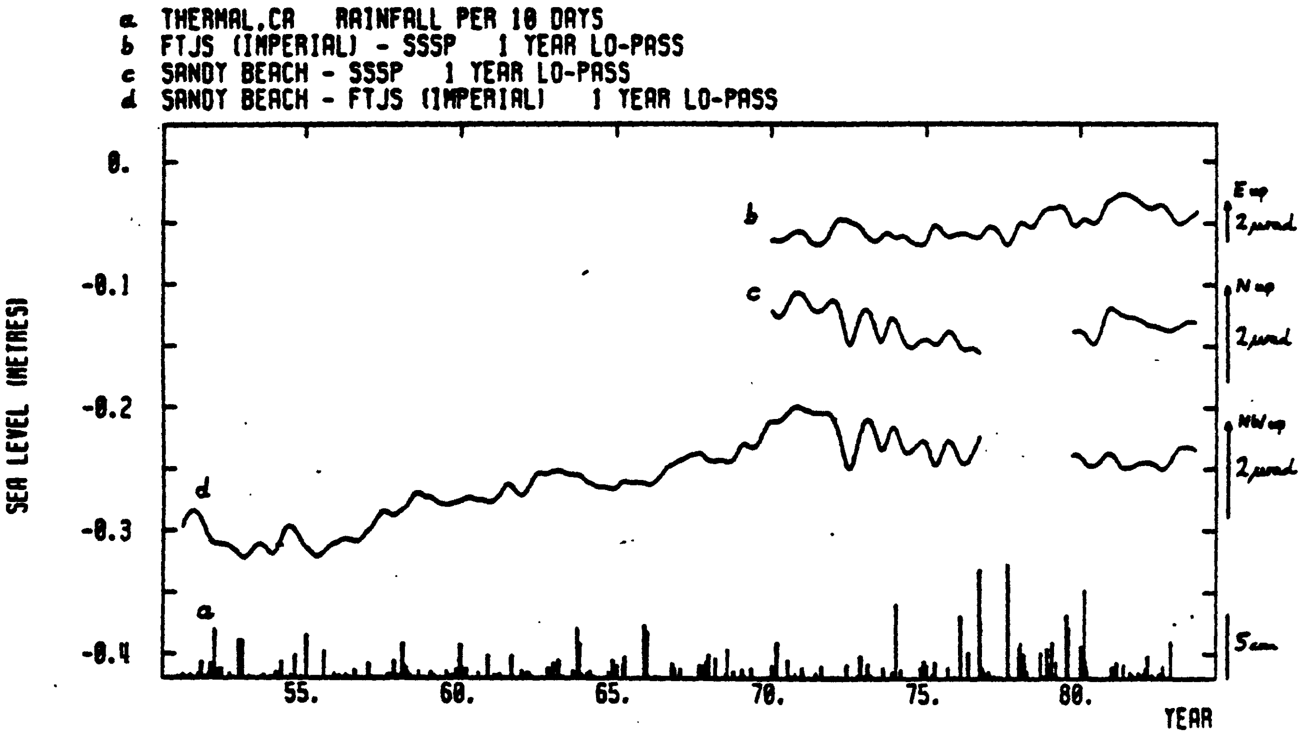

Figure 4 35 years of Salton Sea-level data reduced by John Beavan and Ken Hudnut. Differences between the three gauges have been filtered with a 1-year zero-phase Butterworth low-pass filter. The data were previously reported to 1978 by Wilson and Wood (*Science*, **207**, 183-186, 1980). The new data show that tilt reversed at about the time of the Brawley seismic swarm. The oscillations that occured at this time may be the vertical manifestation of episodic spreading (they are not annual variations), but we cannot exclude the possibility that the USGS gauge at SB was malfunctioning.

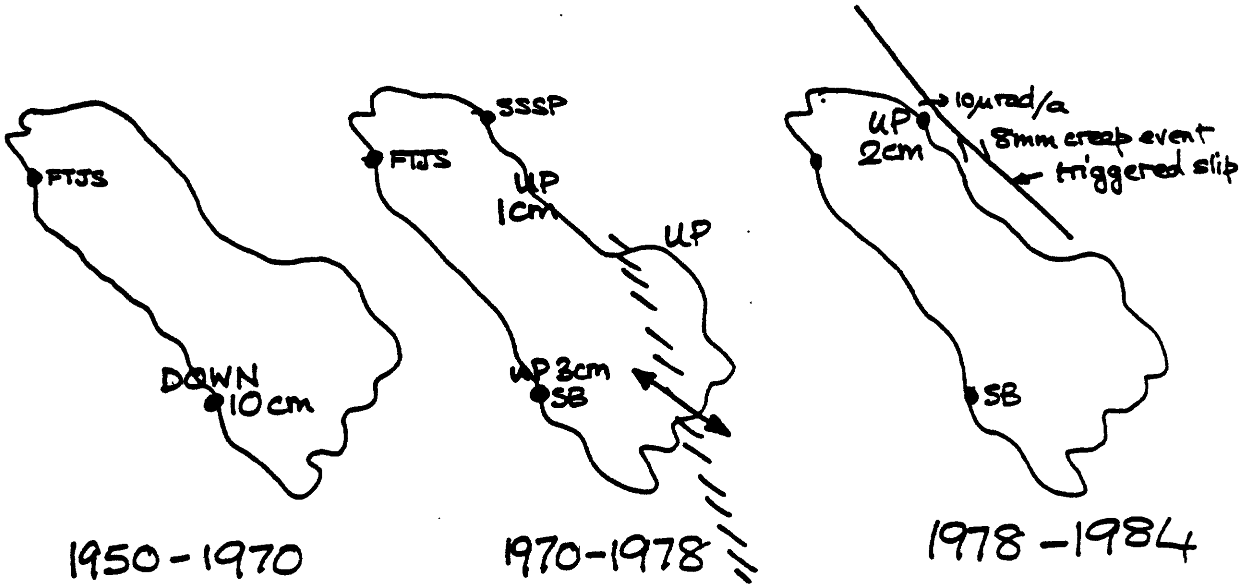
FTJS
DOWN
10 cm
1950-1970
SSSP
FTJS
UP
1cm
UP
UP 3cm
SB
1970-1978
10μrad/a
UP
2cm
8mm creep event
triggered slip
SB
1978-1984

Figure 4b

Possible interpretation of tectonic activity in the Salton Sea region from 1950 to 1984. The three Salton Sea gauges indicate three different periods of tectonic activity. Two gauges suggest a tilt down to the SE before 1970 when a third gauge was added. The tilt reversed in the period 1970-78, at the same time as uplift was observed on a leveling line along the NE shore of the sea. Movement on the fault has been reported recently (Tilt across the fault in 1980-83, (Sharp, 1983), and an 8mm creep event on the fault in 1984,(Louie et al 1985)) that appears to be be related to approximately 2cm of uplift at Salton Sea State Park (SB) since 1978.

The data are consistent with a spreading event of the sort reported in Iceland where uplift of the lips of the spreading center occurs during a dyke-injection phase. Horizontal contraction of surfaces adjacent to the rifting episode should occur simultaneously, an observed feature of several geodetic lines in the Coachella Valley for this period of time.

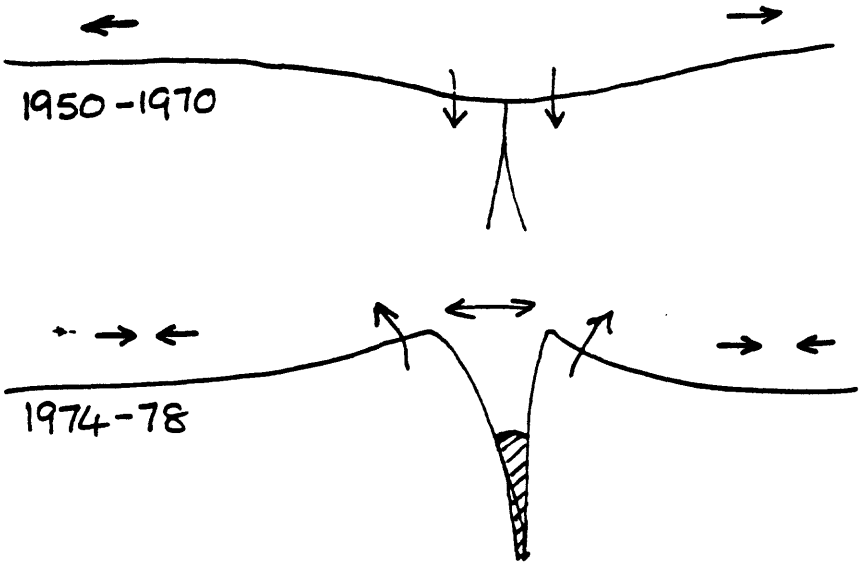
1950-1970
1974-78

Figure 5 Detail of the intersection between the Mecca Hills Segment and the Canal Segment of the San Andreas Fault in the Coachella Valley

The map is that of Clark (1984). A 3.3 degree change in the strike of the San Andreas fault occurs between A and B.

A = C.I.T. Dillon Road Alignment Array (≈2mm/a)
B = 300m long concrete-lined channel known as Wasteway # 3. Dextral flexure but no cracks. Constructed 1951.
C = Trench investigations of Kerry Sieh (Indio Site).
D = Radar mapping of multiple subsurface fault breaks (Bilham et al 1985).
E = Fractured canal lining repaired 11 April 1981. 30cm overthrust removed.
F = Major fracture in Wasteway#3 presumed of hydraulic and/or thermal origin.
G = Wedge-shaped (15°) hill. A similar 15° wedge-shaped hill bounded to the south by an inferred fault occurs approximately 2Km from the SE end of the Mecca Segment.

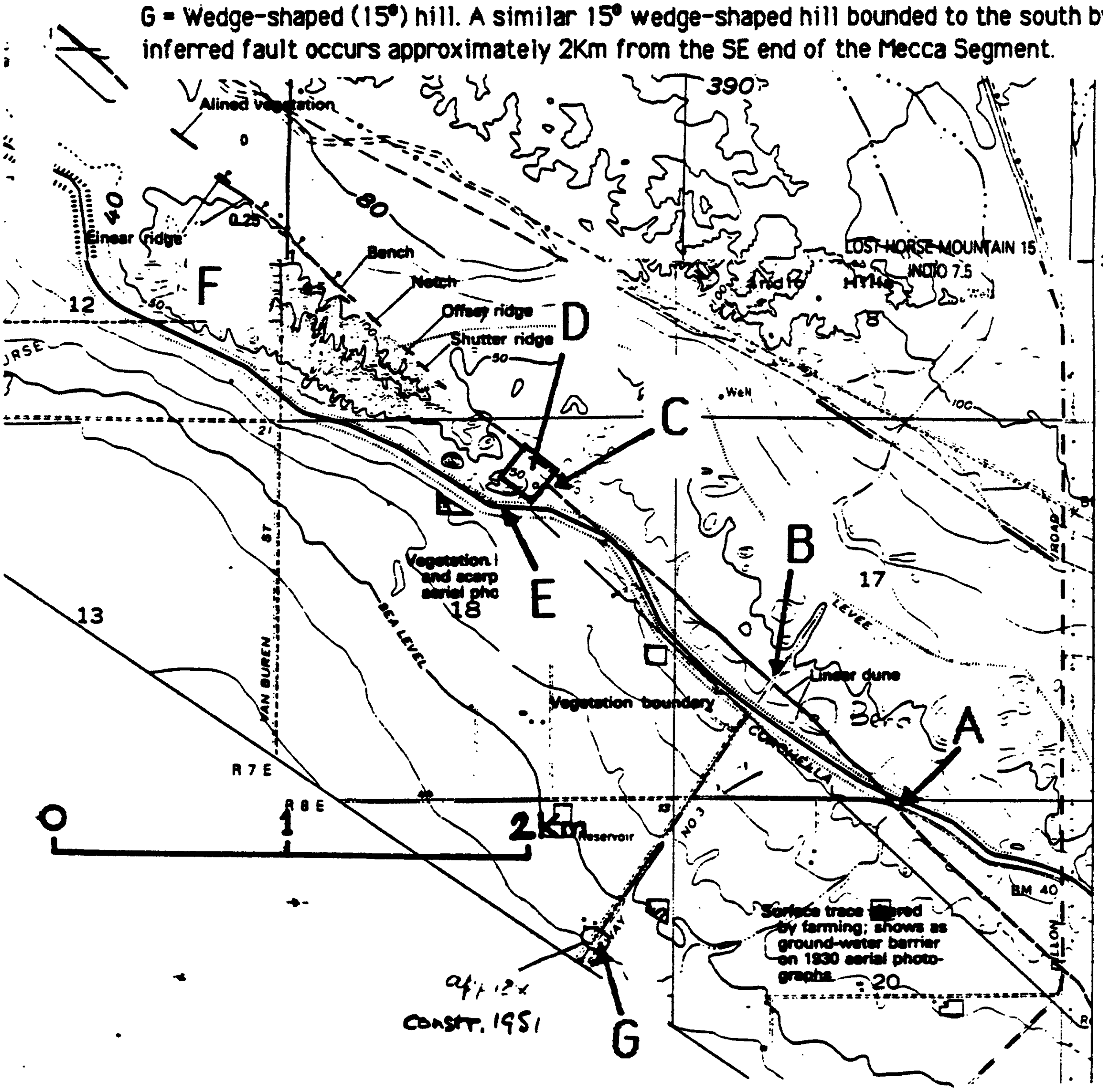
Alined vegetation
390
0
80
40
Linear ridge
0.25
Bench
Notch
F
12
50
Offset ridge
Shutter ridge
D
LOST HORSE MOUNTAIN 15'
INDIO 7.5'
33° 45'
Indio
HYHA
JRSE
21
C
Well
100
50
B
17
Vegetation and scarp aerial pho
18
E
13
ST
VAN BUREN
SEA LEVEL
LEVEE
Linear dune
Vegetation boundary
COACHELLA
A
R 7 E
R 8 E
0
1
2Km
Reservoir
NO 3
BM 40
Surface trace altered by farming; shows as ground-water barrier on 1930 aerial photographs
20
DILLON
ROAD
R
af/p 12x
CONSTT. 1951
G

APPENDIX A. 5.

Slip Rates of Active Faults

Malcolm Clark

3 May 1985

Summary of comments presented to NEPEC March 29, 1985 by Malcolm Clark, USGS

SLIP RATES OF ACTIVE FAULTS

Increased use of late Quaternary slip rates has produced better tectonic analyses and earthquake hazard estimates, yet we are concerned that users may lose sight of the significant limitations in most slip rates. Slip rates (slip/time) are deceptively simple, but estimates of both slip and time generally include crucial assumptions and significant measurement errors.

The principal sources of uncertainties in measurements of slip are (1) imprecise boundaries to the features that have been offset, (2) measurements that fail to span the entire zone of faulting or deformation, (3) no measurement for one of the components of slip, and (4) incorrect identification of apparently offset features.

Most estimates of elapsed time have large uncertainties. Dates commonly must be obtained indirectly from associated deposits or features, and include assumptions about that association. Such dates generally bracket the elapsed time, often by wide margins. Dating techniques themselves may contain major assumptions and analytical uncertainties. In addition, if recurrence interval is large relative to the time period, a major uncertainty in slip rate arises if the measured time period does not begin and end at the same place on an assumed earthquake recurrence cycle.

Estimates of both slip and elapsed time should include minimum and maximum allowed by the data. These extremes should be combined to produce the extreme ranges of resulting slip rate. Those who report slip rates should fully disclose and discuss all aspects of methods, assumptions, and uncertainties that produced those rates. They should also evaluate the quality of the slip and age estimates, and, where possible, give a qualified opinion, based on experience and judgment, of preferred value if the range of slip rates is large.

We have incorporated these suggestions in a recently released slip rate table and map for California assembled from the compiled contributions of 13 U.S. Geological Survey geologists.[1] We intend this table and map to appear in successively revised editions as better data come forth and new sites are measured.

Each contributor is responsible for compiling, calculating, interpreting, and evaluating the slip rates for all available sites within a specific geographic area of the State. We have tried to be both informative and judgmental about each slip rate. Where possible, we report or estimate minimum and maximum values of both slip and age of offset features as allowed by the measurements at each site. We then use the resulting range of values to calculate the probable range in slip rate. In addition, each contributor makes a qualitative estimate of the reliability of the slip and age estimates on the basis of the data and methods used. Although our evaluations are individual and may be somewhat arbitrary, we believe that our informed opinions form a valuable part of the table. Sources and comments for each site will allow users to evaluate the original data and methods by which we or the quoted source derived the slip rates.

---

[1] Preliminary Slip-Rate Table and Map of Late-Quaternary Faults of California, U.S. Geological Survey Open File-Report 84-106. Malcolm M. Clark, Katherine K. Harms, James J. Lienkaemper, David S. Harwood, Kenneth R. Lajoie, Jonathan C. Matti, James A. Perkins, Michael J. Rymer, Andrei M. Sarna-Wojcicki, Robert V. Sharp, John D. Sims, John C. Tinsley, III, and Joseph I. Ziony.

Our slip rate table has only two entries for the San Andreas fault southeast of San Gorgonio Pass. Both are near Indio, and neither is of high quality. Serious uncertainties in estimates of both age and slip occur at one site, and work is still in progress at the other, although it promises good results.

CFS version, edited by MMC, 3 May 1985

Slip Rates for California Faults

Malcolm Clark began the discussion by stating some of the problems with assigning slip rates. In short, he felt that that the present rates are poor but can be improved with more data. He also noted that there is little data for southern San Andreas and San Jacinto faults. Malcolm discussed problems in determining slip rates. Although the formula (rate = displacement/age) is simple, measurements of both slip and time are rarely straight-forward. Such measurements generally include crucial assumptions and significant measurement uncertainties. He advocated that investigators give estimates of minimum and maximum rates and a preferred rate. He also advocated that the investigators give a quality assessment of the rates. Malcolm concluded with a description of the California slip-rate map and table, and cited some examples of the quality assessments he and his colleagues gave to a selected number of southern California slip rates.

APPENDIX A. 6.

Tectonic Framework of the South-Central Transverse Ranges

Jonathan C. Matti

Tectonic framework of the south-central Transverse Ranges

by Jonathan C. Matti

The tectonic framework of the south-central Transverse Ranges includes paleotectonic and neotectonic faults that evolved during late Miocene through Holocene time (Matti and others, 1985). These faults can be grouped into four systems: (1) The San Andreas fault system (2) the San Gorgonio Pass fault system, (3) the Crafton Hill horst-and-graben system, and (4) the Cucamonga fault zone.

San Andreas fault system

Banning fault zone. The Banning fault zone is an old strand of the San Andreas fault system that formerly was a throughgoing fault that extended from the Coachella Valley region, through San Gorgonio Pass, and west to the vicinity of the San Gabriel Mountains; there, the Banning fault probably once was continuous with the San Gabriel fault. The Banning-San Gabriel fault generated about 60 km of right-lateral displacement during the period between 10-12 m.y. B.P. and about 5 m.y. B.P. The Banning-San Gabriel fault was abandoned by the San Andreas system about 5 m.y. ago.

San Andreas fault zone.--In the vicinity of the central Transverse Ranges the San Andreas fault zone consists of these segments that have different degrees of structural complexity (fig. 1). The Mojave Desert segment forms a relatively simple fault zone that extends from the Tejon Pass region to the Cajon Pass region. The segment has been the site of Pliocene through Holocene displacements. The Coachella Valley segment forms a relatively simple fault zone that extends from the Brawley seismic zone northwestward through the Coachella Valley. This segment also has been the site of Pliocene through Holocene displacements. The Transverse Ranges segment forms a complex zone of multiple fault strands that had sequential movement histories; to the northwest and southeast these strands merge to form the Mojave Desert and Coachella Valley segments.

From oldest to youngest, fault strands within the Transverse Ranges segment includes the Wilson Creek, Mission Creek, Mill Creek, and San Bernardino strands (fig. 1). Together, these strands represent the total amount of Pliocene through Recent right-lateral displacement on the San Andreas fault zone (*sensu stricto*) in southern California (4 or 5 m.y. B.P. to Recent). The Wilson Creek strand represents the first generation strand of the San Andreas. Following a prolonged period of right-lateral displacements on a throughgoing fault that generated more than 100 km of offset, the Wilson Creek strand in the vicinity of the San Bernardino Mountains was deformed and compressed into a sinuous trace before being truncated on its outboard side by the Mission Creek strand. The Mission Creek strand in turn generated about 45 km of right-lateral displacement (the same displacement as that of the Punchbowl fault in the San Gabriel Mountains, which I infer to be a continuation of the Mission Creek strand), before it too was deformed in the vicinity of the San Bernardino Mountains and succeeded by the Mill Creek strand. Both the Wilson Creek and Mission Creek strands may have been deformed as a result of left-lateral displacements on the adjacent Pinto Mountain fault. The Mill Creek strand developed inboard (east) of a westward projection of San Bernardino Mountains basement created as the Mission Creek strand and adjacent rocks were deflected and rotated to the west and southwest. Subsequent right-lateral movements on the Mill Creek strand nipped off this projection and displaced it 8 to 10 km to the northwest; subsequently, the Mill Creek strand also was deformed by left-lateral displacements on the Pinto Mountain fault and was terminated as a throughgoing right-lateral strand. The *San Bernardino strand* marks the trace of the modern neotectonic strand of the San Andreas fault within the Transverse Ranges segment. The strand is continuous with the Mojave Desert segment, and extends for 60 km along the western base of the San Bernardino Mountains to the vicinity of the Crafton Hills fault system, beyond which the San Bernardino strand loses its clear surface expression. Continuity of the San Bernardino strand with neotectonic right-lateral faults in the Coachella Valley is doubtful. In my view the San Bernardino strand has reactivated the Mission Creek strand which formerly was an active trace of the San Andreas along the base of the San Bernardino Mountains.

The Wilson Creek, Mission Creek, and Mill Creek strands all merge into the Coachella Valley segment of the San Andreas fault to the southeast; similarly, the Mill Creek, Wilson Creek, and Mission Creek-Punchbowl strands all merge into the Mojave Desert segment to the northwest. This relation requires that while multiple strands were evolving sequentially within the Transverse Ranges segment, the adjacent Mojave Desert and Coachella Valley segments were routinely generating right-lateral displacements within their relatively uncomplicated, narrow fault zones. This contrast in structural style between the Transverse Ranges segment and the two adjacent segments persisted for much of the history of the San Andreas fault (*sensu stricto*), which may require fundamental differences in crustal structure between the complex and simple fault segments.

Complications that developed in the Transverse Ranges segment during Pliocene and early Quaternary time also have characterized the late Pleistocene and Holocene neotectonic regime. Specifically, late Quaternary right-lateral displacements as the Coachella Valley segment of the San Andreas fault apparently are not carried through the southeastern San Bernardino Mountains on any of the throughgoing right-lateral faults: not only are the Mill Creek, Mission Creek, and Wilson Creek strands buried by unfaulted Quaternary alluvium of progressively older age, but the Coachella Valley segment (Mission Creek fault of some workers) appears to lose its fresh appearance and demonstrable Holocene displacements in the vicinity of Desert Hot Springs. The Coachella Valley segment of the Banning fault appears to have fresher tectonic geomorphology in the northwestern Coachella Valley, and I suggest that right-slip on the Coachella Valley segment of the San Andreas fault may have stepped left onto the Banning fault during late Quaternary time (fig. 1). Assuming that right-slip on the Coachella Valley segment is comparable to that on the Mojave Desert in Cajon Pass (25 mm/year), then 25 mm/year may have been transferred from the San Andreas fault to the Banning fault and thence into San Gorgonio Pass. In this capacity the Coachella Valley segment of the fault probably is not a new southern strand of the San Andreas fault zone, but instead represents late Quaternary reactivation of the old Pliocene Banning fault as right-slip is transferred southwestward.

San Gorgonio Pass and Crafton Hills fault system

Late Quaternary tectonism in the San Gorgonio Pass and Crafton Hills fault system represent compressional convergence and extensional pull-apart, respectively. The San Gorgonio Pass fault system is a late Pleistocene and Holocene complex of east-trending reverse and thrust faults separated by northwest-trending faults that I infer to be right-lateral tear or wrench faults developed in the upper plates of the thrusts. The San Gorgonio Pass fault zone thus is a compressional system that is overprinted on the older Banning fault in the San Gorgonio Pass region. The reactivated neotectonic Coachella Valley segment of the Banning fault feeds into the San Gorgonio Pass compressional system, and may or may not work its way through this structural maze and continue on to the northwest. The Crafton Hills fault zone is a northeast-trending series of normal faults that represent late Quaternary crustal extension normal to faults of the San Andreas system.

Neotectonic synthesis

Late Quaternary tectonism in the vicinity of the south-central Transverse Ranges may reflect a regional tectonic regime where right slip is passed from the Coachella Valley segment of the San Andreas fault onto the Banning fault, through San Gorgonio Pass and onto the San Jacinto fault, and then back onto the modern trace of the San Andreas fault in the San Bernardino valley region (fig. 1). The San Gorgonio Pass fault system may have taken up all of the slip on the neotectonic Banning fault through convergence within the thrust-fault belt. Alternatively, an unknown but possibly large amount of slip may have stepped left onto the San Jacinto fault, locally accelerating that fault above the 8 to 12 mm/year rate determined by Sharp (1981). If this extra slip steps back onto the San Andreas fault in the San Bernardino valley, then two relations could be achieved: (1) The modern San Andreas fault would extend as a youthful neotectonic feature southeastward from Cajon Pass to the Crafton Hills region, but would not necessarily continue through the San Gorgonio Pass region and on into the Coachella Valley. This would explain the difficulty most workers have in mapping the modern San Andreas fault through San Gorgonio Pass. The San Bernardino strand shows this distribution pattern. (2) Right-slip on the San Bernardino strand would not continue very far to the southeast beyond the Crafton Hills fault system. As a result, extensional pull-apart would be expected in this zone of normal faults.

Neotectonic relations in the vicinity of the south-central Transverse Ranges thus reflect a complex knot in the modern San Andreas fault zone. However, this setting is not new. Instead, the modern neotectonic framework merely is the latest phase of a complex history that has characterized the Transverse Ranges segment of the San Andreas fault for the last 2 to 2.5 million years. This history can be viewed as a consequence of the repetitive development of a left step in the San Andreas fault zone in the vicinity of the Transverse Range segment. Northwest and southeast of this left step the Mojave Desert and Coachella Valley segments of the San Andreas have relatively uneventful histories; however, where the left step developed, the San Andreas fault has responded by evolving multiple strands that succeeded each other through time as the parent fault attempted to retain its continuity through the region. These successive attempts are represented by the Wilson Creek, Mission Creek, and Mill Creek strands. The modern San Andreas fault is responding to the most recent left step by transferring slip from the

Coachella Valley segment to the Banning fault. Virtually all of the modern neotectonic faults in the vicinity of the south-central Transverse Ranges are a manifestation of this left step in the San Andreas fault zone--which poses challenging problems for siting instrument packages designed to monitor regional strain in anticipation of recognizing premonitory signals for a large earthquake on the San Andreas or San Jacinto fault zone.

References Cited

Matti, J.C., Morton, D.M., and Cox, B.F., 1985, Distribution and geologic relations of fault systems in the vicinity of the central Transverse Ranges, southern California: U.S. Geological Survey Open-File Report 85-365, scale 1:250,000.

Sharp, R.V., 1981, Variable rates of late Quaternary strike slip on the San Jacinto fault zone, southern California: Journal of Geophysical Research, v. 86, no. B3, p. 1754-1762.

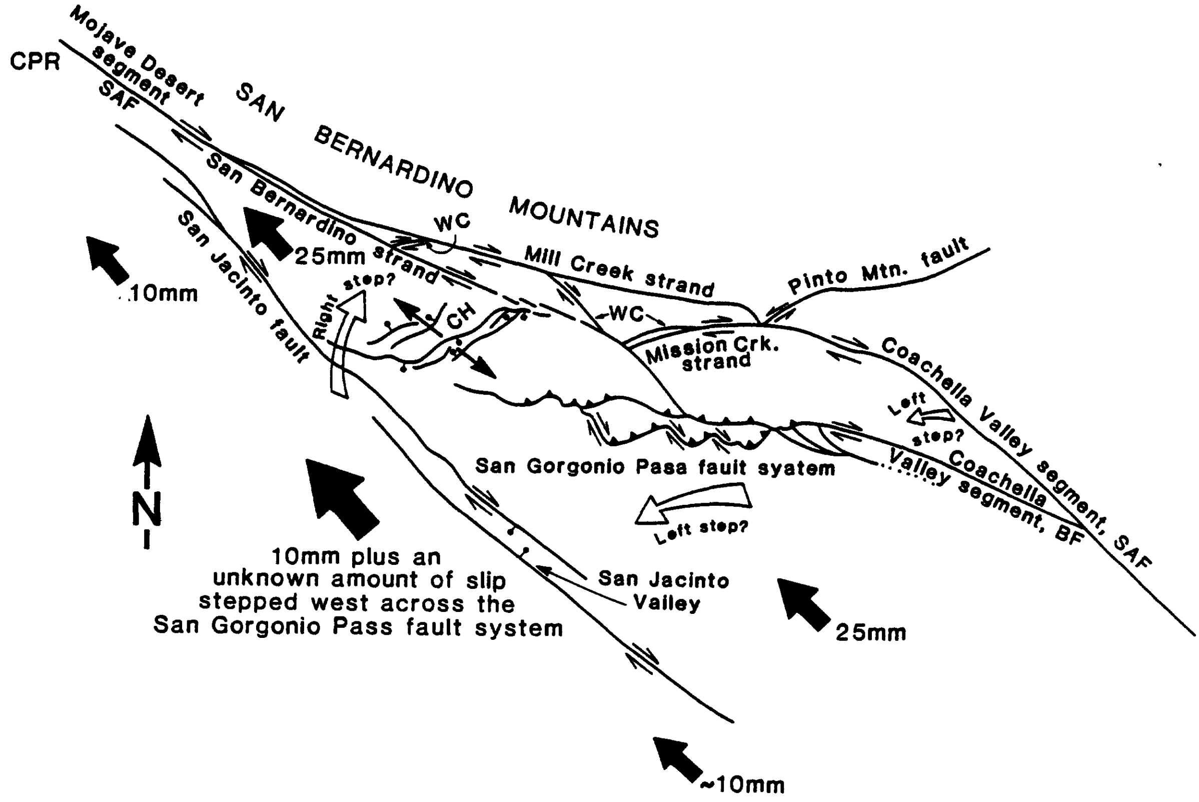
CPR
Mojave Desert segment SAF
SAN BERNARDINO MOUNTAINS
San Bernardino strand
WC
Mill Creek strand
Pinto Mtn. fault
25mm
10mm
San Jacinto fault
Right step?
CH
WC
Mission Crk. strand
Coachella Valley segment, SAF
Left step?
Coachella Valley segment, BF
San Gorgonio Pass fault system
Left step?
N
10mm plus an unknown amount of slip stepped west across the San Gorgonio Pass fault system
San Jacinto Valley
25mm
~10mm

Figure 1. -- Schematic diagram illustrating relations between faults and crustal blocks in the vicinity of the south-central Transverse Ranges, southern California. Large solid arrows indicate the relative motion of crustal blocks; large hollow arrows indicate lateral transfer slip. Small solid arrows in the Crafton Hills area indicate crustal extension in the Crafton Hills fault system. BF, Banning fault; CH, Crafton Hills, CPR, Cajon Pass region; SAF, San Andreas fault; WC, Wilson Creek strand, San Andreas fault. Geology taken from Matti and others, 1985. Ten mm slip-rate on the San Jacinto fault is an average of the 8 to 12 mm rate determined by Sharp (1981).

APPENDIX A. 7.

Evidence on Large Southern California Earthquakes from Historical Records

Duncan Agnew

Evidence on Large Southern California Earthquakes from Historical Records

Duncan Carr Agnew

IGPP A-025
University of California
San Diego

This note is a very preliminary discussion of what evidence the noninstrumental seismicity record gives on large earthquakes on the central San Jacinto fault (the 'Anza gap') and on the southern San Andreas fault (from Cajon pass to the Salton Sea). In order to make any very definite statement it is necessary to fix the size of the earthquake; in doing this I have been guided by the discussion in Sykes and Nishenko [1984]. For the Anza earthquake (called here event A) I have chosen a fault length of 40 km and slip of 1 m, giving a moment of 10^{19} N-m (for depth 8 km) and a repeat time of 100-200 years (for a slip rate of 5-10 mm/yr). For the southern San Andreas I have considered three possible earthquakes:

Event	Length (km)	Slip (m)	Moment (N-m)	Repeat (yr)
B: Cajon–Salton	200	4	$2{\cdot}10^{20}$	160
C: Whitewater–Salton	100	2	$5{\cdot}10^{19}$	80
D: Whitewater–Salton	100	4	10^{20}	160

where the recurrence interval is found using a slip rate of 25 mm/yr. I have considered two fault lengths because of the possibility that rupture does not propagate through San Gorgonio Pass (Banning on the figures), and taken two possible slip amounts to show (see below) how easily an increase in size can cause an earthquake to recede into the unrecorded past (assuming we are now a fixed number of repeat times from it).

For each earthquake there are really two separate problems to be considered. First, are there any events in the historical record which might be the ones under investigation? Before the beginning of instrumental records in 1927-28 it is impossible to associate an earthquake with a particular fault without detailed meizoseismal intensity maps or (better) observed surface rupture. The most conservative approach is to assume that an intensity pattern consistent with an earthquake of interest is evidence for that earthquake. The sparser the data, the more likely it is that the earthquake could have been elsewhere than the place we are concerned with; we naturally may then wish to take the possibility of association less seriously.

If no candidate emerges from the available data, we have the more difficult problem of deciding whether or not the candidate earthquake could have been missed, or at least obscured, in the historical record. This in turn breaks down into three questions:

What intensity distribution would be expected?

What records exist?

How likely is a particular intensity to be recorded in a given class of records?

The first question is a purely scientific one, the second a matter of historical fact, and the third very much a matter of opinion. I begin with the first question since it also bears on the issue of possible candidate earthquakes.

To compute the intensity expected as a function of distance and size I have used the formulation of Evernden *et al.* [1981], which for a single fault segment reduces to

$$I = 3.25 + .75 \log M_0 - 5.25 \log(R + C)$$

where M_0 is the moment in N-m, the magnitude being found using the relation of Hanks and Kanamori [1979], R the distance (km) and C a constant, which Evernden *et al.* take as 25-40 km. Choosing C to be 40 km gives good agreement with the expression of Hanks *et al.* [1975] for the radius of the region with intensity VI or more:

$$\log R_{\text{VI}} = .25 \log M_0 - 2.8$$

(To the degree of crudeness appropriate here we may ignore the distinction between Ross-Forel and Modified Mercalli intensity). We then find the following table of distance *vs* intensity for each event:

Event	Intensity				
	VIII	VII	VI	V	R_{VI}
A	25	60	120	200	90
B	60	110	200	330	200
C	40	90	160	260	140
D	50	100	180	290	170

Figures 1 through 4 show estimated isoseismals (on alluvium) for the four events, together with the extent of faulting; a rough allowance has been made for the finite length of the fault by elongating the isoseismals.

Turning next to the historical record and its interpretation, it must be noted that there is an asymmetry between positive and negative evidence. Any report of an earthquake is evidence for one, but in trying to decide whether the absence of historical accounts genuinely reflects the absence of an earthquake, we must be sure that the shaking could not have been ignored. We may thus ignore places and times which were not continuously inhabited by literate people (in the Californian context we may ignore oral tradition). Passing expeditions cannot be used to rule out seismic activity; even a short time after a large earthquake there are few signs of it in unsettled country. Given continuous habitation, the completeness of reporting depends on the importance of earthquake shaking, the purpose of the document, and the frequency with which entries were made. Other things being equal, the more often a record is made the lower the intensity that is likely to be recorded. A daily newspaper is thus a better record than a weekly, and a weekly very much better than an annual report.

In considering the history of California from the standpoint of earthquake records, the most useful background is provided by accounts which cover social and economic matters, such as Bancroft [1886] and Cleland [1951]. Continuous habitation of the coastal strip began with the founding of the missions: San Diego in 1769, San Gabriel in 1771, San Juan Capistrano in 1773, and San Luis Rey in 1798; the pueblo of Los Angeles was founded in 1782. Before 1790 merely surviving was the most important problem, and reports of earthquakes would be very unlikely. The Los Angeles basin and the San Diego backcountry gradually filled with ranchos, but none were established as far east as San Bernardino until the 1840's. A mission outstation was established near Redlands in 1819 and was at some later time made an asistencia, though it probably was populated mostly by Indian neophytes [Beattie 1929]. It was abandoned after an Indian attack in 1832, though the adobe walls of the one building remained standing into this century [Beattie 1930]. Settlement of San Bernardino did not come until the Mormon colony in

1850 [Raup 1940]. The San Gorgonio pass and northern Coachella valley were unfrequented until 1862, when a road was built through them over east to Arizona, with a branch running from Dos Palmas (near Mecca) to Yuma [Beattie 1925]. Thereafter traffic was fairly frequent, though there were still no white residents until the Southern Pacific built a railroad line through to Yuma in 1877. Actual settlement of the Coachella Valley did not begin until the discovery of artesian water in 1900 [Mendenhall 1909].

Along the San Jacinto fault, Riverside was founded in 1872; San Jacinto had a population of 92 in 1870, 625 in 1880 and 1200 in 1890. Although a post office was established near Anza in 1888, the area remained sparsely populated until recently (the 1890 population of Cahuilla was 90). The USGS San Jacinto quadrangle published in 1900* shows only scattered houses in the Anza valley.

Given a population, there may or may not be surviving written records. Figure 5 attempts to summarize what forms of regular reporting are available for the period 1800-1900. The sources used in compiling this figure are Geiger [1947], Dawson [1951], Gregory [1937], Darter [1942], Pinkett *et al.* [1952], and Agnew *et al.* [1979]. As I am not an expert on the Hispanic period of California history, I have undoubtedly missed possible sources for this time. I have not included all the weather records; particularly in the 1880's and after there are many short series of such data available. I have not included diaries, though they offer the best chance of filling gaps in the 1850-1880 period. I have included newspapers because they were the main source for compilers of earlier lists, and form the basis of much of the Townley-Allen catalog; they have not, however, all been searched.

The historical background to this figure is that from 1769 to 1822 California was under Spanish rule, the main organizations in the province being the missions and the military, with a small number of colonists, mostly former soldiers. The missions made annual reports, largely statistical but also describing building operations [Geiger 1947]. The provincial government and military produced extensive records, primarily administrative and tending to center on the area around the capital at Monterey.† After the revolution in Mexico in 1811, financial support for the military ceased, leading to a general decline. During the Spanish period California was largely closed to foreigners, so that though an increasing number of vessels were on the coast (hunting otter and smuggling) they left little record.

From 1822 through 1847 the province was under Mexican rule, often very loose, and with the military establishment steadily declining. The mission reports become less full with the prospect of impending secularization, and cease in 1832 when it took place; following secularization the mission buildings were often allowed to deteriorate. Less is available from the provincial records, mostly because of the general decline in efficiency but perhaps also because the energies of the governors were primarily spent on fomenting coups. Foreign trade increased throughout this period, but does not seem to have produced any source of regular reports.

With the presence of U.S. troops from 1846 onwards the likelihood of earthquakes being mentioned increases sharply, though at first there were no routine reports. The economic impulse provided by the Gold Rush, though largely passing southern California by, was strong enough to lead to increasing settlement and (more importantly for this

---

*This is Map 15 in the Atlas volume of the 1906 earthquake report [Lawson *et al.*, 1908].

†Those provincial records remaining in California were burned in 1906, though copies of many are preserved in the Bancroft Library.

discussion) the founding of several newspapers [Dawson 1951]. Regular meteorological reports at military posts at Yuma and San Diego [Darter 1942] also begin at this time. Real growth did not begin until after the Civil War, and became especially great in the 1880's. Systematic collection of earthquake reports was begun by C. G. Rockwood (of Princeton) in 1872, and for California only by E. S. Holden in 1888, both relying on newspaper accounts and weather observers for their raw material. Delibrate observation of earthquake intensities was begun by the Weather Bureau in 1915.

The period before 1850 is unfavorable for earthquake reporting in several ways. The economy was pastoral and agricultural, so that until the intensity was very high (at least VII) the shaking would produce no important effects and not be worthy of mention. Most of the records kept concern administrative and commercial matters; there are no detailed records even of the weather, despite its obvious importance. The one regular set of reports is the annual reports of the various missions, but short of outright disaster these had no reason to mention earthquakes. Keeping this in mind, my own interpretation of how likely a given intensity is to be mentioned is:

V (Generally felt, no damage): likely to be mentioned in frequent (weekly or daily) accounts, especially in meteorological records, which were concerned with natural events.

VI (Felt by all; some panic; minor cracking in adobe or weak masonry): Almost certain to be mentioned in frequent accounts; might be mentioned in infrequent ones (annual reports).

VII (Minor damage): likely to be mentioned in infrequent reports.

VIII (Severe damage): certain to be mentioned, except perhaps in reminiscences.

In support of these judgements, it may be noted that almost all the reports of earthquakes in California before 1845 mention damage, the only exceptions being diaries. Figure 6 makes this point in graphical fashion by plotting all reported intensities in San Diego from 1790 through 1980.* Because San Diego is near the Imperial Valley, moderate intensities are fairly frequent there, but before 1850 there is an obvious lack of VI or below. The absence of intensity VI before 1890 probably reflects inhomogeneity in the catalogs, since Agnew *et al.* [1979] did not assign such an intensity unless damage was mentioned.

What does all this mean for our candidate events?

There do not appear to be any earthquakes in the historical lists that correspond to any of these events. There are two shocks that could correspond to an epicenter in the Anza area, on 9 February 1890 and 28 May 1892 (Figures 7 and 8, from Toppozada *et al.*, 1981). However, the absence of reported damage from Indio or San Jacinto is not compatible with the hypothetical event A. Since the locations shown in the figures are very dependent on the isolated reports from Yuma, they should not perhaps be taken too seriously; in any case neither earthquake was large enough to be our event A (Figure 1). For this event, we can also probably rule out the period after 1880, since such a shock would have caused damage at San Bernardino and Riverside; it is unlikely, but not impossible, that it could have been missed after 1870† but before this year it easily could have been. A shock on December 16, 1858 [Toppozada *et al.* 1981], which caused

---

*The data come from Agnew *et al.* [1979], Townley and Allen [1939], and the annual *U.S. Earthquakes*, cross-checked for the larger events against Toppozada *et al.* [1981, 1982].

†Even as late as 1875 widely-felt earthquakes could escape the catalogs; on November 15 of that year an earthquake caused shaking of intensity IV in San Diego, VIII near Mexicali [Agnew *et al.* 1979] and VI in Yuma, but it is not mentioned in Townley and Allen [1939].

damaging shaking in the San Bernardino area. would be consistent with a possible Anza event. and also many others. Before 1850 such an event could easily have passed unrecorded.

Events C and D can certainly be ruled out after 1877, since a railroad ran through the middle of the meizoseismal area. As either event would have created 'newspaper-worthy' shaking in Los Angeles and San Diego and been damaging in San Bernardino, they can almost certainly be ruled out for the years from 1851 until then. For the Spanish and Mexican period it is harder to be definite, but it is my opinion that since neither event would have caused serious damage in centers of population, either could have passed unrecorded, especially in the years 1832-1845. Of course, for event C the short repeat time means that, even putting the event this late, we are long overdue for another; the doubling of the repeat time for event D means that we might well not be. This shows how weak a constraint the historical records provide on possible seismic risk, no doubt inevitably in view of their brevity. Event B, mostly because of the greater rupture length, has much higher intensities in the Los Angeles area and slightly higher ones in San Diego. It very probably would have been reported during the active period of the missions (1790-1832), and probably would have been mentioned even in the 1832-1845 interval. If this type of event is typical we may say that the last one probably occurred before 1790.

This discussion has inevitably involved a great deal of handwaving; can anything be done to improve it? Better modelling of expected intensities would certainly help, though the uncertainties will probably always be large. A systematic search for earthquake reports in the older archives has not been made since Bancroft's work in the 19th century; another search might or might not turn up anything new, but would at least guarantee that what might be there has been looked for. Somewhat the same would be true of a review of the available newspapers before 1880; though there is probably not much that was missed in compiling the Townley-Allen catalogue, some shocks were, and so a thorough search of the Los Angeles and San Bernardino records through about 1880 would be worthwhile.

References

Agnew, D., M. Legg, and C. Strand (1979), Earthquake history of San Diego, pp. 123-138 in *Earthquakes and Other Perils: San Diego Region*, ed. by P. Abbott and W. Elliott (San Diego Association of Geologists, San Diego).

Bancroft, H. H. (1886), *The History of California* (San Francisco: The History Company).

Beattie, G. W. (1925), Development of travel between southern Arizona and Los Angeles as it related to the San Bernardino valley, *Hist. Soc. South. Calif. Quart.*, **13**, 228-257.

Beattie, G. W. (1929), Spanish plans for an inland chain of missions in California, *Hist. Soc. South. Calif. Quart.*, **14**, 243-264.

Beattie, G. W. (1930), *California's Unbuilt Missions* (privately printed).

Cleland, R. G. (1951), *The Cattle on a Thousand Hills: Southern California 1850-1880* (San Marino: Huntington Library)

Darter, L. J. (1942), List of climatological records in the National Archives, *U.S. Nat. Archiv. Spec. List 1* (SuDocs Class. GS4.7:1)

Dawson. M. (1950), Southern California newspapers: 1851-1876, *Hist. Soc. South. Calif. Quart.*, **32**, 5-40. 139-174.

Evernden. J. F.. W. M. Kohler and G. D. Clow (1981). Seismic intensities of earthquakes of conterminous United States — their prediction and interpretation. *U.S. Geolog. Surv. Prof. Pap. 1223*

Geiger, M. J. (1947), *Calendar of Documents in the Santa Barbara Mission Archives* (Washington: Academy of American Franciscan History).

Gregory, W. (1937), *American Newspapers 1821-1936: A Union List of Files Available in the United States and Canada* (New York: Bibliographical Society of America)

Hanks, T. C. and H. Kanamori (1979), A moment magnitude scale, *J. Geophys. Res.*, **84**, 2348-2350.

Hanks, T. C., W. Thatcher, and J. A. Hileman (1975), Seismic moments of the larger earthquakes of the Southern California region, *Geolog. Soc. Amer. Bull.*, **86**, 1131-1139.

Lawson, A. C. *et al.* (1908), *The California Earthquake of April 18, 1906* (Washington: Carnegie Institution)

Mendenhall. W. C. (1909), Ground waters of the Indio region, California, with a sketch of the Colorado desert, *U.S. Geolog. Surv. Water-Supp. Pap. 225*

Pinkett, H. T., H. T. Finneran, and K. H. Davidson (1952), Climatological and hydrological records of the Weather Bureau (Record Group 27) *U.S. Nat. Archiv. Prelim. Invent. 38* (SuDocs Class. GS4.10:38)

Raup, H. F. (1940), San Bernardino, growth and development of a pass-site city, *Univers. Calif. Publ. Geograph.*, **8**, 1-63.

Sykes, L. R. and S. P. Nishenko (1984), Probabilities of occurrence of large plate-rupturing earthquakes for the San Andreas, San Jacinto, and Imperial faults, California, 1983-2000, *J. Geophys. Res.*, **89**,5905-5927.

Toppozada, T. R., C. R. Real, and D. L. Parke (1981), Preparation of isoseismal maps and summaries of reported effects for pre-1900 California earthquakes, *U.S. Geol. Surv. Contract 14-08-001-19200 Ann. Tech. Rep.*

Toppozada, T. R., and D. L. Parke (1982), Areas damaged by California earthquakes, 1900-1949, *U.S. Geol. Surv. Contract 14-08-001-19934 Ann. Tech. Rep.*

Townley, S. D. and M. W. Allen (1939), Descriptive catalog of earthquakes of the Pacific coast of the United States: 1769 to 1928. *Bull. Seismol. Soc. Amer.*, **29**, 1-297.

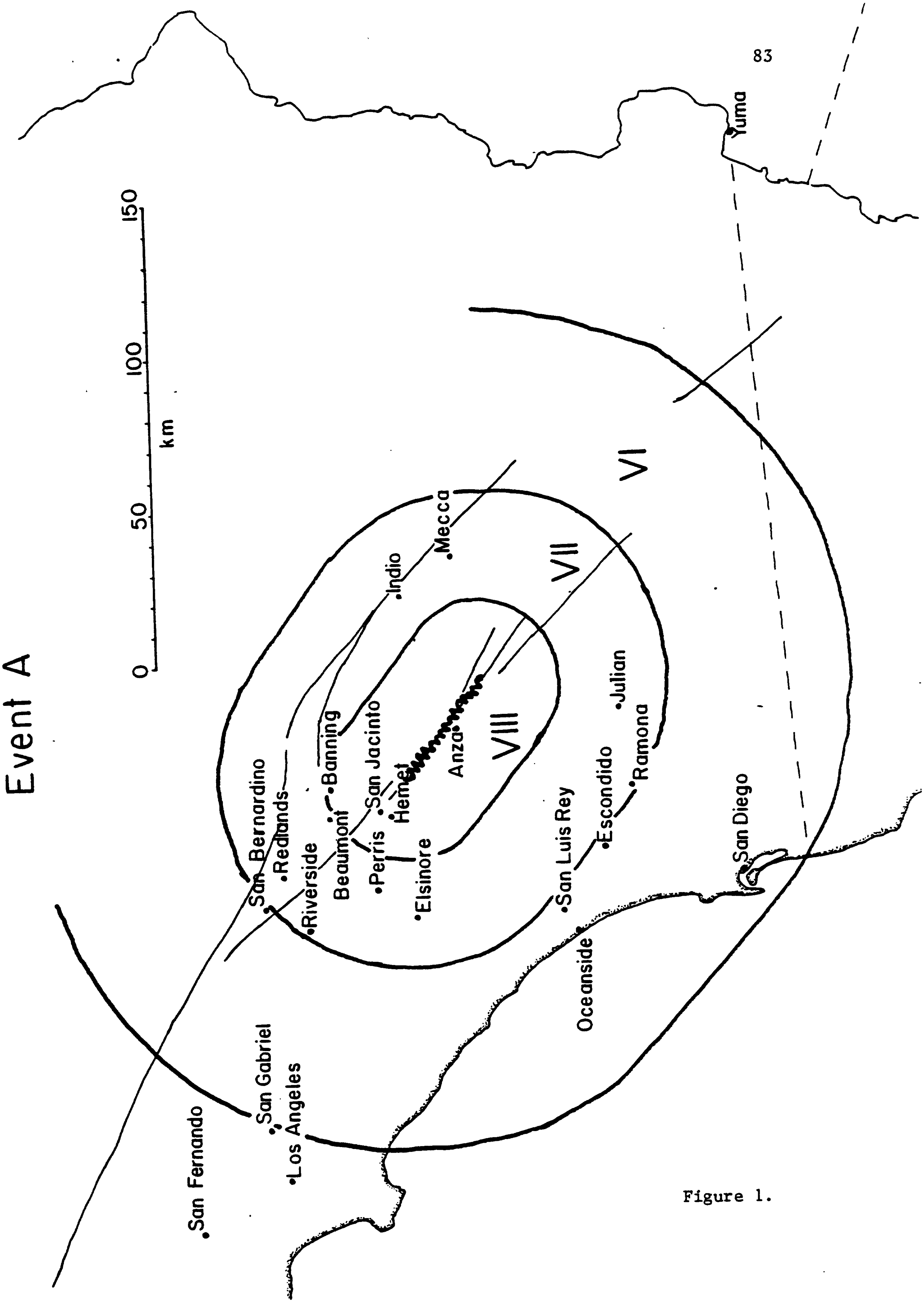
Event A
0
50
100
150
km
VI
VII
VIII
San Fernando
San Gabriel
Los Angeles
San Bernardino
Redlands
Riverside
Beaumont
Banning
San Jacinto
Hemet
Perris
Elsinore
Anza
Indio
Mecca
San Luis Rey
Oceanside
Escondido
Ramona
Julian
San Diego
Yuma

Figure 1.

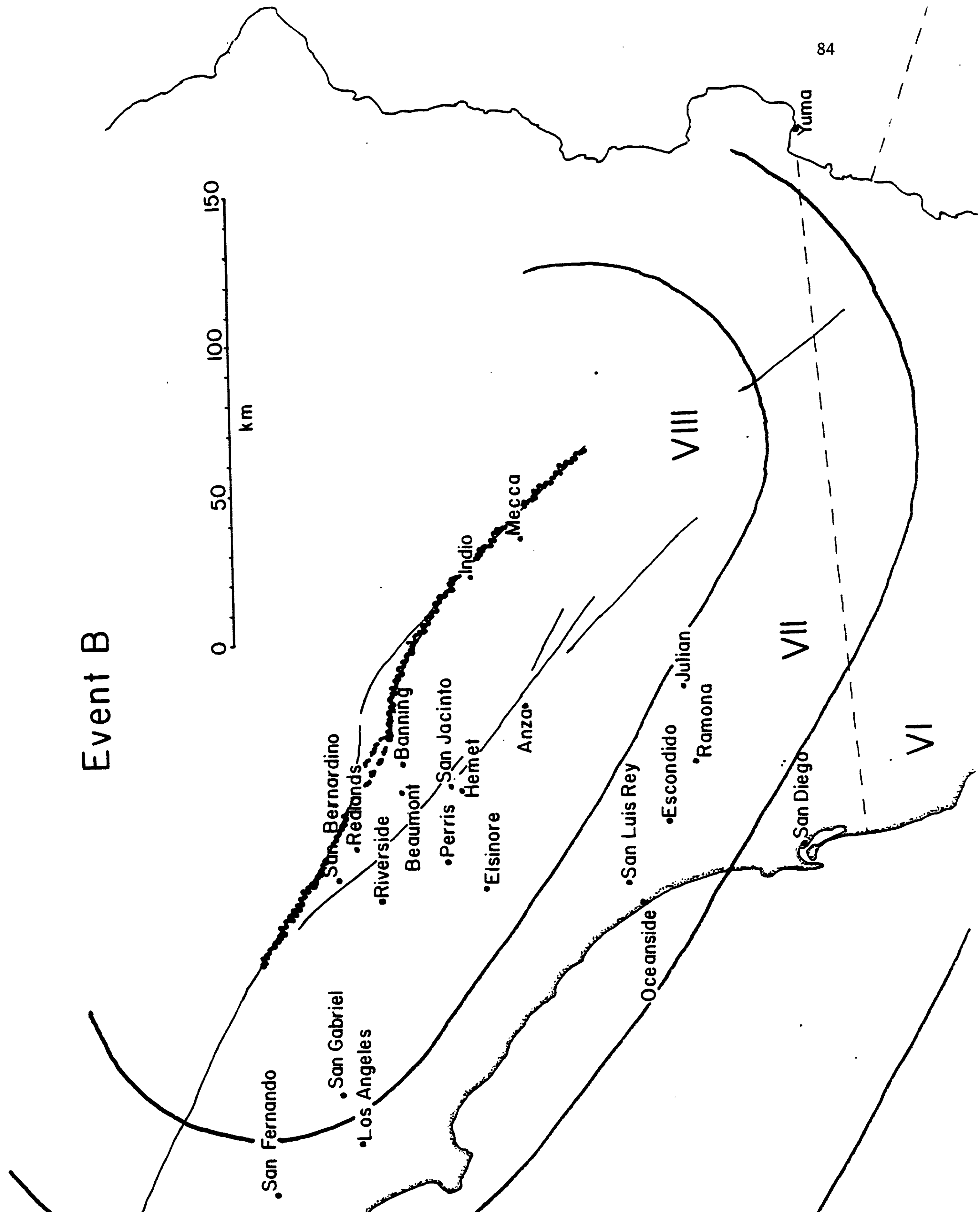
Event B
0
50
100
150
km
San Fernando
San Gabriel
Los Angeles
San Bernardino
Redlands
Riverside
Beaumont
Banning
Perris
San Jacinto
Hemet
Elsinore
Indio
Mecca
Anza
San Luis Rey
Oceanside
Escondido
Julian
Ramona
San Diego
Yuma
VIII
VII
VI

Figure 2

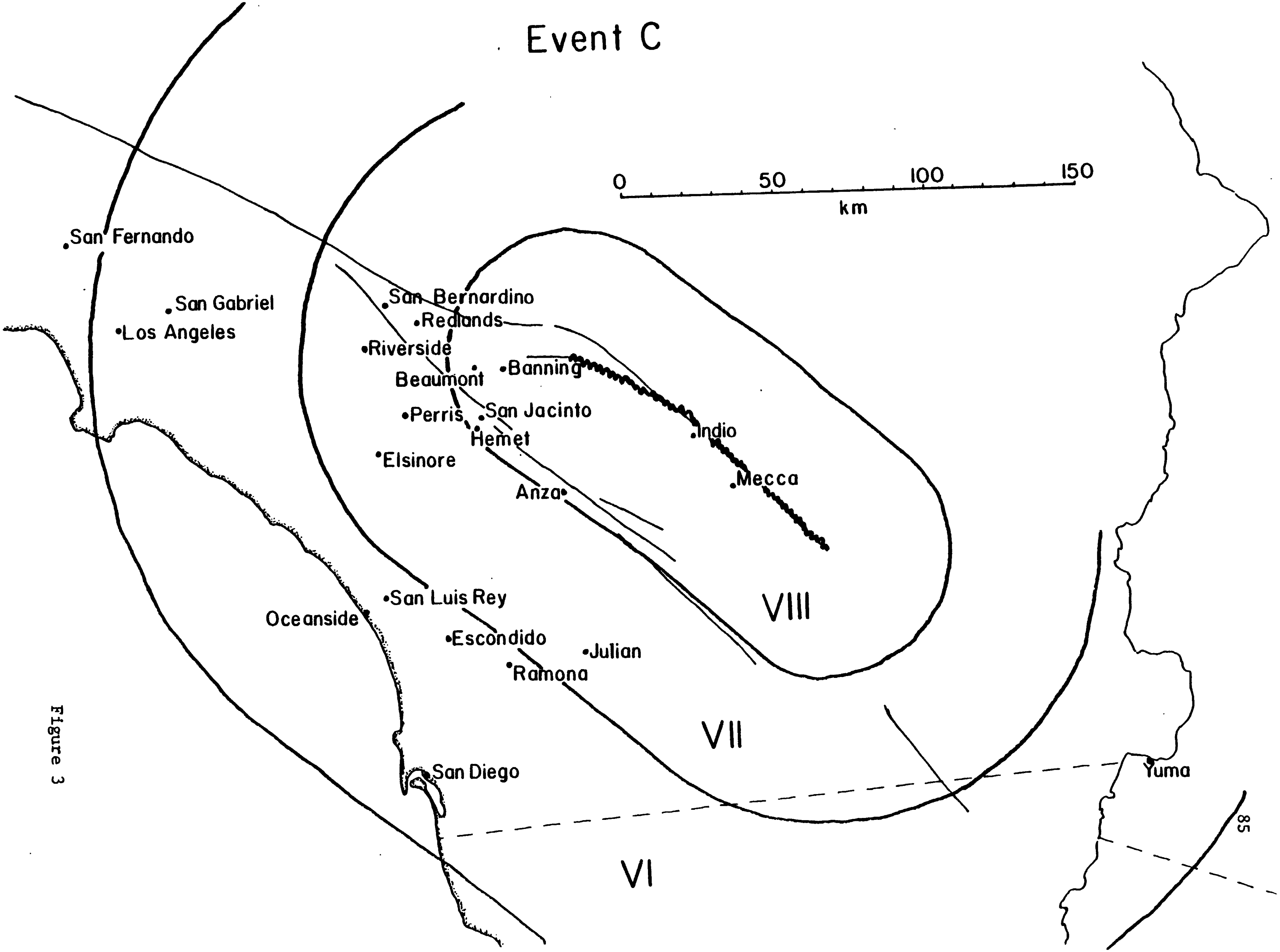
Event C

0
50
100
150
km
San Fernando
San Gabriel
Los Angeles
San Bernardino
Redlands
Riverside
Beaumont
Banning
Perris
San Jacinto
Hemet
Elsinore
Indio
Mecca
Anza
VIII
San Luis Rey
Oceanside
Escondido
Julian
Ramona
VII
San Diego
Yuma
85
VI

Figure 3

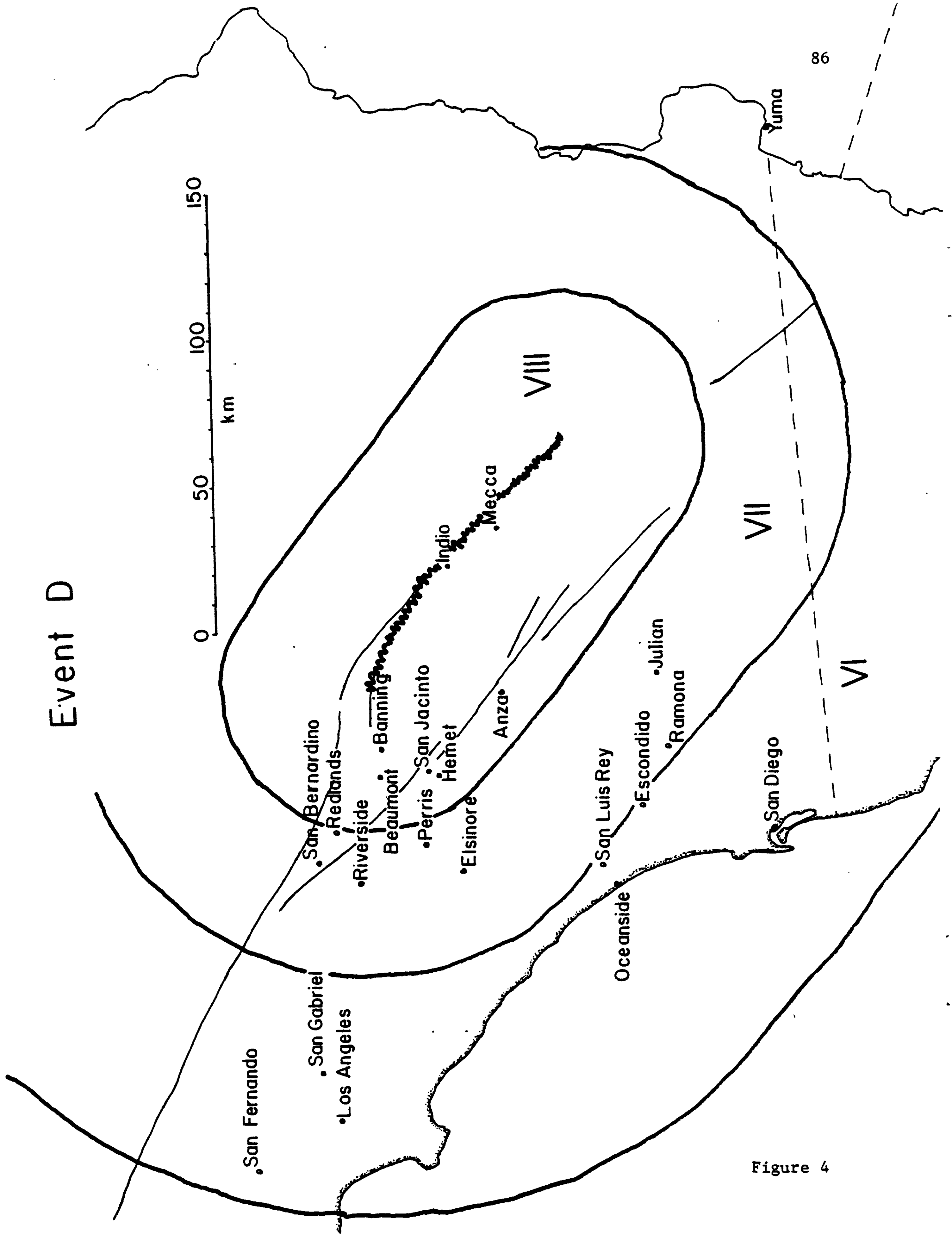
Event D
0
50
100
150
km
VIII
VII
VI
Yuma
Mecca
Indio
Banning
San Jacinto
Hemet
Anza
Julian
Ramona
Escondido
San Luis Rey
San Diego
Oceanside
San Bernardino
Redlands
Riverside
Beaumont
Perris
Elsinore
San Gabriel
Los Angeles
San Fernando

Figure 4

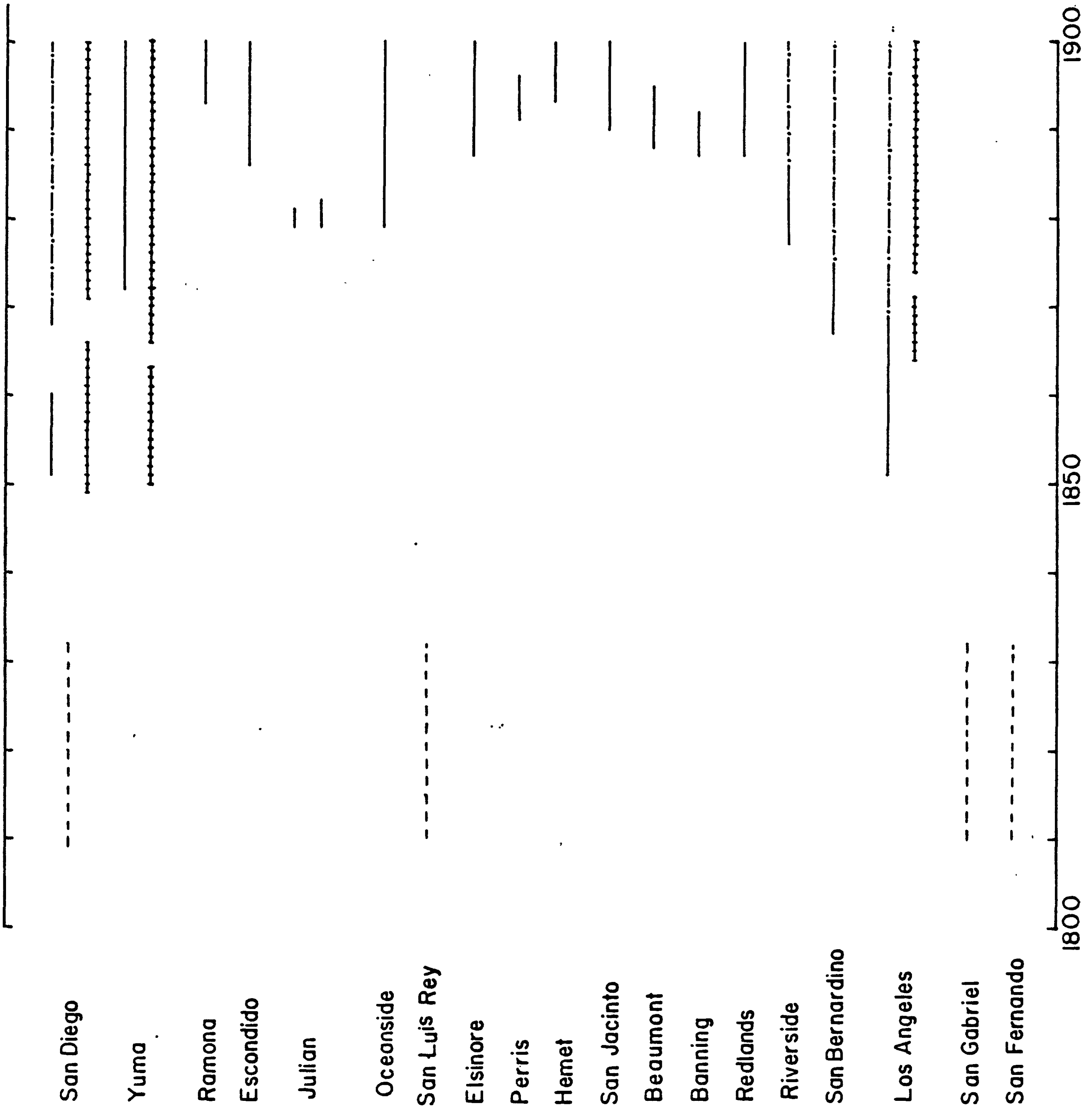

Figure 5. Coverage of the southern California area by regular reports. Dashed lines are mission annual reports, solid lines weekly newspapers and dot-dash daily newspapers; the "railroad-track" lines show weather records.

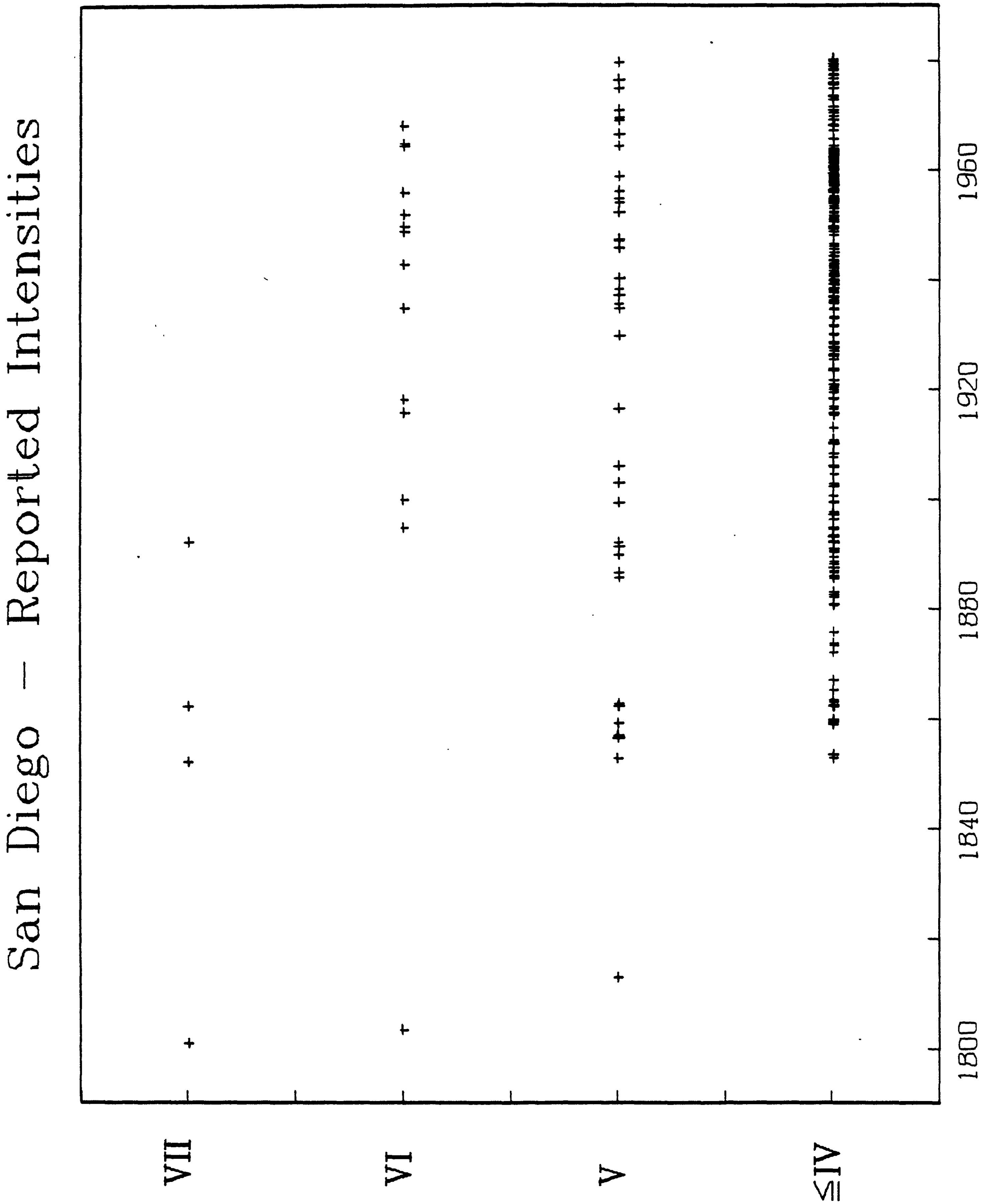
San Diego - Reported Intensities
VII
VI
V
≤IV
1800
1840
1880
1920
1960

Figure 6

CALIFORNIA DIVISION OF MINES AND GEOLOGY

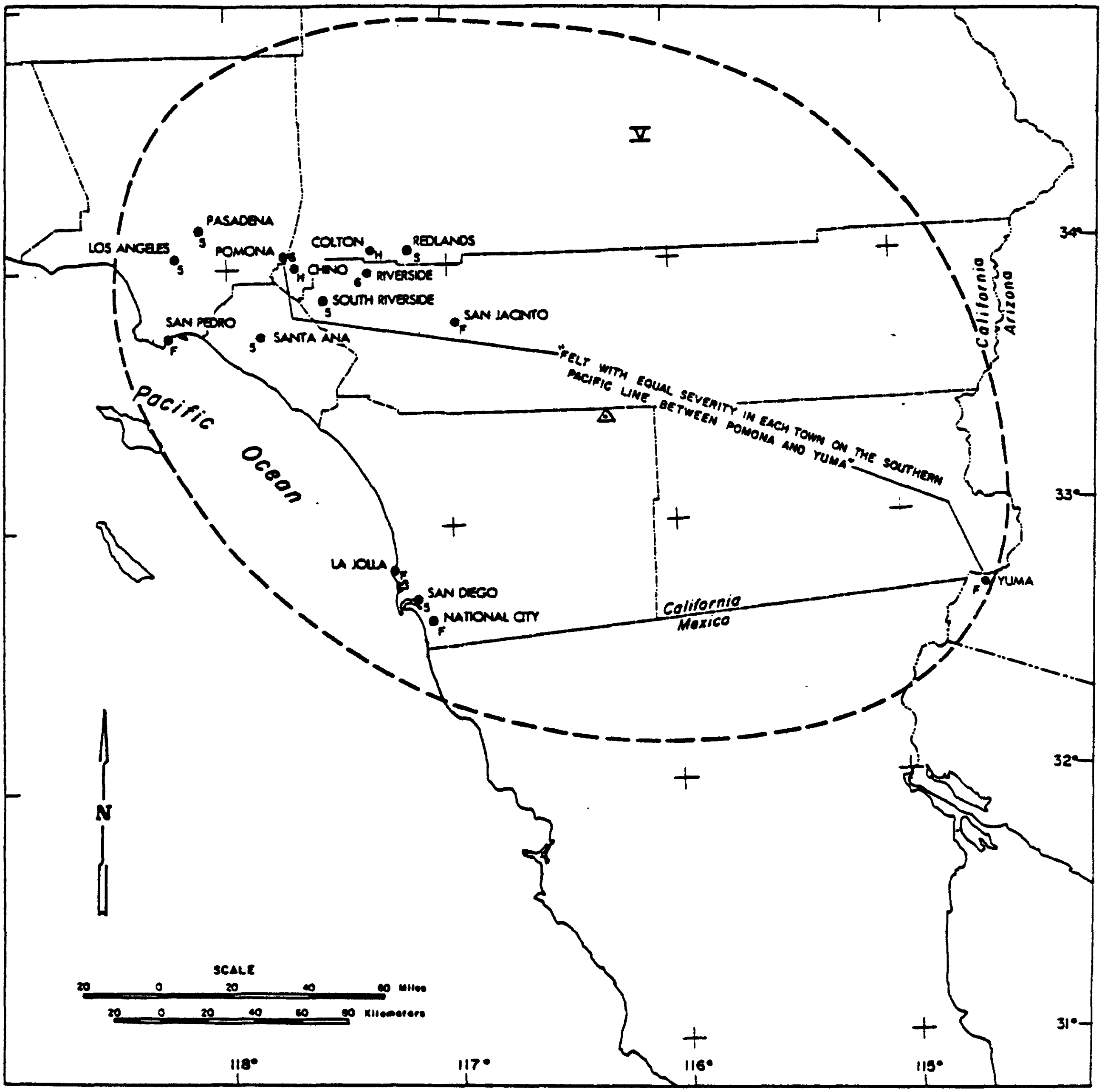
V
PASADENA 5
LOS ANGELES 5
POMONA
COLTON H
REDLANDS S
CHINO H
RIVERSIDE 6
SOUTH RIVERSIDE 5
SAN JACINTO F
SAN PEDRO F
SANTA ANA 5
"FELT WITH EQUAL SEVERITY IN EACH TOWN ON THE SOUTHERN PACIFIC LINE BETWEEN POMONA AND YUMA"
Pacific Ocean
California
Arizona
LA JOLLA F
SAN DIEGO 5
NATIONAL CITY F
YUMA F
California
Mexico
N
SCALE
20 0 20 40 60 Miles
20 0 20 40 60 80 Kilometers
34°
33°
32°
31°
118°
117°
116°
115°

FIGURE 7. MODIFIED MERCALLI ISOSEISMAL MAP

DATE: 9 FEB., 1890 TIME: 12:06 GMT

$\bullet_5$	Site reporting intensity 5 effects	$\bullet_F$	Felt
$\bullet_N$	Reported not felt	$\bullet_L$	Light
V	Zone of intensity 5 effects	$\bullet_H$	Heavy
△	Estimated epicenter	$\bullet_S$	Severe

$\bullet_F$, $\bullet_L$, $\bullet_H$, $\bullet_S$: Indeterminate intensity

——— — — — Smoothed isoseismal line, dashed where data is lacking

1981

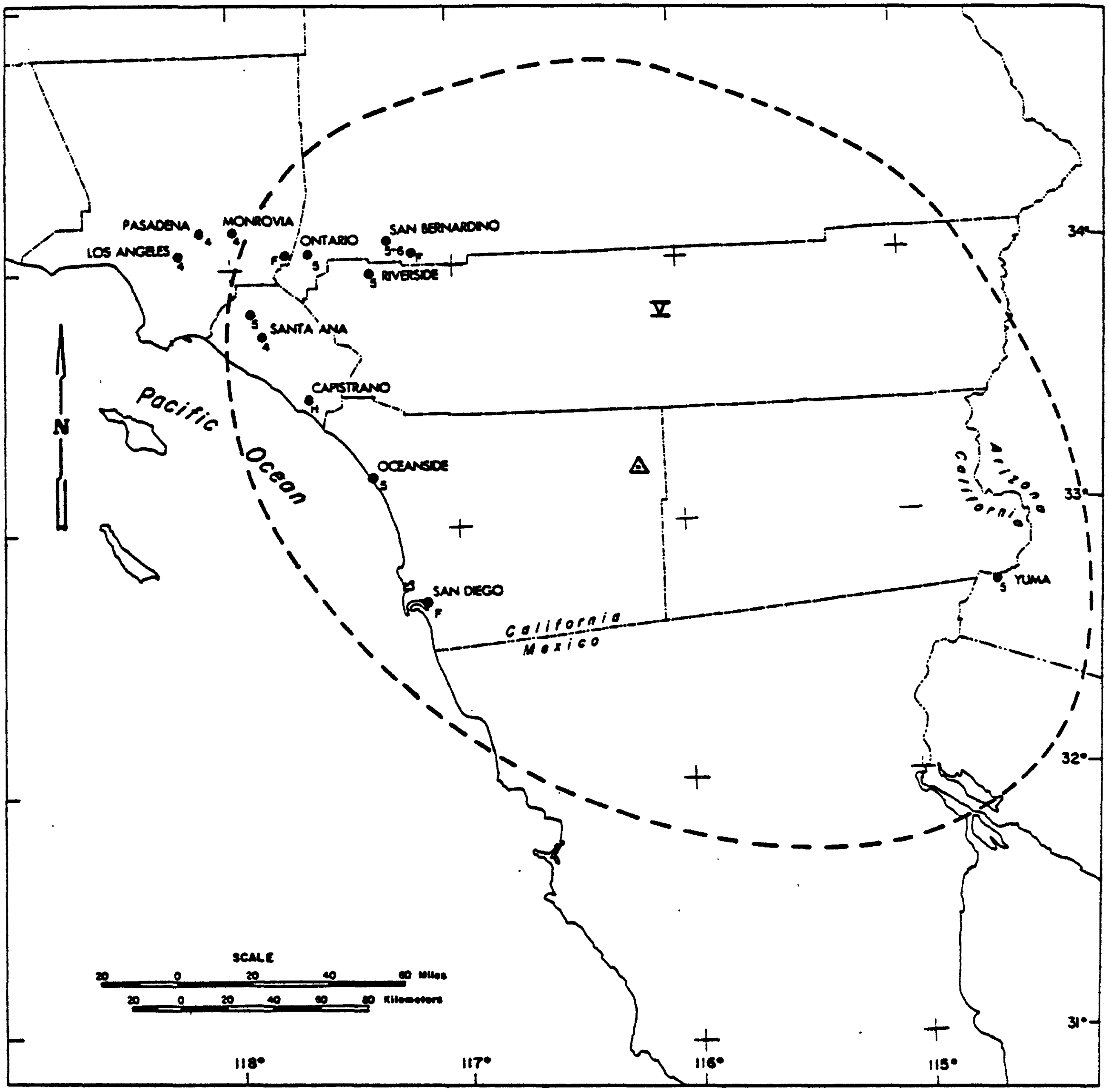
PASADENA 4
MONROVIA 4
LOS ANGELES 4
ONTARIO 5
F
SAN BERNARDINO 5-6
F
RIVERSIDE 5
V
SANTA ANA 5 4
CAPISTRANO H
Pacific Ocean
N
OCEANSIDE 5
SAN DIEGO F
Arizona
California
YUMA 5
California
Mexico
34°
33°
32°
31°
118°
117°
116°
115°
SCALE
20 0 20 40 60 Miles
20 0 20 40 60 80 Kilometers

FIGURE 8 MODIFIED MERCALLI ISOSEISMAL MAP
DATE: 28 MAY, 1892 TIME: 11:15 GMT

$\bullet_5$ Site reporting intensity 5 effects
$\bullet_N$ Reported not felt
V Zone of intensity 5 effects
△ Estimated epicenter

$\bullet_F$ Felt
$\bullet_L$ Light
$\bullet_H$ Heavy
$\bullet_S$ Severe
} Indeterminate intensity

1981

———— — — — Smoothed isoseismal line, dashed where data is lacking

APPENDIX A. 8.

Earthquake Potentials along the San Andreas Fault

Kerry Sieh

Summary Statement for NEPEC March 29, 1985

by Kerry Sieh

Based upon the historical and prehistorical record, three segments of the San Andreas fault in southern California appear to be most likely to generate a larger (M 7) earthquake within the next 50 years. These segments are labeled 2, 5 and 6 in Figure 1. Segments labeled 1, 3 and 4 are unlikely to generate large earthquakes within the next 50 years.

Segment 5 is the southern portion of that reach of the fault which last broke in 1857 (see Fig. 2). Offsets along segment 5, have commonly been about 3 meters (Fig. 3, from Sieh and Jahns, 1984) and the average recurrence interval between the latest 12 large slip events is between 100 and 200 years. (Fig. 4, from Sieh, 1984). The probability of a large (M 7) earthquake along this segment within the next 50 years is about 50%.

Segment 6 is the only portion of the San Andreas fault that has not sustained large offsets in the period of historical record. Nevertheless, the record of the geologically recent past leaves no doubt that this segment is as active as other segments. The long-term slip rate of this segment is about 25mm/yr. (Figs. 2 and 5, from Weldon and Sieh, 1985). Work in progress near Indio suggests that this segment of the fault produces large earthquakes about as often as those historically active sections to the northwest. This observation, coupled with the historical dormancy of this reach and its local low-level creep, lends credence to suggestions that segment 6 has a high probability of generating a large destructive earthquake within the next several decades.

FIGURE: 1

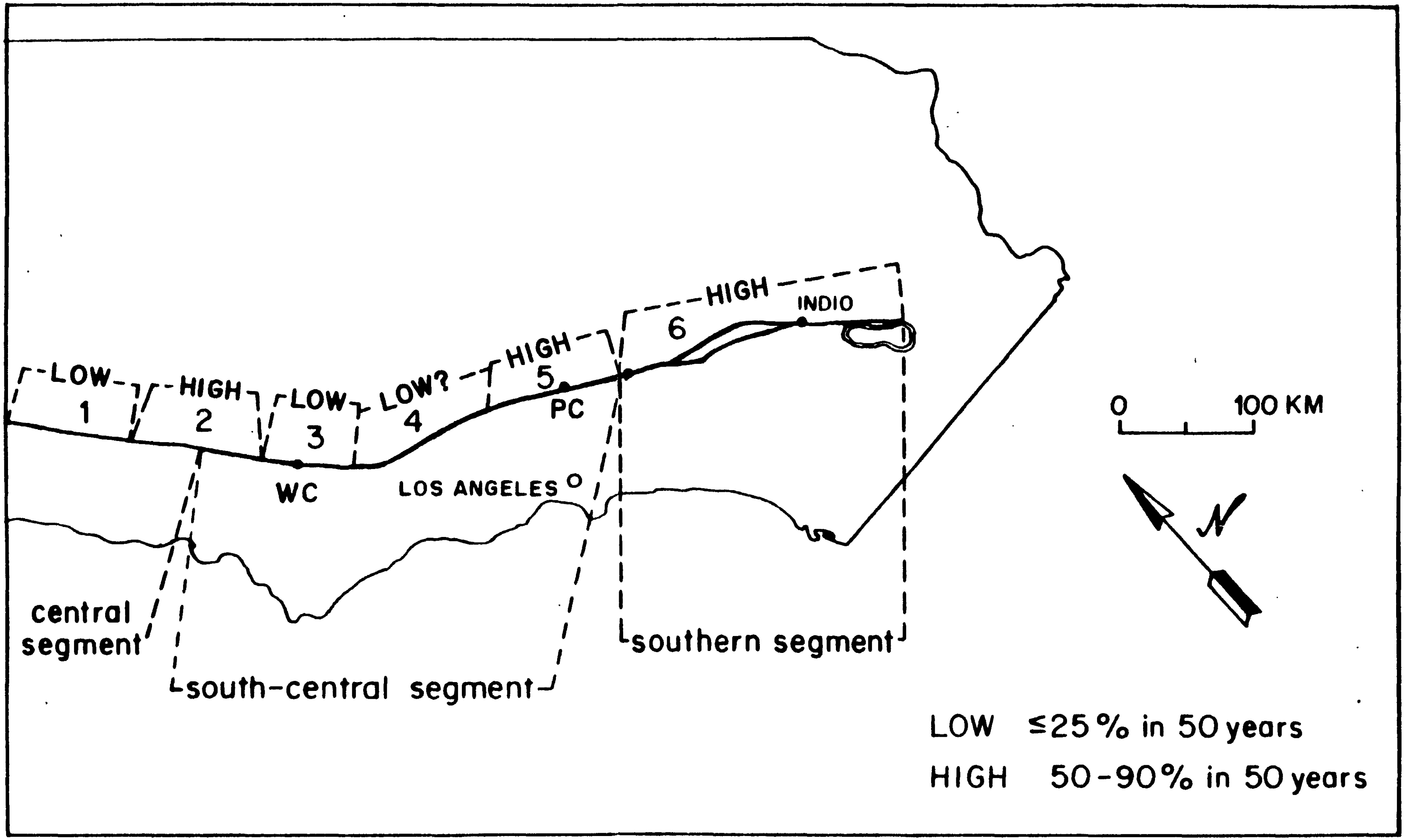
LOW
1
HIGH
2
LOW
3
LOW?
4
HIGH
5
PC
6
HIGH
INDIO
WC
LOS ANGELES
central segment
south-central segment
southern segment
0
100 KM
N
LOW ≤25 % in 50 years
HIGH 50-90% in 50 years

Potentials for earthquakes along the San Andreas Fault over the next 50 years.

FIGURE: 2

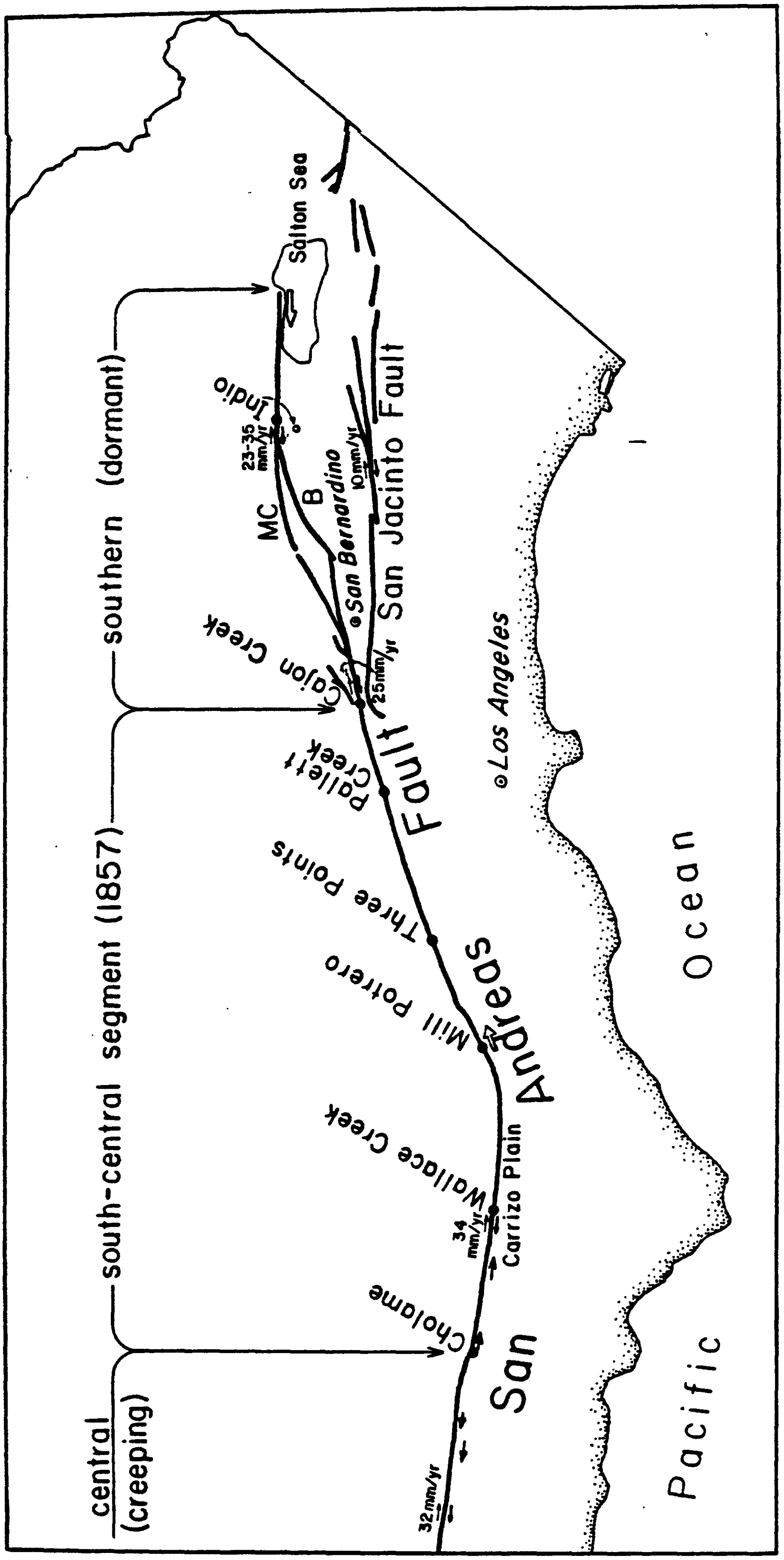
central
(creeping)
south-central segment (1857)
southern (dormant)
Salton Sea
Indio
23-35 mm/yr
MC
B
San Bernardino
10mm/yr
San Jacinto Fault
Cajon Creek
25mm/yr
Los Angeles
Pallett Creek
Three Points
Mill Potrero
Wallace Creek
Carrizo Plain
34 mm/yr
Cholame
32 mm/yr
San Andreas Fault
Pacific Ocean

FIGURE: 3

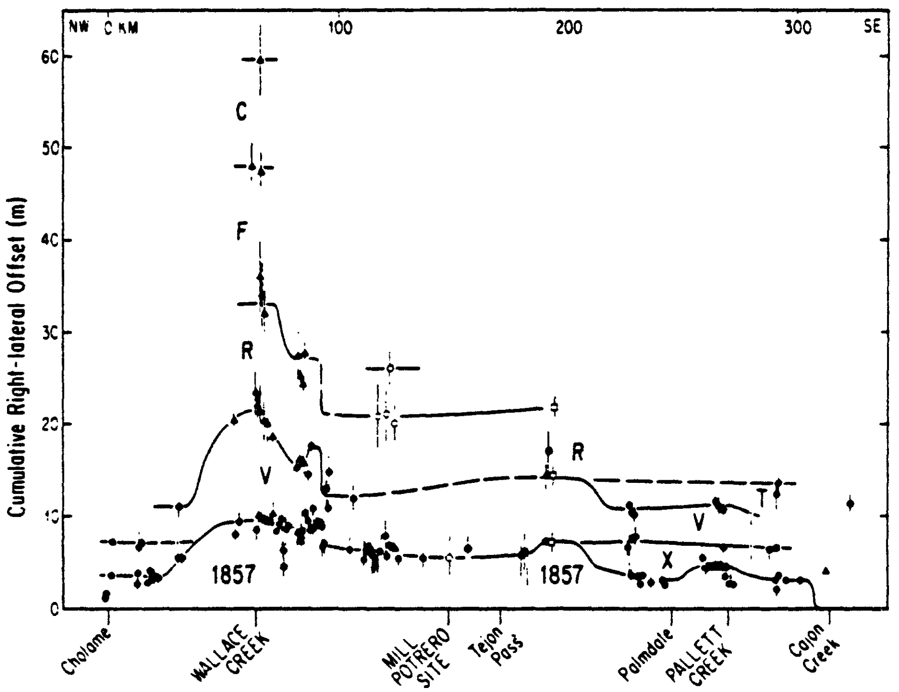

Figure 10. Right-lateral offsets measured along the south-central (1857) segment of the San Andreas fault suggest that slip at each locality is characterized by a particular value. Solid circles are data from Sieh (1978c), with poor-quality data deleted. Open circles are data from Davis (1983). Triangles are new data and remeasurements at sites reported by Sieh (1978c). Open squares are new data. Vertical bars indicate magnitude of imprecision in measurement.

FIGURE: 4

TABLE 2. Estimated Dates of Latest 12 Earthquakes at Pallett Creek

Event	Date.[a] A.D.	Remarks
Z	1857	Historically documented.
X	1720 ± 50	Unit 81 date is within period from 140 to 305 years B.P.[b] (i.e., 1730 ± 80 A.D.); event occurs at top of unit, so ~20 years must be added to unit 81 date[c], thus 1750 ± 80 A.D.; historical record precludes event after 1769, thus 1720 ± 50 A.D.
V	1550 ± 70	Weighted average of upper unit 68 (1405–1630 = 1518 ± 112 A.D.) and unit 72 (1485–1660 = 1573 ± 88 A.D.), which bracket the earthquake horizon.
T	1350 ± 50	Unit 61 date is within period from 1280 to 1380 (i.e., 1330 ± 50 A.D.); event occurs at top of unit, so ~20 years must be added to unit 61 date, thus 1350 ± 50 A.D.
R	1080 ± 65	Weighted average of samples PC-223a, PC-28, and PC-207c, which bracket the earthquake horizon.

TABLE 3. Estimated Dates of Earthquakes A Through N, Using Alternate Method

Event	Date, A.D.
N	1015 ± 100
I	935 ± 85
F	845 ± 75
D	735 ± 60
C	590 ± 55
B	350 ± 80
A	260 ± 90

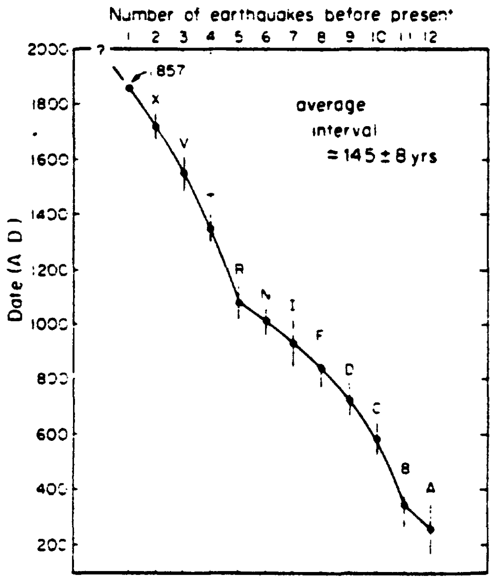

Fig 16 Revised dates of each earthquake at Pallett Creek :

FIGURE: 5

SLIP RATE ON THE SAN ANDREAS FAULT AT CAJON CREEK

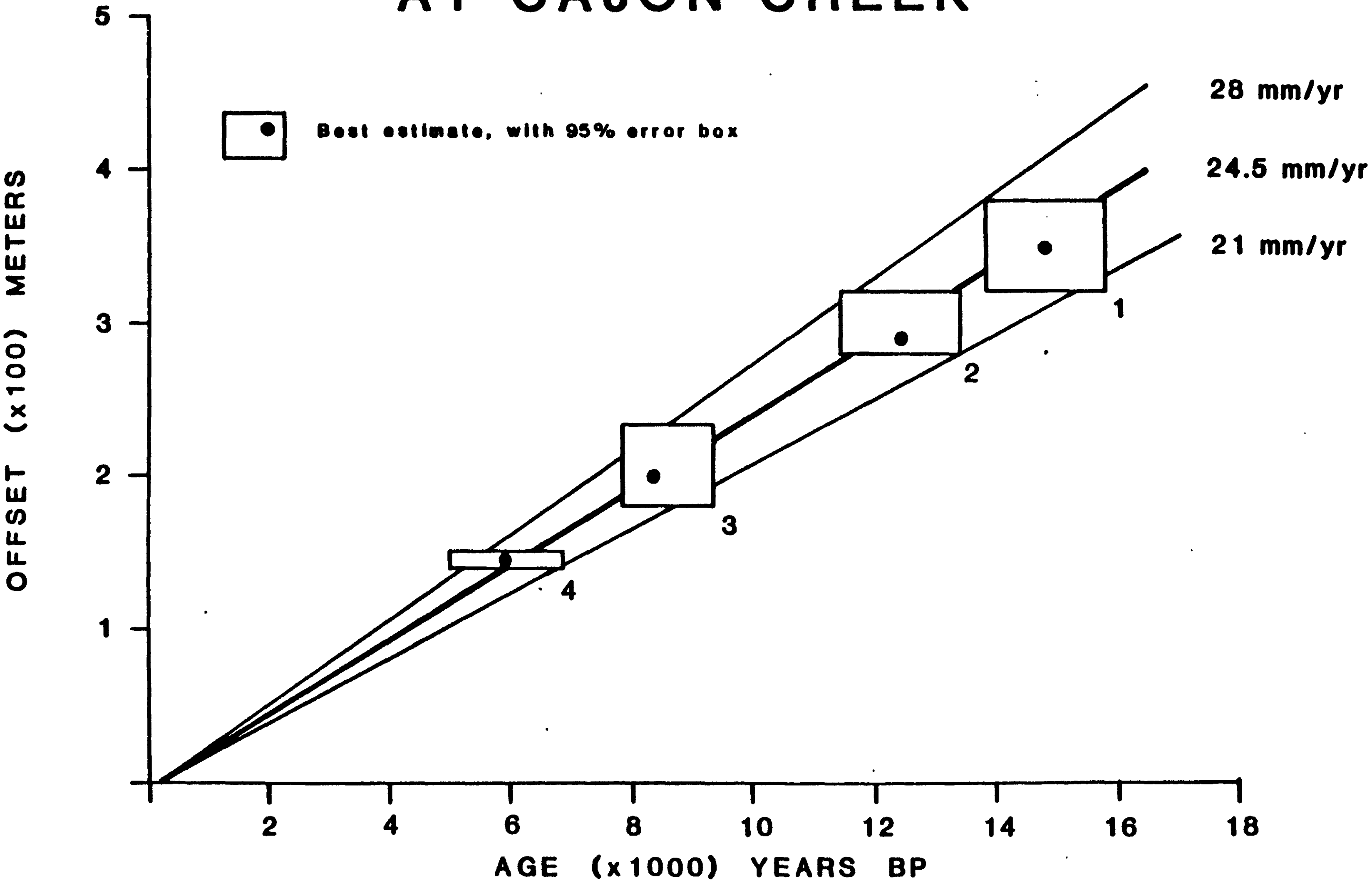

FIGURE 7. Slip rate on the San Andreas fault at Cajon Creek. The points represent our best estimates of the offsets and ages and the boxes represent 95% confidence limits. Each box represents independent offset features, radiocarbon dates and geologic assumptions. The points are not in the center of the boxes due to the asymmetric limits on some of the ages and measurements. The heavy line represents our best estimate of the slip rate at Cajon Creek and the lighter lines are the limits on the rate, constrained to touch each box. The starting point for each line is 170 years ago. This is our best estimate for one-half recurrence intervals after the last earthquake (see text for details).

APPENDIX A. 9.

Forecast Model for Large and Great Earthquakes in Southern California

W. D. Stuart

Forecast Model for Large and Great Earthquakes in Southern California

W. D. Stuart
U.S. Geological Survey
525 S. Wilson Ave.
Pasadena, California 91106

This report describes a procedure for trying to forecast large and great earthquakes on the locked section of the San Andreas fault in southern California. Like numerical weather forecasting, the procedure combines a mechanical theory with repeated field measurements. The mechanical theory is a quasistatic instability model which simulates both pre- and coseismic faulting; the field measurements are a set of lengths, slips, and times of historic and prehistoric earthquake offsets reported in Sieh and Jahns (1984). The field data constrain values of model parameters, such as the shape of an assumed stress-slip law for the fault and the variation of fault strength along strike between Parkfield and the Salton Sea.

Once parameter values are set, the model is potentially useful for earthquake prediction in two ways. First, since model instabilities and offset data for past times agree fairly well, model instabilities corresponding to future times are predictions of future earthquakes. However, the uncertainties of predicted future times would be comparable to uncertainties of recurrence intervals of past earthquakes. Thus a prediction made this way with a model would be no more precise than a prediction made using probabilities and recurrence intervals, except to the extent that the model accounts for variable recurrence times, for example through interaction of different instabilities.

The second way to use a model for prediction is to exploit the accelerated fault slip that occurs shortly before instability. The accelerated fault slip occurs mainly at depth and is large enough to cause recognizable rate changes in lengthening of hypothetical trilateration lines on the ground surface. Since the time scale of the precursory deformation is a fraction of the recurrence interval, the precision of a forecast would be considerably increased over the precision of a forecast based on just recurrence times. In the rest of this report I shall describe the model, then show a comparison of theoretical and observed earthquake times, and finally present computed length changes of hypothetical trilateration lines.

The details of the model are given in Stuart (1984) and Stuart et al. (1985). Figure 1 is a perspective sketch showing the seismogenic part of the fault zone as a long patch of brittle rock. At every position on the patch the fault is assumed to obey a Gaussian shaped stress-slip law, τ^f vs. u, as shown at the bottom of Figure 1. The peak stress (strength) S of the fault varies with depth and distance along strike. Starting at the ground surface, peak stress increases downward to a maximum value at 6 km, then decreases towards greater depth; the patch is effectively 12 km high. The variation of peak stress along strike is a free parameter whose functional values are found by trial so that the model simulates the offsets in Sieh and Jahns (1984). The part of the remaining fault plane closest to the patch is assumed to undergo free slip. The fault plane farther from the patch and surrounding the free slip area is subjected to an imposed fault slip rate which is the forcing in the problem. The increasing imposed slip approximates the relative motion of the North America and Pacific plates, and loads the patch sections toward unstable failure. The failure time of a particular patch section will depend on the patch strength and the prior failure sequence of all patch sections. Immediately after a patch section fails, the section is assumed to heal to full strength so that another instability can occur in the future.

Figure 2 shows the geometry of the boundary value problem for the qualitative model in Figure 1. Figure 2a is a map view showing how the traces of the San Andreas, Imperial, Cerro Prieto, and San Jacinto faults are approximated by straight segments. Each trace segment is the top edge of a vertical, rectangular, planar area which is a dislocation surface. Most of the rectangular areas are divided into smaller rectangular areas; all rectangular areas have uniform slip and are referred to as cells. Figure 2c shows the cells in side view. Cells in shaded areas have the imposed slip rate indicated, whereas slips of all other cells are computed results.

The simulation of fault slip vs. time for all non-imposed slip cells is obtained by numerically solving a system of simultaneous nonlinear equations. Each equation has the form of (1) and expresses

$$\tau^r + \Sigma\tau^d - \tau^f = 0 \qquad (1)$$

shear stress equilibrium at a cell center. The terms in equation (1) are τ^r, the dislocation stress from imposed slip rate cells; $\Sigma\tau^d$, the sum of all other dislocation shear stresses; and τ^f, the Gaussian stress-slip law. In general, fault slip and stress vary with time and from cell to cell. Since the patch is relatively strong, slip of patch sections lags slip elsewhere until the patch sections catch up during unstable slippage. The $\tau^p(\xi)$ plot in Figure 2b shows the inferred variation of patch strength. ^{p}, which is assumed to have piecewise linear variation along strike, is found to have five sections of alternately low and high strength. The high strength sections coincide approximately with the major bends or structural knots of the fault.

Figure 3 is a space-time diagram showing the lengths and dates of instabilities. The names R, T, V, X, and Z correspond to earthquake offsets of the same names in Sieh and Jahns (1984). Numbers in parentheses are estimated dates of offsets at specific field sites. The dates near Indio are from Sieh (1984b) and are preliminary. The remaining dates are from Sieh and Jahns (1984) and Sieh (1984a). The main assumptions for the model are that earthquake R broke the entire locked section of the fault, and that earthquake X broke from Lake Hughes to the Salton Sea. In the simulation, the next future unstable slips occur on patch section 1 in 1993, section 5 in 1993, and section 3 in 2052.

The remaining four figures show the length changes of hypothetical trilateration lines before the two instabilities in 1993. Figures 4 and 5 show the length changes of lines which are respectively lengthening and shortening before unstable slip of section 1. Curves on the plots have been shifted vertically so that from top to bottom they are in north-south order along the fault. The small kinks in computed curves are due to the time step size of one year. The inset diagram in each figure is a fault trace map showing the location and orientation of lines. Line ends are numbered, and a line is identified by a number pair. Locations of line ends are chosen to detect changes in fault slip rate at about 10 km depth, which is where part of the fault patch fails years to decades before instability. Patch section ends are marked by ticks for reference.

In Figures 4 and 5, the lengthening rates are constant until about 15 years before instability, which appears as a jump of line length in the year 1993. Lines 1-2, 2-3, 3-4, and 4-5 show rate changes starting about 1980. The light lines are extrapolations of earlier trends. The predicted rate changes for several of the lines are large enough to be detected by current geodetic techniques using a geodolite. The small symbol just above line 1-2 at the 1980 position is a representative error bar (1 cm) of actual trilateration surveys. For unknown reasons, successive annual measurements often have a scatter about a long term trend line of one or more times an error bar height. Consequently, it appears that several years of semi-annual measurements would be needed to detect the precursory rate change of line 1-2.

Figures 6 and 7 are similar plots for trilateration lines near patch section 5. Preinstability rate changes are much less prominent than in Figures 4 and 5, and start only a few years prior to instability. The height of the error bar symbol above line 27-28 at the 1980 position suggests that such precursory rate changes could be detected in field data.

Results of this and other model simulations suggest that in general accelerated fault slip and ground surface deformation are large enough to detect with existing geodetic instruments. Therefore, if the model is realistic, there is a good chance that a large or great earthquake could be anticipated if a sufficient number of properly located trilateration lines are measured frequently enough. Usually the largest preinstability rate changes occur at patch section ends, where fault strength undergoes a jump, and these locations would be the best locations for installation of new trilateration lines. The model needs more refinement and testing to put bounds on the likely amplitudes and onset times of precursory deformation. The most useful field data for constraining the model would be measurements of repeated earthquake offsets along patch section 1, 4, and 5.

References

Sieh, K. E., Lateral offsets and revised dates of large prehistoric earthquakes at Pallett Creek, southern California, J. Geophys. Res., 89, 7641-7670, 1984a.

Sieh, K. E., Late Holocene behavior of the San Andreas fault, U. S. Geol. Survey Open File Report 84-628, 126-128, 1984b.

Sieh, K. E., and R. H. Jahns, Holocene activity of the San Andreas fault at Wallace Creek, California, Geol. Soc. Am. Bull., 95, 883-896, 1984.

Stuart, W. D., Instability model for recurring large and great earthquakes in southern California, Pure Appl. Geophys., 122, 1984, in press.

Stuart, W. D., R. J. Archuleta, and A. G. Lindh, Forecast model for moderate earthquakes near Parkfield, California, J. Geophys. Res., 90, 592-604, 1985.

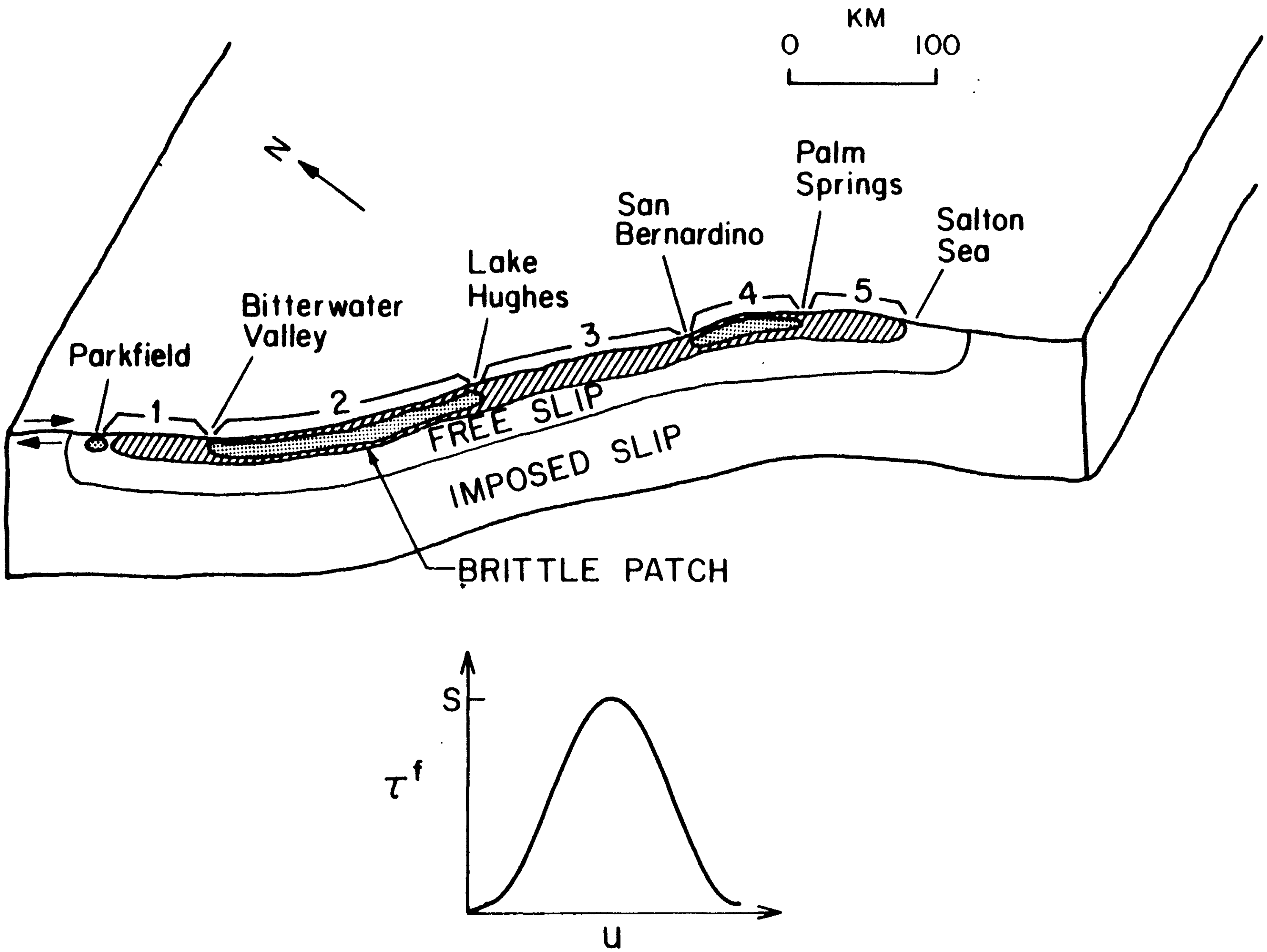
KM
0
100
N
Parkfield
1
Bitterwater Valley
2
Lake Hughes
3
San Bernardino
4
Palm Springs
5
Salton Sea
FREE SLIP
IMPOSED SLIP
BRITTLE PATCH
S
τ^f
u

Figure 1. Qualitative instability model showing five sections of brittle patch on the San Andreas fault.

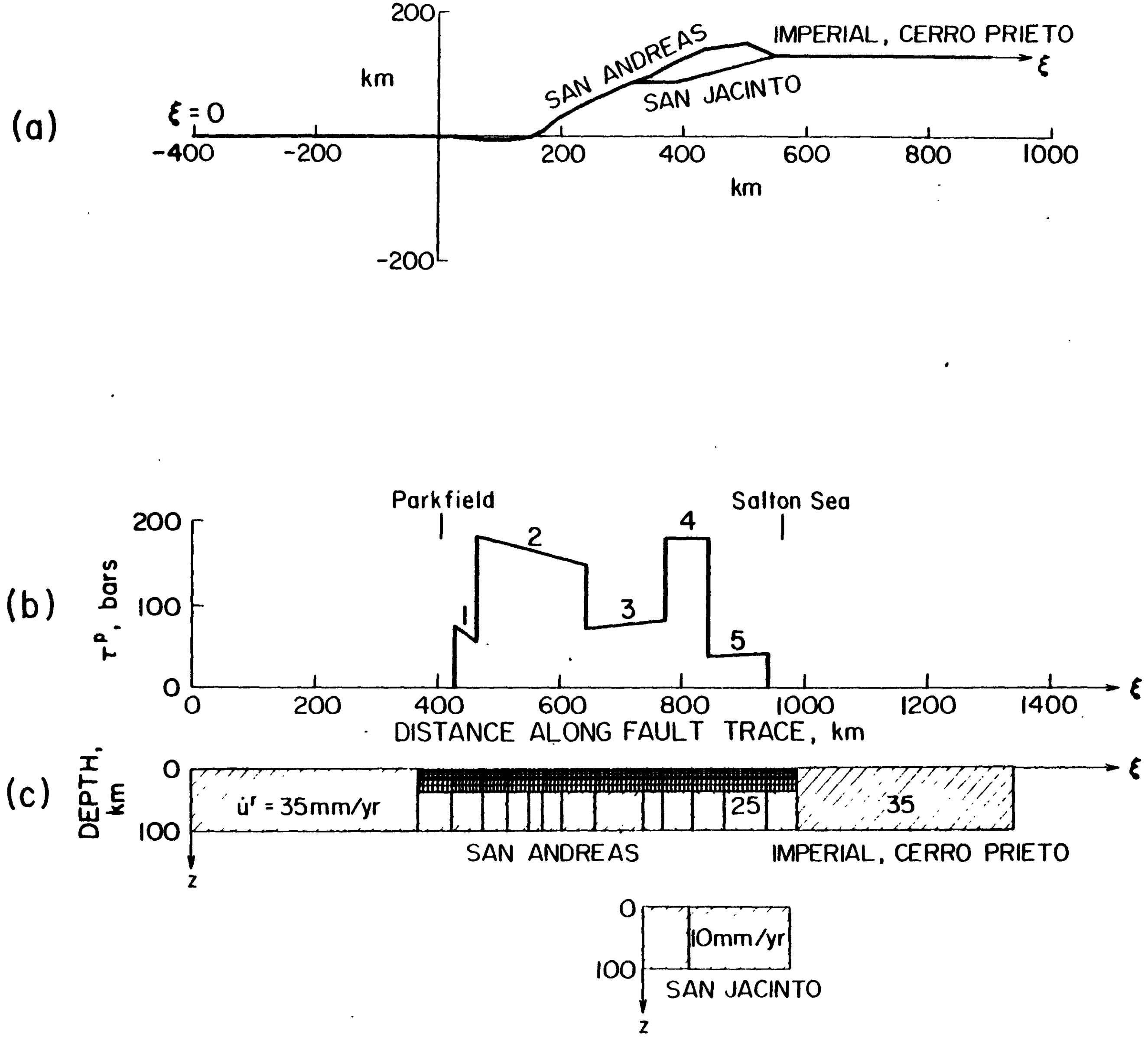
(a)
200
km
-200
ξ = 0
-400
-200
200
400
600
800
1000
km
SAN ANDREAS
SAN JACINTO
IMPERIAL, CERRO PRIETO
ξ
(b)
τ^p, bars
200
100
0
Parkfield
Salton Sea
1
2
3
4
5
0
200
400
600
800
1000
1200
1400
ξ
DISTANCE ALONG FAULT TRACE, km
(c)
DEPTH, km
0
100
u̇^r = 35mm/yr
25
35
ξ
z
SAN ANDREAS
IMPERIAL, CERRO PRIETO
0
100
10mm/yr
SAN JACINTO
z

Figure 2. Boundary value problem for numerical model. (a) Traces of San Andreas, Imperial, Cerro Prieto, and San Jacinto faults showing straight segments of model fault. (b) Fault strength at 6 km depth vs. distance along trace. (c) Side view of flattened fault plane showing cells of uniform slip. Numbers in shaded areas are imposed slip rates.

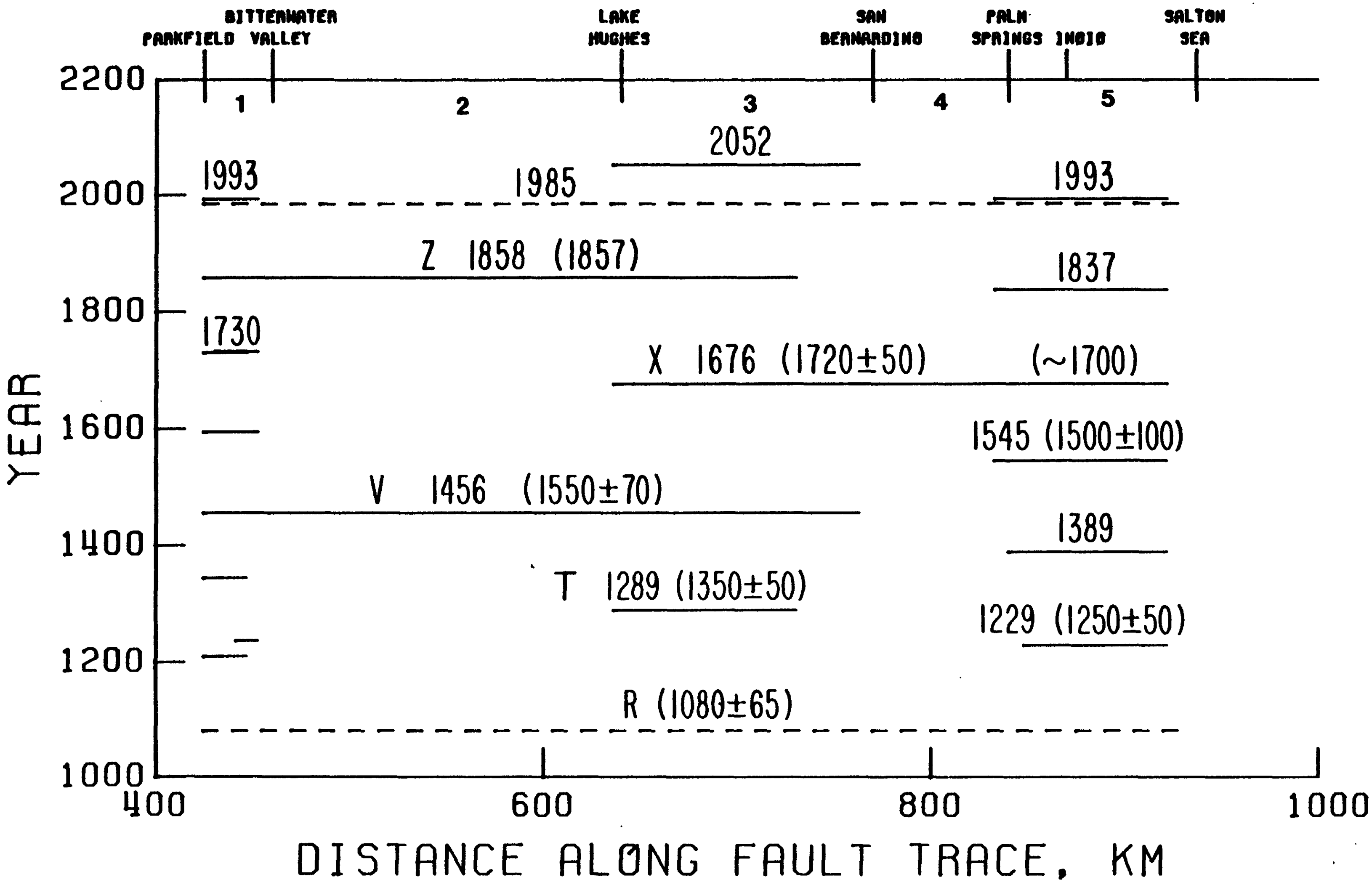

Figure 3. Space-time diagram of computed instabilities. Dashed lines marked R and 1985 are for reference and are not instabilities. The simulation starts at the year 1080 and ends at the year 2079. Dates in parentheses are for earthquake offsets reported in Sieh and Jahns (1984) and Sieh (1984a,b).

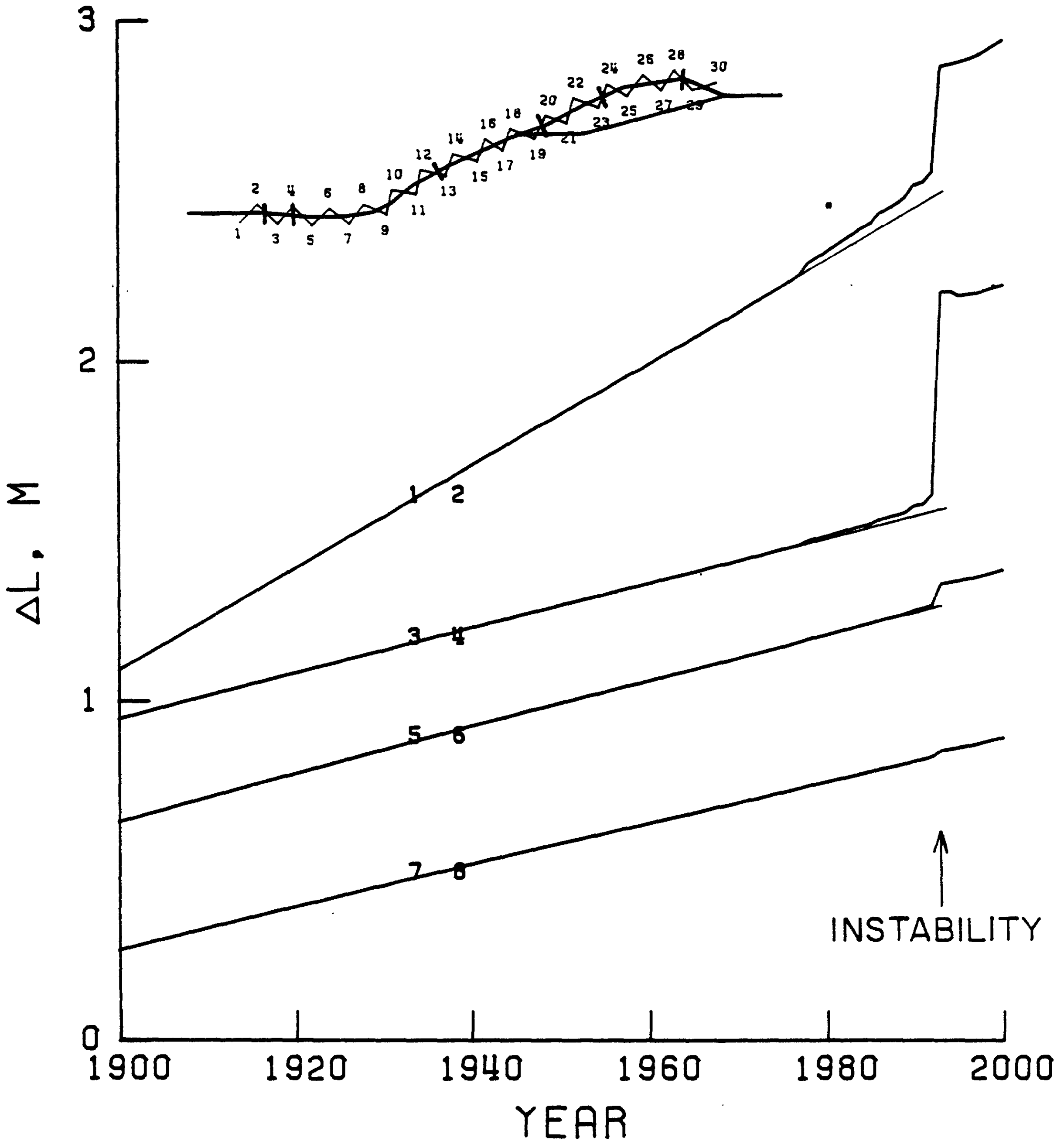

Figure 4. Computed length changes of trilateration lines 1-2, 3-4, 5-6, and 7-8 prior to unstable slip of patch section 1 in 1993. Inset map shows locations of lines and patch sections with respect to fault trace.

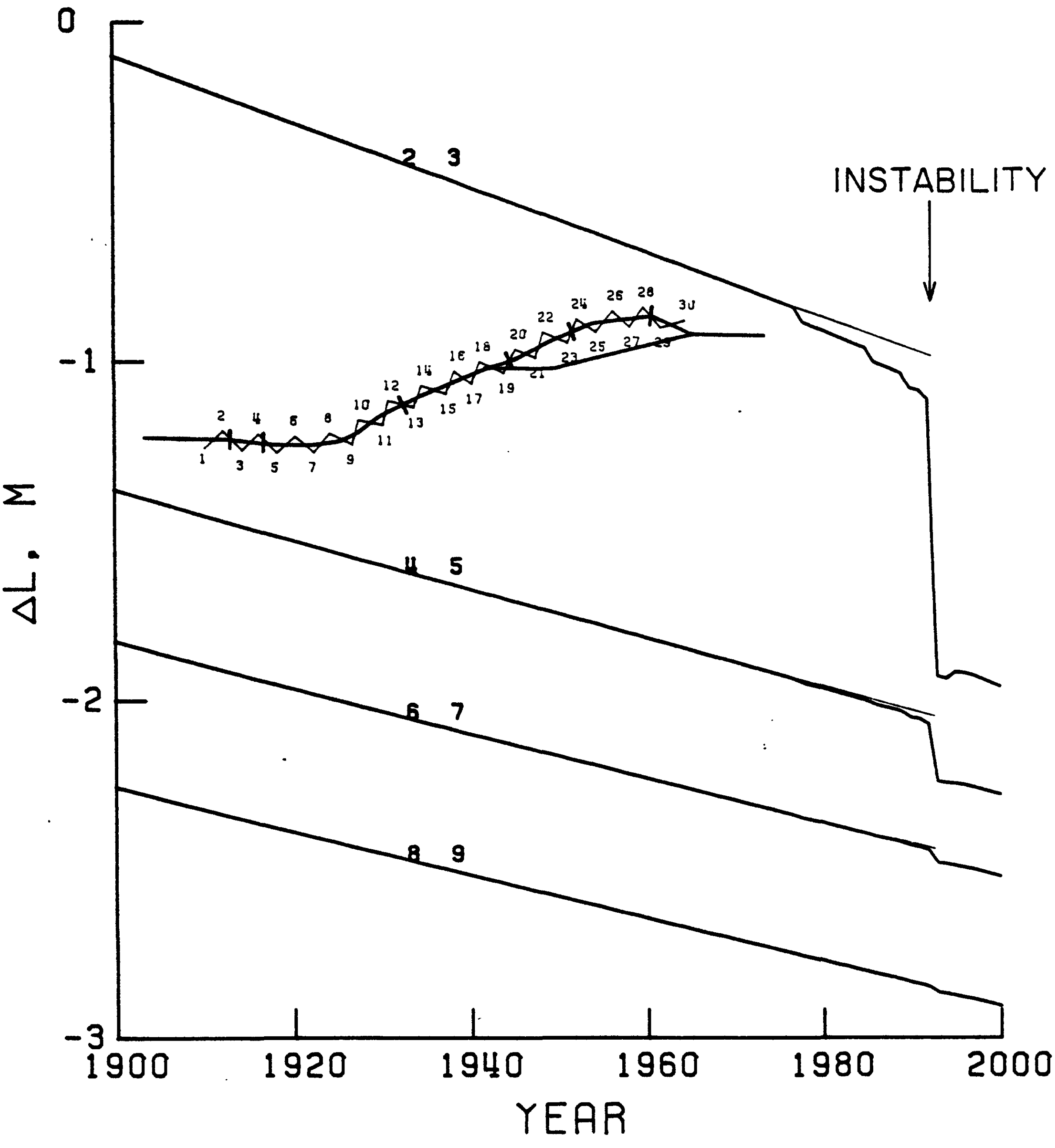

Figure 5. Computed length changes of trilateration lines 2-3, 4-5, 6-7, and 8-9 prior to unstable slip of patch section 1 in 1993. Inset map shows locations of lines and patch sections with respect to fault trace.

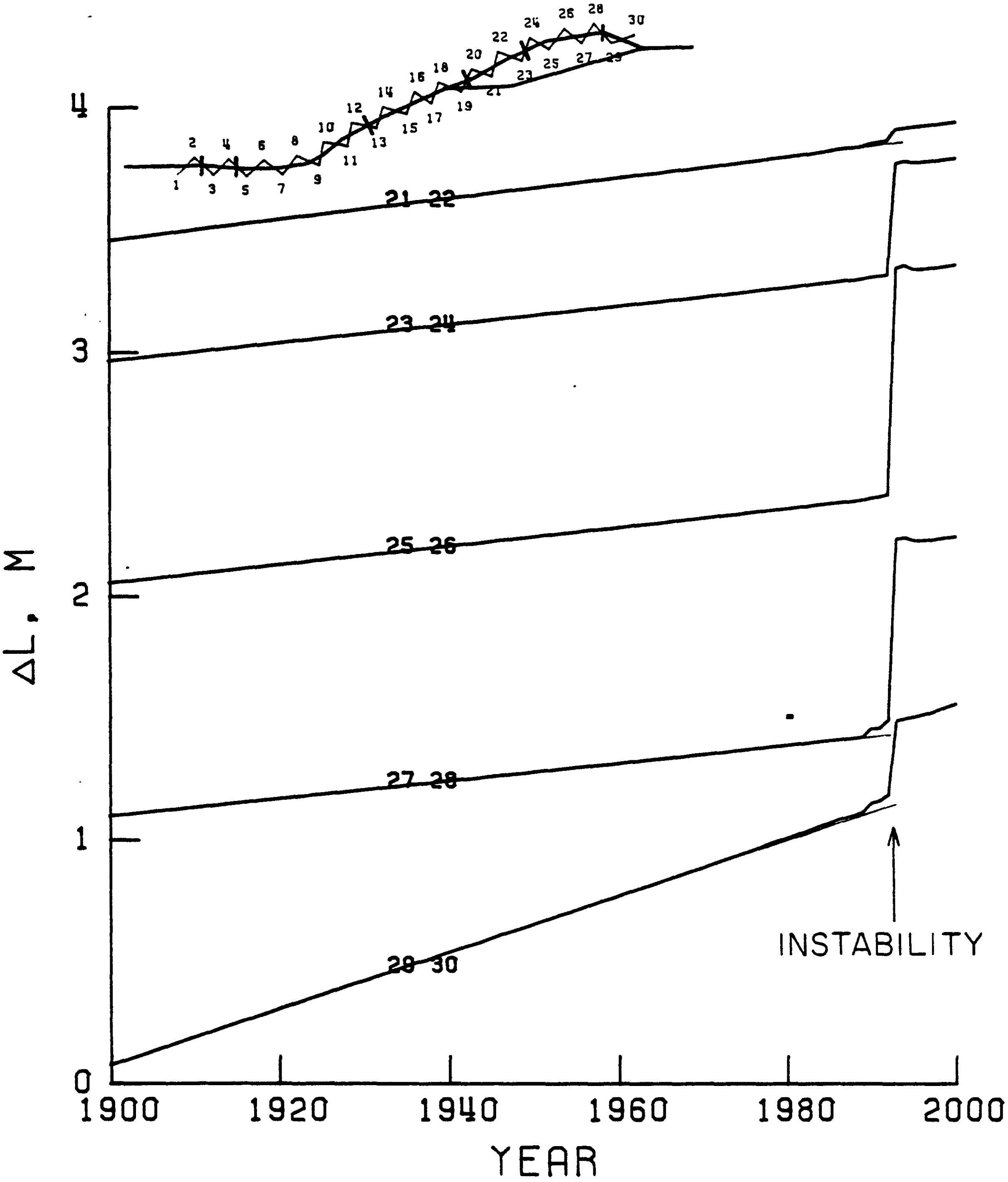

Figure 6. Computed length changes of trilateration lines 21-22, 23-24, 25-26, 27-28, and 29-30 prior to unstable slip of patch section 5 in 1993. Inset map shows locations of lines and patch sections with respect to fault trace.

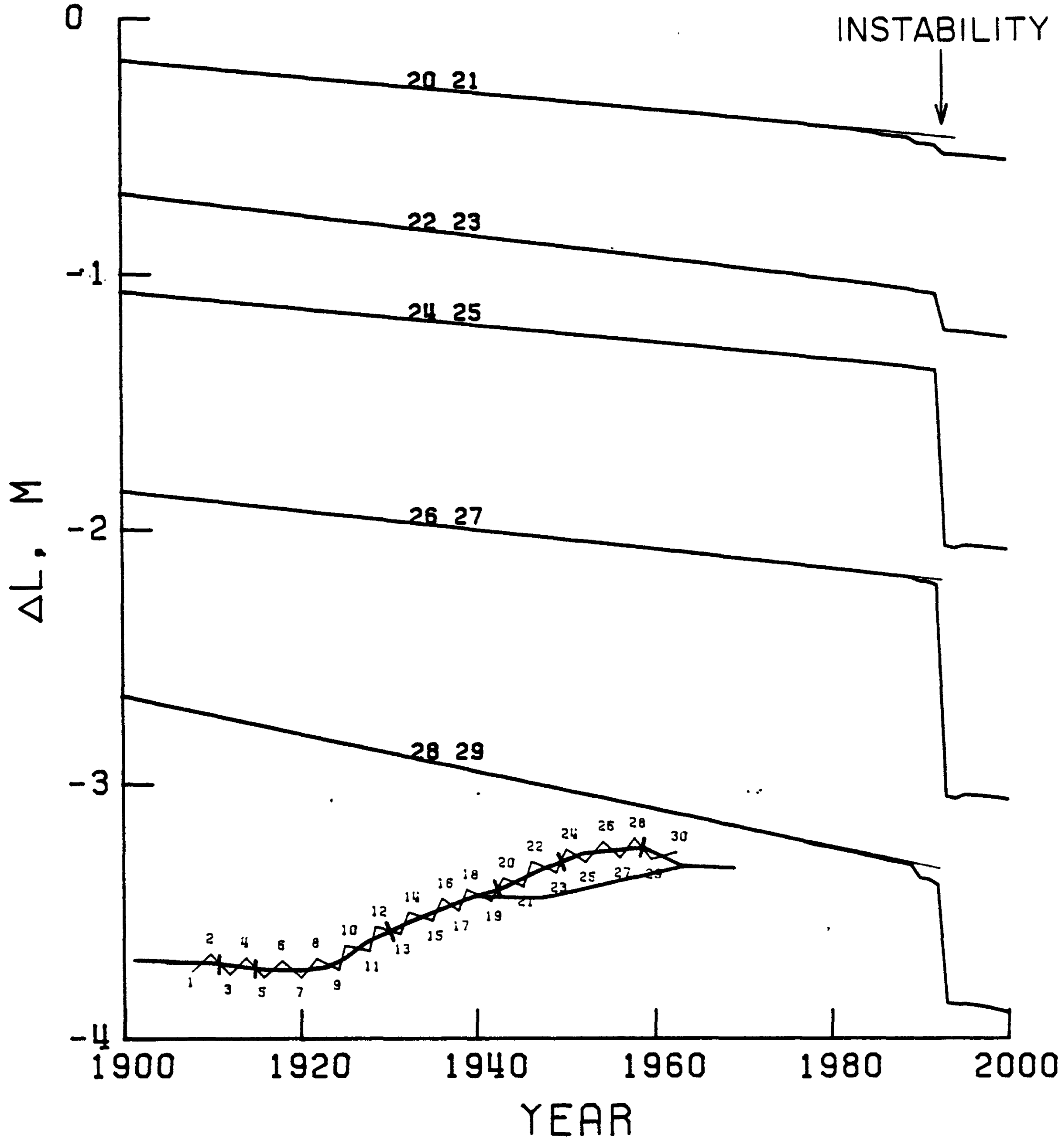

Figure 7. Computed length changes of trilateration lines 20-21, 22-23, 24-25, 26-27, and 28-29 prior to unstable slip of patch section 5 in 1993. Inset map shows locations of lines and patch sections with respect to fault trace.

Forecast Model for Large and Great Earthquakes in Southern California

W. D. Stuart
U.S. Geological Survey
525 S. Wilson Ave.
Pasadena, California 91106

This report describes a procedure for trying to forecast large and great earthquakes on the locked section of the San Andreas fault in southern California. Like numerical weather forecasting, the procedure combines a mechanical theory with repeated field measurements. The mechanical theory is a quasistatic instability model which simulates both pre- and coseismic faulting; the field measurements are a set of lengths, slips, and times of historic and prehistoric earthquake offsets reported in Sieh and Jahns (1984). The field data constrain values of model parameters, such as the shape of an assumed stress-slip law for the fault and the variation of fault strength along strike between Parkfield and the Salton Sea.

Once parameter values are set, the model is potentially useful for earthquake prediction in two ways. First, since model instabilities and offset data for past times agree fairly well, model instabilities corresponding to future times are predictions of future earthquakes. However, the uncertainties of predicted future times would be comparable to uncertainties of recurrence intervals of past earthquakes. Thus a prediction made this way with a model would be no more precise than a prediction made using probabilities and recurrence intervals, except to the extent that the model accounts for variable recurrence times, for example through interaction of different instabilities.

The second way to use a model for prediction is to exploit the accelerated fault slip that occurs shortly before instability. The accelerated fault slip occurs mainly at depth and is large enough to cause recognizable rate changes in lengthening of hypothetical trilateration lines on the ground surface. Since the time scale of the precursory deformation is a fraction of the recurrence interval, the precision of a forecast would be considerably increased over the precision of a forecast based on just recurrence times. In the rest of this report I shall describe the model, then show a comparison of theoretical and observed earthquake times, and finally present computed length changes of hypothetical trilateration lines.

The details of the model are given in Stuart (1984) and Stuart et al. (1985). Figure 1 is a perspective sketch showing the seismogenic part of the fault zone as a long patch of brittle rock. At every position on the patch the fault is assumed to obey a Gaussian shaped stress-slip law, τ^f vs. u , as shown at the bottom of Figure 1. The peak stress (strength) S of the fault varies with depth and distance along strike. Starting at the ground surface, peak stress increases downward to a maximum value at 6 km, then decreases towards greater depth; the patch is effectively 12 km high. The variation of peak stress along strike is a free parameter whose functional values are found by trial so that the model simulates the offsets in Sieh and Jahns (1984). The part of the remaining fault plane closest to the patch is assumed to undergo free slip. The fault plane farther from the patch and surrounding the free slip area is subjected to an imposed fault slip rate which is the forcing in the problem. The increasing imposed slip approximates the relative motion of the North America and Pacific plates, and loads the patch sections toward unstable failure. The failure time of a particular patch section will depend on the patch strength and the prior failure sequence of all patch sections. Immediately after a patch section fails, the section is assumed to heal to full strength so that another instability can occur in the future.

Figure 2 shows the geometry of the boundary value problem for the qualitative model in Figure 1. Figure 2a is a map view showing how the traces of the San Andreas, Imperial, Cerro Prieto, and San Jacinto faults are approximated by straight segments. Each trace segment is the top edge of a vertical, rectangular, planar area which is a dislocation surface. Most of the rectangular areas are divided into smaller rectangular areas; all rectangular areas have uniform slip and are referred to as cells. Figure 2c shows the cells in side view. Cells in shaded areas have the imposed slip rate indicated, whereas slips of all other cells are computed results.

The simulation of fault slip vs. time for all non-imposed slip cells is obtained by numerically solving a system of simultaneous nonlinear equations. Each equation has the form of (1) and expresses

$$\tau^{r} + \Sigma\tau^{d} - \tau^{f} = 0 \qquad (1)$$

shear stress equilibrium at a cell center. The terms in equation (1) are τ^{r}, the dislocation stress from imposed slip rate cells; $\Sigma\tau^{d}$, the sum of all other dislocation shear stresses; and τ^{f}, the Gaussian stress-slip law. In general, fault slip and stress vary with time and from cell to cell. Since the patch is relatively strong, slip of patch sections lags slip elsewhere until the patch sections catch up during unstable slippage. The $\tau^{p}(\xi)$ plot in Figure 2b shows the inferred variation of patch strength. ^{p}, which is assumed to have piecewise linear variation along strike, is found to have five sections of alternately low and high strength. The high strength sections coincide approximately with the major bends or structural knots of the fault.

Figure 3 is a space-time diagram showing the lengths and dates of instabilities. The names R, T, V, X, and Z correspond to earthquake offsets of the same names in Sieh and Jahns (1984). Numbers in parentheses are estimated dates of offsets at specific field sites. The dates near Indio are from Sieh (1984b) and are preliminary. The remaining dates are from Sieh and Jahns (1984) and Sieh (1984a). The main assumptions for the model are that earthquake R broke the entire locked section of the fault, and that earthquake X broke from Lake Hughes to the Salton Sea. In the simulation, the next future unstable slips occur on patch section 1 in 1993, section 5 in 1993, and section 3 in 2052.

The remaining four figures show the length changes of hypothetical trilateration lines before the two instabilities in 1993. Figures 4 and 5 show the length changes of lines which are respectively lengthening and shortening before unstable slip of section 1. Curves on the plots have been shifted vertically so that from top to bottom they are in north-south order along the fault. The small kinks in computed curves are due to the time step size of one year. The inset diagram in each figure is a fault trace map showing the location and orientation of lines. Line ends are numbered, and a line is identified by a number pair. Locations of line ends are chosen to detect changes in fault slip rate at about 10 km depth, which is where part of the fault patch fails years to decades before instability. Patch section ends are marked by ticks for reference.

In Figures 4 and 5, the lengthening rates are constant until about 15 years before instability, which appears as a jump of line length in the year 1993. Lines 1-2, 2-3, 3-4, and 4-5 show rate changes starting about 1980. The light lines are extrapolations of earlier trends. The predicted rate changes for several of the lines are large enough to be detected by current geodetic techniques using a geodolite. The small symbol just above line 1-2 at the 1980 position is a representative error bar (1 cm) of actual trilateration surveys. For unknown reasons, successive annual measurements often have a scatter about a long term trend line of one or more times an error bar height. Consequently, it appears that several years of semi-annual measurements would be needed to detect the precursory rate change of line 1-2.

Figures 6 and 7 are similar plots for trilateration lines near patch section 5. Preinstability rate changes are much less prominent than in Figures 4 and 5, and start only a few years prior to instability. The height of the error bar symbol above line 27-28 at the 1980 position suggests that such precursory rate changes could be detected in field data.

Results of this and other model simulations suggest that in general accelerated fault slip and ground surface deformation are large enough to detect with existing geodetic instruments. Therefore, if the model is realistic, there is a good chance that a large or great earthquake could be anticipated if a sufficient number of properly located trilateration lines are measured frequently enough. Usually the largest preinstability rate changes occur at patch section ends, where fault strength undergoes a jump, and these locations would be the best locations for installation of new trilateration lines. The model needs more refinement and testing to put bounds on the likely amplitudes and onset times of precursory deformation. The most useful field data for constraining the model would be measurements of repeated earthquake offsets along patch section 1, 4, and 5.

References

Sieh, K. E., Lateral offsets and revised dates of large prehistoric earthquakes at Pallett Creek, southern California, J. Geophys. Res., 89, 7641-7670, 1984a.

Sieh, K. E., Late Holocene behavior of the San Andreas fault, U. S. Geol. Survey Open File Report 84-628, 126-128, 1984b.

Sieh, K. E., and R. H. Jahns, Holocene activity of the San Andreas fault at Wallace Creek, California, Geol. Soc. Am. Bull., 95, 883-896, 1984.

Stuart, W. D., Instability model for recurring large and great earthquakes in southern California, Pure Appl. Geophys., 122, 1984, in press.

Stuart, W. D., R. J. Archuleta, and A. G. Lindh, Forecast model for moderate earthquakes near Parkfield, California, J. Geophys. Res., 90, 592-604, 1985.

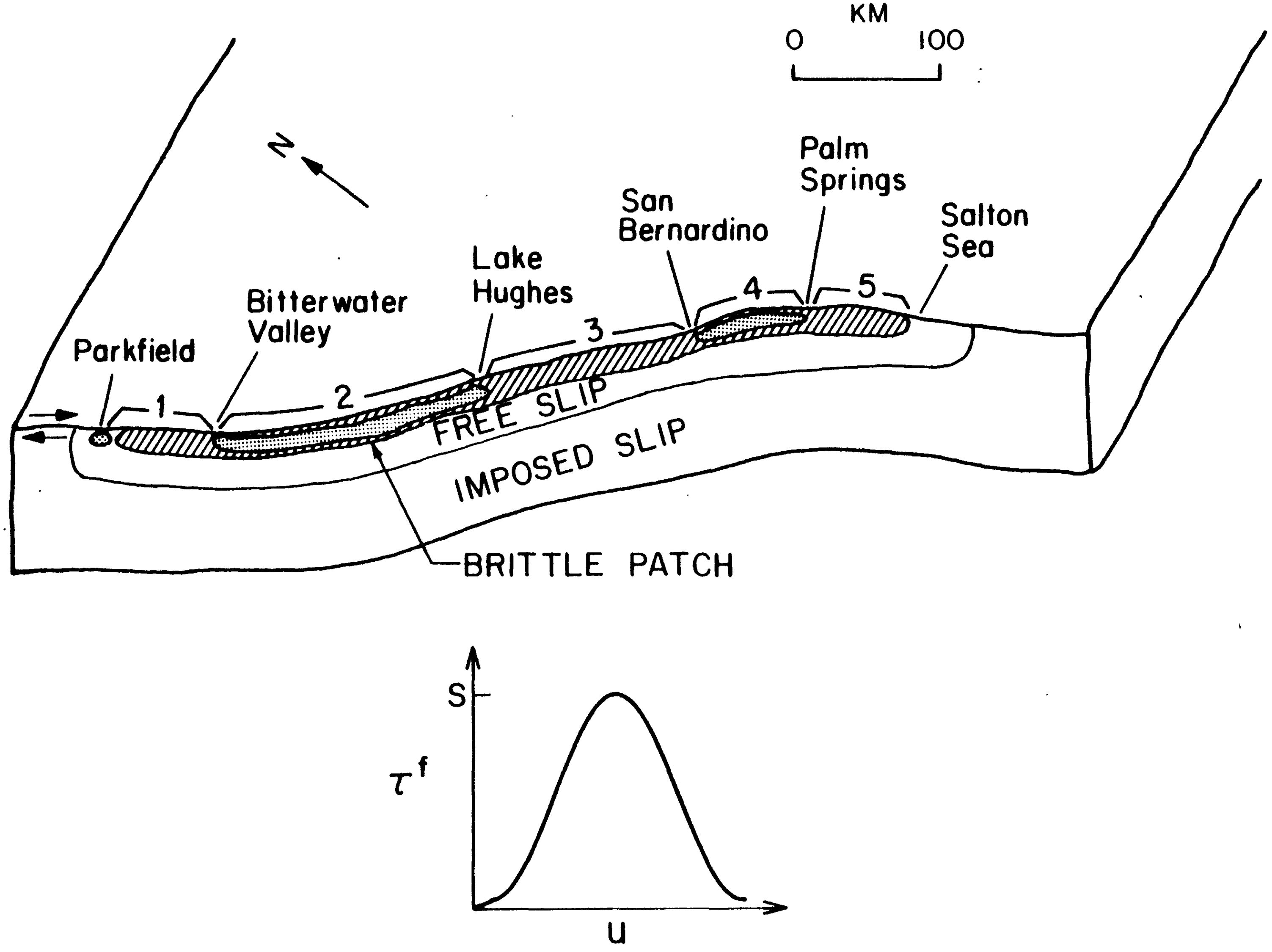
KM
0
100
N
Palm
Springs
San
Bernardino
Salton
Sea
Lake
Hughes
Bitterwater
Valley
Parkfield
1
2
3
4
5
FREE SLIP
IMPOSED SLIP
BRITTLE PATCH
S
τ^f
U

Figure 1. Qualitative instability model showing five sections of brittle patch on the San Andreas fault.

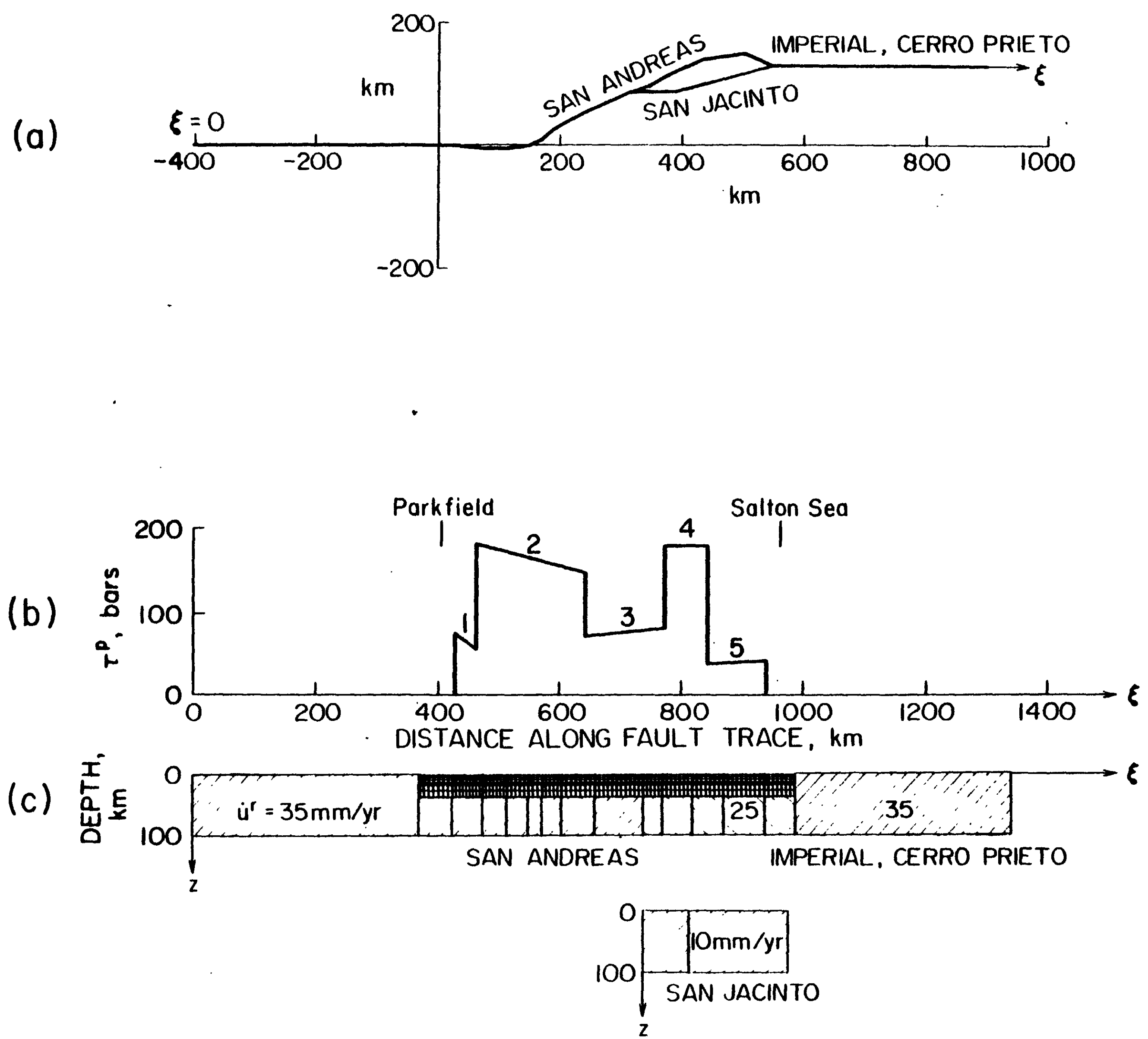
(a)
200
km
ξ = 0
-400
-200
200
400
600
800
1000
km
-200
SAN ANDREAS
SAN JACINTO
IMPERIAL, CERRO PRIETO
ξ
(b)
τ^P, bars
200
100
0
Parkfield
Salton Sea
1
2
3
4
5
0
200
400
600
800
1000
1200
1400
ξ
DISTANCE ALONG FAULT TRACE, km
(c)
DEPTH, km
0
100
$\dot{u}^r$ = 35mm/yr
25
35
ξ
z
SAN ANDREAS
IMPERIAL, CERRO PRIETO
0
100
10mm/yr
SAN JACINTO
z

Figure 2. Boundary value problem for numerical model. (a) Traces of San Andreas, Imperial, Cerro Prieto, and San Jacinto faults showing straight segments of model fault. (b) Fault strength at 6 km depth vs. distance along trace. (c) Side view of flattened fault plane showing cells of uniform slip. Numbers in shaded areas are imposed slip rates.

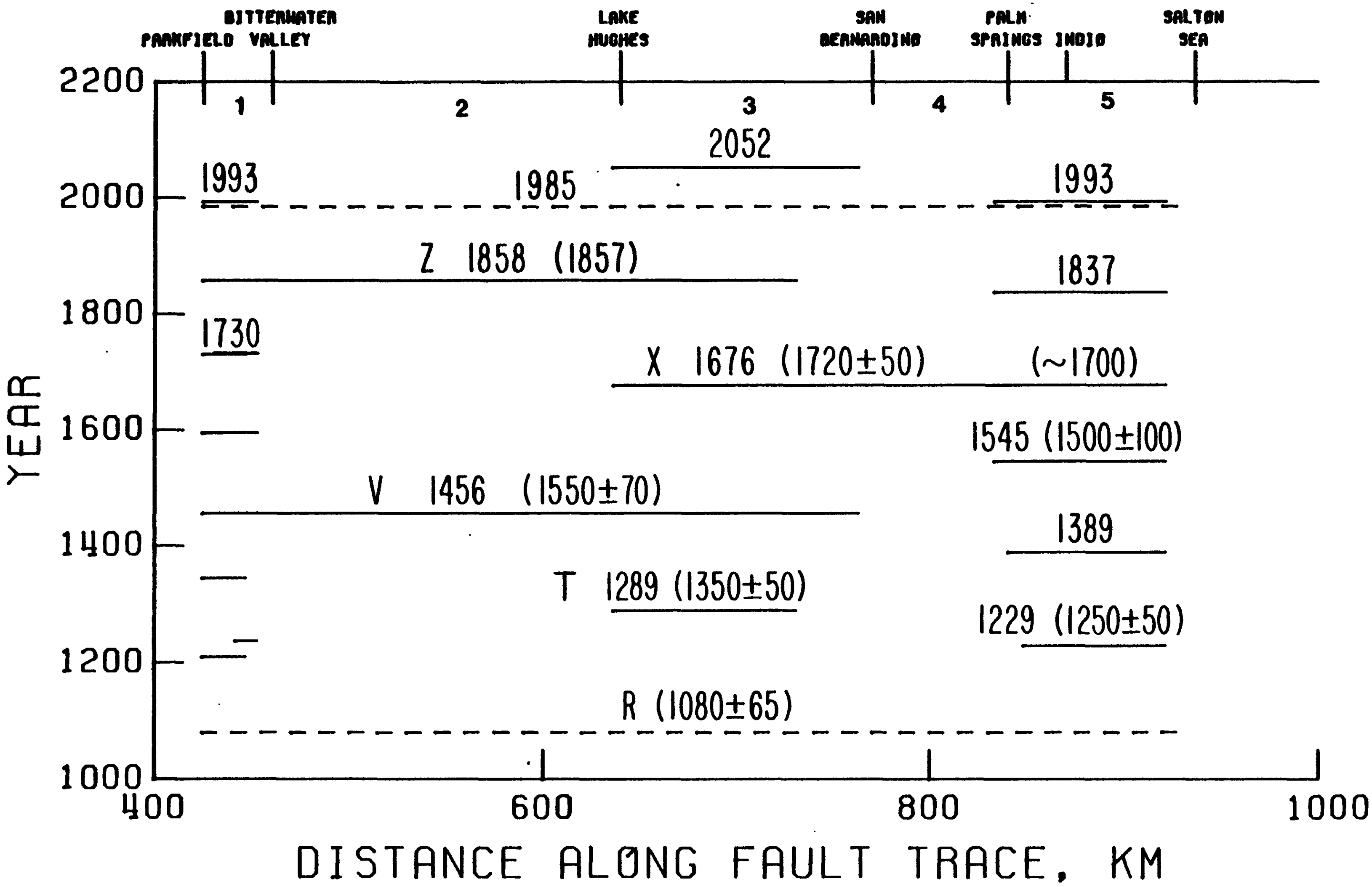

Figure 3. Space-time diagram of computed instabilities. Dashed lines marked R and 1985 are for reference and are not instabilities. The simulation starts at the year 1080 and ends at the year 2079. Dates in parentheses are for earthquake offsets reported in Sieh and Jahns (1984) and Sieh (1984a,b).

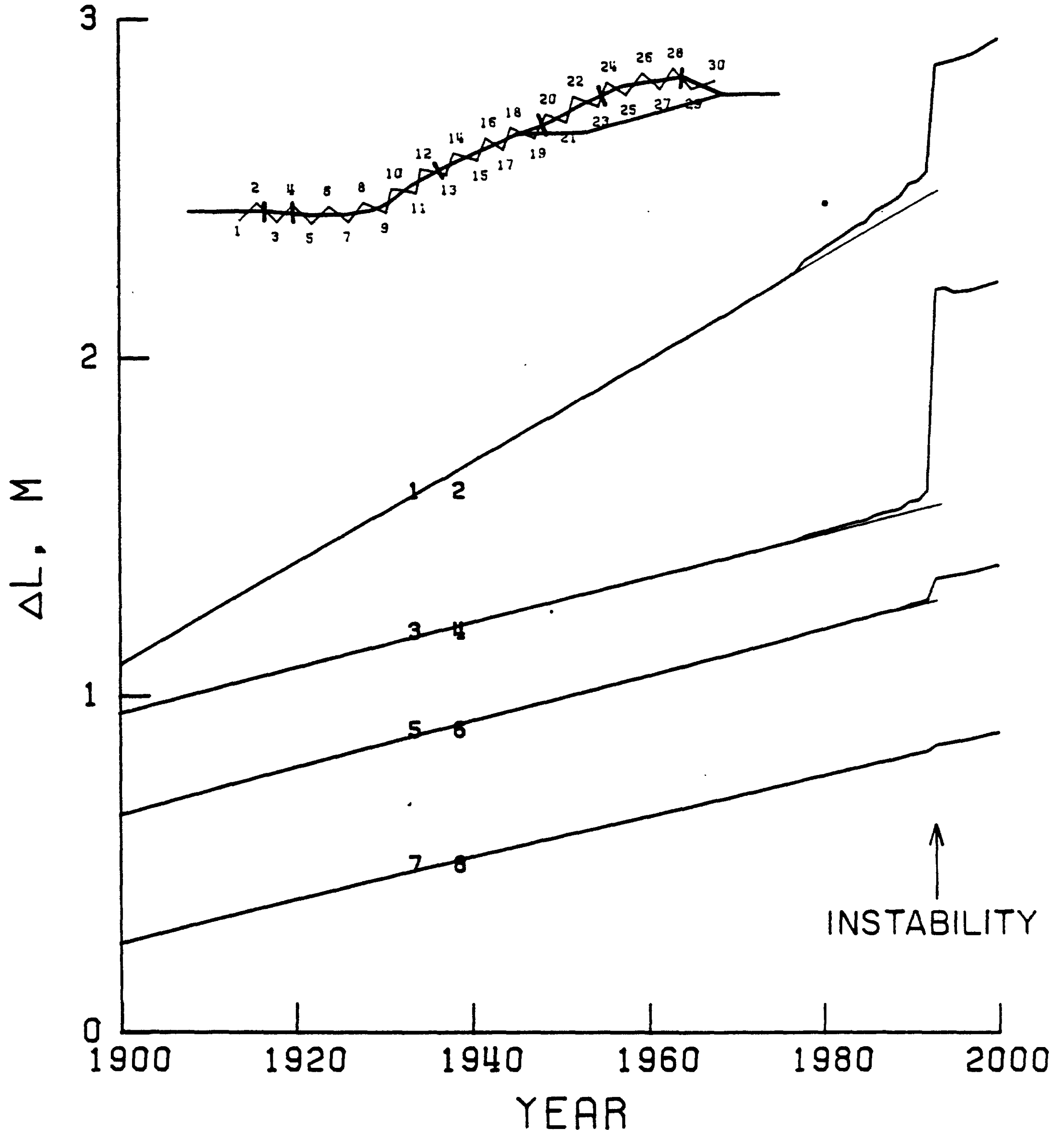

Figure 4. Computed length changes of trilateration lines 1-2, 3-4, 5-6, and 7-8 prior to unstable slip of patch section 1 in 1993. Inset map shows locations of lines and patch sections with respect to fault trace.

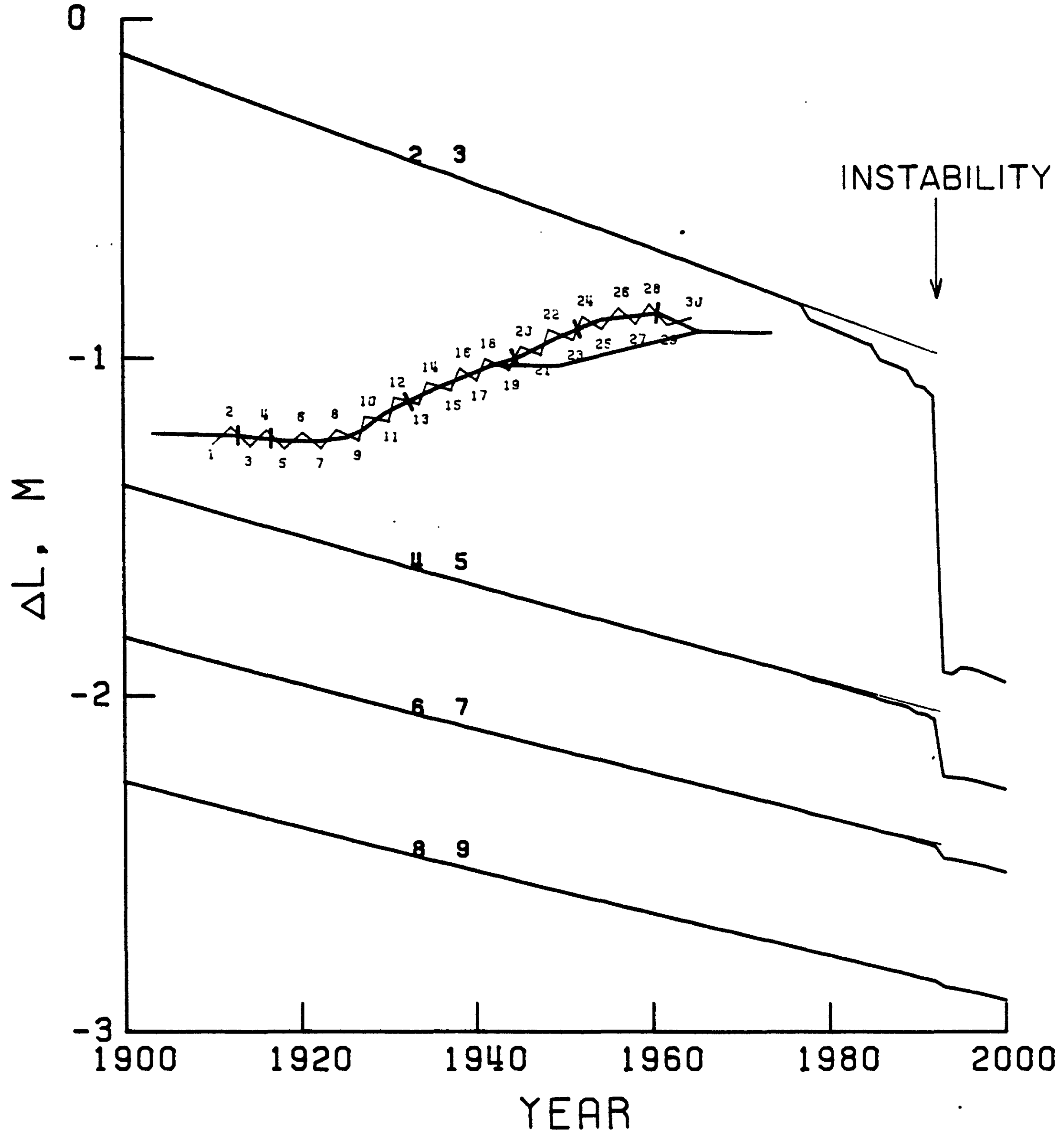

Figure 5. Computed length changes of trilateration lines 2-3, 4-5, 6-7, and 8-9 prior to unstable slip of patch section 1 in 1993. Inset map shows locations of lines and patch sections with respect to fault trace.

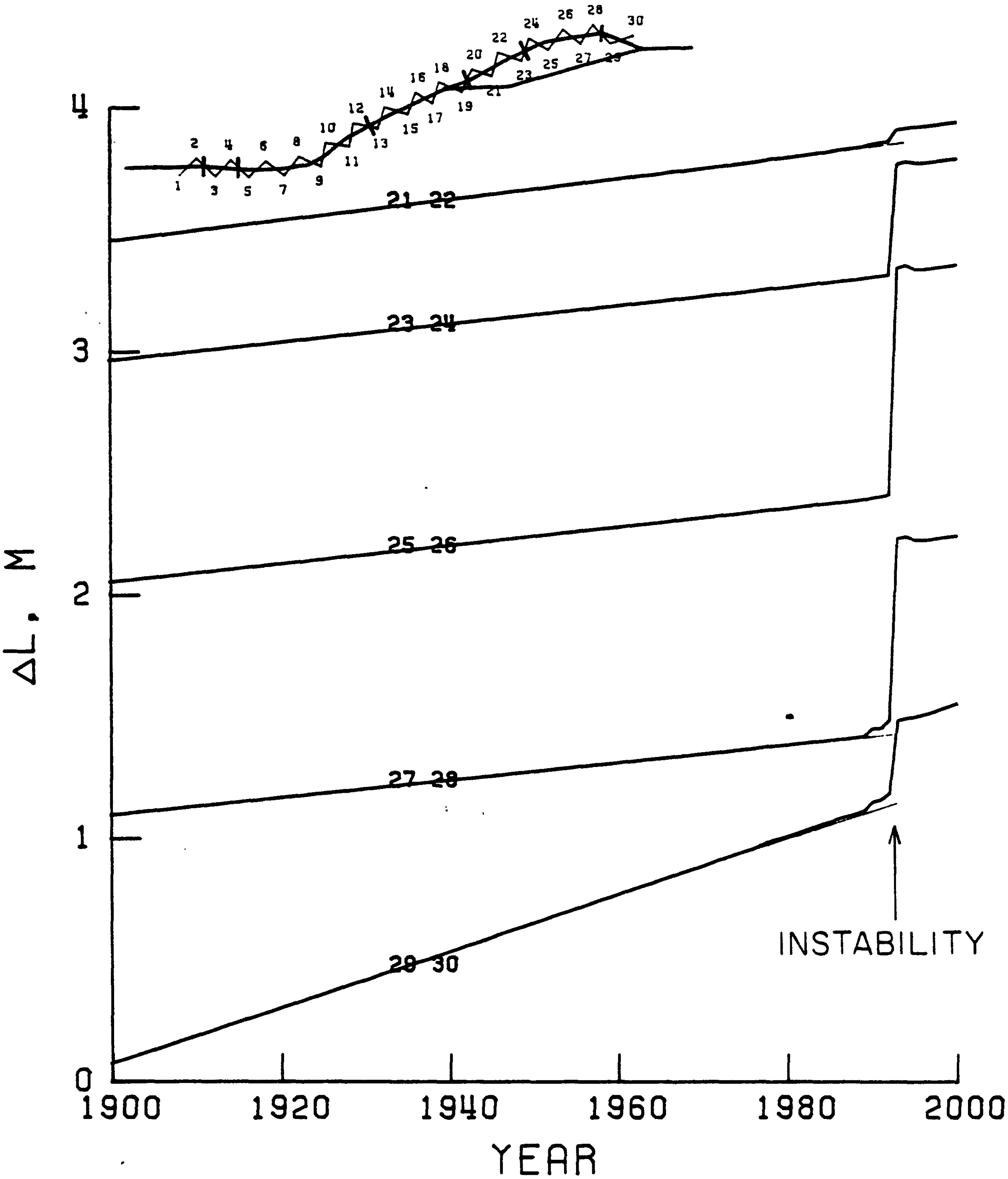

Figure 6. Computed length changes of trilateration lines 21-22, 23-24, 25-26, 27-28, and 29-30 prior to unstable slip of patch section 5 in 1993. Inset map shows locations of lines and patch sections with respect to fault trace.

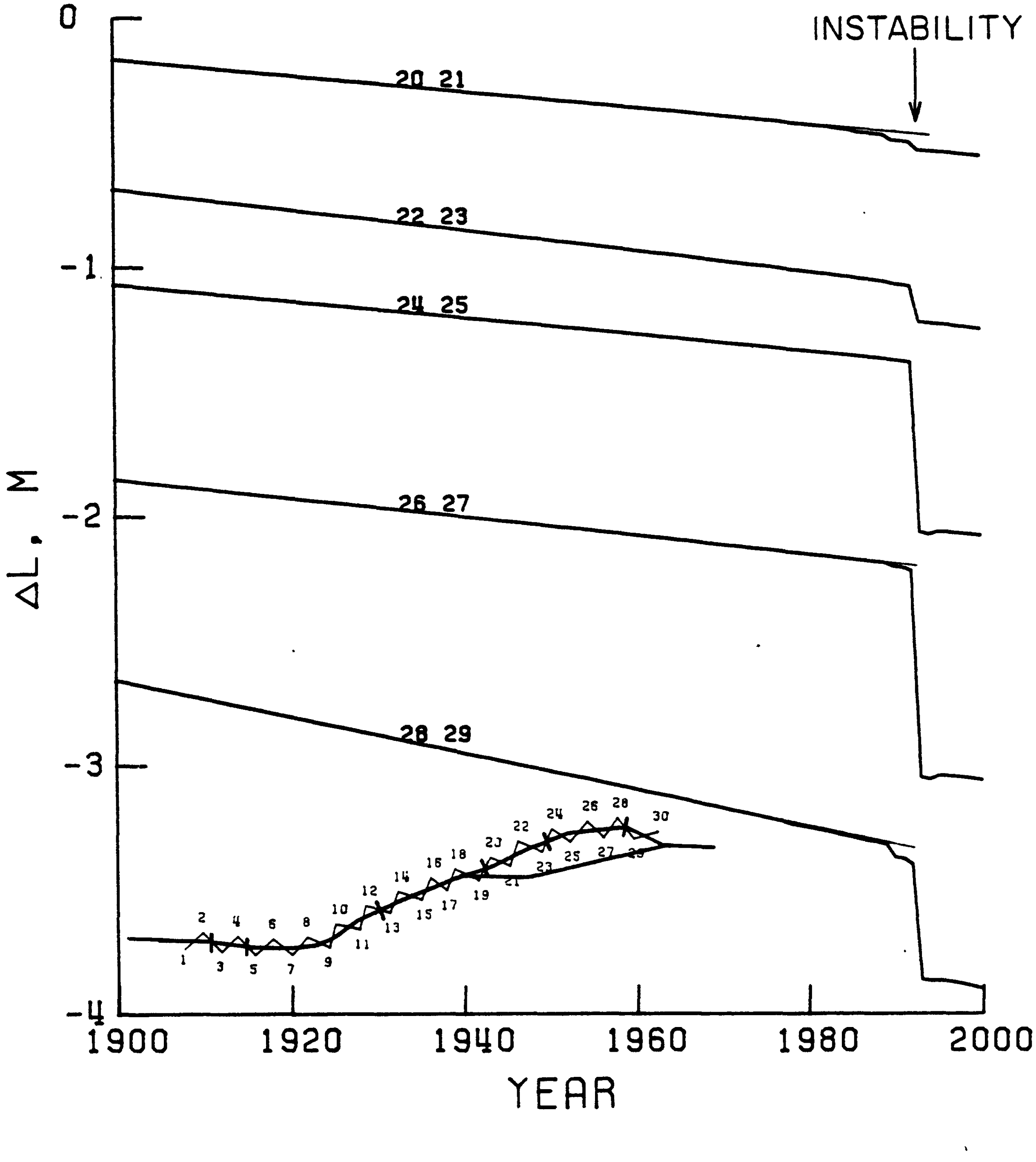

Figure 7. Computed length changes of trilateration lines 20-21, 22-23, 24-25, 26-27, and 28-29 prior to unstable slip of patch section 5 in 1993. Inset map shows locations of lines and patch sections with respect to fault trace.

APPENDIX A. 10.

Foreshocks and Time-Dependent Earthquake Hazard Assessment in Southern California

Lucille M. Jones

FORESHOCKS AND TIME-DEPENDENT EARTHQUAKE HAZARD ASSESSMENT IN SOUTHERN CALIFORNIA

Lucile M. Jones
U.S. Geological Survey
Seismological Laboratory
California Institute of Technology
Pasadena, CA 91125

ABSTRACT

The probability that an earthquake in southern California ($M \geq 3.0$) will be followed by an earthquake of larger magnitude within 5 days and 10 km (i.e., will be a foreshock) is shown to be 6% ± .5% (1 S.D.), and to be independent of the magnitude of the possible foreshock between M=3 and M=5. The probability that an earthquake will be followed by a $M \geq 5.0$ mainshock, however, increases with magnitude of the foreshock from less than 1% at $M \geq 3$ to 6.5% ± 2.5% (1 S.D.) at $M \geq 5$. The mainshock is most likely to occur in the first hour after the foreshock and the probability that a mainshock will occur decreases with elapsed time from the occurrence of the possible foreshock by approximately the inverse of time. Hence, the occurrence of an earthquake of $M \geq 3.0$ in southern California increases the earthquake hazard within a small space-time window several orders of magnitude above the normal background level.

INTRODUCTION

Previous studies of the nature of foreshocks [e.g., 1, 2, 3, 4, 5, 6, 7] have concentrated on estimating the rate of foreshock occurrence before moderate and large earthquakes and thus have looked backwards in time (i.e., given a group of mainshocks, how many were preceded by foreshocks?) These studies have shown that a significant percentage of earthquakes have been preceded by foreshocks (5% [6] to 50% [1] depending on the tectonic regime and definition of foreshock; 35% in southern California [7]) suggesting that foreshocks could be a useful tool for short-term earthquake hazard assessment. Obviously, whether or not an earthquake was preceded by a foreshock is known by the time the mainshock occurs. For real time earthquake hazard assessment, the probability that a given earthquake will be a followed by a mainshock, rather than preceded by a foreshock is needed.

This paper determines the percentage of earthquakes by magnitude that were followed by earthquakes of larger magnitude in southern California in the last 52 years and from this the probability that an earthquake will be a foreshock. The distribution of the temporal spacing between foreshocks and mainshocks is also analyzed to provide an estimate of the decay in earthquake hazard with time after a possible foreshock has occurred.

DATA

All earthquakes recorded in the catalogue for southern California (from 32°0'N to 36°30'N and 122°0'W to 115°0'W) from 1932 to July 1983 with a local magnitude (M_L) greater than 3.0 have been considered. The data were obtained from the southern Californian catalogue compiled and updated by the California Institute of Technology [8]. Only $M \geq 3.0$ earthquakes have been included because that is the estimated level of completeness of the catalogue for this time [9] and also because most of the foreshocks to damaging earthquakes have been above that magnitude [10].

Aftershocks were removed from the data set since the probability that an obvious aftershock will be followed by a larger earthquake is not the objective of this study. This was done by defining an aftershock as an earthquake with a magnitude smaller than that of the mainshock within a space-time window whose size is determined by the magnitude of the mainshock. The space-time window used was $(M_{main} - 3.)* 40$

days and (M_{main}^3 * 0.2) km. Excluding these aftershocks, a total of 4811 earthquakes has been reported in southern California of $M \geq 3.0$ from 1932 to July 1983.

Each non-aftershocks was were followed by a larger event within 5 days was considered to be a foreshock, so that if multiple foreshocks preceded a mainshock each foreshock was counted individually. This does not strongly affect the results since most mainshocks were preceded by only one foreshock as is shown in Table 1 where the number of mainshocks preceded by a given number of foreshocks is shown. Moreover, in all 18 sequences with 3 or more foreshocks of $M \geq 3.0$, every foreshock had a magnitude equal to or greater than the preceding foreshocks.

ANALYSIS

Identifying Foreshocks. A precise definition of foreshocks (a space-time window in which a possible mainshock could occur) is required to allow probabilities to be calculated. The optimum space-time window should be large enough that most (but not necessarily all) foreshock-mainshock sequences will be included but small enough that the resulting probabilities of a larger earthquake occurring within that window will be significantly above background level and thus useful for earthquake hazard assessment.

The observed distribution of earthquakes with magnitudes larger than the first earthquake in a 30 km circle (by km) for 30 days (by day) after all non-aftershocks is shown in Figure 1. Clearly, the distribution in space and time of mainshocks after foreshocks is not uniform. Mainshocks occur most frequently in the first day after the foreshocks and within 1 km of the foreshock epicenter; the rate of occurrence decays strongly with time and distance from the foreshock. Since the purpose here is to maximize the usefulness of a definition of foreshocks rather than to ensure that all foreshock-mainshock pairs are included, the space-time window for defining a foreshock was chosen to be 5 days and 10 km. Beyond this window, the occurrence of earthquakes is no more than 100% above the mean rate of occurrence. This spacing between foreshock and mainshock is comparable to those found in studies of recent sequences [7,11]. When the term "foreshock" is used in the rest of this paper, it will mean that another earthquake, larger than the foreshock, was listed in the catalogue within 5 days after the foreshock and with an location less than 10 km from the epicenter of the foreshock.

Probabilities by Magnitude. Available earthquake catalogues can be used to predict future patterns of seismicity by assuming that the foreshock process is stationary, i.e., that foreshocks are as likely to occur in the next 50 years as in the last 50 years. It is then possible to consider the distribution of foreshocks in the set of all earthquakes as a binomial distribution and the earthquakes that have been recorded in the last 52 years as a random selection of all of the earthquakes that have and will occur in southern California. The percentage, p, of earthquakes that are foreshocks is then an estimate of the probability that a future earthquake will be a foreshock. The first standard deviation of this estimate is $(np(1-p))^{1/2}$ where n is the total number of earthquakes [12].

The cumulative number of earthquakes at or above a given magnitude is shown in Fig 2 for a) all earthquakes in the data set, b) all foreshocks by the above definition, c) foreshocks followed by $M \geq 4.0$ mainshocks, and d) foreshocks followed by $M \geq 5.0$ mainshocks [13]. Using the maximum likelihood method [14], the relationship between the cumulative number of earthquakes, N, and magnitude, M, was found to be,

$$\log(N) = 6.18 - (0.83\pm.02)*M \qquad (1)$$

for all earthquakes, and

$$\log(N) = 4.85 - (0.83\pm.10)*M \qquad (2)$$

for the foreshocks. The magnitude coefficients (called b-values) are the same for both foreshocks and all earthquakes (0.83) suggesting a lack of dependence on magnitude for the distribution of foreshocks.

The probability that an earthquake of $M \geq 3.0$ in southern California will be followed by an earthquake of a larger magnitude within 5 days and 10 km is approximately 6% ± .5% (1 SD) (Fig 3). The probability that an earthquake will be a foreshock and the standard deviation of that probability, shown as a function of magnitude in figure 3, were calculated by dividing the total number of foreshocks at or above a given magnitude by the total number of earthquakes at that or greater magnitude. As suggested by the b-values, no strong dependence on magnitude can be seen. The standard deviations of the estimates increase with magnitude because of the decrease in size of the data set so the lack of magnitude dependence is not definitive. Because no foreshock has been reported in southern California larger than $M = 5.4$ the probability that a larger earthquake will be a foreshock cannot be estimated.

A dependence on magnitude is seen in the probability that an earthquake will be a foreshock to a potentially damaging $M \geq 5.0$ mainshock (Fig 3). A $M \geq 3.0$ earthquake has a 1% chance of being followed by a $M \geq 5.0$ mainshock but a $M \geq 5.0$ earthquake has a 6.5% chance of being followed by another $M \geq 5.0$ earthquake. This magnitude dependence is shown more clearly in figure 4 where the difference in magnitudes between foreshocks and their mainshocks is plotted against the cumulative number of foreshock-mainshock pairs with that or greater difference in magnitude. A maximum-likelihood fit to this data shows that the number of foreshock-mainshock pairs (N) with a magnitude difference greater than or equal to ΔM is;

$$\log(N) = 2.4 - (0.73 \pm .12) * \Delta M. \qquad (3)$$

Thus, the magnitude distribution of mainshocks after foreshocks is approximately the same as independent earthquakes (Eq. 1) The average difference in magnitude of foreshocks and mainshocks is not 2.0 units of magnitude as has been suggested previously [15].

Decay in Earthquake Hazard with Time. The probability that an earthquake will be a foreshock is observed to decrease quickly with elapsed time from the occurrence of the foreshock. Figure 5 shows the number of mainshocks still to occur plotted against the time (by hour) from the foreshock for the 287 foreshock-mainshock pairs in the data set. The first hour after the foreshock is the most likely to contain the mainshock; 26% of the mainshocks occur within that time. Within one day, 70% of the mainshocks will have occurred. Fitting a power curve to these data gives a rate of decay in hazard of time $^{-.9}$. The rate of occurrence of mainshocks of $M \geq 4.0$ and $M \geq 5.0$ also decays with time after the foreshock by time$^{-.7}$ and time$^{-.6}$ respectively. This suggestion of a slower time decay for larger mainshocks is smaller than the errors. The temporal decay in the occurrence of mainshocks after foreshocks is thus very similar to the decrease in the occurrence of aftershocks after mainshocks which is inversely proportional to time.

DISCUSSION

The occurrence of an earthquake of $M \geq 3.0$ in southern California increases the probability of a larger earthquake occuring within 10 km and 5 days to 6%. The magnitudes of the possible mainshocks have a normal b-value distribution above the magnitude of the foreshock. The probability of a larger earthquake occurring decays rapidly with time after the possible foreshock. Combining these results, the probability per hour, $P(M_m)$, that an earthquake of $M \geq M_m$ will occur within one hour after time t(hr) after an earthquake of $M = M_f$ is;

$$P(M_m) = 0.02 * 10^{-b*(M_m - M_f)} * (t+1 \text{ hr})^{-.9} \qquad (4).$$

Although the short-term earthquake hazard increases several orders of magnitude above the background rate after the occurrence of an earthquake as shown here, the absolute probability of an earthquake occurring is still quite low. Aki [16] has shown, however, that increased earthquake hazard resulting from independent precursors can be combined by considering the probability gain resulting from each precursor. If the probabilities are small, the probability of an earthquake occurring is

$$P = P_o * (P_a/P_o) * (P_b/P_o) * \ldots \qquad (5)$$

where P_o is the background rate of occurrence, P_a is the probablility due to precursor a, P_b is the probability from precursor b, etc. The ratio of P_a/P_o for foreshocks can be quite high depending on the size of the possible foreshock and the background rate.

The potential usefulness of this method can be shown by considering the probablity of a major earthquake occurring on the San Andreas Fault. This southern most section of the fault (called the Indio section, from the Salton Sea to Cajon Pass) is estimated to have a recurrence interval of 250 yrs for M 7.5 earthquakes [17]. This gives a background rate of 0.004/yr or 4.6×10^{-7}/hr. It has been about 300 years since the last earthquake in Indio so the present probability of a M = 7.5 earthquake is .03/yr [17] or 3.5×10^{-7}/hr. This gives a probability gain from being at the end of the seismic cycle of 7.5. If a M=5.5 earthquake were to occur at one end of this section, either at Mecca Beach on the Salton Sea or at Cajon Pass, the probability of a M=7.5 earthquake occurring in the next hour would be (by Eq. 4) .0008. By Eq. 5, the total probability of a M=7.5 earthquake occurring in the next hour would be .0008 times the probability gain of 7.5 or .6%, or 1.8% in the next 5 days. The probability of a M=7.5 earthquake occurring after a M=6.0 earthquake in Mecca Beach or Cajon Pass would be, by the same rationale, 1.4% for the first hour and 4.2% for the first 5 days.

The well constrained spatial and temporal limits of this earthquake hazard means that any earthquake preparation measures that were undertaken on this basis would only be required within a limited region and need only be maintained for a few days. However, the transitory nature of the hazard and the high probability of the mainshock occuring within the first hour also means that a decision to undertake any earthquake preparation measures on the basis of these probabilities would have to be made before the possible foreshock occurs. In addition, for this hazard assessment to be of use, information about the location and magnitude of the possible foreshock would have to ba quickly proccessed and disseminated.

Acknowledgements. The author would like to thank E. Hauksson, P. Reasenburg, A. Lindh, W. Ellsworth, and T. Heaton for helpful advise and criticism. This work was conducted while the author was a National Research Council Fellow at the U. S. Geological Survey.

REFERENCES

1. Mogi, K., Bull. Earthq. Res. Inst., 47, 429-451, (1969).

2. Utsu, T., J. Fac. Sci., Hokkaido Univ., Series VII (Geophysics), 3, 197-266, (1970).

3. Kagan, Y., and L. Knopoff, Geophys. J. Roy. Astron. Soc., 55, 67-86, (1978).

4. Jones, L. and P. Molnar, J. Geophys. Res., 84, 3596-3608, (1979).

5. von Seggern, D., S. Alexander, and C. Baag, J. Geophys Res., 86, 9325 - 9351, (1981).

6. Bowman, J., and C. Kisslinger, Bull. Seism. Soc. Am., 74, 181-198, (1984).

7. Jones, L., Bull. Seism. Soc. Am., 74, 1361-1380 (1984).

8. Hileman, J., C. Allen, and J. Nordquist, Seismicity of the Southern California Region, 1 January 1932 - 31 December 1972, (Seismological Laboratory, Calif. Inst. Tech., Pasadena, CA, 1973).

9. Hileman, Ph.D. Thesis, Calif. Inst. Tech., (1978).

10. No earthquake of $M \geq 5.0$ in southern California in the last 20 years when the level of completeness of the catalogue is closer to $M = 2.0$ has had its largest foreshock smaller than $M = 3.0$ [7].

11. The distance spacing of 10 km is slightly larger than previously found and may result from the larger errors in the locations of earthquakes in the early part of the catalogue.

12. Bevington, P. R., Data Reduction and Error Analysis for the Physical Sciences (McGraw-Hill, New York, NY, 1969).

13. The obvious offsets in the cumulative number of earthquakes in Fig 1 result from the practise of assigning magnitudes only to the nearest half-unit of magnitude at Caltech until 1943.

14. Aki, K. Bull. Earthq. Res. Inst., Tokyo Univ., 43, (1965).

15. Papazachos, B., Tectonophysics, 28, 213-226 (1975).

16. Aki, K., in Earthquake Prediction, An International Review, (Amer. Geophys. U., Washington, DC, 1981).

17. Sykes, L., and S. Nishenko, J. Geophys. Res., 89, 5905-5928, (1984).

FIGURE CAPTIONS

Fig 1. A 3-dimensional histogram of the number of earthquakes recorded within 30km (by km) and 30 days (by day) after all of the 4811 non-aftershocks in the southern California catalogue larger than the original earthquake. The peak at 1 day and 1 km has been halved (from the actual 120 events) for plotting.

Fig 2. The cumulative number of earthquakes recorded in southern California from 1932 to July 1983 at or above each magnitude level as a function of magnitude. Also shown are the cumulative number of foreshocks, foreshocks to $M \geq 4.0$ mainshocks and foreshocks to $M \geq 5.0$ mainshocks. Equations 1 and 2 are shown by the solid lines.

Fig 3. The probability that an earthquake in southern California will be followed by a larger earthquake within 5 days and 10 km as a function of the magnitude of that earthquake (solid line). The dashed line shows the probability of being followed by a $M \geq 4.0$ mainshock and the dotted line shows the probability that an earthquake will be followed by a $M \geq 5.0$ mainshock. The vertical bars show the standard deviation in the estimates of probability for each magnitude level.

Fig 4. The cumulative number of foreshock-mainshock pairs with a difference in magnitude at or above each magnitude level as a function of difference in magnitude. Only pairs recorded after 1943 (when magnitudes were first given to the nearest .1 unit instead of .5 unit) are used.

Fig 5. The number of mainshocks still to occurr as a function of elapsed time from the foreshock.

# of foreshocks in sequence	Magnitude of Mainshock				
	3.0–3.9	4.0–4.9	5.0–5.9	≥ 6.0	Total
1	102	51	11	2	166
2	14	13	4	0	31
3	3	8	0	0	11
4	0	4	1	1	6
5	1	0	0	0	1

Table 1. The number of mainshocks preceded by a given number of foreshocks as a function of the magnitude of the mainshock.

Fig. 1

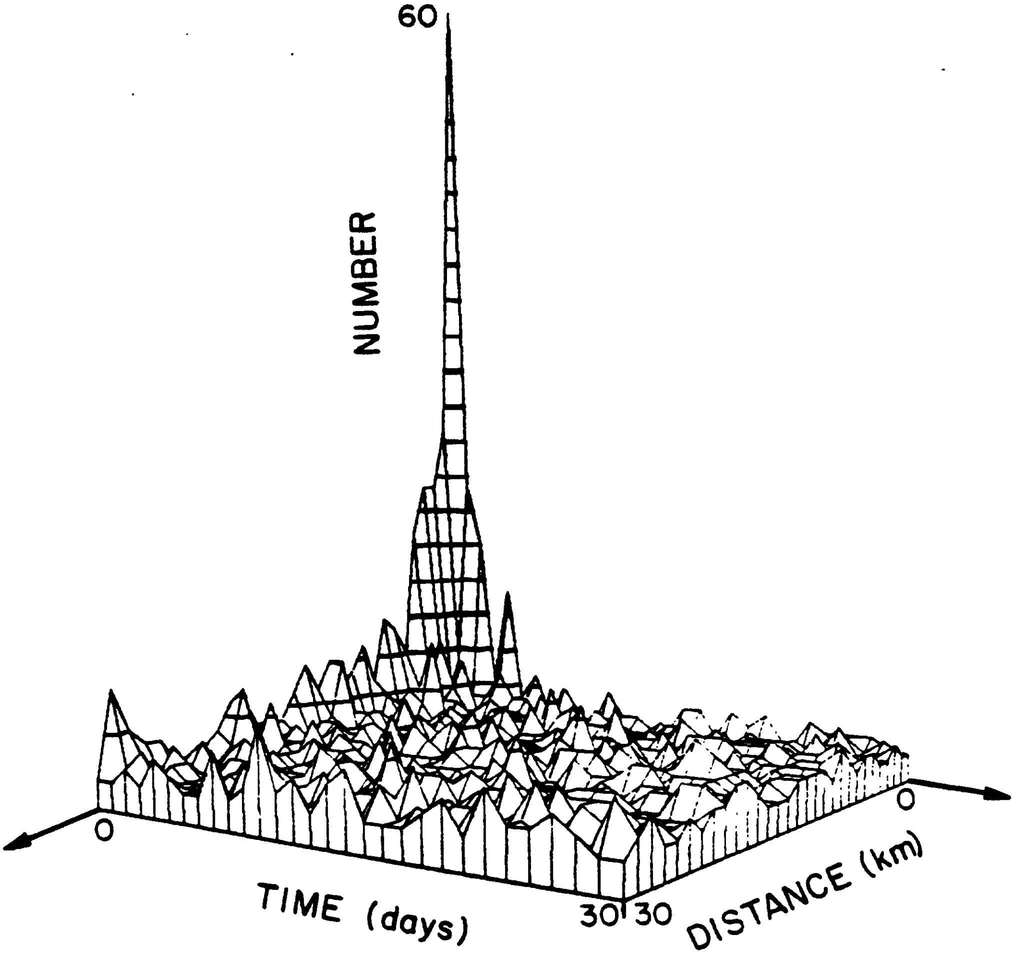

Fig 2

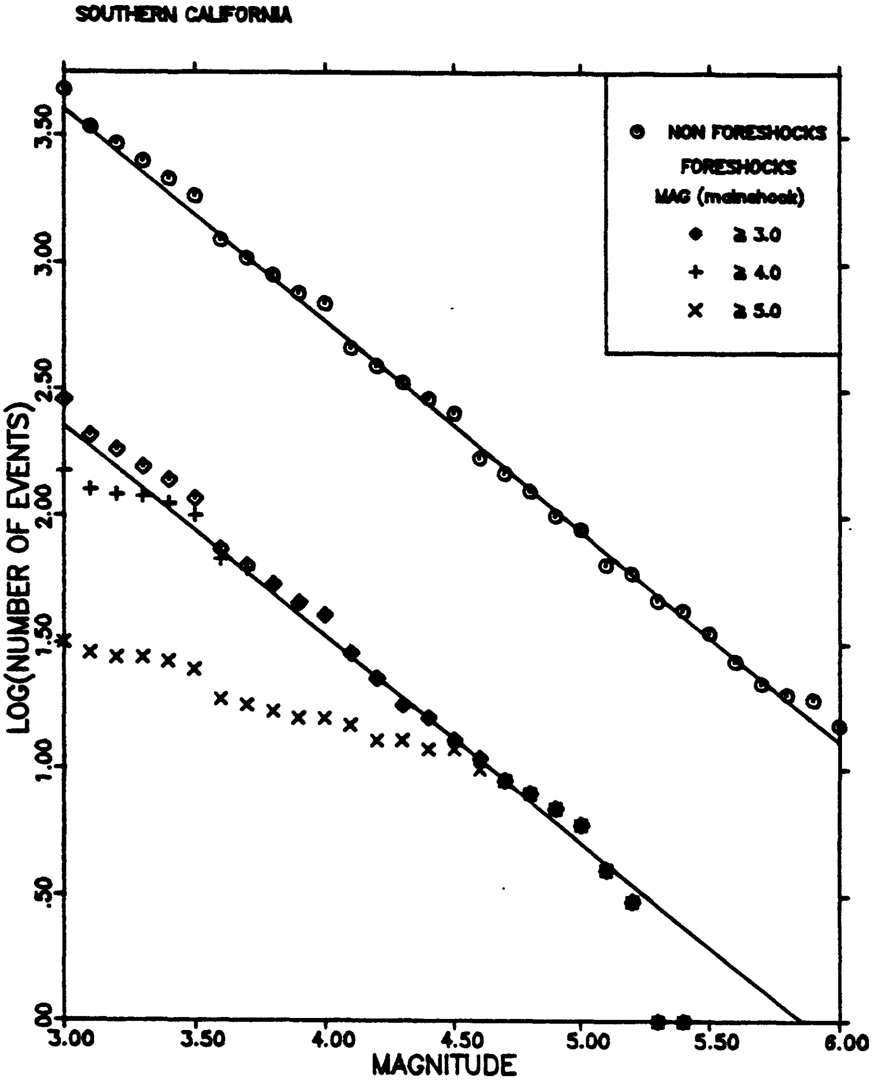
SOUTHERN CALIFORNIA
● NON FORESHOCKS
FORESHOCKS
MAG (mainshock)
◆ ≥ 3.0
+ ≥ 4.0
× ≥ 5.0
LOG(NUMBER OF EVENTS)
3.50
3.00
2.50
2.00
1.50
1.00
.50
.00
3.00
3.50
4.00
4.50
5.00
5.50
6.00
MAGNITUDE

Fig 3

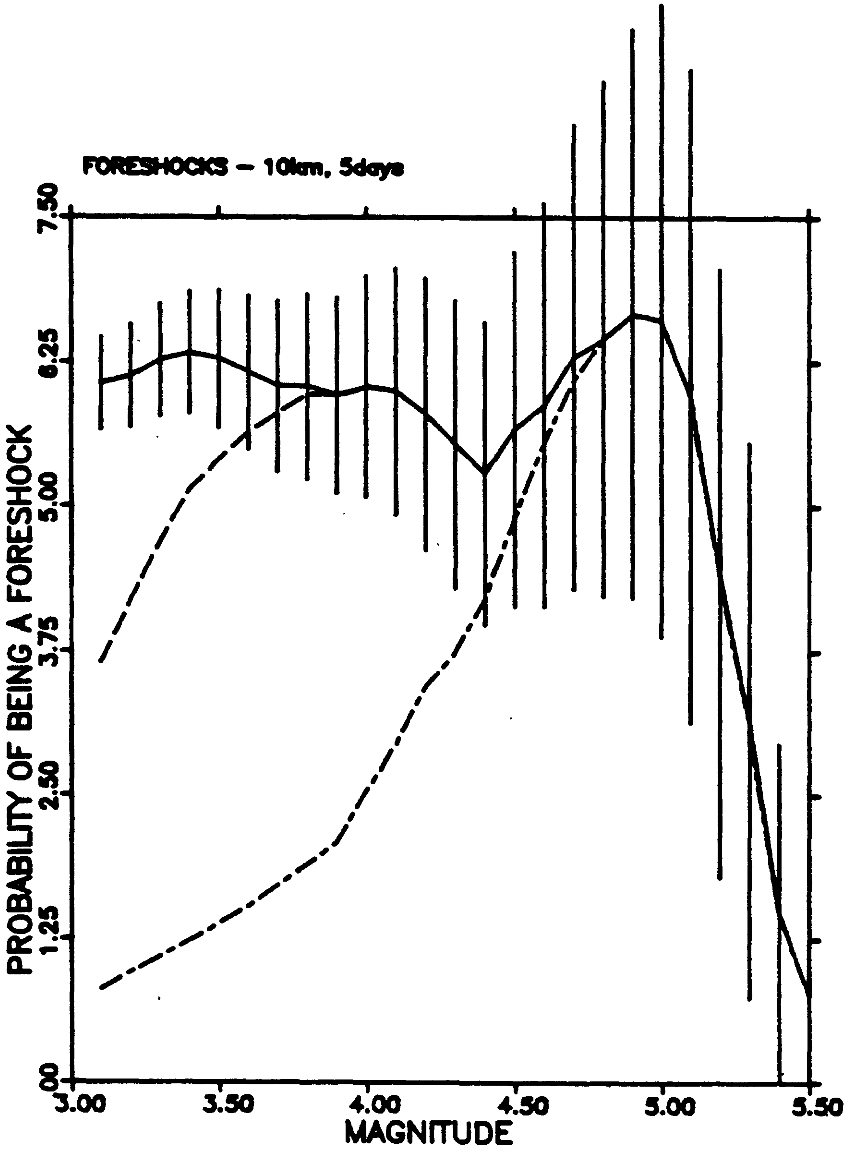
FORESHOCKS — 10km, 5days
PROBABILITY OF BEING A FORESHOCK
0.0
1.25
2.50
3.75
5.00
6.25
7.50
3.00
3.50
4.00
4.50
5.00
5.50
MAGNITUDE

Fig 4

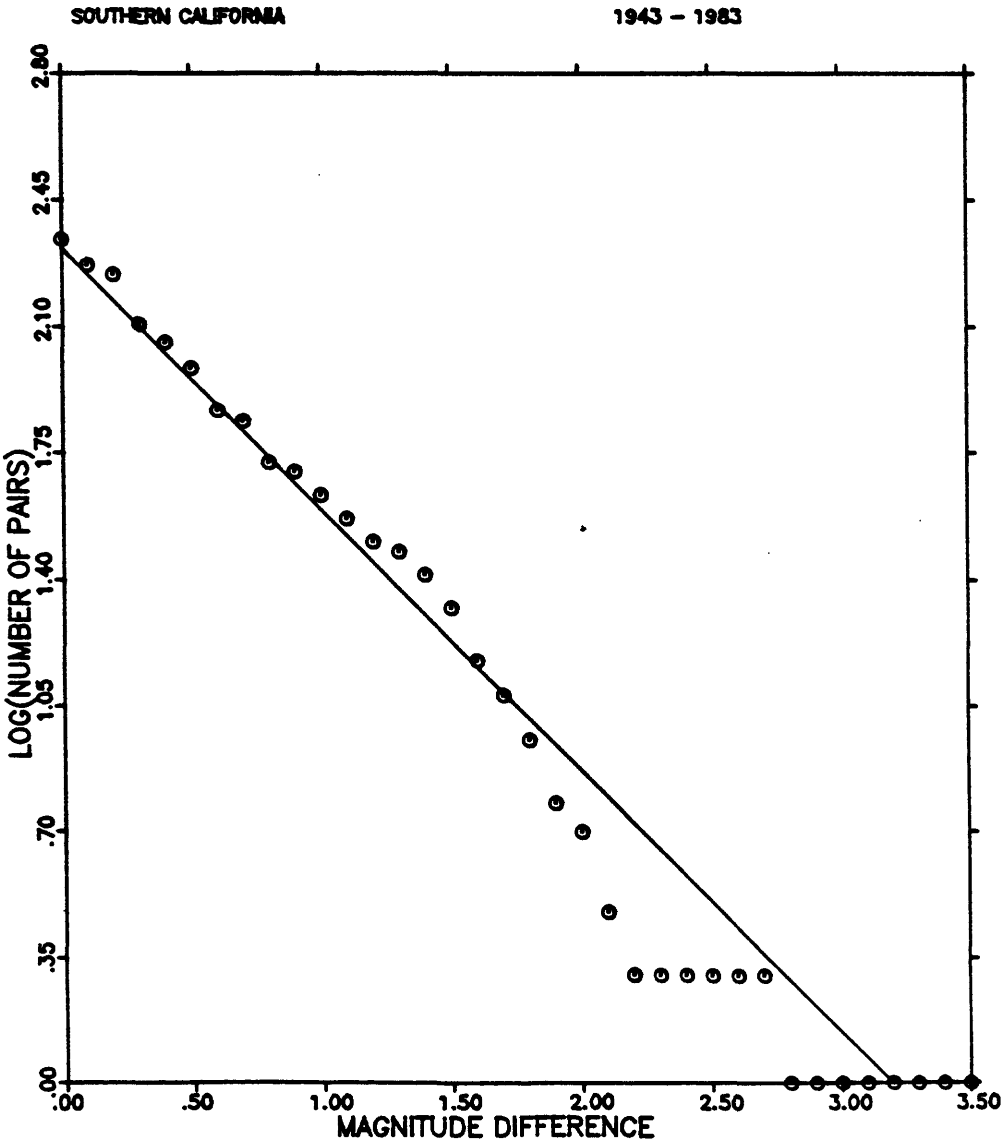
SOUTHERN CALIFORNIA
1943 - 1983
LOG(NUMBER OF PAIRS)
2.80
2.45
2.10
1.75
1.40
1.05
.70
.35
.00
.00
.50
1.00
1.50
2.00
2.50
3.00
3.50
MAGNITUDE DIFFERENCE

Fig. 5

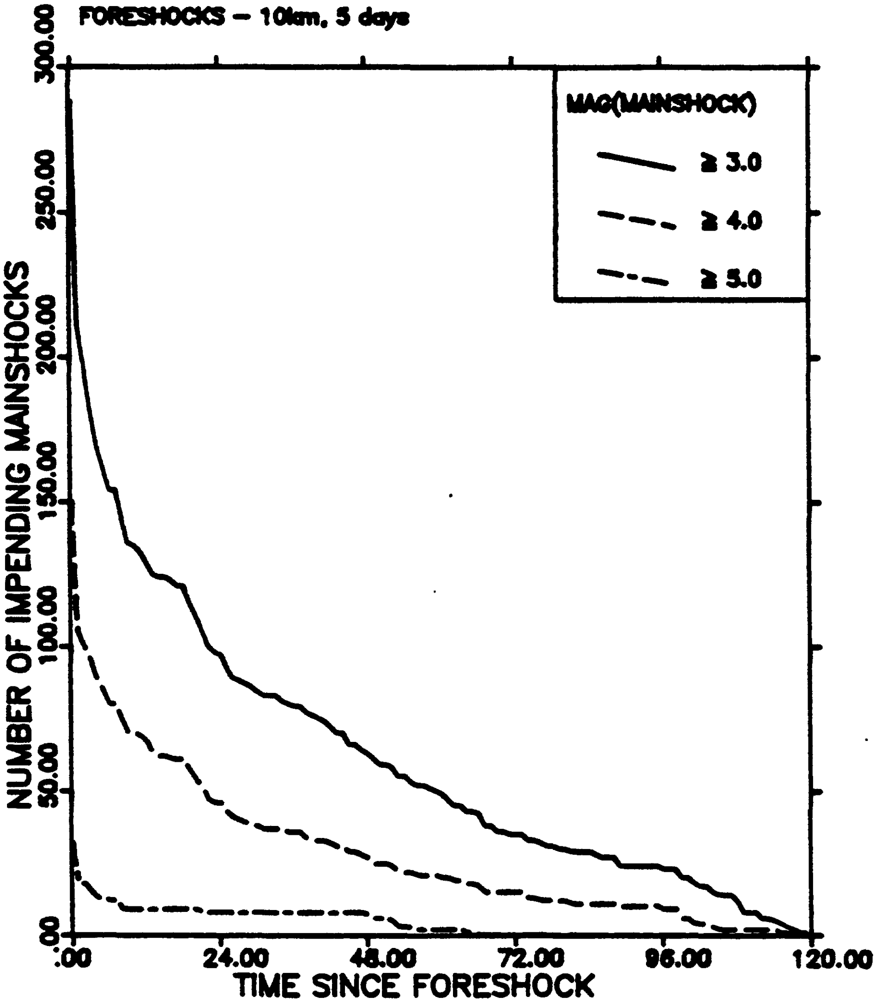
FORESHOCKS – 10km, 5 days
MAG(MAINSHOCK)
≥ 3.0
≥ 4.0
≥ 5.0
NUMBER OF IMPENDING MAINSHOCKS
300.00
250.00
200.00
150.00
100.00
50.00
.00
.00
24.00
48.00
72.00
96.00
120.00
TIME SINCE FORESHOCK

APPENDIX A. 11.

CIT (California Institute of Technology) - USGS Catalog Events 1979-1984

C. Johnson

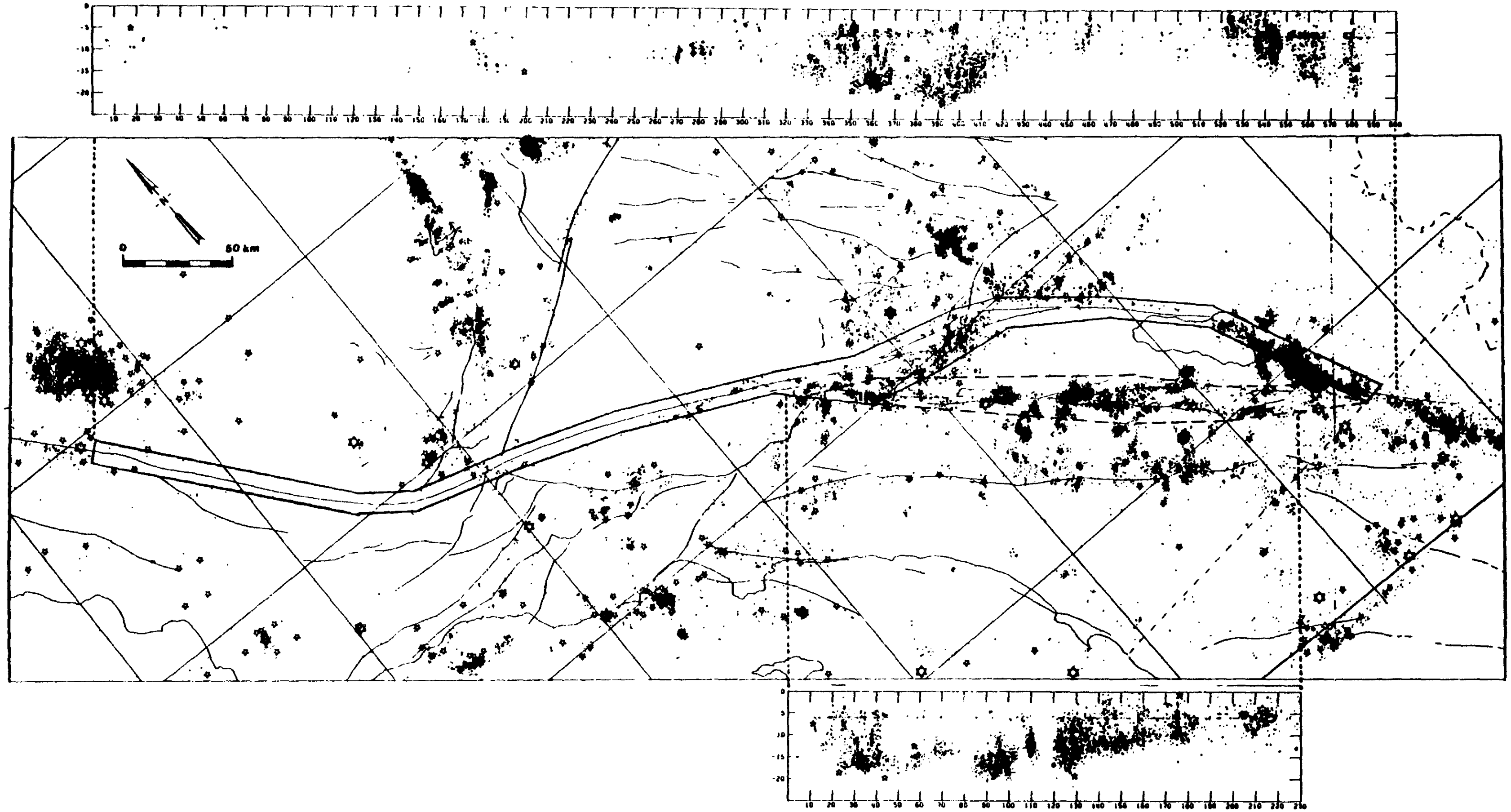

ALL CIT-USGS CATALOG EVENTS 1979-1984
(APPROX. 65,000 EVENTS)

APPENDIX A. 12.

A Review of Earthquake Stress Drop Determination Along the San Andreas and San Jacinto Fault Zones, Southern California

Arthur Frankel

A Review of Earthquake Stress Drop Determinations Along the San Andreas and San Jacinto Fault Zones, Southern California

Arthur Frankel

Jet Propulsion Laboratory, California Institute of Technology, Pasadena, Ca. 91109

There have been several studies in the past fifteen years of the stress drops of earthquakes in southern California. In this summary, I will concentrate on determinations of static stress drops for events along the San Andreas and San Jacinto faults made from recordings at local and regional distances (excluding data from the Anza seismic network), since these calculations are the most common. My major conclusion is that we actually know very little about the spatial and temporal variations of seismic stress drop along these fault zones in southern California. Our knowledge is limited by the inadequacy of the present instrumentation in this critical region of the United States. However, there is encouraging, albeit limited, evidence that stress drop determinations, when carefully corrected for path effects, are useful to the prediction of moderate-sized earthquakes in this area.

It should be noted that stress drop determinations are highly model dependent, so that absolute values are less reliable than relative differences in stress drop determined from the same technique and source model. Static stress drop calculations require estimates of the seismic moment and faulting dimension. The source size can be determined from the corner frequency of the displacement spectrum (Brune, 1970) or from the duration of the displacement or velocity pulse. In general, the highest stress drops reported in southern California are in the hundreds of bars.

Wyss and Brune (1971) determined the apparent stress (*rigidity · energy / moment*) for about 300 events (M_L 3-6) in southern California, using the ratio of short (1 sec) to long ($\approx$ 20 sec) period seismic amplitudes. They concluded that most events along the San Andreas and San Jacinto fault zones (excluding aftershocks of the Borrego Mountain earthquake) had average apparent stresses. Earthquakes near San Gorgonio Mountain in the Big Bend region of the San Andreas fault had higher than average apparent stresses. However, the study had many limitations, such as the lack of depth and path corrections and the inadequacy of the M_L scale as a measure of energy. Thus, these reported regional differences in apparent stress must be considered highly tentative. Analysis of recordings from broad-band instruments at closer epicentral distances is required to substantiate these variations.

Thatcher and Hanks (1973) calculated the stress drops of over a hundred events in southern California using spectra from analog recordings of torsional instruments at epicentral distances ranging up to about 300 km (Figure 1). The central finding of this study was that stress drops generally ranged from about 1 to 100 bars, independent of seismic moment for events between magnitudes 3.5 and 6.8 (Figure 2). Some regional variations in stress drop were tentatively identified in the paper. Earthquakes near the San Andreas and San Jacinto fault zones were characterized by average stress drops (1-30 bars). A notable exception was the 1948 Desert Hot Springs earthquake ($M_L = 6.5$), which had a relatively high stress drop of 140 bars. Again, confirmation of the regional differences in stress drop awaits higher quality recordings at smaller epicentral distances.

Estimates of the stress drops of three $M_L \approx 5$ earthquakes along the San Jacinto fault zone near Anza have been obtained from the records of close-in (Δ < 20 km) strong-motion accelerographs (Figure 3). These events occurred within the Anza seismic slip gap identified by Thatcher et al (1975) and surround the seismicity gap reported by Sanders and Kanamori (1984). Hartzell and Brune (1979) calculated a stress drop of 225 bars for the 1975 Horse Canyon event (M_L 4.8), using corner frequency measurements. Frankel (1984) used displacement pulse widths to determine stress drops of 110 and 100 bars for the 1980 (M_L 5.5) and 1982 (M_L 4.8) events, respectively. Stress drop calculations derived from corner frequency observations varied from the time domain results by as much as a factor of two. Similar time domain measurements made from close-in strong motion recordings for an M_L 4.7 aftershock of the 1975 Oroville earthquake (data from Fletcher et al, 1980) and an M_L 5.0 aftershock of the 1979 Imperial Valley shock yielded stress drops of 180 and 130 bars, respectively (Figure 4). Thus, the stress drops of the events near Anza do not appear to be unusually high, relative to those of aftershocks in other parts of California. However, it is not yet known whether the two aftershocks studied had representative stress drops for their source regions or had untypically high stress drops. In this regard, Hartzell and Brune (1977) calculated a stress drop of about 640 bars for an M_L 4.3 event that occurred during the 1975 Brawley swarm in the Imperial Valley, using spectral measurements derived from records of a single strong motion instrument. Therefore, stress drops of at least some events in the Imperial Valley are as high as those found for earthquakes near Anza.

Many seismologists have suggested the use of stress drop determinations of microearthquakes (M_L < 3) for earthquake prediction purposes. However, recent observations of the spectra and pulse widths of microearthquakes have indicated that path effects often contaminate stress drop determinations for these small events. A general observation of microearthquake studies in California and other areas is that the corner frequencies of small earthquakes (M_L < 3) remain roughly constant as their seismic moments decrease below about 10^{20} dyne cm (Figure 5; see, e.g., Archuleta et al, 1982). This observation contrasts with the finding of Thatcher and Hanks (1973) that corner frequencies increase with decreasing seismic moment for events larger than M_L 3, so that stress drops are independent of moment. There is substantial evidence that the corner frequencies observed in microearthquake spectra are produced by severe attenuation at shallow depths under the receiver sites (Frankel, 1982; Hanks, 1982) and are not indicators of the rupture dimension of the source. Malin and Waller (1985) report severe attenuation at depths less than 500m using a vertical array of seismometers placed in a borehole drilled through the Cleveland Hill fault zone near Oroville. Apparent corner frequencies observed in records taken from surface seismometers were absent from the seismograms recorded by the borehole receivers. Thus spectra of ground motions recorded by seismometers at the surface may not reflect the source spectra of small events.

This site response problem is clearly apparent in the P-wave velocity spectra of a magnitude 2.0 event in the San Gorgonio Pass area (depth= 19 km), derived from digital recordings of the southern California array (Figure 6). The spectrum at station RAY (hypocentral distance r=21 km) is much lower in frequency than that of station MLL which is more distant (r= 30 km; compare Figures 7 and 8). This effect cannot be attributed to source directivity, since both stations are at similar azimuths and incidence angles from the source. In fact, station GAV, 75 km from the source, has much higher frequency content than RAY (Figure 9). Thus, attenuation near the RAY site must be producing the apparent corner frequency of the signal at that site. Although other sites may record higher frequency energy than RAY, this observation calls into question whether the corner frequencies accurately represent the source spectrum. This example also points out the inadequacy of the sampling rate used by the southern California network (50 samples per second), since the velocity spectrum at MLL appears to be increasing up to the Nyquist frequency of 25 hz.

The severity of path effects on microearthquake waveforms can actually be quite useful in the determination of stress drops of earthquakes with magnitudes greater than about 3.5, whose source durations are long enough to be separated from pulse broadening caused by path effects. Frankel and Kanamori (1983) determined the stress drops of ten events ($M_L \approx 4$) using the waveforms of adjacent small earthquakes ($M_L \leq 2.2$) as empirical Green's functions (Figure 10). The pulse widths of these small earthquakes were generally observed to decrease to some minimum pulse width with decreasing magnitude (Figures 11-13). Thus the pulse widths of the smallest events were interpreted as the impulse response of that particular path between the source region and the receiver. The waveforms of the smaller events were approximately deconvolved from the waveforms of the larger events, to obtain an estimate of the source duration of the larger event that was corrected for all path effects, including the site response (Figure 14). The limited dynamic range of the network caused the waveforms for the larger events to be clipped. This study relied on the measurement of the time between the P-wave onset and the first zero crossing ($\tau_{1/2}$) to quantify source duration.

Frankel and Kanamori (1983) found that earthquakes in southern California exhibit significant differences in stress drop (Figures 15 and 16) and that these differences may sometimes be indicative of impending larger shocks. The event with the highest stress drop of those studied (event #6, 11:51 UT, 2 July 1979, M_L 3.8, 860 bars) was located 10 km south of the trifurcation of the San Jacinto fault zone (Figure 17). This earthquake was followed an hour later by an event 1.5 km away (event #7, M_L 3.6) with a stress drop of only 88 bars. The M_L 5.5 February 1980 earthquake occurred within eight months of the high stress drop event and its hypocenter was located about 2 km away. The large variation in stress drop between the two adjacent events in July 1979 may imply that stress drops reflect very localized stress conditions along a fault zone and may be useful for the identification of asperities where moderate-sized earthquakes may nucleate.

The other event with a stress drop significantly higher than average for this study occurred near the San Andreas fault about 30 km northwest of Cajon Pass, near Wrightwood (event #8, Figure 16). The location of this high stress drop event (350 bars) near the southern terminus of the great 1857 earthquake should prompt further study of the source parameters of earthquakes in this area. Stress drops of shallow earthquakes near the intersection of the Banning and Mission Creek faults were between 40 and 70 bars, average for events in this study.

In conclusion, it is premature to evaluate the limited stress drop calculations available for earthquakes in the vicinity of the San Andreas and San Jacinto faults in terms of earthquake prediction. Seismic network instrumentation with reasonable sampling rates (100-200 samples/sec) and high dynamic range are required to obtain stress drops of $M_L > 3.5$ events, corrected for path effects. The upgrade of relatively few ($\approx$20) stations of the southern California network would provide the necessary data to judge the utility of seismic stress drop for the monitoring of tectonic stress levels and the discrimination of foreshock sequences.

References

Archuleta, R. J., E. Cranswick, C. Mueller and P. Spudich (1982), Source parameters of the 1980 Mammoth Lakes, California, earthquake sequence, *J. Geophys. Res.*, *87*, p. 4595-4608.

Brune, J. N. (1970), Tectonic stress and the spectra of seismic shear waves from earthquakes, *J. Geophys. Res.*, *75*, p. 4997-5009.

Fletcher, J. B., A. G. Brady, and T. C. Hanks (1980), Strong-motion accelerograms of the Oroville, California aftershocks: data processing and the aftershock of 0350 August 6, 1975, *Bull. Seismol. Soc. Am.*, *70*, p. 243-267.

Frankel, A. (1982), The effects of attenuation and site response on the spectra of microearthquakes in the northeastern Caribbean, *Bull. Seismol. Soc. Am.*, *72*, p. 1379-1402.

Frankel, A. (1984), Source parameters of two $M_L \approx 5$ earthquakes near Anza, California, and a comparison with an Imperial Valley aftershock, *Bull. Seismol. Soc. Am.*, *74*, p. 1509-1527.

Frankel, A., and H. Kanamori (1983), Determination of rupture duration and stress drop for earthquakes in Southern California, *Bull. Seismol. Soc. Am.*, *72*, p. 1527-1551.

Given, D. (1983), Seismicity and structure of the trifurcation in the San Jacinto fault zone, Southern California, Master's thesis, California State University, Los Angeles, 73 pp.

Hanks, T. C. (1982), $f_{\max}$, *Bull. Seismol. Soc. Am.*, *72*, p.1867-1880.

Hartzell, S. H. and J. N. Brune (1977), Source parameters for the January 1975 Brawley-Imperial Valley earthquake swarm, *Pageoph.*, *115*, p. 333-355.

Hartzell, S. H. and J. N. Brune (1979), The Horse Canyon earthquake of August 2, 1975 - two-stage stress release process in a strike-slip earthquake, *Bull. Seismol. Soc. Am.*, *69*, p. 1161-1174.

Hartzell, S. H., and D. V. Helmberger (1982), Strong-motion modeling of the Imperial Valley

Earthquake of 1979, *Bull. Seismol. Soc. Am.*, *72*, p. 571-596.

Malin, P. E. and J. A. Waller (1985), Preliminary results from vertical seismic profiling of Oroville microearthquake S-waves, preprint.

Sanders, C. O., and H. Kanamori (1984), A seismotectonic analysis of the Anza seismic gap, San Jacinto fault zone, Southern California, J. Geophys. Res., 89, p. 5873-5890.

Thatcher, W. and T. C. Hanks (1973), Source parameters of southern California earthquakes, J. Geophys. Res., 78, p. 8547-8575.

Thatcher, W., J. A. Hileman and T. C. Hanks (1975), Seismic slip distribution along the San Jacinto fault zone, Southern California and its implications, *Geol. Soc. Am.*, *Bull.*, *86*, p. 1140-1146.

Wyss, M. and J. N. Brune (1971); Regional variations of source properties in southern California estimated from the ratio of short- to long-period amplitudes, *Bull. Seismol. Soc. Am.*, *61*, p. 1153-1167.

Figure Captions

Figure 1. Map of earthquakes studied by Thatcher and Hanks (1973), from their paper.

Figure 2. Log moment plotted against log corner frequency for earthquakes in southern California, along with lines of constant static stress drop (from Thatcher and Hanks, 1973).

Figure 3. a) Map of Anza area with three events $M_L \approx 5$, studied using records from SMA instruments (circles; map from Frankel, 1984). Focal mechanisms from Given (1983) and Given personal communication (1984). b) Map of Imperial Valley area showing location of the aftershock of the 1979 shock studied by Frankel (1984). Lower map is adapted from Hartzell and Helmberger (1982).

Figure 4. Log displacement pulse width plotted against log moment for the two events near Anza, an aftershock of the 1975 Oroville event and an aftershock of the 1979 Imperial Valley shock (after Frankel, 1984).

Figure 5. Log moment as a function of log corner frequency for Mammoth Lakes earthquakes (from Archuleta et al, 1982).

Figure 6. Map of southern California showing location of earthquake in the San Gorgonio Pass region and stations of the southern California network used for the spectral analysis.

Figure 7. P-waveform and velocity spectrum (on linear axes) at station RAY for the event in Figure 6.

Figure 8. Same as Figure 7, for station MLL.

Figure 9. Same as Figure 7, for station GAV.

Figure 10. Map of earthquakes $M_L \approx 4$ (filled circles with ID numbers) and stations (open circles), from Frankel and Kanamori (1983).

Figure 11. Waveforms of a mainshock and two small foreshocks recorded by a station of the southern California array (from Frankel and Kanamori, 1983).

Figure 12. Half-pulse width ($\tau_{1/2}$) plotted against magnitude for mainshock #11 and its accompanying events (from Frankel and Kanamori, 1983).

Figure 13. Same as Figure 12, for mainshock #3 and its foreshocks and aftershocks.

Figure 14. Original (open circles) and path corrected (filled circles) values of $\tau_{1/2}$, from Frankel and Kanamori (1983).

Figure 15. Stress drops of mainshocks (given by their ID numbers) from Frankel and Kanamori (1983).

Figure 16. Map of mainshocks with their ID numbers and stress drops (in bars) from Frankel and Kanamori (1983).

Figure 17. Map showing event #6 (11:51 UT) and event #7 (12:42 UT) and epicenter of subsequent M_L 5.5 earthquake (from Frankel and Kanamori, 1983). Top trace in each panel is the waveform of event #6, middle trace is for event #7 and bottom trace is the waveform of a small event used as the empirical Green's function.

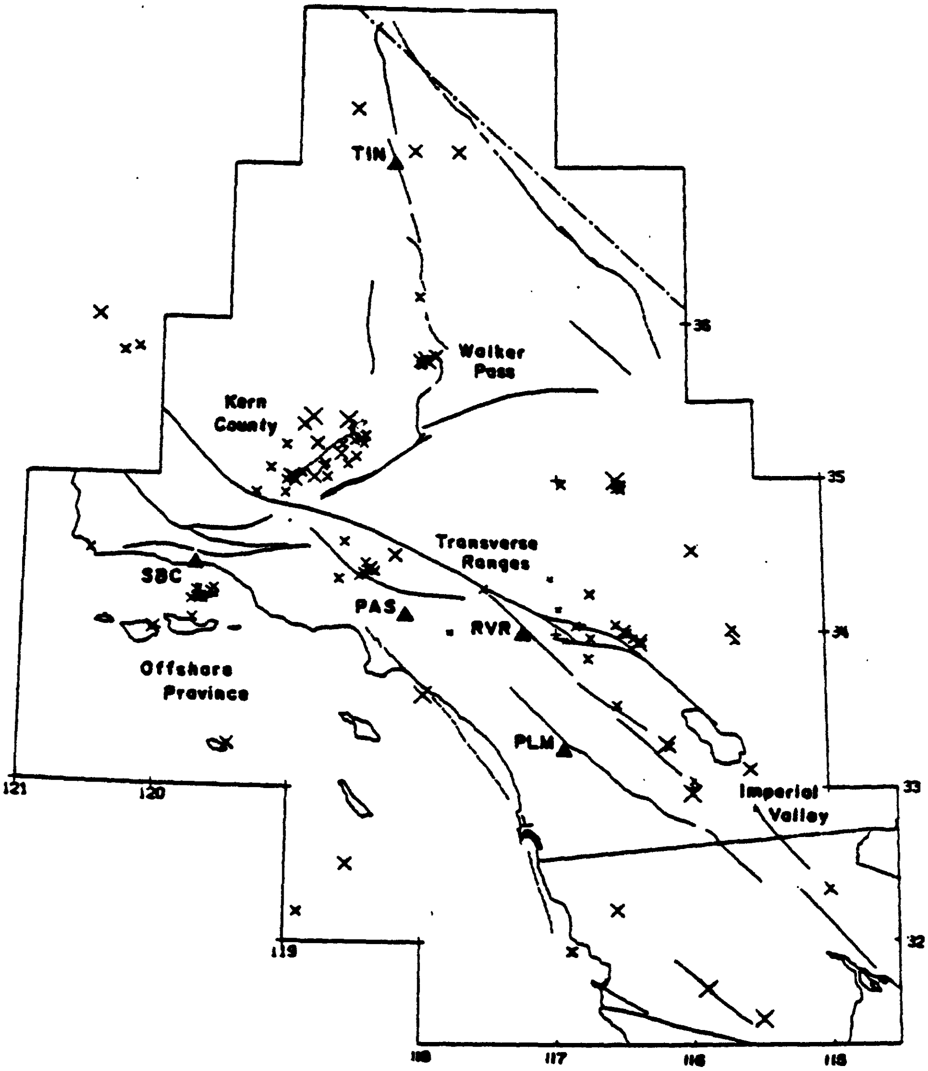
TIN
Walker Pass
Kern County
Transverse Ranges
SBC
PAS
RVR
Offshore Province
PLM
Imperial Valley
36
35
34
33
32
121
120
119
118
117
116
115

Fig. 1. Southern California, showing active faults, earthquake epicenters (crosses), and seismograph stations (triangles) used in this study. The size of the crosses is proportional to earthquake magnitude.

FIGURE 1

From: Thatcher and Hanks (1973)

THATCHER AND HANKS: SOUTHERN CALIFORNIA EARTHQUAKES

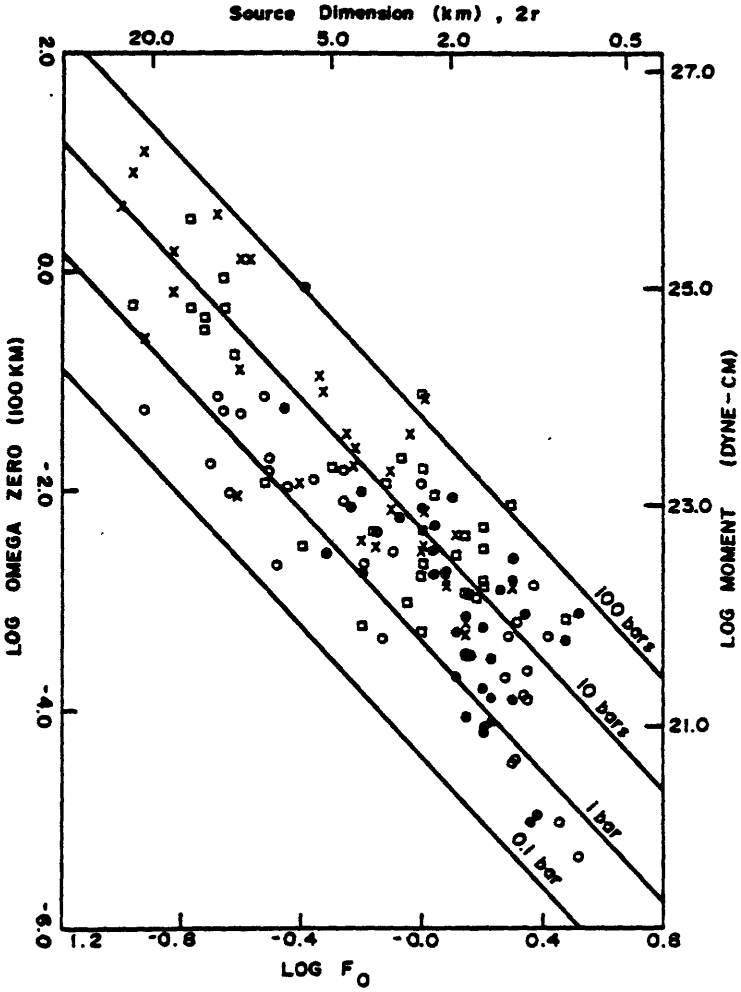

Fig. 6. Representation of Ω_0—f_0 for all southern California earthquakes studied in this paper. The observed spectral quantities are shown scaled to source dimension $2r$ and seismic moment by using *Brune's* [1970] theory. Open circles represent earthquakes in offshore province and San Andreas fault; solid circles, in Transverse Ranges; squares, in Kern county; crosses, in other southern California locations.

FIGURE 2

From: Thatcher and Hanks (1973)

Focal mechanisms from D. Given

Lower map adapted from Hartzell and Helmberger 1982

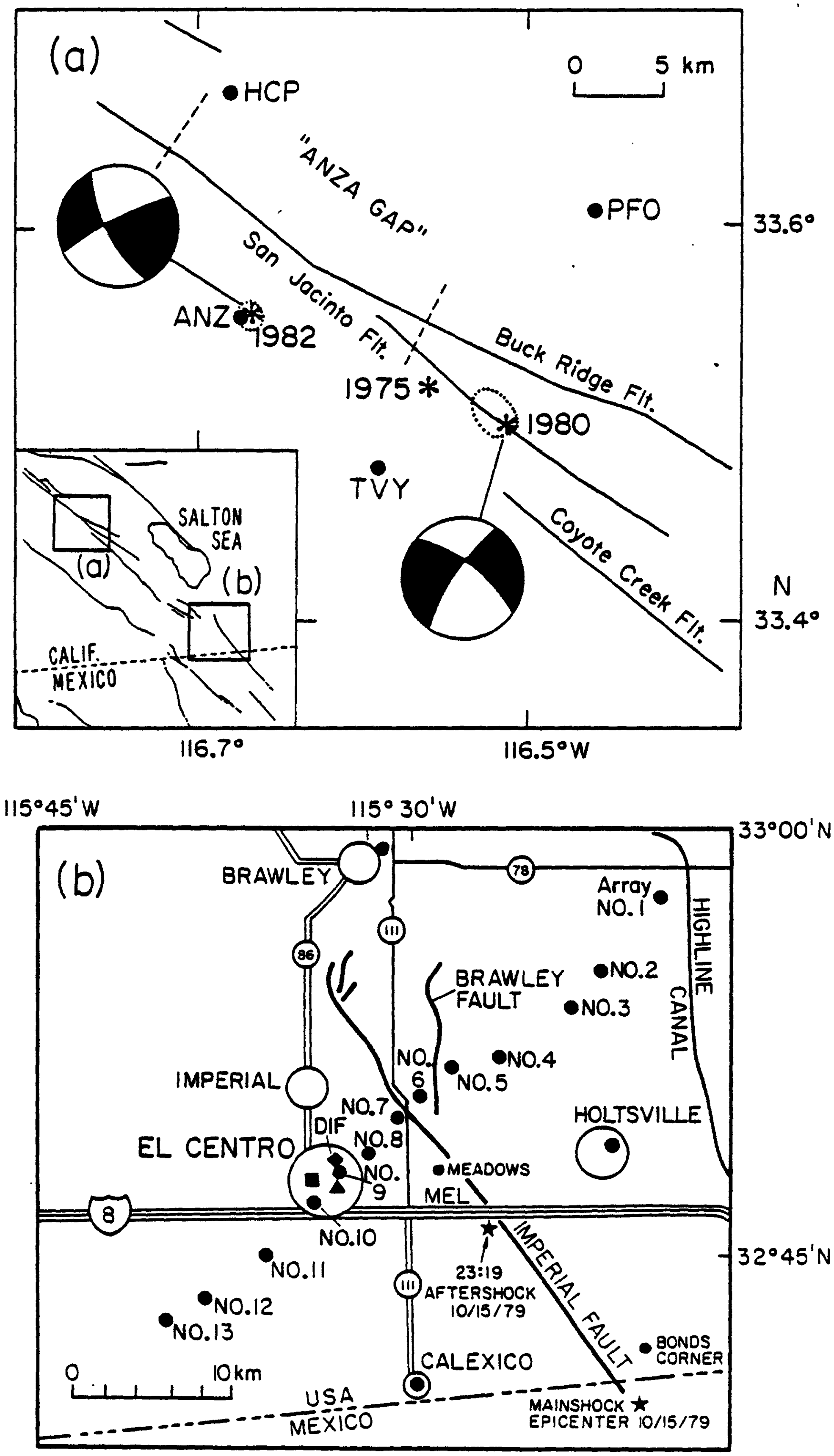
(a)
0 5 km
HCP
"ANZA GAP"
PFO
33.6°
San Jacinto Flt.
ANZ
1982
1975
Buck Ridge Flt.
1980
TVY
SALTON SEA
(a)
(b)
CALIF.
MEXICO
Coyote Creek Flt.
N
33.4°
116.7°
116.5°W
115°45'W
115° 30'W
33°00'N
(b)
BRAWLEY
78
Array NO. 1
HIGHLINE CANAL
111
86
BRAWLEY FAULT
NO.2
NO.3
NO. 6
NO.5
NO.4
IMPERIAL
NO.7
HOLTSVILLE
DIF
EL CENTRO
NO.8
MEADOWS
NO. 9
MEL
8
NO.10
IMPERIAL FAULT
32°45'N
NO.11
23:19 AFTERSHOCK 10/15/79
NO.12
NO.13
BONDS CORNER
0
10km
CALEXICO
USA
MEXICO
MAINSHOCK EPICENTER 10/15/79

FIGURE 3

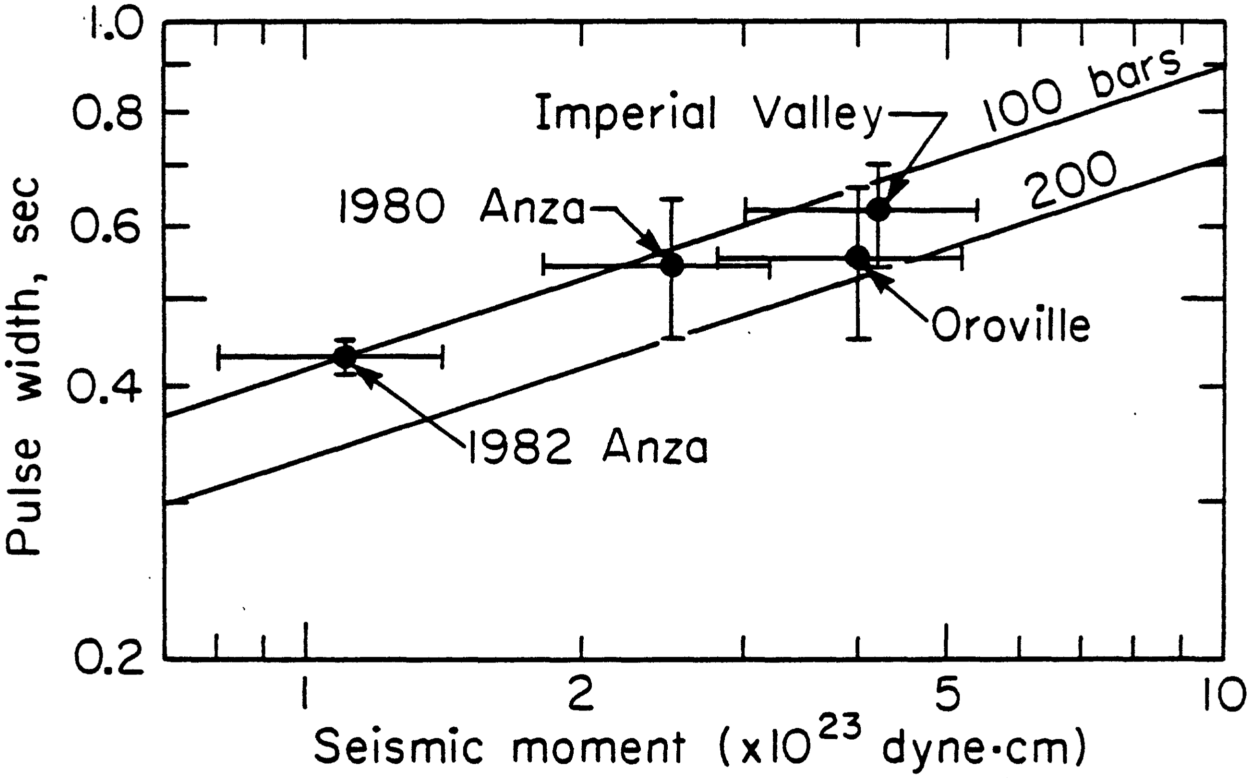
1.0
0.8
0.6
0.4
0.2
Pulse width, sec
1
2
5
10
Seismic moment (x10^23 dyne·cm)
Imperial Valley
100 bars
200
1980 Anza
Oroville
1982 Anza

FIGURE 4

FIGURE 5

Data from:
Archuleta et al (1982)

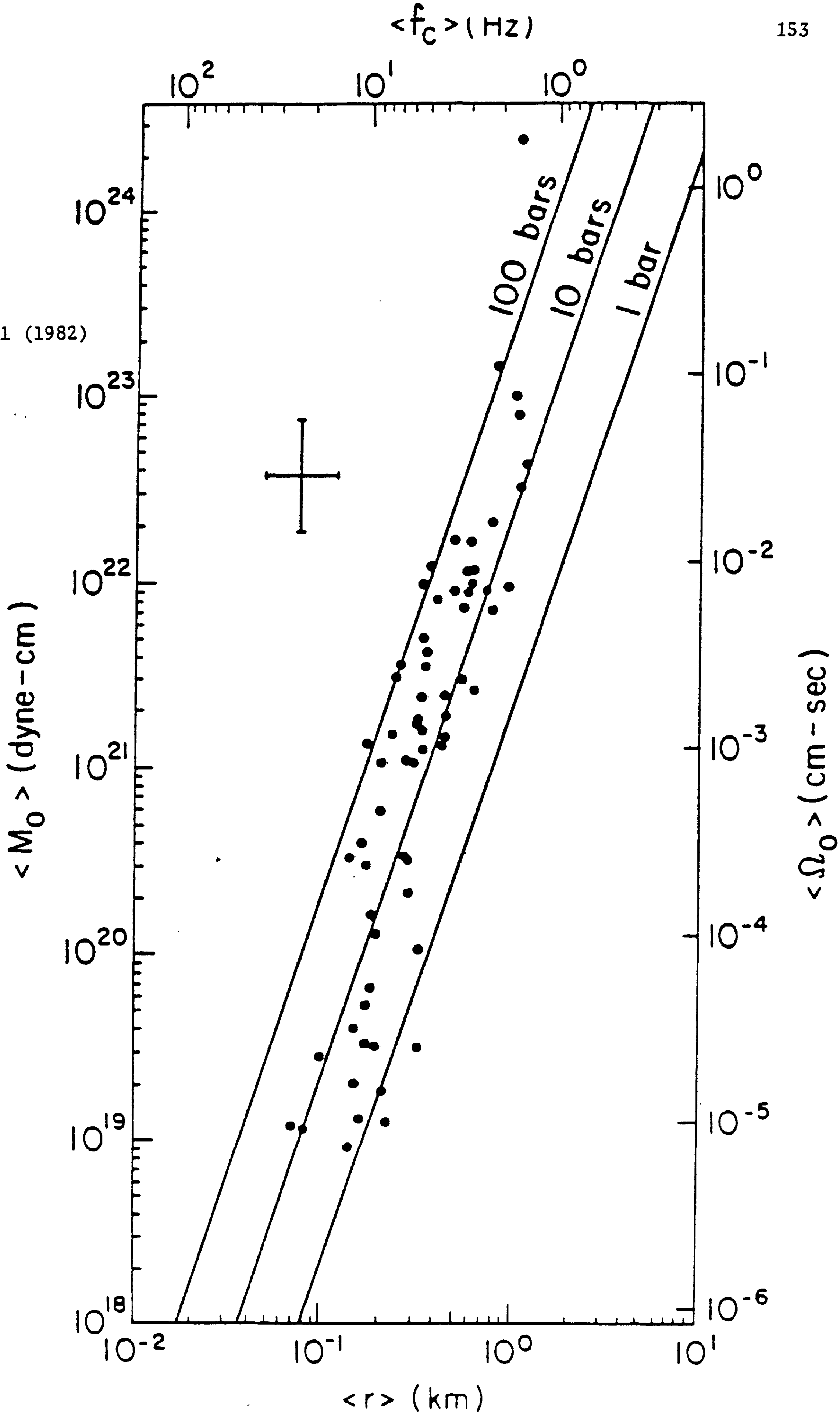

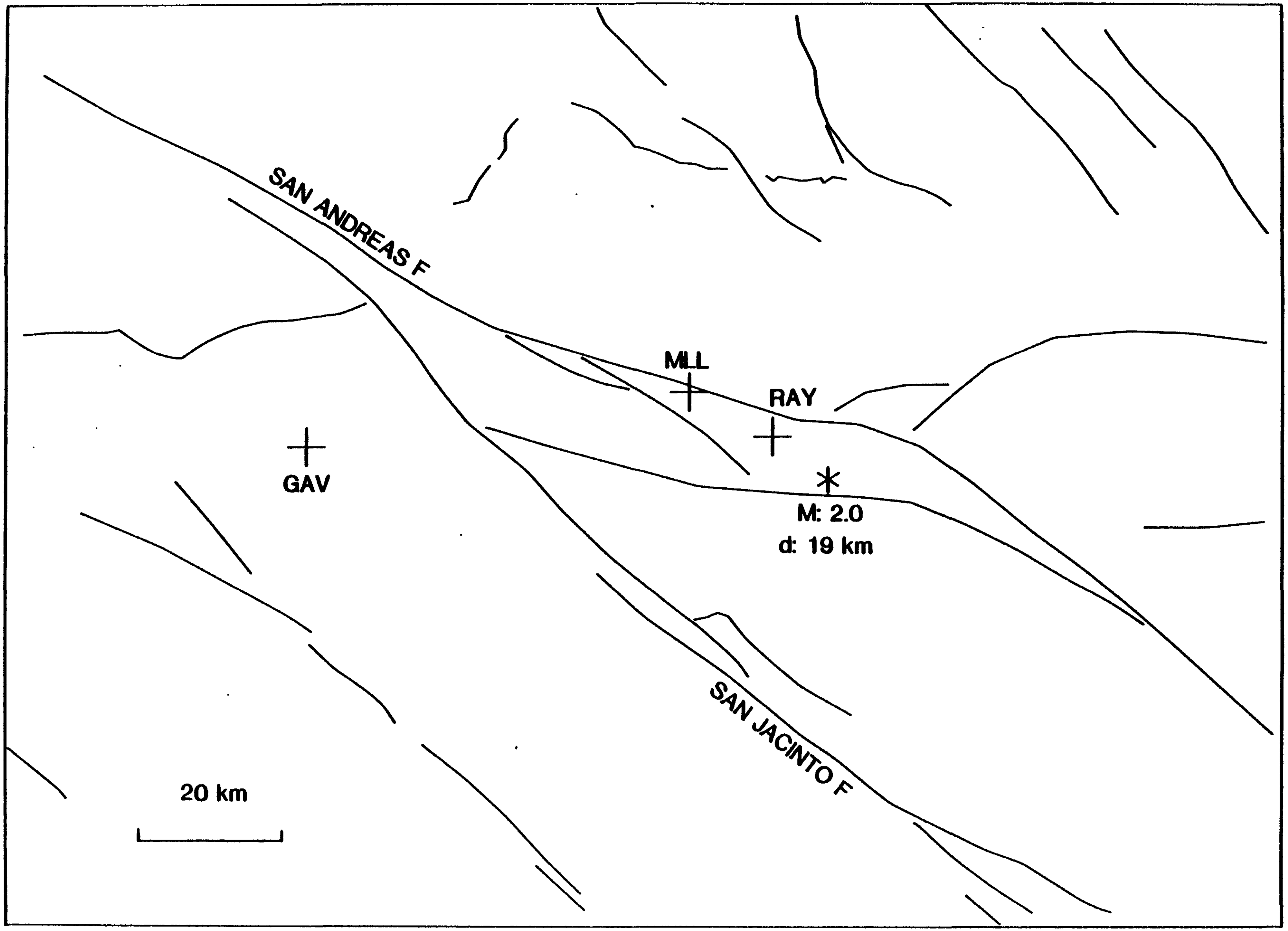
SAN ANDREAS F
MLL
RAY
GAV
M: 2.0
d: 19 km
SAN JACINTO F
20 km

FIGURE 6

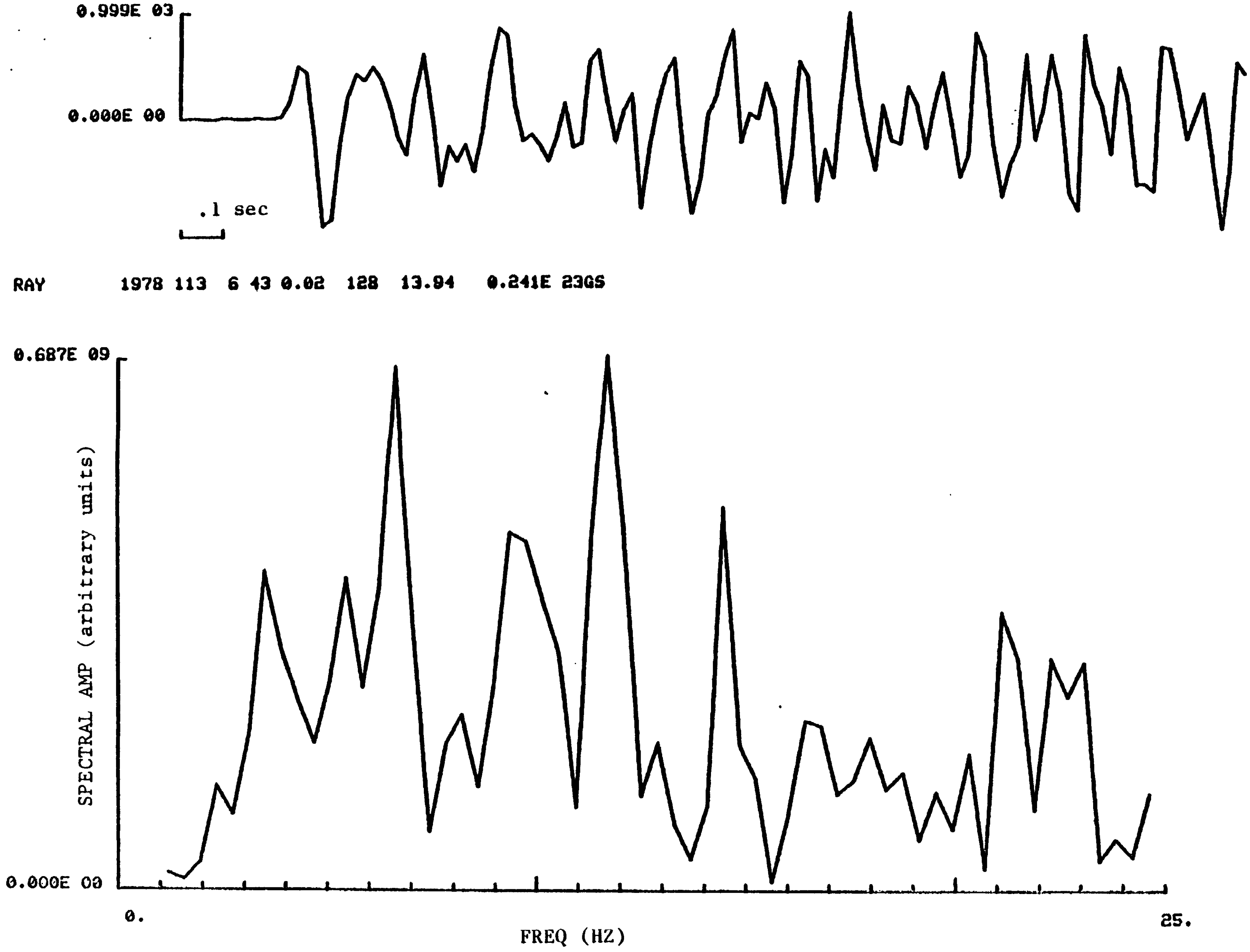

FIGURE 7

P-waveform and velocity spectrum (on linear axes) at RAY (r=21 km)

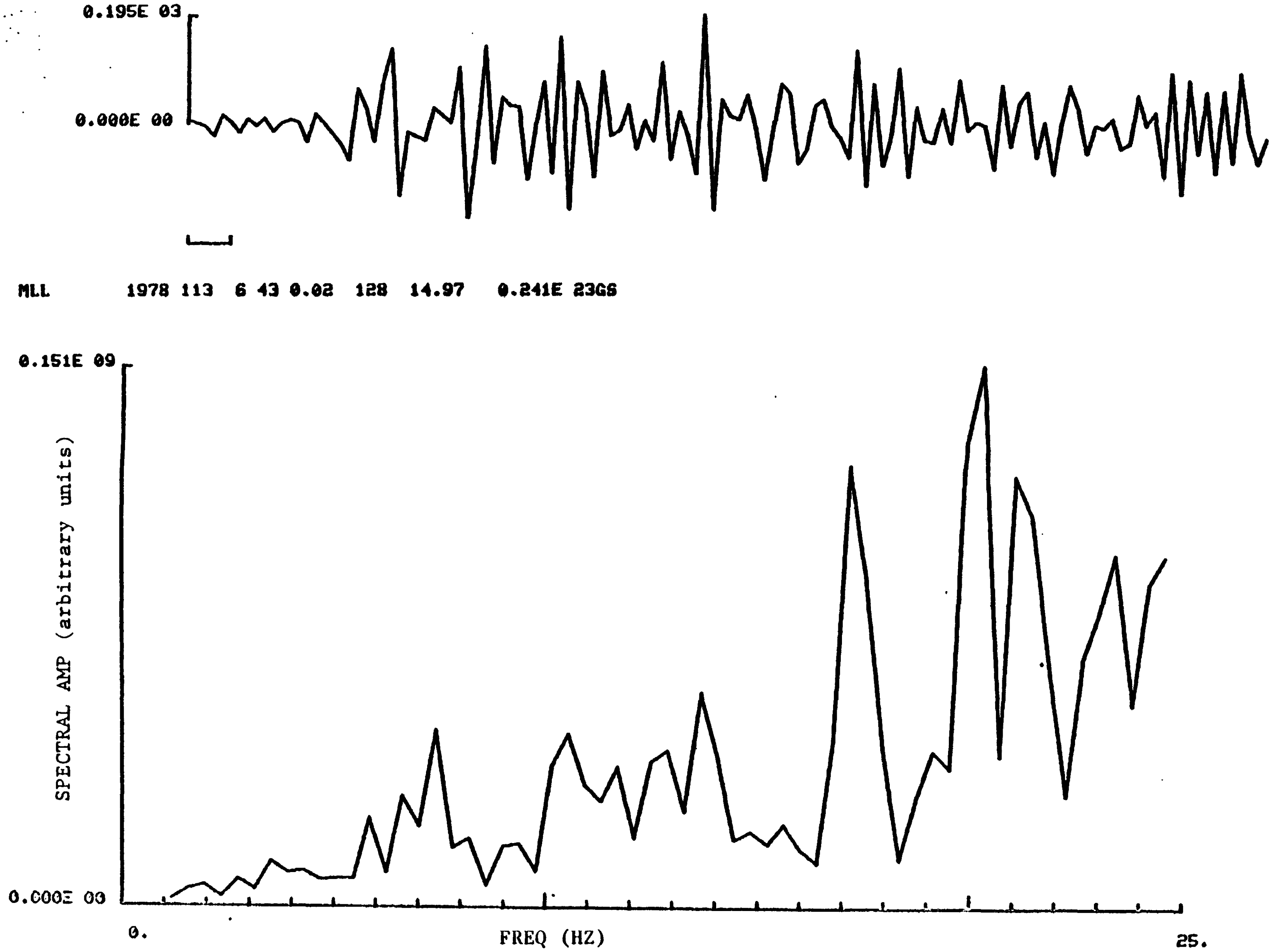

FIGURE 8
STATION MLL (r= 30 km)

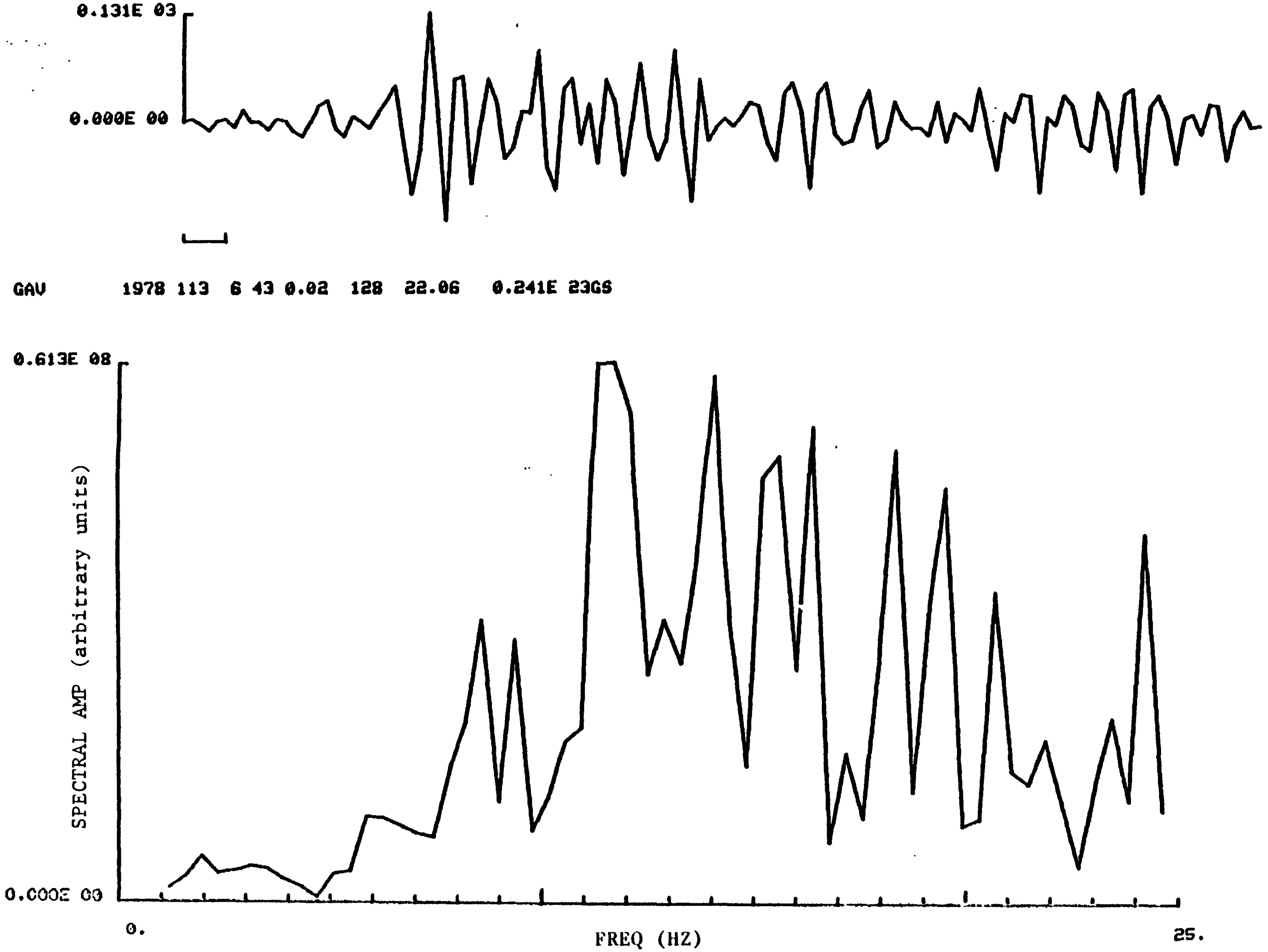

FIGURE 9 STATION GAV (r= 75 km)

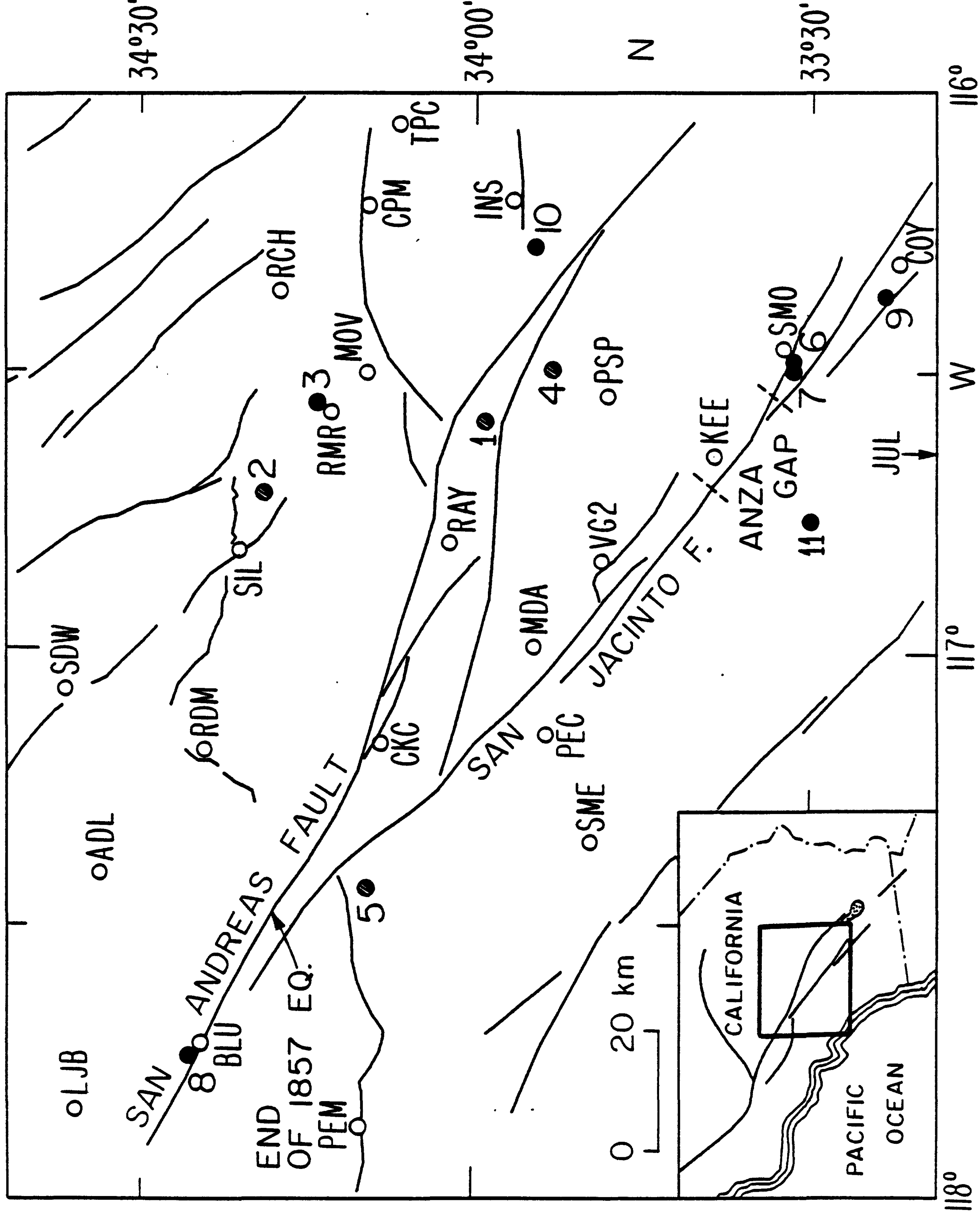
34°30'
34°00'
33°30'
118°
117°
116°
N
W
SAN ANDREAS FAULT
SAN JACINTO F.
END OF 1857 EQ.
ANZA GAP
20 km
0
20
CALIFORNIA
PACIFIC OCEAN
LJB
BLU
PEM
ADL
SDW
RDM
CKC
SME
PEC
MDA
SIL
RAY
VG2
RMR
MOV
RCH
CPM
TPC
INS
PSP
KEE
SMO
JUL
COY
1
2
3
4
5
6
7
8
9
10
11

FIGURE 10

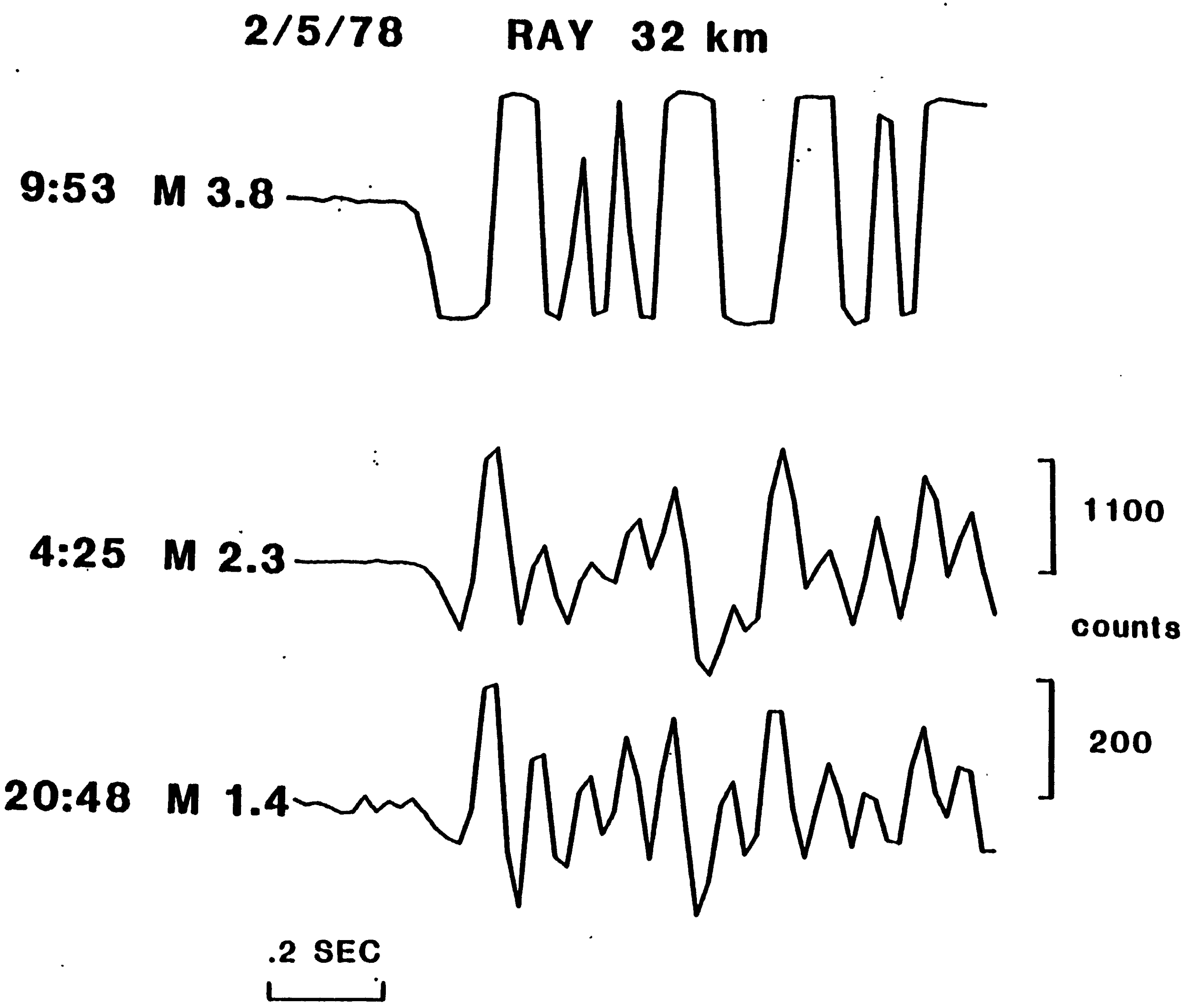

FIGURE 11

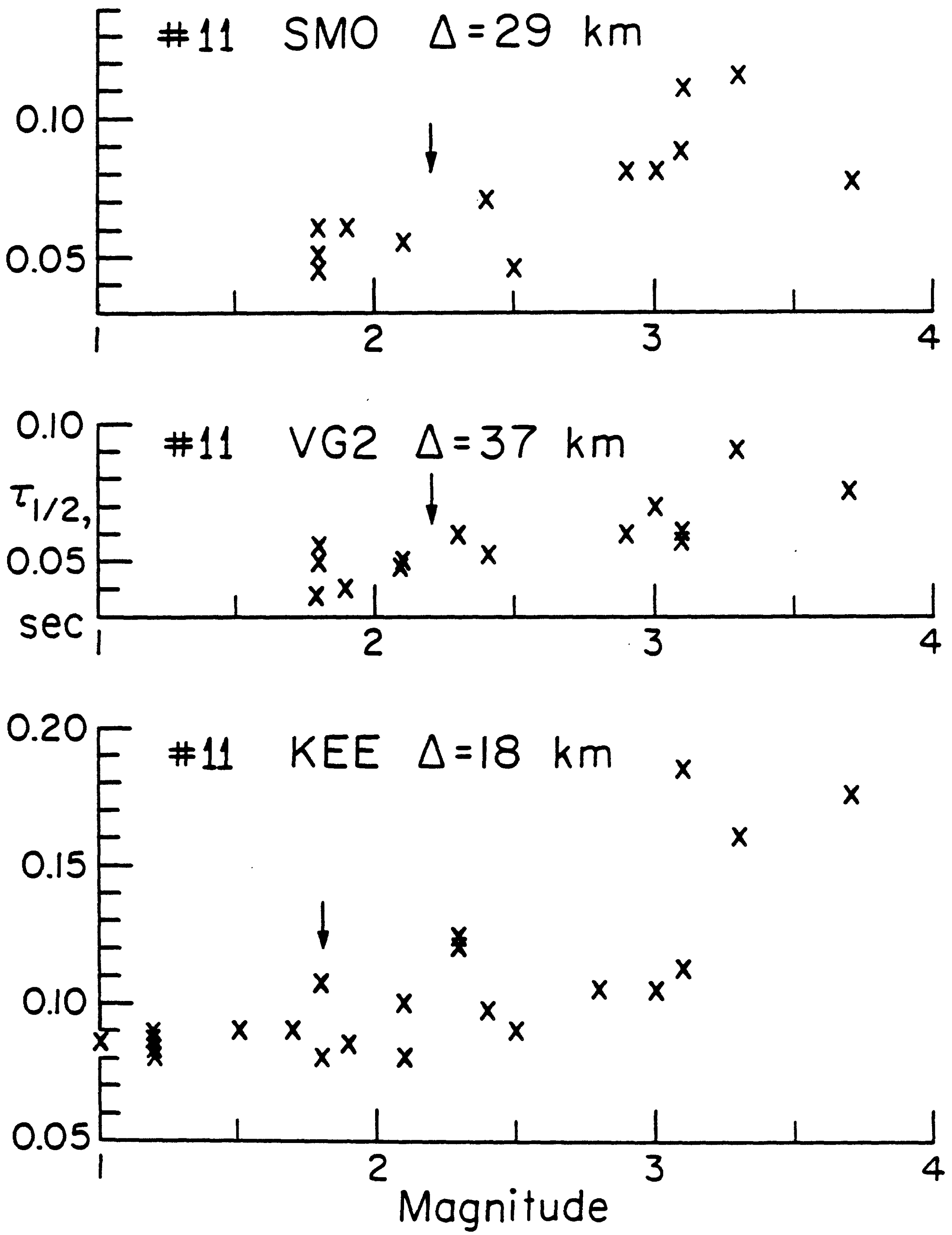
#11 SMO Δ=29 km
0.10
0.05
1
2
3
4
#11 VG2 Δ=37 km
0.10
$\tau_{1/2}$, sec
0.05
1
2
3
4
#11 KEE Δ=18 km
0.20
0.15
0.10
0.05
1
2
3
4
Magnitude

FIGURE 12

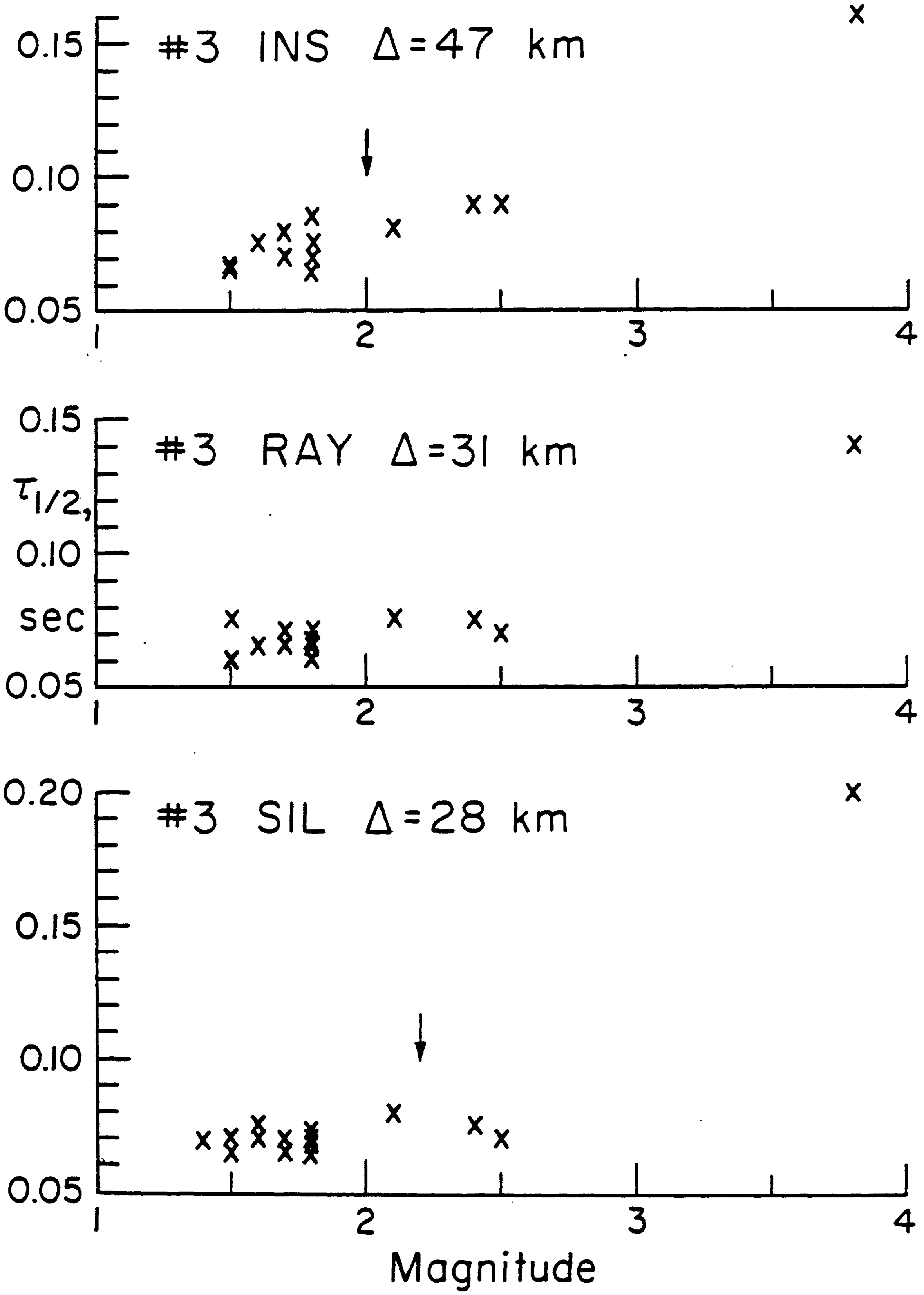
#3 INS Δ=47 km
#3 RAY Δ=31 km
#3 SIL Δ=28 km
$\tau_{1/2}$, sec
0.05
0.10
0.15
0.20
1
2
3
4
Magnitude

FIGURE 13

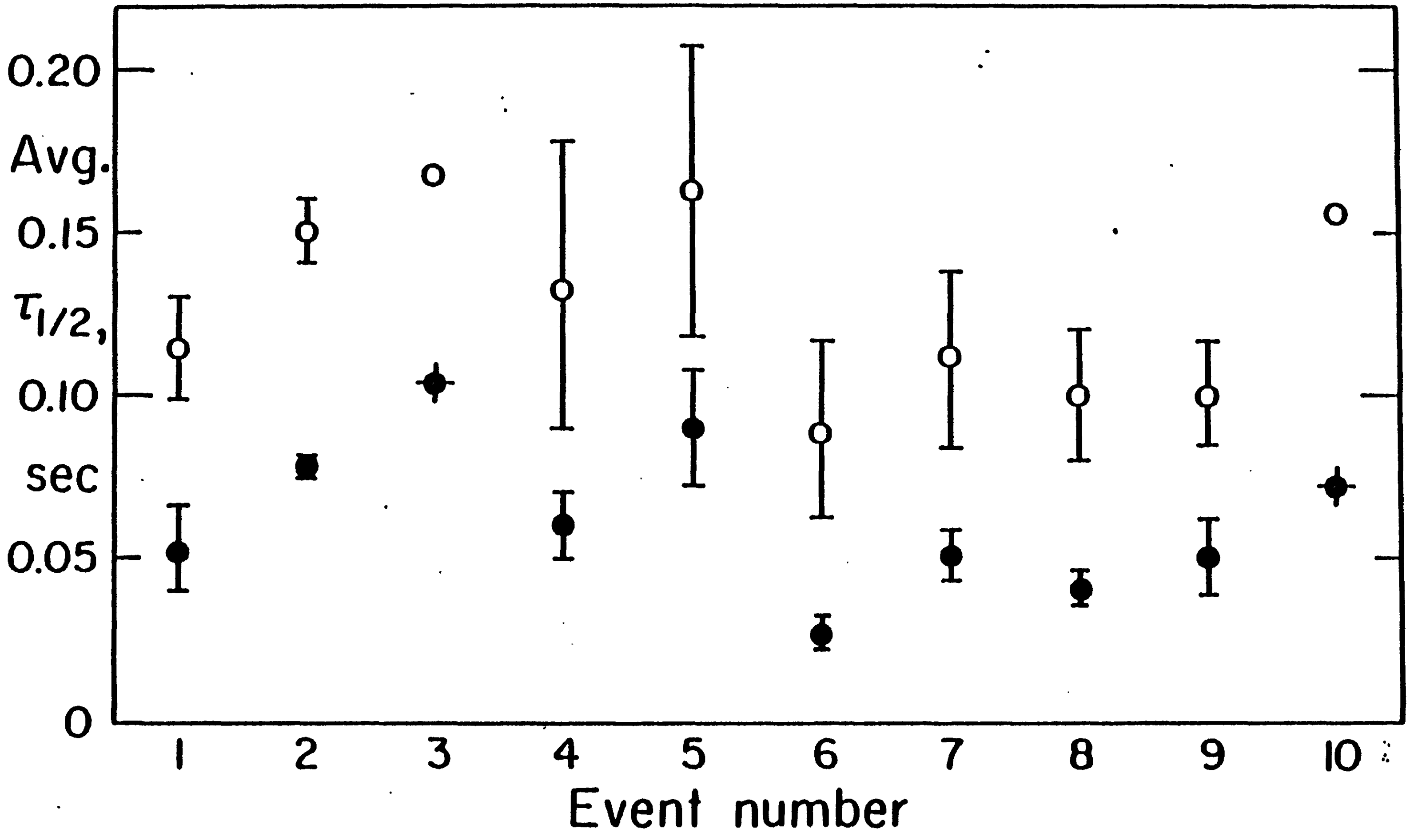

FIGURE 14 Open circles: before path corrections
Filled circles: after empirical path corrections

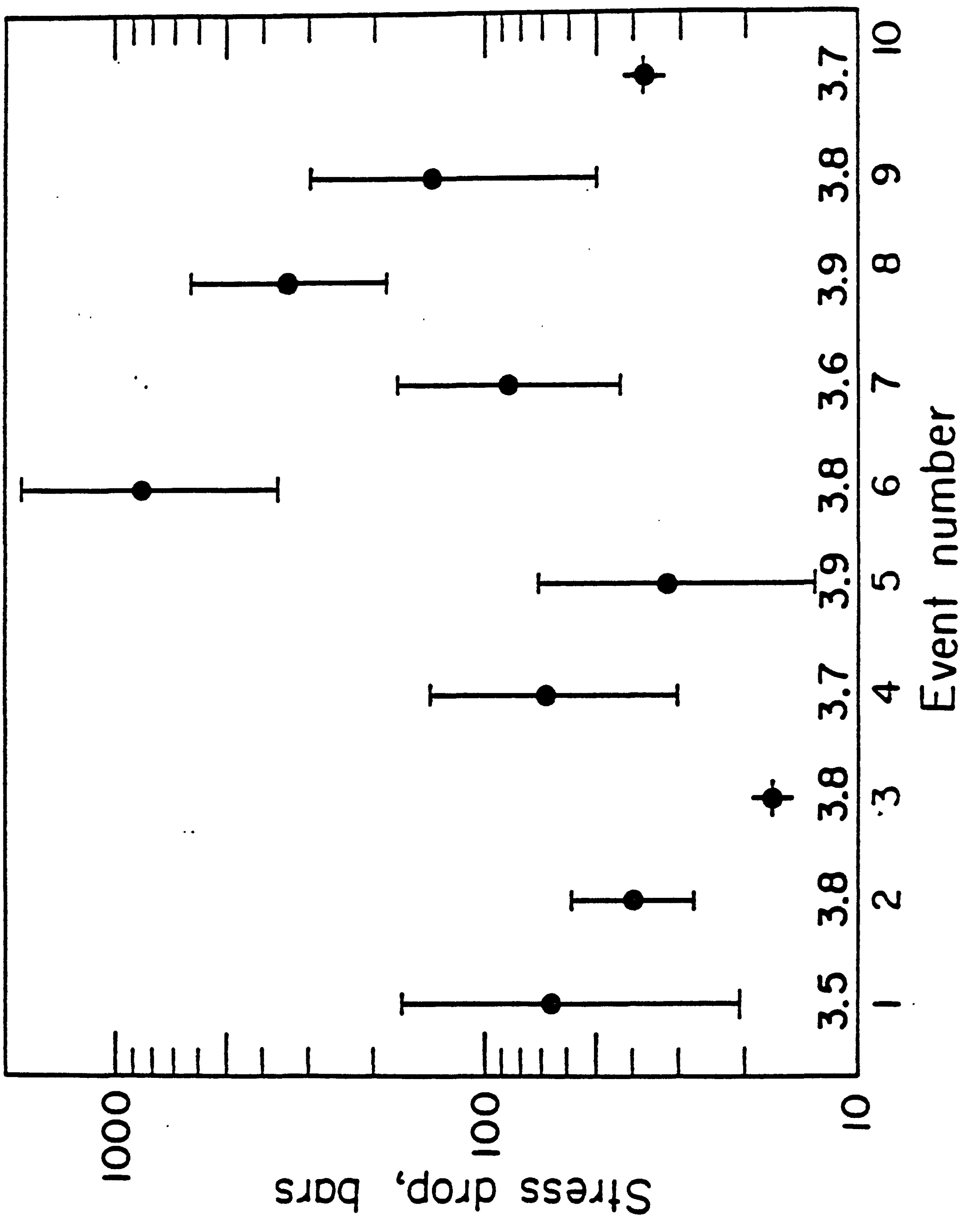
Stress drop, bars
1000
100
10
Event number
1
2
3
4
5
6
7
8
9
10
3.5
3.8
3.8
3.7
3.9
3.8
3.6
3.9
3.8
3.7

FIGURE 15

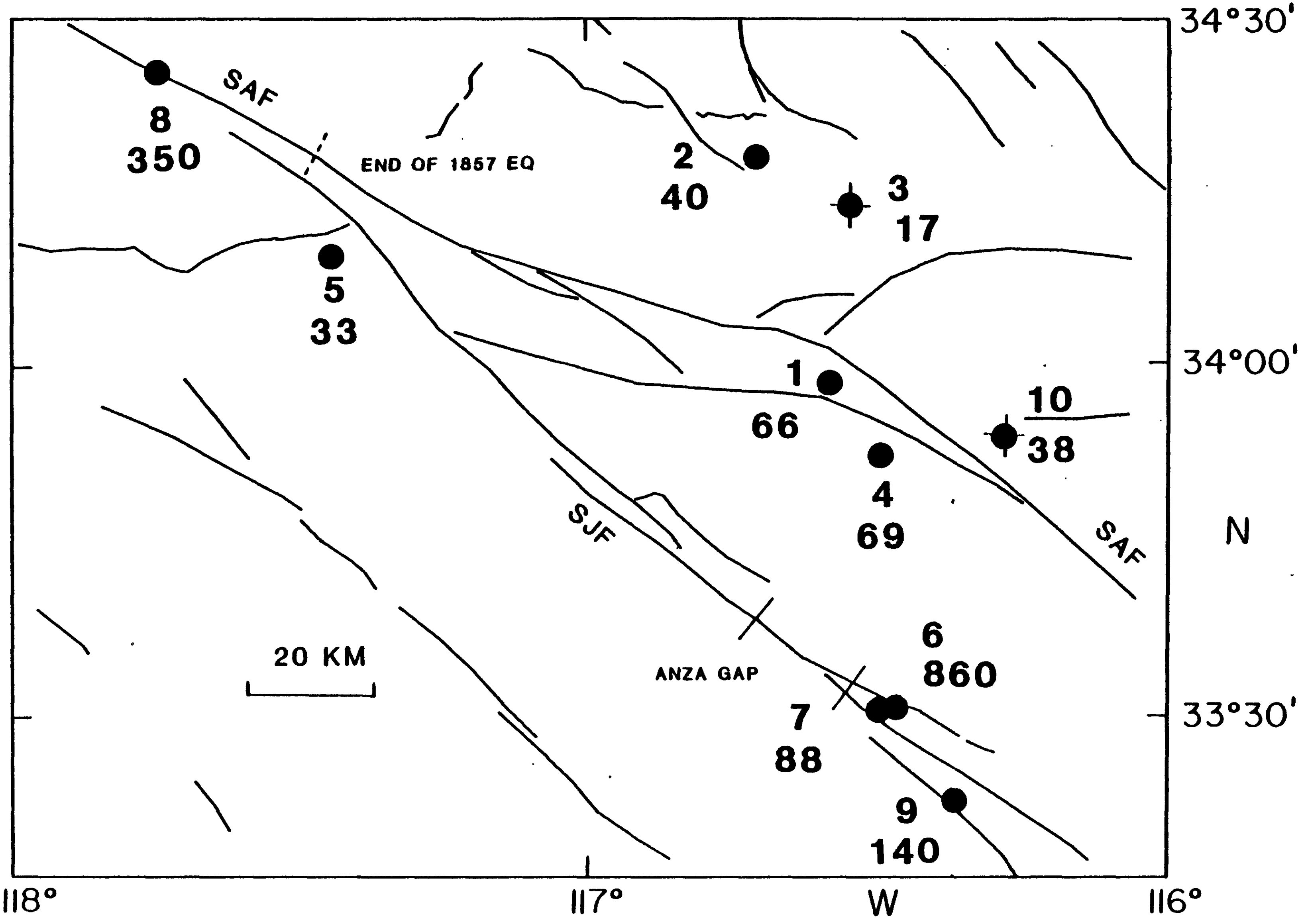
34°30'
34°00'
33°30'
N
118°
117°
W
116°
SAF
SAF
SJF
END OF 1857 EQ
ANZA GAP
20 KM
8
350
2
40
3
17
5
33
1
66
10
38
4
69
6
860
7
88
9
140

FIGURE 16

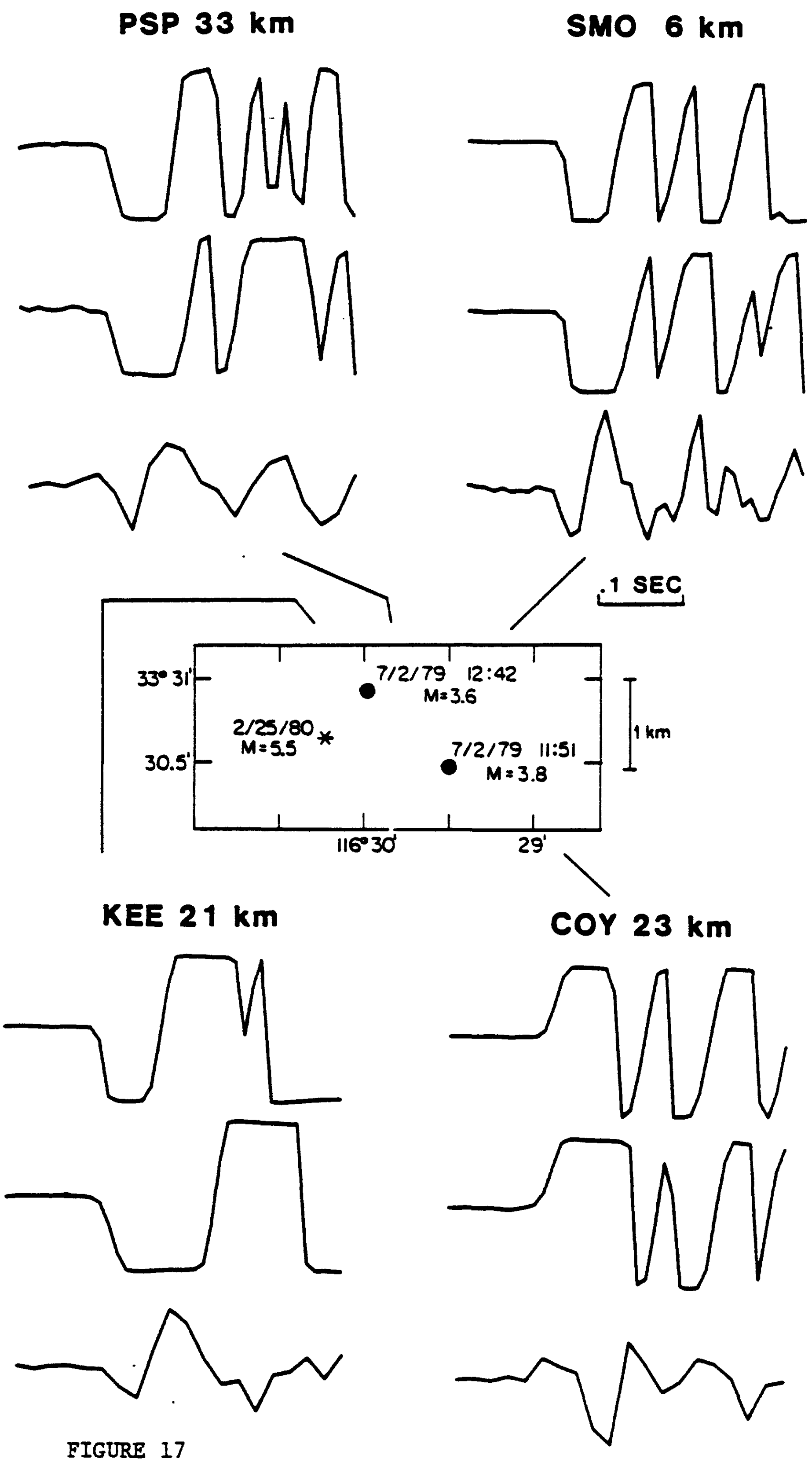

FIGURE 17

Top trace: 11:51 event
Middle trace: 12:42 event
Bottom trace: empirical Green's function

APPENDIX B. 1.

Council letter to Director, U.S. Geological Survey

Lamont-Doherty Geological Observatory of Columbia University | *Palisades, N.Y. 10964*

Cable: LAMONTGEO
Palisades New York State
TWX-710-576-2653

Telephone: Code 914, 359-2900

10 July 1985

Dr. Dallas Peck
Director
U.S. Geological Survey
MS 106, National Center
12201 Sunrise Valley Drive
Reston, Virginia 22092

Dear Dallas,

I am writing to you about the results of the meeting of the National Earthquake Prediction Evaluation Council (NEPEC) of March 29 and 30, 1985. Most of that meeting was devoted to a review, discussion and synthesis on the San Andreas and San Jacinto faults in southern California. The Council heard 14 invited presentations on various aspects of those two faults, an update on Parkfield and a review by Thatcher of a special studies area workshop held by the USGS in San Diego from February 28 to March 2, 1985. That workshop's goal was to identify and reach a consensus of specific segments of those two fault zones appropriate for detailed earthquake prediction studies. Copies of the presentations at that workshop were made available to NEPEC members. The NEPEC meeting was also preceded by the semi-annual review of data from southern California, which several NEPEC members attended.

The minutes of the March meeting are being sent separately to you along with copies of the technical presentations and figures. Those presentations, the papers presented at the workshop and the minutes of the March meeting will be included in an open-file report. The Council agreed to meet in July to discuss methodologies for identifying intermediate and short term precursory effects of earthquakes with emphasis on Parkfield.

Dr. John Filson had asked the Council at an earlier meeting to consider sending your office advice about updating or modifying letters that were sent to the State of California in 1976, 1980 and 1981 about the earthquake hazard situation in southern California. The information stated below is our assessment of that situation for southern California, particularly for the two faults that we reviewed. Since there is a great deal of new information available for those two faults, the Council believes that it is appropriate to recommend that a revised statement be issued by your office on southern California. The Council was also notified that an update of such a statement on a yearly basis would be welcome and desirable.

It is clear that there have been several major advances in our understanding of the earthquake hazard related to the San Andreas and San Jacinto faults in southern California. Geological excavations or trenching have been carried out at several places along the San Andreas fault in southern California. Those data have been particularly important in extending back the short record of historic earthquakes (about 100 to 200 years) to periods of several hundreds to 2000 years. Prehistoric earthquakes have been recognized in several excavations. While the studies are still in their infancy and much work remains to be done, the data already permit approximate repeat times of large shocks to be calculated for a few places and for long-term slip rates to be measured for several segments of the San Andreas fault in southern California.

A very important result from analyses of prehistoric and historic large shocks is that repeat times, average displacements and magnitudes for several segments of faults a few tens of kilometers long appear to be very similar from one large shock to another. In contrast, repeat times and other properties of large or great earthquakes vary considerably from one segment of the San Andreas fault to another. For example, the largest shocks that break the Parkfield segment have been accompanied by displacements of 0.5 to 1 m and occur about every 21 years. In contrast, at Wallace Creek in the Carrizo Plain the past three largest displacement events have been about 10 m.

Preliminary excavations along the southernmost San Andreas fault between Palm Springs and the Salton Sea indicate that the chance that that segment could break in a large earthquake is greater than had been previously thought. That segment, which shows abundant Quaternary evidence of faulting, has not broken historically. The Council heard evidence that a shock on that segment probably would have not been recorded if it had occurred before 1845. Preliminary trenching data indicate repeat times of the order of 150 years. It should be remembered that the date that segment last ruptured is not known nor are repeat times known to better than several decades.

Three groups have now made independent estimates of the probabilities of large earthquakes breaking various parts of the San Andreas fault in southern California during the next few decades. Qualitatively the estimates show remarkable similarity for most of the segments examined. The uncertainty of these probability estimates ranges from being relatively small for Parkfield to very uncertain for segments such as that near San Gorgonio Pass. Average repeat times of about 150 years appear to characterize the 40-km segment of the San Andreas to the south of Cholame, the segment of the San Andreas between Tejon and Cajon passes and (as mentioned above) that segment from Palm Springs to the Salton Sea. The first two segments broke in the Fort Tejon earthquake of 1857 while the latter segment probably has not broken since at least 1845. It is reasonable to assume we are in a period, albeit one spanning several decades, in which major earthquakes are more likely to occur along those three segments than, say, in the period 1870-1970.

In constrast, the segment of the San Andreas fault in the Carrizo Plain appears to have a low probability of rupturing in a great earthquake during the next few decades. Between Cajon Pass and Palm Springs the San Andreas fault is extremely complicated and has several major branches. Analysis of historic data indicates that it probably has not ruptured since at least 1790. It may have last broken in a great (magnitude near 8) earthquake about 1710. Our knowledge of prehistoric earthquakes in that area and of repeat times of large or great shocks is almost non-existent. Tentative estimates would give it a moderate probability of rupturing in a large or great earthquake during the next few decades.

The northern half of the San Jacinto fault, particularly those segments near Anza and at the fault's northern end, have moderate to high probabilities of rupturing in earthquakes of magnitude 6 1/2 to 7 during the next few decades. Our knowledge of the long-term slip rate along those segments of the San Jacinto faults is quite poor as are estimates of repeat times of large shocks.

In reviewing the San Andreas and San Jacinto faults the Council was well aware that major and damaging earthquakes in southern California have occurred on other faults as well. We chose the above two faults for our initial consideration since they have some of the largest rates of long-term movement. Earthquakes as large as magnitude 6.5 can occur on a great number of faults in southern California; a few shocks of that type can be expected during the next few decades. Major faults like the Garlock and Sierran frontal faults, which were not reviewed in March, have lower rates of long-term slip than the San Andreas but could also be sites of future large earthquakes.

Seismicity in southern California has shown no dramatic changes during the last several months. The general level of intermediate-size earthquakes (magnitude 5 and above) compared to the period 1953-1978, remains high.

While the greatest progress to date in earthquake prediction has been for longer time scales, i.e., one to a few decades, a focussing of our efforts in those areas that have higher probabilities should permit us to obtain more data on intermediate and short-term precursory effects.

The designation Long-Term Earthquake Potential is appropriate for a number of the segments discussed above or for southern California in general. The designation Long-Term Prediction (for which a time window of a few years to a few decades is used by the Council) is applicable to the Parkfield segment. The Council found no definite evidence that other segments of the San Andreas and San Jacinto faults should be put in that category. That statement probably reflects our poor state of knowledge of those segments and should not be construed as indicating the earthquake risk is low.

Our knowledge of various segments of the San Andreas and San Jacinto faults in southern California is evolving rapidly. Geological data such as those from trenching and various types of geophysical monitoring need to be expanded greatly for several of the above fault segments if we are to have a reasonable chance of either obtaining data on intermediate or short term precursors or of making predictions on those time scales.

In the light of these observations, we see no reason to alter the earthquake hazard situation in southern California that was portrayed in letters to the State in 1980 and 1981. However, in light of the new terminology adopted by the U.S. Geological Survey for geologic hazards, the situation does not meet the criteria for a Hazard Warning. We recommend, therefore, that the assessment presented above be formally passed to the State of California as information regarding a hazardous condition (long-term earthquake potential) as provided for under U.S.G.S. procedures.

You may wish to include the following summary points in a letter to the State of California:

- Considerable progress has been made in the last few years in long-range prediction and in estimates of long-term earthquake potential, i.e., for time scales of one to a few decades.
- Probabilistic estimates of the likelihood of large earthquakes during the next few decades along various parts of the San Andreas fault in southern California made by 3 different groups are in substantial agreement for many parts of the fault.
- Three segments of the San Andreas fault in southern California have average repeat times of about 125 to 175 years, have not ruptured in large earthquakes in more than 128 years and have moderate to high probabilities of being sites of large earthquakes during the next few decades. These are the 40-km zone south of Cholame, that between Tejon and Cajon passes and the segment between Palm Springs and the Salton Sea. New data indicate that the latter segment, which has not broken historically, has a higher potential than previously thought.
- The northern half of the San Jacinto fault, especially segments near Anza and at its northern end near San Bernadino and Riverside, has a moderate to high probability of rupturing in shocks of magnitude 6 1/2 to 7 during the next few decades.
- The Parkfield segment of the San Andreas fault has a high probability of rupturing in an event of magnitude near 6, similar to that of 1966, within ±4 years of 1988. That estimate is considered by NEPEC to be a Long-Term Prediction, i.e., one in which the expected time window for occurrence is a few years to a few decades.
- The segment of the San Andreas fault in the Carrizo Plain appears to have a low probability of rupturing in a large earthquake like that of 1857 during the next few decades. Estimates of repeat times of large shocks and probabilities for the complex section of the San Andreas fault system between Cajon Pass (San Bernadino) and Palm Springs are very uncertain. Tentative estimates indicate that it has a moderate probability of rupturing within the next few decades.
- Since the last major breakage of the San Andreas fault in southern California occurred in 1857, it is reasonable to assume that we are in a period, albeit one spanning several decades, when another major earthquake is more likely than, say, in the period 1870-1970.
- Earthquakes of magnitude up to 6 1/2 have occurred in the past and can be expected to occur in the future along many faults in southern California other than along major throughgoing faults like the San Andreas. A few other major faults with long-term slip rates less than that of the San Andreas fault could also be sites of major earthquakes during the next few decades.
- The general level of intermediate-size earthquakes (magnitude 5 and above), in southern California, compared to the period 1953-1978, remains high.
- In light of these observations, the earthquake hazard for southern California is considered to be high (as it was in previous communications

to the State of California). The probability is moderate to high that a large to great (magnitude 7.5 to 8) earthquake will occur in southern California during the next 30 years.

- It should be noted that the U.S. Geological Survey changed its terminology for Geological Hazards Warning in 1984. In statements issued in 1980 and 1981 southern California was considered to be in a Hazard Watch State, the second of three categories of hazard information used prior to 1984.
- The earthquake hazard in California for the next decade is high enough that a greater effort needs to be devoted to earthquake monitoring, prediction and preparedness. A designation like "Region of Intensive Observation" would seem appropriate for several parts of southern California.

Sincerely yours,

Lynn R. Sykes
Chairman, National Earthquake Prediction
Evaluation Council

LRS/llm

APPENDIX B. 2.

U.S. Geological Survey Statement to California Office of Emergency Services

March 3, 1849

United States Department of the Interior

GEOLOGICAL SURVEY
RESTON, VA. 22092

OFFICE OF THE DIRECTOR

APR 4 1985

In Reply Refer To:
WGS-Mail Stop 106

Mr. William M. Medigovich
Director, California Office of
  Emergency Services
P.O. Box 9577
2300 Meadowview Road
Sacramento, California 95823

Dear Mr. Medigovich:

This letter is to review the earthquake hazard situation in the Parkfield, California, region. The results of geological investigations in the region, which were recently reviewed by the National Earthquake Prediction Evaluation Council (NEPEC), indicate that there is a high probability of an earthquake of about magnitude 6 within the next several years in the Parkfield region. We do not consider that the evidence and evaluation warrant issuance of a "geologic hazard warning" by the U.S. Geological Survey (USGS) at this time (see definitions as published in Federal Register, January 31, 1984, enclosed), but the following information may be of use to State and local officials in hazard mitigation or emergency response planning.

Specifically, the results of our studies as concurred in by NEPEC indicate three essential points.

1. There is evidence that earthquakes have occurred on the San Andreas fault in central California near Parkfield in 1857, 1881, 1901, 1922, 1934, and 1966, or about every 22 years.

2. The last three of these earthquakes were all similar, leading to the hypothesis of a characteristic magnitude 6 Parkfield earthquake with recurring features.

3. There is a high probability that another magnitude 6 earthquake will occur on the San Andreas fault near Parkfield in the next several years. Statistical calculations indicate there is a 95 percent probability that this earthquake will occur in the 1985-1993 interval. The model on which these statistics are based is developed in reports by W. H. Bakun of the USGS, one written with A. G. Lindh of the USGS and another with T. V. McEvilly of

the University of California. Copies of these reports are enclosed. NEPEC concluded that these findings constitute a long-term prediction, a term taken to include a specific place and a time interval of a few years to a few decades for occurrence of an earthquake.

It is our understanding that the California Earthquake Prediction Evaluation Council has reviewed the Parkfield studies and endorses the points made above.

The last damaging Parkfield earthquake on June 28, 1966, was slightly less than magnitude 6 and caused only minor damage. If a larger earthquake were to occur, damage would be sustained over a wider area. There is some geological evidence that an earthquake larger than magnitude 6 is possible in the Parkfield area, with the fault breaking up to 25 miles further south than it did in 1966. The significance of this evidence is more equivocal and additional study and review of it are needed.

The USGS has been conducting an experiment in the area in an attempt to detect instrumentally the premonitory features of the earthquake before it occurs. We stress, however, that both the anticipated earthquake and perhaps a larger event could occur without the detection of any clear premonitory features. We shall continue our efforts and will notify your office immediately if conditions so warrant and of any changes in our assessment of the situation. The USGS remains available to explain its research and findings to State, county, and local officials.

Sincerely yours,

Director

Enclosures

APPENDIX B. 3.

U.S. Geological Survey Press Release

United States
Department of the Interior
Geological Survey, National Center
Reston, Virginia 22092

Public Affairs Office
Donovan Kelly (703) 860-7444

For release: April 5, 1985

STUDIES FORECASTING MODERATE EARTHQUAKE NEAR PARKFIELD, CALIF., RECEIVE OFFICIAL ENDORSEMENT

The forecast that an earthquake of magnitude 5.5 to 6 is likely to occur in the Parkfield, Calif., area within the next several years (1985-1993) has been reviewed and accepted by state and federal evaluation panels according to an announcement today (April 5, 1985) by the U.S. Geological Survey.

A letter summarizing the results of the scientific review of the Parkfield forecast was sent to Mr. William Medigovich, Director of the California Office of Emergency Services, by Dr. Dallas Peck, Director of the U.S. Geological Survey.

Parkfield has been the site of a USGS earthquake prediction experiment that is using sophisticated distance measuring devices and other monitoring equipment in an attempt to determine and monitor signals that might presage an earthquake.

The research that led to today's statement has been carried out by William H. Bakun and Allan G. Lindh of the U.S. Geological Survey and Thomas V. McEvilly of the University of California. Their conclusions are based on analyses of reports of earthquakes in the Parkfield area in 1857, 1881, and 1901 and seismograph records of events near Parkfield in 1922, 1935, and 1966. The average interval between these events is 22 years and statistical analyses indicate a high probability (over 90 percent) of another earthquake in the region within the 1985-1993 interval. The seismograph records of the last three Parkfield earthquakes are very similar, leading to the hypothesis of a characteristic earthquake in the Parkfield region of about magnitude 6 on the Richter Scale.

Parkfield lies along the San Andreas fault in a sparsely populated region about 170 miles south of San Francisco and 180 miles north of Los Angeles. An earthquake of magnitude 6 is of moderate size, at the threshold of being able to cause modest damage to some structures that have not been designed for earthquake resistance.

The last characteristic Parkfield earthquake occurred on June 28, 1966, registered a magnitude slightly less than 6, and caused only minor damage to wood-frame houses in the region.

(more)

The results of the Parkfield studies by Bakun, Lindh, and McEvilly have recently been reviewed and endorsed by the National Earthquake Prediction Evaluation Council and the California Earthquake Prediction Evaluation Council. These bodies advise federal and state officials respectively on the validity of statements and studies regarding the occurrence of future earthquakes. The national council concluded that the findings at Parkfield constitute a long-term prediction, a term adopted by both councils to describe a statement on the occurrence of an earthquake at a specific place and within a time interval of a few years to a few decades.

In their evaluation of the research, the two prediction review panels said that the potential exists for the next earthquake in the Parkfield region to be larger than the 1966 shock, and for the fault rupture to extend southeast into the adjacent 25-mile segment of the San Andreas fault. Both panels agreed, however, that the evidence for this larger earthquake was speculative and required additional data and review.

Under a program of earthquake prediction research, the U.S. Geological Survey maintains an array of sensitive geophysical monitoring instruments in the Parkfield region in an attempt to predict the occurrence of the expected earthquake more precisely. The California Division of Mines and Geology also maintains a large number of instruments to measure the effects of the earthquake.

The California Office of Emergency Services has reviewed the evaluation with local officials and will take coordinated action should the extensive monitoring equipment arrayed throughout the Parkfield region indicate that the anticipated earthquake is imminent.

* * * USGS * * *

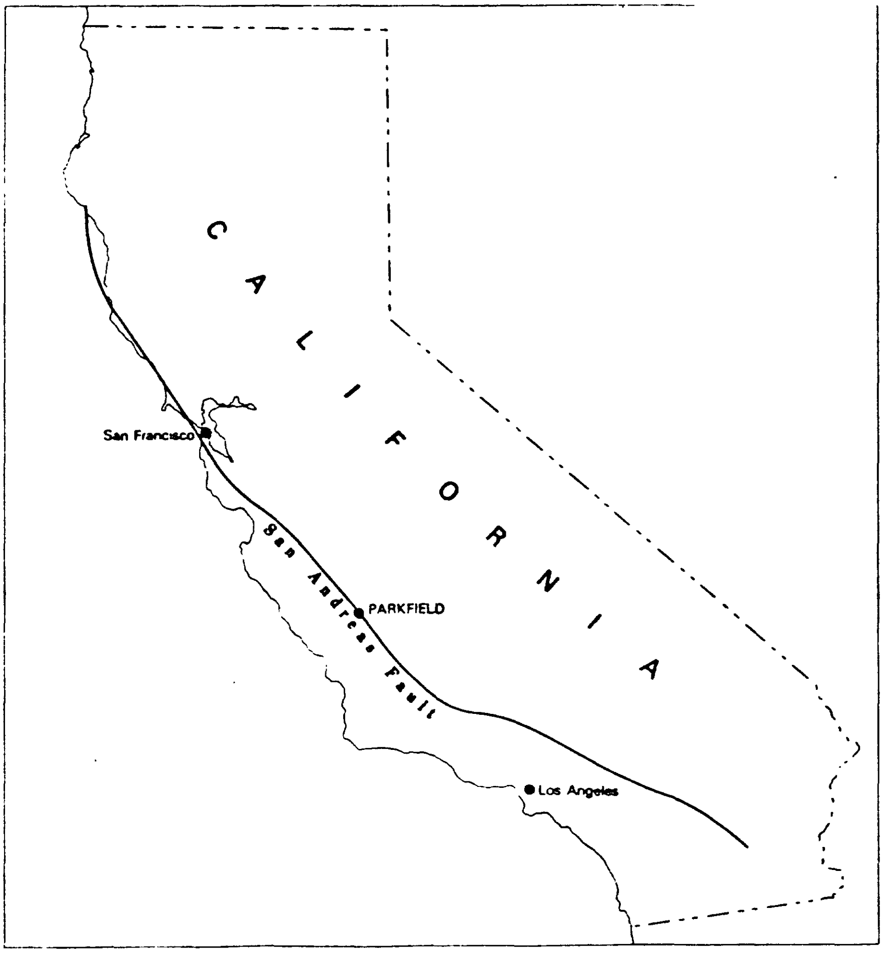

APPENDIX C. 1.

1976 letter to Alex Cunningham, Director, Office of Emergency Services, California

Hamil

United States Department of the Interior
GEOLOGICAL SURVEY
RESTON, VIRGINIA 22092

MAR 3 1976

Honorable Edmund G. Brown, Jr.
Governor of California
Sacramento, California 95814

Dear Governor Brown:

Recent investigations by the Geological Survey indicate that there is increasing cause for concern over the possibility of a major earthquake in the Los Angeles area. The land surface along the San Andreas fault north of Los Angeles has risen by almost a foot over the last 15 years, with the maximum uplift reaching about 10 inches in the vicinity of Palmdale. This finding was announced in a press release of the Department of Interior on February 13, 1976, a copy of which is enclosed, and was described in many California newspapers soon thereafter.

Some earthquakes are known to have been preceded by uplift, including the 1971 San Fernando, California, quake and the 1964 Niigata, Japan, quake. The occurrence of an uplift does not necessarily portend a great shock, however, and there is some evidence that an uplift may have occurred in the region of the present uplift around 1900 without a subsequent earthquake.

The region of the uplift last experienced a major earthquake of magnitude greater than 8 in 1857. Through this century, the section of the San Andreas fault north of Los Angeles has been seismically quiet and is one of the "locked" or presently inactive sections of the fault. While this part of the fault has been locked, adjacent parts have been moving by creep or active faulting to accommodate, at least in part, the general movement of the Pacific plate on the west side of the San Andreas fault past the North American plate on the east side. There is little doubt, therefore, that strain energy has accumulated. The earthquakes near Bakersfield in 1952 and San Fernando in 1971 may be indications that the stress in the region is approaching the level for major failure.

I believe it would be helpful if we, together with a few members of our staffs, could meet to discuss the new observations and our plans for further studies. This might assist you in deciding what defensive actions might be taken to prepare for such an event in ways that are effective but not disruptive.

Let's Clean Up America For Our 200th Birthday

Of equal importance is the need for us to discuss procedures for communication of information should additional anomalies be observed. This could include the issuance of an earthquake prediction. In the enclosed Geological Survey Circular 729, I have described how I am proposing to disseminate earthquake prediction information. The diagram on page 11 shows our intention to send information about California earthquakes to your office. It would be very helpful to me to get your reaction to this plan first hand and to have your suggestions for changes.

I will be in California for a visit to Stanford University on March 18 and 19. I could meet with you on March 17 if you so desire. If another date would be preferable, I will be pleased to try to adjust my schedule.

Sincerely yours,

V. E. McKelvey

Director
V. E. McKelvey

Enclosures

APPENDIX C. 2.

1980 letter to Alex Cunningham, Director, Office of Emergency Services, California

United States Department of the Interior

GEOLOGICAL SURVEY
RESTON, VA. 22092

In Reply Refer To:
EGS-Mail Stop 720

JUL 3 1980

Mr. Alex R. Cunningham
Director, Department of Emergency Services
Post Office Box 9577
Sacramento, California 95814

Dear Mr. Cunningham:

In March 1976, we wrote to Governor Edmund G. Brown, Jr. expressing our increased concern over the possibility of a major earthquake in the Los Angeles area (copy of letter enclosed). The cause of our concern at that time was the uplift of the land area along the San Andreas fault in southern California during the period 1961-1974. Although the uplift was centered in the vicinity of Palmdale, a broad region of southern California increased in elevation 10-15 inches. The total area affected was 32,000 square miles. Analyses of data from surveys taken since 1974 indicate that by 1978 the uplift had subsided rapidly to approximately one-third of its pre-1974 amplitude.

Our March 1976 letter to Governor Brown was sent prior to the development of our current Geologic Hazard Warning and Preparedness procedures. Under our current procedures, our March 1976 notification of the southern California uplift would be described as a Hazard Watch. A Hazard Watch is the second of three levels of hazard information; it gives notification "that a potential catastrophic event of a generally predictable magnitude may occur within an indefinite time (possibly months or years)." Thus, this letter is essentially an update of an existing Hazard Watch for southern California.

The reduction of the uplift and additional recent geophysical observations indicate that changes or adjustments are continuing within the Earth's crust in southern California. Geological investigations undertaken since 1976 have yielded estimates of the dates of previous large earthquakes associated with movement along the San Andreas fault in this region. Due to these additional observations and studies, our concern over the possibility of a major earthquake in California is greater now than in 1976.

Below, we outline briefly the causes of our increased concern:

o In 1857 the San Andreas fault broke for some 200 miles, from Cholame to just north of San Bernardino, giving rise to an earthquake of estimated magnitude 8.3. Detailed geologic studies of the fault along this zone of historical breakage indicate that events similar to the 1857 earthquake have occurred at intervals from 100-230 years and on the average every 140 years. Since the last major breakage of the San Andreas fault in this region was in 1857, it is reasonable to assume that we are in a period, albeit one spanning several decades, when another major earthquake is more likely than, say, in the period 1860-1960.

o For the past 8 years, we have been making regular geodetic surveys in southern California to observe patterns of strain in the Earth's uppermost crust. Initially, these surveys indicated that the uppermost crust in southern California was in a general state of increasing north-south compression. Given the geometry of the region, this strain pattern tended to push the sides of the fault together and this, in a simple model, might reduce the likelihood of slippage or breakage along the fault. Beginning in 1979, we observed a dramatic change in the crustal strain pattern. The magnitude of the strain rate increased to about three or four times that previously observed, and its orientation was such that the crust in southern California was being subjected to east-west tension. Our model indicates that the San Andreas would be more likely to fail under these conditions than under north-south compression. Early results from surveys conducted this spring show that the strain condition is returning to the pre-1979 pattern; nevertheless, the magnitude of the recent strain changes, greater than any observed in the previous 6 years, are disconcerting.

- Over the last year, we have observed increases in the quantity of radon in the ground water of certain wells in southern California. Similar increases have been observed prior to earthquakes in Japan and the Soviet Union. (Many rocks, particularly granites, contain trace amounts of radioactive elements. As these elements decay, they give off harmless quantities of radon, a radioactive gas with a short half-life. Because of its radioactive nature, this gas can be detected in minute quantities in ground water.)

- The level of seismicity in the State has also recently increased. During the past 10 months, there have been 11 earthquakes of magnitude exceeding 5.5 in the region; this is about twice the total of similar events in the previous 6 years. Although the previous 6 years may have been abnormally quiescent, the recent seismicity may indicate an increase in regional crustal stress.

We shall continue to intensify our observational efforts in southern California, and we intend to conduct periodic reviews of these observations and their significance. The reviews will be made by the U.S. Geological Survey (USGS) scientists, scientists under contract to the USGS and the National Earthquake Prediction Evaluation Council if appropriate. We shall keep you informed of the results of these reviews and any new developments.

We hope this information is useful to you, and we look forward to working with you toward the reduction of earthquake hazards in California. We shall be happy to receive your comments or questions resulting from this letter.

Sincerely yours,

HW Menard

H. William Menard
Director

Enclosure

Copy to: Honorable Edmund G. Brown, Governor of California
State Geologist, California
Dr. Charles C. Thiel, Federal Emergency Management Agency, Washington, D.C.

APPENDIX C. 3.

1981 letter to Alex Cunningham, Director, Office of Emergency Services, California

United States Department of the Interior
GEOLOGICAL SURVEY
RESTON, VA. 22092

OFFICE OF THE DIRECTOR

October 9, 1981

Mr. Alex R. Cunningham
Director, Office of Emergency Services
Post Office Box 9577
Sacramento, California 95418

Dear Mr. Cunningham:

On July 3, 1980, we wrote to you to review the earthquake hazard situation in southern California and to notify you that, under our current Hazard Warning procedures, we considered the region to be in a Hazard Watch state. A Hazard Watch is the second of three levels of hazard information formally issued by the U.S. Geological Survey; it gives notification "that a potential catastrophic event of generally predictable magnitude may occur within an indefinite time (possibly months or years)."

In that letter, we cited the observations of rapid crustal strain variation, increases in radon in ground water, and an increase in the level of seismicity as the basis of our concern; this concern was reinforced by new data on the recurrence interval of large earthquakes on the southern San Andreas fault. We also indicated that we would review the situation periodically and keep you informed of new developments.

The purpose of this letter is to meet this latter commitment.

e salient features of our most recent observations are summarized briefly below:

The radon content of certain water wells in southern California continues to show strong variations. Wells near Lake Hughes and Lytle Creek show marked increases while six others show no strong, recent trend and one indicates a marked decrease. Measurements of soil radon show a general increase in the region during the past several months.

* We have received several reports of changes in the water-table level near San Bernardino and renewed spring activity along the San Andreas fault near Palmdale. We are in the process of confirming and making further determinations on these and other reports related to unusual water flow or level.

* Seismicity in southern California has shown no dramatic changes during the last several months. Small clusters of earthquakes have occurred near San Bernardino and Bombay Beach, but these are not particularly unusual. The general level of intermediate-size earthquakes (magnitude 5 and above), compared with the period 1971-1978, remains high. Beginning about the summer of 1978, we observed a marked increase in the seismicity in southern California that was recently sustained by a magnitude 5.5 earthquake just off the coast on September 4, 1981.

In the light of these observations, we see no reason to alter our Hazard Watch notification for southern California. We plan to hold a meeting in early November to review and discuss the most recent geophysical and geochemical observations in southern California. We shall contact you shortly with information on the date and location of this meeting. We look orward to reviewing our data more fully with you at that time.

Sincerely yours,
Dallas L. Peck, Director

Copy to: State Geologist, California
Ugo Morelli, Federal Emergency Management Agency, Washington, D.C.

APPENDIX D.

Proceedings of Southern California Special Study Areas Workshop, San Diego, California, February 28-March 2, 1985

REPORT ON SOUTHERN CALIFORNIA SPECIAL STUDY AREAS WORKSHOP

San Diego, California
28 February - 2 March 1985

Wayne Thatcher and Bill Ellsworth
U.S. Geological Survey
Menlo Park, California

The goal of the workshop was to identify specific 30-km-long segments of the southern San Andreas and San Jacinto fault zones appropriate for detailed earthquake prediction studies.

The attached agenda, program, extended abstracts and post-meeting comments of nine workshop participants are included here. They provide some flavor of the informal proceedings and of the range of opinions of the participants.

There was considerable unanimity on the need to focus efforts in selected regions of southern California. While the Parkfield prediction experiment provides the best conceptual model for such focussed studies, there was a widespread sentiment that experiments had to be tailored to take account of the geological and geophysical characteristics of each region to be studied. For example, given a 150-km-long fault zone with high seismic potential, several years of intensified seismic and geodetic measurements throughout this zone would be needed to establish criteria for selecting a 30-km-long segment for detailed monitoring. Nonetheless, the necessity of addressing the high seismic risk of southern California with clustered monitoring efforts was clearly recognized, and there was wide if perhaps not unanimous agreement on where these studies should be located: the Anza slip gap on the nothern San Jacinto fault, the southernmost end of the San Andreas fault near the Salton Sea, and the complex junction zone of the San Andreas and San Jacinto faults near Cajon Pass.

WORKSHOP ON

SPECIAL STUDY AREAS IN SOUTHERN CALIFORNIA

SUMMARY

Southern San Andreas fault - Tejon Pass to San Bernardino
Central San Andreas fault - Parkfield to Tejon Pass

Special studies along segments of the San Andreas fault between Parkfield and San Bernardino should consider four primary approaches, a discussion of which follows:

1 **Regional Outlook** -- If the large southern California earthquakes of 1857, 1872, 1927 and 1952 were to recur today, it is quite possible that we would predict only the 1857 event. The other events were located in areas away from the San Andreas fault where our monitoring equipment is currently sparse. More than a decade of effort clearly shows that there are more than 95 active faults in the Los Angeles Basin. A M6.5 earthquake on a fault system such as the Newport-Inglewood could have as large an impact on Los Angeles as an M8 earthquake on the San Andreas fault, located about 30 miles to the northeast. Consideration, therefore, should be given to a regional monitoring scheme that includes the San Andreas and San Jacinto faults and other structures as well. Detecting earthquake precursors is not easy and if we are not to miss a major earthquake, selective equipment upgrading should be done throughout southern California.

Studies should be geared to maintaining a regional perspective in order to gain a comprehensive picture of the earthquake process and the interrelationship of individual segments of the San Andreas system. Greater understanding of the slip rates of individual fault segments and of the variation of those rates with time (uniform(?)) are necessary in order to understand the long-term behavior of the San Andreas fault and major changes between active and "inactive" segments In addition, they provide important data on the kinematic character of multiple segments of fault systems for forecast modelling such as time - dependent and instability models. A regional approach also provides greater latitude for developing new, innovative instruments, and would allow us to coordinate experiments that employ these instruments.

2. **Pre- or syn- cluster developmental program** -- In order to best determine where instrument clusters should be installed, a developmental program should be initiated to address specific problems and to formulate models of how data should be collected. Of particular importance, is the continuation of geologic mapping and trenching of the type being done by Kerry Sieh, John Matti, Joe Ziony, and others to accurately map geologic units and the structural framework, to determine the chronologic history of fault activity, to establish local and regional fault slip rates, and to calculate earthquake recurrence intervals Groups of people should be identified for coordinated pre- and syn- cluster studies. From the standpoint of political support. it should be kept in mind that Congress associates an augmented earthquake prediction program with increased monitoring focused on areas of high seismic potential. The program design, therefore, should include the simultaneous development of clusters and pre-cluster investigations.

Problems to be addressed include:

a. Determination of the long-term tectonic behavior of the San Andreas fault. From Cholame to Tejon Pass M8 events occur about every 250-450 years, with surface offsets on the order of 7m. Between Tejon Pass and Cajon Pass, on the other hand, there is about 145 years between M8 events and these are associated with surface offsets of about 3.5m. The entire interval, however, is believed to have a relatively uniform fault slip rate of 35mm/yr and there are no obvious gross differences in surface geology or in strain levels at the Garlock fault (Tejon Pass) where the seismic character of the fault changes. What, then, are the reasons for these changes? And what are the coupling mechanisms between segments that allow ruptures to propagate long distances during great earthquakes?

b. Between Parkfield and San Bernardino do fault ruptures begin in generally simple or complex areas?

c. Creep is occurring on the southern San Andreas fault from Thousand Palms to Bombay Beach (on the Salton Sea). Apparently, there is no current seismicity along this stretch of the fault. Why is this segment of the creeping fault aseismic while the central California creeping segment displays relatively abundant low-magnitude seismicity?

d. What mechanisms control how fault segments interact and how is total fault slip accommodated by tangential or en echelon systems? Why do events migrate and what controls the migration rate?

e. What effects do secondary structures and seismicity have on the occurrence, size, and nucleation point of major earthquakes?

f. Are premonitory signals present in our micro-earthquakes?

g. If the crust is locked at depths shallower than 20-25KM from Tejon Pass to Cajon Pass as geodetic data suggest, then it seems that prior to a large event the lower part of this zone must break (because recent earthquakes do not involve a thickness as large as 25KM). What experiments might we initiate to detect this premonitory rupture?

h. How do we determine that part of the strain budget that is accommodated by folding and minor fracturing as compared to faulting?

3. **Instrumentation at Parkfield** -- The current monitoring network at Parkfield is insufficient and should be augmented before a major effort is made to add new clusters in southern California. Our achievements at Parkfield may well determine our ability to secure new funding for an operational prediction network for southern California. What we learn at Parkfield may not be transferable to southern California but it should provide a good physical model that assists our research in network deployment strategy. Sufficient instrumentation at Parkfield is also

important to be able to properly evaluate the likelihood of a "run-on" of the expected Parkfield earthquake for 20 or so miles to the southeast, possibly producing an earthquake as large as M7

4. **Suggested cluster sites** -- Sites of concentrated monitoring in southern California probably should not be developed as replicates of the Parkfield cluster. Each new site will be tectonically and seismologically unique and so monitoring must be tailored to the physical characteristics and the logistical realities of the site.

The suggested sites are listed in the order in which they were mentioned most frequently, beginning with those mentioned the most.

a. Cajon Pass

The region from Pallet Creek to Cajon Pass was considered by many to be one of the strongest candidates for a cluster. It is the location where the fault rupture associated with the 1857 earthquake terminated and it marks a transition from a generally simple to complex segments of the San Andreas fault. It is, of course, the junction of the San Andreas and the San Jacinto fault systems and the seismicity increases south of the pass Recent movement on the San Jacinto fault may have produced sinuous bulges on the San Andreas fault, thus affecting the seismic potential at this location In terms of monitoring, we already have a baseline of data from the 2-color laser operations at nearby Pearblossum. In addition, downhole experiments and the development of a deep earth observatory in the Cajon Pass drill hole will provide data valuable for a more comprehensive evaluation of the tectonic and seismologic environment.

b. Cholame area, southeast of Parkfield

The concern of a run-on of the next Parkfield earthquake argues that the area where the potential fault rupture will occur be adequately instrumented. The same area could possibly be the nucleation point of a repeat of the 1857 earthquake as well and so instrumentation should be increased in an effort to detect precursors.

c. Tejon Pass

The seismic and tectonic character of the San Andreas fault change across the Garlock fault. How do these changes affect earthquake potential on the San Andreas and how dangerous is the Garlock fault and the Big Pine fault? The intersection of major faults and the change in seismic character support the installation of a cluster between Tejon Pass and Lake Hughes.

d. Mojave

A cluster on a relatively simple stretch of the San Andreas fault may provide valuable data that can be applied to a better understanding of earthquake generation on more complex segments of the fault.